Neutrophil-derived microvesicle-induced blood brain barrier dysfunction and white matter lesion formation in the ageing brain

By:

Anjana Ajikumar

A thesis submitted in partial fulfilment of the requirements for the degree of Doctor of Philosophy

Department of Neuroscience

Faculty of Medicine, Dentistry & Health

The University of Sheffield

September 2020

Abstract

Age-associated white matter lesions (WML), an independent risk factor for dementia, are histologically characterised by endothelial cell activation, blood brain barrier dysfunction and microglial activation. Systemic inflammation can interact with brain endothelium and exacerbate neurodegenerative processes, leading to accelerated progression of dementia. The mechanisms by which systemic inflammation affects WM pathology and cognitive decline in the ageing population are, as yet, unknown. Neutrophils, first responder cells of the innate immune system, are significantly higher in dementia patients and are associated with cognitive decline in Alzheimer's disease (AD) patients who are hospitalised due to infection. Activated neutrophils produce neutrophil-derived microvesicles (NMVs) which modulate systemic endothelial function but, to date, the effect of NMVs on brain endothelial cells is unknown. We hypothesise that during an inflammatory event, NMVs interact with brain microvascular endothelial cells leading to dysfunction of the blood brain barrier (BBB), microglial activation, WML formation and cognitive decline.

Specifically, this study investigated the interaction between NMVs and the human cerebral microvascular endothelial cell line (hCMEC/D3) and determined whether NMVs alter BBB integrity and gene expression *in vitro*. Flow cytometry and confocal imaging demonstrated that NMVs are internalised by brain endothelial cells. To understand how these cells internalise NMVs, hCMEC/D3 were incubated with various pharmacological inhibitors targeting different modes of internalisation. Results from this study revealed that NMVs are internalised via a variety of energy-dependent mechanisms, including clathrin-mediated endocytosis and macropinocytosis. Furthermore, some of the NMVs co-localised with early endosomal markers when analysed under confocal microscopy. Microarray analysis was performed on cells treated with NMV (300 NMV/µL) to compare the transcriptome to control untreated cells. The internalisation of NMVs significantly altered the transcriptomic profile of hCMEC/D3 cells, including ubiquitin mediated proteolysis, p38 and SNARE mediated vesicular transport pathways. Functional grouping analysis highlighted dysregulation of genes associated with tight junction proteins, vesicle mediated transport, protein transport and RNA localisation. Since the microarray data indicated that vascular integrity was impacted after NMV internalisation, this was validated by assessing the permeability of the brain endothelial monolayer by measuring paracellular leakage (using 10 kDa and 70 kDa FITC-Dextran) and transendothelial electrical resistance (TEER). Results indicated that NMV significantly increase the flux of both 10-kDa and 70-kDa FITC-Dextran, indicating BBB leakage.

Internalisation of NMV also decreased TEER in a time-dependent manner. These finding indicate that NMVs interact with and can alter gene expression of brain microvascular endothelial cells and impact the integrity of the BBB.

The current study also characterised the transcriptomic profile of endothelial cells in age-associated WML. Laser capture microdissection (LCM) was employed to isolate endothelial cells from lesions, normal appearing white matter (NAWM) and non-lesional control WM. Transcriptomic analysis indicated microvessels in WML are associated with the dysregulation of genes involved in ubiquitin mediated proteolysis, endocytosis and p53. Furthermore, this study also highlighted that although NAWM is radiologically normal, the gene expression profile of vessels suggest WML arise in a field effect of vascular changes which extend beyond the established lesion.

Evidence presented throughout this thesis conclude that NMVs may play an important role in modulating the integrity of the BBB. Moreover, vascular-associated transcriptomic changes in ageing WM may lead to BBB dysfunction, and represent potential therapeutic targets to prevent the pathogenesis of age-associated WML.

ACKNOWLEDGMENTS

First and foremost, I would like to acknowledge my supervisor- Dr. Julie Simpson for her scientific wealth, constant support and at times personal guidance throughout my PhD. I am forever grateful for her positive attitude and constant encouragement. Most of all, thank you for all the positivity when things were not going as planned.

I would like to thank my second supervisor – Dr. Victoria Ridger. Thank you for sharing the knowledge with me and for your support and encouragement. Thank you for my greater understanding of neutrophils and shear stress.

Thank you to Alzheimer's Research UK for funding my PhD and the CFAS study for the generous donation of tissue for the study- without it, this work would not have been possible. Thank you to all my donors who showed up every time to donate blood mostly at short notices- I am forever grateful.

Thanks to all my colleagues and friends both at Department of infection, immunity and cardiovascular diseases (IICD) and SITraN for being there for me, answering all the questions and all the help throughout the PhD. A special mention to Merete- thank you for the countless cups of tea, dinners, and falafels that we shared. Without you, I wouldn't have lasted through the PhD.

Special thanks to my parents and my siblings – Ajay and Ami. Thank you for the constant encouragement and love. Your never-ending questions about science was my comfort away from all of you. Thank you for always sneaking Lyons into my suitcase each time because Tea is not the same in UK!

Finally, a huge thank you to Manoj. Without you being my rock, this would not be a reality. You took this journey along with me, believed in me when I lost sight. You have suffered a lot of sleepless nights along with me without ever complaining. You have been my rock throughout sharing my lows and celebrating my highs. Thank you for your never fading positivity and your sense of humour – your love was the guiding light.

Table of Contents

List of Figures

List of Tables

Abbreviations

% P	Percent present
ABC-HRP	Avidin-biotin horseradish peroxidase
AD	Alzheimer's Disease
ANOVA	Analysis of variance
ApoE	Apolipo protein E
AU	Absorbance unit
BBB	Blood brain barrier
BMEC	Brain microvascular endothelial cells
CAA	cerebral amyloid angiopathy
cDNA	Complimentary DNA
CFAS	Cognitive Function and Ageing Study
CNS	Central nervous system
DAVID	Database for annotation, visualisation and integrated discovery
ds-cDNA	Double stranded cDNA
DSCL	Deep subcortical lesion
EDTA	Ethylenediaminetetraacetic acid
EIPA	5-(N-Ethyl-N-isopropyl) amiloride
fMLP	*N*-Formylmethionyl-leucyl-phenylalanine
FoxO	Forkhead box proteins class O
FSC-A	Forward Scatter Area
FSC-W	Forward Scatter Width
FU	Fluorescence unit
GAPDH	Glyceraldehyde 3-phosphate dehydrogenase

GWAS	Genome wide association study
H&E	Haematoxylin and eosin
HCAEC	human coronary artery endothelial cells
hcMEC/D3	Human cerebral microvascular endothelial cell line
HUVEC	human umbilical vein endothelial cells
ICAM-1	Intercellular adhesion molecule 1
IHC	Immunohistochemistry
IL	Inter leukin
IMPaLa	Integrated molecular pathway level analysis
iNOS	Nitric oxide synthase
kDA	Kilo Dalton
KEGG	Kyoto encyclopaedia of genes and genomes
LCM	Laser capture microdissection
LPS	Lipopolysaccharide
MCI	Mild cognitive impairment
MDC	Monodansylcadaverine
MHC	Major histocompatibility complex
miRNA	Micro RNA
MMP	Matrix metalloproteinase
MRC	Medical Research Council
MRI	Magnetic Resonance Imaging
mRNA	Messenger RNA
MS	Multiple Sclerosis
MS	Multiple sclerosis

MV	Microvesicle
NAWM	Normal appearing white matter
NMV	Neutrophil-derived microvesicle
NVU	Neuro vascular unit
PBS	Phosphate buffered saline
PCA	Principal component analysis
PMD	Post-mortem delay
PVL	Periventricular Lesion
RIN	RNA Integrity Number
RNA	Ribonucleic acid
ROS	Reactive oxygen species
RPMI	Rosa Park Memorial Institute Medium
RT	Room temperature
SNP	Single nucleotide polymorphism
SVD	Small vessel disease
TEER	Trans endothelial electrical resistance
TEM	Transmission electron microscopy
TJ	Tight junction
TLR	Toll-like receptors
TNF-α	Tumour necrosis factor – alpha
VaD	Vascular Dementia
VCAM-1	Vascular cell adhesion molecule 1
WHO	World Health Organisation
WM	White Matter

WML	White Matter Lesion
ZO-1	Zonula Occludens -1

Chapter 1: General Introduction

1.1 Epidemiology of Dementia

The proportion of ageing adults (aged 65y and older) in the general population in developed countries is on the rise due to falling birth rates and increased longevity, attributed to advanced health care. It is estimated that by 2050, the number of elderly people will surpass the number of children under 15 in the United Kingdom i.e. one in four will be aged 65 and over (Office of National Statistics, 2018). This will result in increased incidences of age-associated neurodegenerative disorders, which will have long-term effects on the social policies of developed countries. One of the major health problems of an ageing population is dementia. The World Health Organisation (WHO) defines dementia as a syndrome that affects the cognitive ability of an individual and is different from the decline associated with the normal ageing process. Dementia is considered as one of the major causes of dependency among the older population. WHO estimate that currently 46.8 million people worldwide are living with dementia, and these figures are projected to increase to 75.6 million by 2030. The Alzheimer's Society UK reported in 2015 that there are 850,000 people living with dementia in the UK and this is set to increase to a million by 2025. Alzheimer's disease (AD) is the biggest cause of dementia, followed by vascular dementia (VaD) and dementia with Lewy bodies (DLB) (Mount and Downton, 2006). Understanding the underlying mechanisms that contribute to the development of cognitive decline and dementia is crucial for identifying novel therapeutic treatments.

1.2 Vascular Dementia

Vascular dementia (VaD) is the second most common cause of dementia in the elderly population, accounting for 20-30% of total dementia cases. VaD and AD have many overlapping risk factors and pathophysiology, making it very difficult to distinguish these subtypes. Factors that mainly contribute to VaD are atherosclerosis, small vessel disease and cerebral amyloid angiopathy (McAleese et al., 2016). Atherosclerosis is a condition in which fibro-fatty deposits are commonly formed in the basilar artery and the circle of Willis, resulting in plaques causing degeneration of the vessels (Beach et al., 2007). These plaques narrow arteries thereby reducing the cerebral blood flow and resulting in a hypoxic environment, which ultimately disrupts brain homeostasis.

Small vessel disease (SVD) is a general term that refers to the damage of small arteries, arterioles and brain capillaries (Poggesi et al., 2012). SVD can affect different regions of the brain such as grey and white matter. As the atherosclerotic changes in the small vessels increases, it can lead to

ischemic conditions in the area, to which the microvasculature is vulnerable (Ho et al., 2000; Kalaria and Erkinjuntti, 2006). As the disease progresses, it can present itself as deep white matter hyperintensities, microbleeds, lacunar infarcts and cortical atrophy (Pantoni, 2010). SVD is strongly associated with stroke, and it is estimated that at least one in every five stroke cases is associated with SVD, especially in the elderly population (Wardlaw et al., 2013b). Furthermore, the presence of SVD correlates with a worse clinical outcome in patients with stroke, and with delayed recovery (van Uden et al., 2016). Although SVD was described over a century ago, it is only with the recent neuroimaging advances that the disease is finally taking to the main stage.

SVD is also generally associated with lifestyle factors such as sedentary lifestyle, smoking, obesity along with other vascular factors such as diabetes, hypertension and hyperlipidaemia (O'Donnell et al., 2010; Posner et al., 2002). Obesity and diabetes can significantly increase inflammation and has been associated with development of dementia in later life (Pedditzi et al., 2016; Shalev and Arbuckle, 2017). Furthermore, hypertension is a major risk factor for SVD (Abraham et al., 2016). In a trial with very elderly patients (80 years or older), it was reported that reduction of hypertension reduced stroke mortality (Beckett et al., 2008). All of this suggest that SVD is a multi-factorial disease.

Another major factor in development of VaD is cerebral amyloid angiopathy (CAA), which results from the cerebrovascular deposition of β-amyloid protein (Vinters, 1987; Viswanathan and Greenberg, 2008). Deposition of this protein causes vessel wall thickening and narrowing of the lumen resulting in perivascular microhaemorrhage. Another common pathological feature of CAA is cortical microinfarctions, which are frequently located in subcortical white matter (Gurol et al., 2013; Reijmer et al., 2016). WML were reported to be severe in patients diagnosed with CAA than healthy age matched controls and patients with AD (Gurol et al., 2013; Holland et al., 2008)

In the general population, the prevalence of SVD is increasing as the population is ageing, and since SVD is associated with altered cerebral blood flow it can play a significant role in the development of dementia (Hakim, 2019). In fact, vascular dysregulation was reported to be an early event in the disease progression cascade when over 7,700 brain images from Alzheimer's Disease Neuroimaging Initiative (ADNI) were analysed (Iturria-Medina et al., 2016). This suggests that early disruption of cerebral blood flow can initiate may events in the brain that can eventually lead to dementia.

As discussed before, altered cerebral blood flow can lead to SVD, which can often lead to cerebrovascular lesions, which can be commonly observed on MRI scans. Although the changes

in WM are regarded as the radiological signature of SVD, the exact pathological mechanism underlying these WM changes is still unclear.

1.3 White Matter

Cerebral white matter (WM) is an area rich in neuronal connections that are essential for processing information (Vernooij et al., 2008). It is enriched with fibre pathways that connect cortical and subcortical structures (Schmahmann et al., 2008) and is responsible for effective cognition and behaviour (Madden et al., 2009). The WM contains a variety of cells including astrocytes, microglia, pericytes, oligodendrocytes and endothelial cells, and accounts for approximately 50% of the total brain volume. The region is white in colour due to the high myelin content which is made up of complex lipids. Myelin supports fast axonal conduction of the nerve impulse. The process of myelination happens rapidly in the first few years of life (Barkovich et al., 1988) and is a tightly controlled process. Although myelination happens mostly during the early years, increasing evidence suggest that remyelination processes continue in the adult brain helping to maintain homeostasis (Gensert and Goldman, 1997; Piaton et al., 2011; Zhang et al., 1999).

Understanding how changes in microstructure of WM occur is essential in understanding normal ageing and disease pathologies. As we age, cortical disconnection due to axonal demyelination increases (Bartzokis et al., 2004; Chang et al., 2012; O'Sullivan et al., 2001), leading to reduced transfer efficiency of information. Analysis of brain white matter structure using MRI scans in UK biobank participants demonstrated that the older the age of the participant, the greater the changes in the white matter, supporting the finding that white matter pathology associates with ageing (Cox et al., 2016).

1.3.1 Age- associated White Matter Lesions (WML)

Post-mortem tissue studies have indicated that white matter pathology is a key contributor to dementia that can develop independently of other cortical pathologies, and is associated with co-morbidity pathologies including diabetes, vascular disease and hypertension (Bronge et al., 2002; Brun and Englund, 1986; Kalaria, 2002, 2000; King et al., 2014), all of which are risk factors for developing dementia (Cukierman-Yaffe et al., 2009; Kivipelto et al., 2002; Spauwen et al., 2013). White matter lesions (WML) present as high signal intensity areas in T_2- weighted and diffusion tensor magnetic resonance imaging (MRI) (Ovbiagele and Saver, 2006). WML, also referred to as white matter hyperintensities, are a common feature in the over-65s (Knopman et al., 2003; Wharton et al., 2011) and are considered to be a part of normal ageing (Ylikoski et al., 1995).

WML can be classified into two groups according to their neuroanatomical location; deep subcortical lesions (DSCL) and periventricular lesions (PVL) (Enzinger et al., 2006; Fazekas et al., 1993; Rostrup et al., 2012; Spilt et al., 2006). The presence of either WML on T2-weighted MRI can predict AD (Brickman et al., 2012; Sachdev et al., 2013), and are associated with an increased rate of cognitive decline (De Groot et al., 2002; Devine et al., 2013). In patients with dominantly inherited AD, WML form independent of cortical AD-associated pathology (Lee et al., 2016). Furthermore, cerebral amyloid accumulation and clinical hypertension are independently associated with greater WML volume (Scott et al., 2015), highlighting the need to study WML independently of cortical pathology.

Although the biggest risk factor for developing WML is ageing, genetics also play a role in some cases (Atwood et al., 2004). Genome wide association studies (GWAS) have highlighted the potential role of several genes and biological processes in the pathogenesis of WML, including the involvement of cytokines such as *IL-5* and *IL5RA* (Fernandez-Cadenas et al., 2011), ApoE regulation (Nebes et al., 2001) and matrix metalloproteinase (MMP) regulation of neuroinflammation (Smith et al., 2009). WM-related SNPs are mainly associated with a region in chromosome 17, which mainly harbours immune regulatory genes, such as *TRIM65* (Fernandez-Cadenas et al., 2011). Additional GWAS of larger, well characterised ageing cohorts are needed to identify new loci associated with VaD and WML.

While WML are a feature of normal ageing and SVD it should be noted that changes in WM are related to other disorders, including cerebrovascular diseases such as stroke (Fazekas et al., 1993; van Uden et al., 2016; Wen and Sachdev, 2004), chronic inflammation (Raz et al., 2012; Yao et al., 2019) and inflammatory diseases such as multiple sclerosis (Frischer et al., 2015; Huang et al., 2017) psychiatric disorders such as depression (Krishnan et al., 1988; O'brien et al., 1996), bipolar disorder (Dupont et al., 1990) and schizophrenia (Kubicki et al., 2005).

The microstructure of WM is susceptible to environmental factors. Systemic-induced changes to cerebral blood vessels, including the formation of atherosclerotic plaques and arterial stiffness, occur both in normal ageing and in dementia patients (Brown and Thore, 2011; Gouw et al., 2011). Changes in cerebral blood flow and/or blood vessels are suggested to underlie WML pathogenesis, likely through hypoperfusion giving rise to a hypoxic environment (Choi et al., 2015; Lee et al., 2011; Wardlaw et al., 2014)(Black et al., 2009; Gouw et al., 2011). Future studies are required to determine how cerebrovascular-related changes contribute to the WML formation and/or progression in the ageing brain.

1.4 Blood brain barrier

The concept of the blood brain barrier (BBB) was originally proposed by Paul Ehrlich in 1885, but the debate of its existence carried on well into 20th century. Seminal experiments by Goldmann (1909), one of Ehrlich's student, who administered trypan blue intravenously into mice, demonstrated the exclusion of the dye from the CNS. This paved the way for establishing the BBB as a barrier between the CNS and periphery. Physiological experiments carried out in the sixties and seventies, as reviewed by Daneman and colleague (Daneman and Engelhardt, 2017), demonstrated that the BBB is not an impermeable barrier, but a highly regulated active barrier. The BBB is comprised of highly specialised brain microvascular endothelial cells (BMEC) that regulate the movement of molecules between the periphery and the CNS (***Figure 1. 1***). BMECs are characterised by the presence of intercellular tight junction proteins (TJP) and adherens junctions (AJ) (Daneman and Engelhardt, 2017; Hawkins and Davis, 2005; Obermeier et al., 2013). Together these proteins form junctional complexes between BMEC that regulate the permeability of BBB (Sweeney et al., 2018). BMEC are also characterised by their low pinocytic activity and restricted passage of molecules from the circulation to the brain. BMECs express energy dependent, receptor-mediated transport systems that selectively transport molecules across the barrier (Grammas et al., 2011; Sweeney et al., 2018). In other organs of the body, endothelial cells have small fenestrations that allow movement of molecules, however BMEC lack these pores and are connected to each other by TJP thus allowing the cells to control the movement of molecules. Most neurons are in close proximity to a capillary (Zlokovic, 2005) thereby facilitating rapid diffusion of receptor-mediated transport and rapid efflux of neurotransmitters and metabolic products from neurons and synapses into the blood. Endothelial cells are encased by processes extending from pericytes and the endfeet of astrocytes (Bell and Zlokovic, 2009; Cheslow and Alvarez, 2016), forming the neurovascular unit which is essential for brain homeostasis and maintaining normal neuronal function.

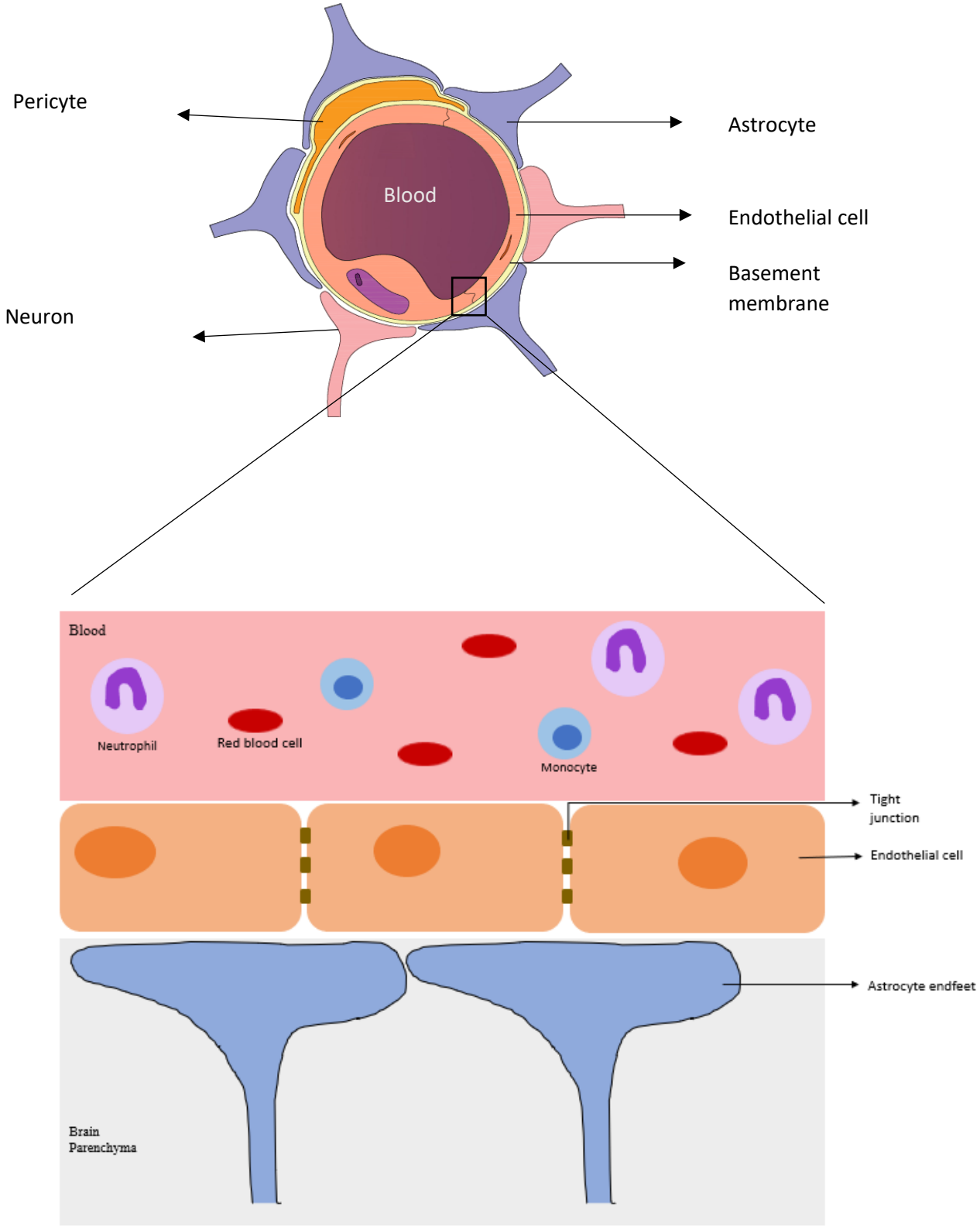

Figure 1. 1 Schematic representation of the major components of BBB. Endothelial cells line the capillaries and are tightly adhered to each other through tight junction (TJ) proteins, which control the movement of molecules between blood and brain parenchyma. Pericytes are embedded in the basement membrane. Along with this, astrocytic endfeet and neuronal processes make up the neurovascular unit (NVU).

1.4.1 Blood brain barrier dysfunction in the WM

Studies in the 1990s reported that the BBB is intact and functional during normal physiological ageing (Mooradian and McCuskey, 1992; Vorbrodt and Dobrogowska, 1994; Wadhwani et al., 1991). However, more recent studies have demonstrated increased evidence of BBB vulnerability in ageing cohorts (Goodall et al., 2018; Hafezi-Moghadam et al., 2007; Hosokawa and Ueno, 1999; Janota et al., 2015). Furthermore, changes in vascular integrity precedes cognitive decline in AD, suggesting that it is an early event in disease pathogenesis (Bell and Zlokovic, 2009; Stolp and Dziegielewska, 2009; Zlokovic, 2011).

Pathogenic changes in the cerebrovasculature are common in VaD patients, including increased BBB permeability (Bell et al., 2010). Post-mortem studies using electron microscopy have shown that BMEC from AD patients have reduced number of mitochondria and reduced frequency of the TJP zonula occludens at cell junctions (Stewart et al., 1992). BBB dysfunction can lead to the accumulation of serum proteins, such as albumin and fibrinogen, in the brain parenchyma and this can be utilised as a tool to measure BBB permeability. A meta-analysis of the literature reported that BBB permeability increases in normal ageing and in dementia patients, as evident by the increased CSF/albumin ratio (Farrall and Wardlaw, 2009). Histological characterisation of MRI-identified WML demonstrates that loss of BBB integrity is a feature of WML (Young et al., 2008). Furthermore, when BBB leakage was analysed in a cohort of 201 patients with stroke and WML using contrast-enhanced MRI, it was reported to be significantly higher in WML and appeared to be increasing in NAWM depending on the proximity to the lesion (Wardlaw et al., 2017). This suggests that BBB dysfunction is a feature of WML and it may be present in NAWM, affecting the blood flow to the region. In animal models of vascular cognitive impairment and dementia, severe vascular pathologies were present (detailed review by Gooch and Wilcock (2016)) (Gooch and Wilcock, 2016). Additionally, in animal models of stroke, transmission electron microscopy (TEM) and western blot analysis of the microstructure of BBB in WML has detected a decrease in expression of ZO-1 and occludin (Fan et al., 2015). Since these proteins are an integral part of TJP that play a key role in maintaining the integrity of the BBB, this further confirms the association of BBB dysfunction with WML. Overall, the relationship between BBB dysfunction and dementia is complex and requires detailed studies to elucidate the interplay between BBB dysfunction and the pathogenesis of disease.

1.4.2 Cerebral endothelial activation and dysfunction in WML

A prominent feature of age-associated WML is the activation of endothelial cells, associated with increased expression of adhesion molecules including intracellular adhesion molecule -1 (ICAM-1) and vascular cell adhesion molecule-1 (VCAM-1). Both ICAM-1 and VCAM-1 may regulate vascular permeability and play a role in the recruitment of inflammatory cells to the site of injury (Auerbach et al., 2007). Human post- mortem studies demonstrate that increased expression of ICAM-1 is a feature of age-related WML (Fernando et al., 2004). A positive correlation between ICAM-1 expression and progression of WML is reported by various studies (Hassan et al., 2003; Markus et al., 2005) suggesting endothelial activation plays a crucial role in the progression and development of WML. Endothelial dysfunction and the resulting extravasation of serum proteins modulates the neuroinflammatory response, which may further contribute to the pathogenesis of WML (Huang et al., 2010; Simpson et al., 2010). Levels of soluble ICAM-1 are significantly higher in the serum of patients with AD compared to age-matched controls, and the circulating levels of soluble VCAM-1 correlate with the severity of dementia (Huang et al., 2015). This collective evidence demonstrates cerebral endothelial cell activation and associated BBB dysfunction is a prominent feature of age associated WML and may play a major role in their pathogenesis. However, the precise mechanism(s) of BMEC activation resulting in BBB dysfunction in ageing WM is still largely unknown and needs to be investigated.

1.5 Neuroinflammation

As the CNS has a low regenerative ability, strictly monitored damage control during an infection is essential for survival (Galea et al., 2007). Inflammation has been known to be neurotoxic for many decades, but the effects were considered to be transient. It is now well established that neuroinflammation plays a significant role in several neuropathological conditions, including dementia, motor neurone disease and multiple sclerosis (as reviewed by (Guzman-Martinez et al., 2019). Neuroinflammation is primarily mediated by the resident immune cells of the brain, namely microglia. Although age is the biggest risk factor for development of neurodegenerative diseases, microglia-induced inflammation plays a role in the initiation and pathogenesis of neurodegeneration (Heppner et al., 2015; Krstic and Knuesel, 2013). This inflammatory response can lead to a cascade of inflammation within the brain, which can be fatal if not monitored (Heppner et al., 2015). Evidence from post-mortem studies demonstrates microglial activation is a feature of age-associated WML (Simpson *et al.*, 2007; Waller *et al.*, 2019). Moreover, immune-

activated microglia are a prominent feature of PVL, expressing high levels of MHC-class II, while microglia in DSCL primarily adopt a phagocytic phenotype, expressing high levels of CD68, indicating that microglial activation is location-dependent. Although phagocytic activity of microglia is hugely important in white matter as it aids in clearing myelin debris and recruitment of oligodenritic precursor cells to the site of damage (Franklin and Ffrench-Constant, 2008; Kotter et al., 2006), persistent activation and the secretion of pro-inflammatory cytokines may lead to neurodegeneration. A systematic review of post-mortem analysis of brain samples of dementia patients with age matched neurological controls verified microglial activation markers are a consistent feature of AD (Hopperton et al., 2018). However, research in this field is limited and more studies into the mechanisms underlying microglial activation are required.

1.5.1 Microglia

As mentioned before, microglia are the resident effector cells of innate immunity in the CNS. These antigen-presenting cells (APC) express a set of proteins called major histocompatibility complex II or MHC class II antigens along with co-stimulatory molecules and, together with perivascular macrophages, drive the innate immune response in the brain. Under normal resting conditions, microglia have a ramified morphology and adopt an inactive, resting state constantly surveying the environment. Simultaneously, they are also responsible for the maintenance of neuronal circuits and synaptic remodelling (Ji et al., 2013). Any change in the microenvironment leads to rapid activation of microglia which undergo morphological changes, retracting their processes to adapt a large, round morphology associated with a phagocytic phenotype. This is accompanied by up-regulation of surface antigens, including MHC Class II, and upregulation of key inflammatory cytokines (Hugh Perry, 1998; Kreutzberg, 1996; V Hugh Perry et al., 1993), and is mediated by specialised receptors known as danger-associated molecular patterns (DAMPs) or pathogen-associated molecular patterns (PAMPs). Depending on the type of injury, microglia can display two distinct phenotypes- namely M1 and M2 (***Figure 1. 2***). Classically activated microglia polarise to an M1 phenotype in response to an injury or infection, and secrete pro-inflammatory cytokines, such as IL-1β, TNF-α and inducible nitric oxide synthase (iNOS) (Orihuela et al., 2016). Even though killing the invading pathogens is clearly beneficial, pro-inflammatory cytokines can also induce neurotoxicity (Block et al., 2007). To minimise the damage, an anti-inflammatory phase is initiated where microglia polarise to a M2 phenotype to assist repair through secretion of anti-inflammatory factors, such as IL-4, IL-13, IL-10 and TGF-β (Tang and Le, 2016; Zhou et al., 2012). In addition, M2 microglia also secrete insulin-like growth factor 1 (IGF-1) which promotes neuronal survival (Suh et al., 2013). However, it should be noted that this is an overly simplified

way of categorising microglia, and it is highly likely that a heterogeneous population of M1 and M2 microglia, along with intermediate phenotypes, co-exist in the brain and are essential for tissue homeostasis.

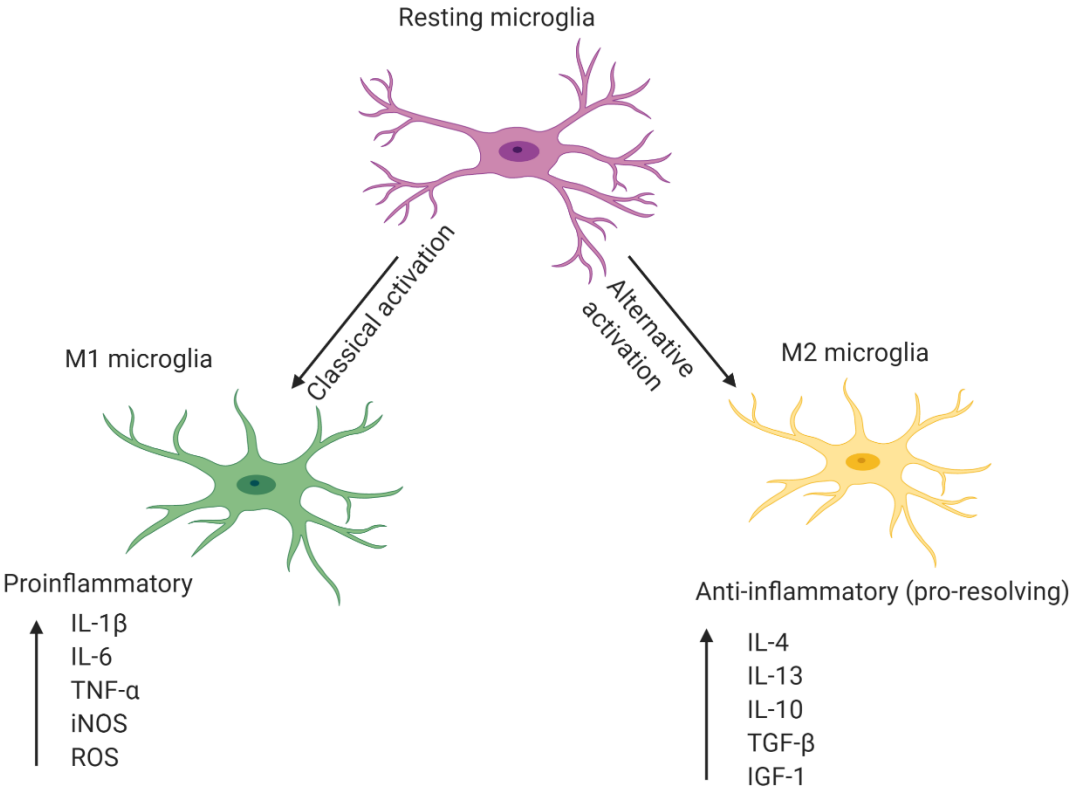

Figure 1. 2 Classical phenotypes of microglia. Microglia can by activated either through classical activation (in response to inflammation or infection) or alternative activation (pro-resolving / anti-inflammatory). Diagram created using BioRender.com

1.4.2 Microglial priming

Changes in the homeostatic environment of the brain can trigger microglial activation. Microglia become primed during neurodegeneration, neuroinflammation and also as part of the normal ageing process. These primed microglia have a lower threshold for activation and when stimulated produce an exaggerated inflammatory response, which may contribute to neurodegeneration and cognitive impairment (Perry and Holmes, 2014). They have a similar morphology to activated microglia with higher expression of MHC-class II molecules and are hyper-responsive towards secondary stimuli, resulting in the heightened production of pro-inflammatory cytokines, including IL-1β and IL-10 (Cunningham, 2013).

Infections in the body or systemic inflammation trigger a heightened inflammatory response in microglia. This response is extensively studied in animal models by challenging the immune system with bacterial endotoxins, such as lipopolysaccharide (LPS), which can lead to an exaggerated neuroinflammatory response and increased neurodegeneration (Cunningham, 2013; Holmes et al., 2009). Peripheral administration of LPS activates microglia, stimulating increased expression of TNF-α and IL-1β in the CNS, causing learning and memory impairment in animal models (Tanaka et al., 2011). Furthermore, low dose of peripheral challenge is reported to cause microglial activation and sickness behaviour both in humans and primates (Brydon et al., 2008; Hannestad et al., 2012; Harrison et al., 2009; Henry et al., 2009), supporting the hypothesis that systemic inflammation activates microglia. Perry et al., (1993) first demonstrated the aggregation of MHC class II positive microglia adjacent to ageing white matter in older rats compared to juvenile rats. The presence of activated microglial clustering is a feature of the radiologically normal appearing white matter surrounding WML (de Groot et al., 2013; Waller et al., 2019; Yuan et al., 2017), suggesting a role for microglia in the pathogenesis of WML.

1.4.3 Peripheral Inflammation and cognitive impairment

As discussed above, primed microglia have a heightened response to peripheral immune challenges. The central neuroinflammatory response following peripheral administration of LPS is exaggerated and prolonged in ageing (Godbout et al., 2005; Li et al., 2012), suggesting that repeated challenge of the immune system can negatively impact on the CNS. Evidence of a peripheral challenge affecting the CNS is not limited to animal models. In healthy male adults,

mild stimulation of innate immunity by endotoxin injection has negative effects on memory function (Reichenberg et al., 2001). Additionally, ageing population studies reveal that hospitalisation due to infections are associated with lower scores on cognitive testing (Benros et al., 2015). Furthermore, hospitalisation due to pneumonia increases the risk of developing dementia in well- functioning older adults (Tate et al., 2014).

Longitudinal studies have demonstrated a negative correlation between systemic inflammation and cognitive function (Dimopoulos et al., 2006; Komulainen et al., 2007; Marioni et al., 2009). Sepsis is a systemic inflammatory response to an infection causing organ dysfunction and contributing to the morbidity and mortality of hospitalised patients (Opal, 2003; Russell, 2006). In patients with sepsis, several studies have reported that there is a significant decline in cognition in the elderly (Guerra et al., 2012; Iwashyna et al., 2010), indicating that peripheral infection play a role in driving cognitive impairment. Together, these studies indicate that peripheral inflammation can have a profound impact on the cognitive status of an individual.

Further evidence to support the hypothesis that systemic inflammation exacerbates dementia come from delirium studies. Delirium is a sudden state of severe confusion where a patient's cognitive function, perception and emotions are disturbed. Dementia is one of the biggest risk factors for developing an episode of delirium (Fong et al., 2015; Morandi et al., 2017). In elderly and demented cohorts, mild inflammatory stimuli can trigger an episode of delirium (Inouye and Charpentier, 1996), leading to longer hospital stays and a greater risk of developing further complications, such as infection, thus creating a vicious loop of within the body. Delirium is linked with a significant decline in cognitive function (Girard et al., 2010; Jackson et al., 2004), leading to exacerbated dementia (Fong et al., 2009; Witlox et al., 2010)(Witlox et al., 2010). Furthermore, when cognitive function was assessed 6-12 months after an episode of delirium, a significant number of patients did not regain their baseline cognitive status (Saczynski et al., 2012). In a longer term follow-up study of AD patients, those who developed delirium had a more rapid cognitive deterioration throughout the subsequent 5 years than patients who did not develop delirium (Gross et al., 2012). All of this indicates that systemic inflammation can lead to progression of dementia and can be considered as an important clinical target.

Numerous clinical studies have reported the link between systemic inflammation and cognition, where chronic infections in patients with cardiovascular diseases are associated with cognitive decline (Li et al., 2011; Snyder et al., 2015; Strandberg et al., 2003). Infections, such as upper respiratory tract infections (URTIs) or urinary tract infections, are very common among the elderly

and can have a marked effect on their cognition (Bucks et al., 2008). Similarly, reports indicate that AD patients with periodontitis have a significant decline in their cognitive function (Ide et al., 2016). Furthermore, in a population-based cohort study, the patient group with periodontitis who did not receive any treatment had a significantly higher incidence of dementia (Lee et al., 2017), demonstrating that systemic inflammation can be a risk factor for the progression of dementia.

Additional evidence to support the link between systemic infection and cognitive decline come from studies of non-steroidal anti-inflammatory drugs (NSAIDs), which are prescribed to treat peripheral inflammatory conditions such as pain, inflammation and fever. Epidemiological studies indicate mid-life use of NSAIDs are protective against the development of dementia (Broe et al., 2000; Etminan et al., 2003; Stewart et al., 1997)(Breitner et al., 2009; Chang et al., 2016; Cote et al., 2012), and their findings have increased the research into the use of anti-inflammatory drugs to reduce cognitive decline. While clinical trials using NSAIDs such as naproxen or celecoxib report no improvement in cognitive function (Aisen et al., 2003; Martin et al., 2008; Thal et al., 2005), these findings suggest that multiple mechanisms underlie disease pathogenesis and that intervention with NSAIDs may need to occur before neuronal dysfunction/loss. Furthermore, pioglitazone a drug commonly used to treat type II diabetes has a beneficial effect on hypertension induced WMLs (Lan et al., 2015), indirectly confirming that systemic therapies may prevent WM pathology. Together, these studies provide compelling evidence that elements of peripheral inflammation have a profound effect on the cognitive status of an individual and support a key role of systemic inflammation in the progression of dementia.

Further evidence of peripheral immune activation during ageing affecting cognitive impairment come from gene expression studies. In ageing mice, transcriptomic analysis of brain regions reported immune activation as a result of ageing (Lee et al., 2000). Meta-analysis of gene expression studies (datasets from human, mice and rats) revealed that there is an increased expression of inflammation and immune response related genes during ageing (De Magalhães et al., 2009). Functional analysis of these transcriptomic datasets reveals that the innate immune response is associated with cognitive decline in the ageing population (Avramopoulos et al., 2011; Cribbs et al., 2012), supporting the hypothesis that innate immune activation plays a key role in progression of dementia. Microarray analysis of ageing WM demonstrates an up-regulation of numerous immune-related genes in WML, including pro-inflammatory cytokine signalling, antigen presentation and phagocytosis (Simpson et al., 2009). In a non-neurological normal ageing cohort, higher levels of inflammatory markers such as IL-6 and C reactive protein (CRP) in the serum negatively associate with cognitive function (Yaffe et al., 2003). In contrast, a study has

reported that inflammation contributes to the development of depressive symptoms but not cognitive decline (van den Biggelaar et al., 2007).

Clinical studies show that systemic inflammation has a detrimental effect on the white matter during development by reduced myelination, immature cerebrovascular development and long lasting cognitive deficits (Kadhim et al., 2001; Rezaie and Dean, 2002). *In utero* inflammation, also called chorioamnionitis, can cause adverse injury to the brain via upregulation of foetal systemic inflammation. In babies with chorioamnionitis, white matter microstructures are altered compared to healthy controls (Anblagan et al., 2016), suggesting inflammation can play a role in WM pathology. *In vivo* experiments demonstrate that peripheral inflammation exerts an effect on the CNS leading to white matter damage (Lehnardt et al., 2002; Pang et al., 2003). New-born mice exposed to moderate levels of IL-1β present increased numbers of non-myelinated axons and long lasting cognitive deficits (Favrais et al., 2011), further suggesting that systemic inflammation during development has a lasting effect on the white matter. Other *in utero* studies have also reported white matter pathology, including gliosis and brain endothelial cell activation, after endotoxin exposure (Bonestroo et al., 2015; Duncan et al., 2002; Stolp et al., 2009, 2005). Although these studies cannot predict long-term consequences or if WM can recover from these alterations, these studies highlight the vulnerability of WM to systemic inflammation. Furthermore, following systemic inflammation, there is significant dysfunction of the BBB, affecting the integrity of the barrier with the loss of TJP and associated with white matter pathology (Bonestroo et al., 2015; Favrais et al., 2011; Rosenberg, 2009; Stolp et al., 2005; Trickler et al., 2010). It should be noted that microstructural changes in WM are associated with peripheral inflammation in AD patients (Swardfager et al., 2017). All this evidence suggest that peripheral inflammation is a risk factor for white matter lesion formation and associated dementia. There are various hypotheses, but the exact mechanism(s) linking peripheral inflammation, BBB dysfunction and white matter damage are currently unknown.

1.5 Neutrophils

As discussed above, the innate immune response is linked to cognitive impairment in the ageing population. Leukocytes, such as neutrophils, play a key role in host defence, releasing a range of pro-inflammatory cytokines (chemokines) that can recruit inflammatory cells to the site of infection (Leliefeld et al., 2016). Neutrophils are the most abundant circulating white blood cells in the body. They are the first line of defence and typically survive for less than 24 hours in

circulation (Athens et al., 1961; Galli et al., 2011). Neutrophils are recruited to the site of infection or inflammation via a chemotactic gradients, such as CXCL8 (Amulic et al., 2012). They are readily activated and migrate to the area of infection releasing a range of secretory vesicles in the process called degranulation, which can also cause collateral damage through their toxic contents. These granules are a rich source of antimicrobial molecules, including elastase, MMP-9 and human neutrophil peptide-1 (Borregaard et al., 2007). Another mechanism by which neutrophils fight pathogens is by releasing neutrophil extracellular traps (NETs) (Brinkmann et al., 2004; Jenne et al., 2013; Saitoh et al., 2012) or by releasing microvesicles (Pitanga et al., 2014; Ridger et al., 2017; Timár et al., 2013) providing critical immunity. Activated neutrophils can express MHC class II and co-stimulatory molecules, acting as APCs (Abi Abdallah et al., 2011; Culshaw et al., 2008) suggesting that neutrophils play diverse roles in clearing infections.

1.5.1 The role of neutrophils in dementia

Although it is much debated how short lived neutrophils can contribute to progression of AD, in the early 1990's it was reported that neutrophils from patients with dementia had higher activity than healthy controls (Licastro et al., 1994). Significantly higher levels of circulating neutrophils have been detected in dementia patients compared to non-neurological control patients (Rai et al., 2012; Shad et al., 2013). Additionally, AD patients have significantly higher blood neutrophil-lymphocyte ratio than healthy age-matched controls (Kuyumcu et al., 2012). In transgenic mouse models of AD, neutrophils interact with brain endothelial cells through ICAM-1/LFA-1 (Zenaro et al., 2015). This interaction can induce rapid changes in the endothelial cells to increase BBB permeability through cytoskeletal changes. Additionally, depletion of neutrophils significantly improves memory function in the early stages of AD (Zenaro et al., 2015), suggesting that neutrophils may play a role in the initiation of cognitive dysfunction. Neutrophil adhesion itself is sufficient to induce changes in endothelial sites by upregulation of ICAM-1 and VCAM-1 (DiStasi and Ley, 2009; Fabene et al., 2008; Zarbock and Ley, 2008). This suggests that neutrophils may also play in the role of activation of endothelial cells, which is also a feature of WML. However, as neutrophils are not a feature of age-associated WM pathology it is still unclear how they exert their effect and contribute to WML pathogenesis. One potential indirect mechanism of neutrophil-induced BBB dysfunction is via their release of microvesicles.

1.6 Microvesicles

Microvesicles (MVs) are increasingly recognised as important mediators of cell to cell communication. They are complex structures that originate from donor cells and can travel to

distant sites of action in the body (Barry and FitzGerald, 1999; Hugel et al., 2005; Ratajczak et al., 2006). Although cell-derived vesicles were postulated in the 1940s (Chargaff and West, 1946) when the authors conducted preliminary studies to understand the "biological significance of the thromboplastic protein of blood", their presence was confirmed only later by electron microscopy (Wolf, 1967). Wolf suggested that microvesicles derived from lipid-rich particles and coined the term 'platelet-dust', which had some of the parent properties such as coagulation. As technology advanced, the field demonstrated that MVs are a part of the larger family of extracellular vesicles which bud directly from the plasma membrane in a general physiological process called membrane vesiculation, and are involved in cell-to-cell communication (Ratajczak et al., 2006). MVs are distinguished from other extracellular vesicles by their size, typically ranging 0.1-1 μm in diameter, whereas exosomes are smaller and apoptotic bodies larger. MVs are also referred to as 'microparticles' in the literature, with the terms microvesicles and microparticles being largely interchangeable. In this thesis, the term 'microvesicles' will be used instead of microparticles, as the latter term can also be used to describe non-biological structures.

MVs are implicated in several pathological processes including inflammation and angiogenesis (Ciardiello et al., 2016; Puddu et al., 2010), and can be shed in low levels from healthy cells under normal physiological conditions (Greenwalt, 2006; Taubert et al., 2010). Shedding of MV from the parent cell involves an influx in Ca^{2+} into the cytosol. Biogenesis of MVs are a result of extensive phospholipid redistribution which is tightly controlled by amino phospholipid translocases, initiated by Ca^{2+} influx into the cells. MV formation is induced by the translocation of phosphatidylserine by Ca^{2+} dependent enzymes such as scramblases which also activate the proteolytic enzyme calpain, resulting in disrupt of the actin cytoskeleton, stimulating vesiculation (Olivier et al., 2011). MVs are released by most type of cells upon activation by various methods such as physical or chemical stress, hypoxia and shear stress (Ratajczak et al., 2006)

In the last decade, the role of MVs in intercellular communication acting as paracrine/endocrine effectors has greatly advanced, however the ability of MVs to package their contents in response to various stimuli is still underexplored. Interestingly, it was discovered that MVs can transfer genetic information horizontally. Many studies have shown that MVs contain mRNA, which can be transferred in co-culture conditions. Endothelial progenitor cell-derived MVs interact with endothelial cells, promoting cell survival and proliferation, however when endothelial progenitor cell-derived MVs are incubated with RNAse, they fail to induce the proliferative and angiogenic changes both *in vitro* and *in vivo* (Deregibus et al., 2007). MVs also contain microRNA (miRNAs), which can affect the gene expression of the target cells. miRNAs are a class of small noncoding,

evolutionary conserved RNAs involved in regulation of gene expression, achieved either by degradation of target mRNA or inhibition of translation (Macfarlane and Murphy, 2010). MVs released by mesenchymal stem cells contain more than 40 mature miRNA that are also expressed by the parent cells (Collino et al., 2010).. miRNAs are selectively packaged to MVs (Diehl et al., 2012), and can drive disease pathology (Gomez et al., 2020; Hulsmans and Holvoet, 2013). Together these findings demonstrate that MVs are emerging to be key effectors in the pathogenesis of a variety of diseases.

There is a growing body of evidence supporting that MVs not only transfer content between cells but also can drive disease pathology in various conditions. MVs from cancer cell lines can support tumour growth by helping them evade the immune system (Valenti et al., 2007). They also contain proteinases, including MMP-2 and 9, which can cause extracellular matrix degradation (Ginestra et al., 1998), facilitating invasion. In other inflammatory conditions such as sepsis, leukocyte derived MVs are significantly elevated (Fujimi et al., 2003). In atherosclerosis, several types of MVs are elevated including platelet-derived MVs and monocyte-derived MVs (Mallat et al., 1999; Merten et al., 1999)

Increasing evidence suggest that MVs can contribute to the overall inflammatory response. MVs derived from non-primed primary macrophages have the potential to activate macrophages (Thomas and Salter, 2010). Macrophages can also release MVs in response to TLR ligands (Gauley and Pisetsky, 2010). Tumour cells treated with doxorubicin, or other small molecules such as cisplatin, release microvesicles that contain the drug, acting as a potential drug-efflux mechanism resolving drug resistance (Safaei et al., 2005; Shedden et al., 2003), demonstrating that MVs have the ability to have an enormous impact on therapeutic strategies.

MVs have an immune-modulatory response in the host. MVs released from the placenta of pre-eclampsia patients induces a systemic maternal inflammatory reaction (Holder et al., 2012; Messerli et al., 2010). Elevated myeloid-derived MVs have been detected in the CSF of experimental autoimmune encephalomyelitis (EAE) mice, an animal model for studying MS, and can activate microglia (Verderio et al., 2012). Furthermore, MV levels are higher in patients with clinical symptoms of MS or in a relapsing state when compared to stable disease state or healthy controls, suggesting the peripheral immune system can modulate the CNS, which may act as a useful tool to monitor disease status. In another inflammatory disease, rheumatoid arthritis (RA), platelet-derived MVs are elevated in patients compared to controls, correlating with the severity of the disease (Knijff-Dutmer et al., 2002). Leukocyte-derived MVs are elevated in synovial fluids

of RA patients, suggesting these MVs play a role in inflammation and cause local joint destruction (Gyorgy et al., 2012; Sellam et al., 2009). Interestingly, another study reported that MVs isolated from neutrophils from healthy controls and RA patients reduced monocyte and fibroblast-like synoviocyte activation *in vitro* (Rhys et al., 2018). This suggests that MVs can also act as anti-inflammatory and may play a role in inflammation clearance. All of this points towards the complex mode of action of MVs and how they exert their effect on the target cell, however more studies are required to fully elucidate the role of each MV population in disease pathogenesis.

1.6.1 Neutrophil-derived microvesicles

Neutrophils release MVs known as neutrophil-derived microvesicles (NMVs) in response to various inflammatory or infectious stimuli such as formyl-methionyl-leucyl phenylalanine (fMLP) or lipopolysaccharide (LPS) (Gasser and Schifferli, 2004; Hess et al., 1998; Mesri and Altieri, 1998). NMVs are formed by budding of the plasma membrane (see ***Figure 1. 3***). This process is initiated with an influx of calcium into the cell. The increased cytosolic Ca^{2+} activates a calcium-sensitive protease called calpain, which can remodel the cytoskeleton (Pasquet et al., 1996). The neutrophil plasma membrane is made up of a lipid bilayer. Under resting conditions, phosphatidylserine, which is negatively charged is located on the inner leaflet on the bilayer. When the neutrophil is activated, increased cytosolic calcium recruits and activates various enzymes such as floppase and scramblase, causing lipid movement to the outer membrane and inactivation of flippase eventually leading to the flopping of phosphatidylserine to the outer leaflet (Turturici et al., 2014), eventually leading to the blebbing off of NMVs from plasma membrane. There is evidence that NMV cargo is not randomly allocated; instead it is selectively recruited and dependent on the mechanisms of stimulation (D'Souza-Schorey and Clancy, 2012; Dalli et al., 2013).

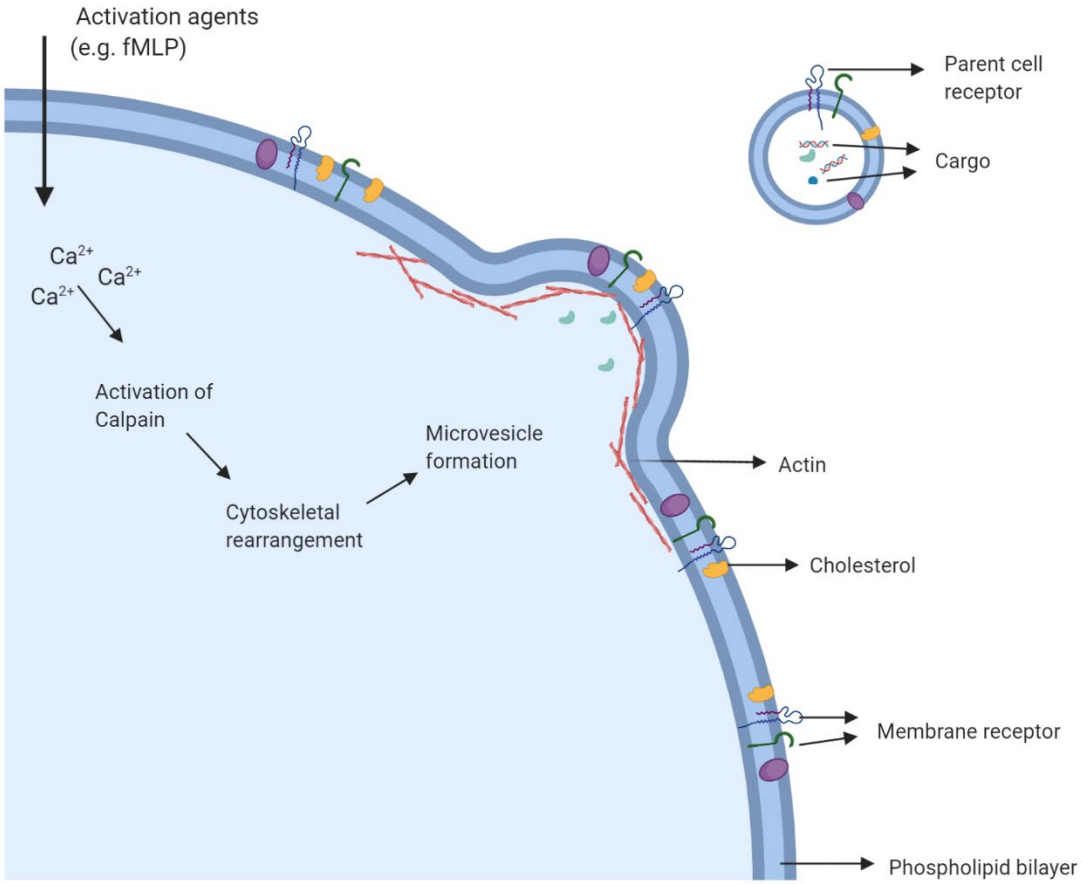

Figure 1. 3 Formation of a microvesicle. When a neutrophil is activated (for e.g. by fMLP), it increases cytosolic calcium, which can activate Calpain leading to cytoskeletal rearrangement. The outward budding of the plasma membrane will eventually lead to fission and separation of microvesicle (MV) from the parent cell. MVs are loaded with genetic material such as mRNAs, miRNAs and proteins (enzymes, cytokines, growth factors). MVs also contain some but not all of the surface receptors of the parent cell.

NMVs express neutrophil specific surface markers such as CD66b and adhesion molecules such as CD11a (Hong et al., 2012; Jaffe et al., 1973), and are enriched in phosphatidylserine and L-selectin (Mesri and Altieri, 1998). The role of NMVs in disease pathologies is slowly being understood. NMVs are elevated at inflammatory locations in severe inflammatory conditions, such as sepsis and atherosclerosis (Berckmans et al., 2005; Prakash et al., 2012). NMVs exert an anti-inflammatory response through several mechanisms: they act on macrophages to inhibit their inflammatory properties (Gasser and Schifferli, 2004; Rhys et al., 2018), reduce the phagocytic activity of dendritic cells and modify the release of TGF-β1, a potent regulator of macrophage activation (Eken et al., 2008). NMVs also contain annexin A1, an endogenous anti-inflammatory protein which confers anti-inflammatory properties (Dalli et al., 2008). However, other several studies report NMVs induce a pro-inflammatory phenotype on endothelial cells (Hong et al., 2012; Mesri and Altieri, 1998; Pitanga et al., 2014; Terrisse et al., 2010). These contrasting reports suggest that NMVs exert a pro- or anti-inflammatory response dependent on the target cell.

1.6.2 Neutrophil-derived microvesicles and endothelial dysfunction

NMVs are emerging to be inflammatory mediators that increase vascular permeability (Mesri and Altieri, 1999, 1998) in endothelial cell lines, including human umbilical vein endothelial cells (HUVECs) and human coronary artery endothelial cells (HCAECs) (Dalli et al., 2008; Gomez et al., 2020). NMVs activate the JNK1 pathway leading to increased endothelial cell activation (Mesri and Altieri, 1999). Furthermore, miRs in NMVs can increase inflammation by targeting a negative regulator of NF-κβ pathway, leading to increased expression of adhesion molecules in HCAECs, leading to endothelial dysfunction in HCAECs (Gomez et al., 2020).

Activated neutrophils from patients suffering from sepsis, which is a systemic inflammatory response to an infection can produce higher levels of NMVs with increased levels of adhesion molecule expression (Fujimi et al., 2002). Sepsis is often characterised by an impaired immune response as well as endothelial dysfunction (Wheeler and Bernard, 1999). The septic environment contains a variety of neutrophil stimulators, such as inflammatory cytokines, bacteria and bacterial by-products which may induce heightened production of NMVs. These studies demonstrate that NMVs play a role in endothelial activation, which may result in endothelial dysfunction.

NMVs can induce upregulation of inflammatory gene expression, including pro-inflammatory cytokines such as IL-6 and IL-8, leading to cell injury *in vitro* (Mesri and Altieri, 1998; Pitanga et al., 2014). Additionally, NMVs can bind to endothelial cells via CD18, leading to increased

expression of adhesion molecules such as ICAM-1 along with increased ROS production (Hong et al., 2012). Interestingly during leukocyte extravasation, NMVs are deposited at the basement membrane where they can regulate vascular integrity (Lim et al., 2013). Moreover, inhibition of NMV formation dramatically increases vascular leakage, suggesting that NMVs play a role in maintaining vascular integrity. While several reports have shown that NMVs play a role in modulating the integrity of the endothelial barrier, to date no studies have studied the interaction of NMVs with brain endothelial cells.

1.6.3 Neutrophil-derived microvesicles and brain endothelial cells

Patients with dementia have significantly higher levels of circulating neutrophils than non-neurological control patients (Shad et al., 2013). However, to date, no study has reported NMV levels in dementia patients. Analysis of the NMV-induced genetic and proteomic changes induced in HUVECs suggest NMVs modulate expression of a number of immune and immune-modulatory genes, including upregulation of cytokines and chemokines (Dalli et al., 2013). These findings suggest that NMVs have the ability to modulate gene expression changes in endothelial cells. Interestingly, platelet-derived MVs from MS patients significantly increase BBB permeability *in vitro*, demonstrating their role in breakdown of BBB (Marcos-Ramiro et al., 2014). MVs from activated monocytes contain miRNAs that trigger a NF-κB mediated inflammatory response and increased expression of adhesion molecules in brain endothelial cells (Dalvi et al., 2017). Inhibition of extracellular vesicle release can reverse endothelial activation, leading to reduction in inflammation, demonstrating that peripheral immune cells have the ability to modulate CNS inflammation. To date, research has focused on the interaction of NMV with peripheral endothelial barriers, however, as the brain endothelium has unique properties studies investigating the impact of NMVs on BBB function are needed. Such studies will further aid in understanding how systemic inflammation can modulate disease progression.

1.7 Hypothesis

While significantly higher levels of circulating neutrophils have been identified in patients with cognitive impairment, neutrophil extravasation is not a feature of the neuropathology of dementia. How neutrophils impact dementia and the mechanism of this interaction is currently unknown.

We hypothesise that NMVs interact with cerebral endothelial cells inducing BBB dysfunction and upregulating the neuroinflammatory response, thereby contributing to white matter damage in the ageing brain.

1.7.1 Aims of the project

1. To determine if NMVs interact with human cerebral microvascular endothelial cells *in vitro*. Specifically, NMVs will be incubated with hCMEC/D3 and the interaction/internalisation assessed using confocal imaging and flow cytometry. This study also aims to identify the mechanism of NMV internalisation by employing specific pathway inhibitors.

2. To assess the impact of the NMV internalisation on the integrity of the hCMEC/D3 monolayer. Permeability will be assessed by measuring the trans-endothelial electrical resistance (TEER) and permeability of the tracer molecule FITC-dextran (10kDa) across a transwell system.

3. To profile NMV-induced changes in the transcriptome of hCMEC/D3 cells by microarray analysis, and identify NMV-induced changes in key pathways and functional groups.

4. To characterise the transcriptomic profile of microvessels in age-associated WML and identify specific BBB-associated gene expression changes which may contribute to lesion pathogenesis.

Chapter 2: Interaction of neutrophil-derived microvesicles with hCMEC/D3 cells

2.1 Introduction

Neutrophils play a role in several inflammatory conditions such as rheumatoid arthritis, cystic fibrosis and atherosclerosis (detailed reviews in Gifford and Chalmers, 2014; Mócsai, 2013; Wright et al., 2014), yet the role of neutrophils in neurodegenerative diseases such as AD is relatively unexplored. In transgenic mouse models of AD, depletion of neutrophils is associated with a reduction in AD neuropathology and improved cognition (Zenaro *et al*., 2015). Dementia patients have significantly increased levels of neutrophils compared to healthy age matched non-neurological controls (Shad *et al.,* 2013), and neutrophils from AD patients display a pro-inflammatory, hyperactive phenotype that is associated with cognitive decline, suggesting that neutrophils have the ability to modulate changes in CNS (Dong et al., 2018). However, to our best knowledge, the mechanism of how these circulating neutrophils impact cognitive decline in dementia patients is currently unknown.

There are various mechanisms by which neutrophils and other immune cells exert their effect, depending on their target cells. One mechanism is by releasing MVs, which play a role in cell-cell communication. Neutrophils release MVs into the circulation in response to various stimuli such as viruses, bacteria and their by-products, shear stress and cytokines. NMVs can act directly as inflammatory mediators and modulate changes in vascular permeability in endothelial cells (Mesri and Altieri, 1999, 1998), including human umbilical vein endothelial cells (HUVEC) (Dalli et al., 2008), human coronary artery endothelial cells (HCAEC) (Gomez et al., 2020) and epithelial cells (Slater et al., 2017). NMVs either directly bind to the endothelial cells, causing activation and stimulating pro-inflammatory cytokine release (Mesri and Altieri, 1998), or they release their contents causing endothelial cell activation and cell injury (Pitanga et al., 2014). Although NMVs have been shown to interact with endothelial cells, their interaction with brain endothelium is unexplored.

Various sources of brain endothelial cells have been reported in the literature to model the BBB *in vitro.* Ideally, primary human cerebral microvessel endothelial cells are the best choice to study the BBB, however isolating these cells is challenging. There are some commercially available sources of primary brain endothelial cells, but these are expensive and lack detailed information

regarding the brain tissue source. Alternative models of the BBB can be created from cells derived from stem cells, including pluripotent stem cells and cord blood-derived stem cells. Pluripotent stem cells can be obtained from either human blastocysts or can be induced by reprogramming somatic cells (Takahashi et al., 2007; Takahashi and Yamanaka, 2006; Thomson et al., 1998). This method requires a co-differentiation protocol where the cells are treated with unconditioned and then conditioned media, forcing them to differentiate to endothelial progenitor cells (Lippmann et al., 2012), which have the ability to form a pure monolayer and develop tight junction proteins with expression of claudin-5, occludin and ZO-1. Stem cell-derived brain endothelial cells are known to have higher transendothelial electrical resistance (TEER) values, which is a measure of electrical resistance between two cells. Stem cell derived brain endothelial cells have a TEER of ~250 Ωcm^2, but this can exceed 1000 Ωcm^2 when co-cultured with other component cells of the BBB, such as astrocytes (Lippmann et al., 2012). Cord-derived brain endothelial cells also express tight junction proteins and have a TEER above 150 Ωcm^2. However, much more detailed characterisation of these stem cell derived models is required. Another drawback is that the protocol to obtain endothelial cells from stem cells is quite lengthy. To overcome these issues, various cell lines have been developed, including one of the most widely reported human cerebral microvascular endothelial cell lines, hCMEC/D3, which was developed in 2005 (see ***Table 2. 1***) hCMEC/D3 cells express various endothelial cell markers including CD34, CD40 and CD144 (Weksler et al., 2013), tight junction proteins, including claudins and occludins, and scaffolding proteins such as ZO-1 (Afonso et al., 2008; Weksler et al., 2013), with levels decreasing under pro-inflammatory stress (Forster et al., 2008). This cell line has been extensively used to study brain endothelial cell permeability using tracer molecules such as lucifer yellow, low and high molecular weight dextrans (Poller et al., 2008; Weksler et al., 2005).

Based on this evidence, the current *in vitro* research was carried out using hCMEC/D3 cells to study the interaction of NMVs with human brain endothelial cells and to determine the mechanism of internalisation.

Table 2. 1 Characteristics and limitations of commercially available human immortalised brain endothelial cells

Brain endothelial cell lines	TEER ($\Omega.cm^2$)	Year	Limitation	References
hCMEC/D3	20 - 40	2005	Low TEER under routine culture; loss of TJ characteristics after P35	(Weksler et al., 2005)
HBMEC	N/A	2001	Limited passages	(Stins et al., 2001)
BB19	N/A	1996	N/A	(Kusch-Poddar et al., 2005; Prudhomme et al., 1996)
NKIM	100	2007	No data available on expression of various transporters	(Ketabi-Kiyanvash et al., 2007)
HBMEC/ciβ	2-20	N/A	Not extensively characterised	(Furihata et al., 2015)
TY10	45	2013	Low occludin expression	(Maeda et al., 2013; Sano et al., 2013)

2.2 Aims and Objectives

Studies in transgenic mouse models of AD have suggested that neutrophils play a role in driving cognitive decline in AD (Zenaro et al., 2015), and demonstrated that depletion of neutrophils leads to improvement of memory in mice that already show signs of cognitive impairment. Although levels of NMVs in dementia patients have not been the focus of research, given that circulating levels of neutrophils are significantly higher in dementia patients and that cognitive function rapidly declines during an infection, we hypothesise that NMVs are internalised by human brain endothelial cells, decreasing vascular integrity and increasing their permeability. Specifically, this chapter aims to:

- Determine if NMVs interact with and are internalised by the human cerebral microvascular endothelial cell line hCMEC/D3.

- Investigate the mechanism of internalisation of NMVs by hCMEC/D3 cells using chemical inhibitors of specific pathways.

2.3 Materials and Methods

2.3.1 Volunteer Information and Ethics

Healthy volunteers aged between 18-45 were recruited for this study. Prior to the commencement, ethical approval was obtained from the University of Sheffield Research Ethics Committee (see appendix I). Participants were provided with a detailed information sheet outlining the aims of the research, what the study involved and their rights. Volunteers were also informed not to give blood if they have any known chronic or acute medical conditions are if they are taking any medication that may affect leukocyte function. Consent was taken after 24 hours and a signed copy the consent form was provided to the participants and to the University. All subjects were healthy with no known anomalies. Blood withdrawal was performed by a trained phlebotomist. Participants were asked about their general health on the day of donation and no temperature was taken. Full blood count, erythrocyte sedimentation rate and CRP were not performed on any of the donation to determine the inflammatory status of the donor.

2.3.2 Human Neutrophil Isolation

The neutrophil isolation method used for the experiments was based on that described by Haslett et al., (1985) with some modifications. Care was taken throughout to avoid changes in temperature, introduction of bubbles and long incubation periods in order that neutrophils remained as inactivated as possible. Approximately 36 mL of venous blood was taken from healthy donors and collected in a tube containing 4 mL of anti-coagulant sodium citrate (3.8 mg/mL; Sigma). The tube was centrifuged at 260 *g* for 20 mins with acceleration 5, brake 0 at room temperature (RT). Plasma was discarded and 6 mL of 6% dextran (Sigma-Aldrich, USA; 1.5 mL/10 mL blood) at RT was added to the remaining cells and made up to 50 mL using sterile saline. Dextran enables the sedimentation of red blood cells to the bottom of the tube. The tube was gently inverted ten times, avoiding the production of any bubbles. The cap was replaced, and the tube was left to sediment for 30 minutes at RT. In a fresh tube, 16 mL of Histopaque 1077 (Sigma, UK) was added and left to warm to RT. Histopaque 1077 allows separation by density gradient (Swamydas and Lionakis, 2013). After 30 minutes, the leukocyte rich layer was removed from the dextran and gently layered over 16 mL of Histopaque (4mL/ 10 mL blood), ensuring a well-defined separated layer. The solution was made up to 50 mL using sterile saline and centrifuged at 400 *g* for 25 minutes (acceleration 5, brake 0) to pellet the neutrophils. The PBMC layer was carefully removed and red blood cells present in the neutrophil rich pellet were exposed to hypotonic lysis buffer (0.6% NaCl)

by adding 1 mL and gently resuspending. The solution was made up to 25 mL using the hypotonic solution and was gently inverted for 30–45 seconds. Exposure to the hypotonic solution was strictly monitored to avoid lysing of neutrophils. 25 mL of hypertonic solution (1.6% NaCl) was added to make a final volume of 50 mL and inverted once. The tube was centrifuged at 250 *g* for 7 minutes at acceleration 5, brake 3. The supernatant was discarded and 10 mL of Roswell Park Memorial Institute (RPMI) medium (Fisher Scientific, US) was added to the tube. 10 µL of suspension was removed and added into 90 µL of RPMI media in a 1.5 mL tube for cell counting and the remaining cell suspension was centrifuged at 250 *g* for 7 minutes to pellet neutrophils. The cell count was determined using a haemocytometer with the following formula.

No. of neutrophils = $\frac{No.from\ haemocytometer}{4}$ ×Dilution Factor × Volume of RPMI = X × 10^4 neutrophils

2.3.3 Neutrophil- derived microvesicle preparation

NMVs were prepared using the method described by Nolan et al., (2008) with slight modifications. Isolated neutrophils were resuspended in phosphate buffered saline (PBS) supplemented with Calcium (Ca^{2+}) and Magnesium (Mg^{2+}) (1ml/10 million neutrophils) as calcium influx into the cell is essential for MV formation (Pasquet et al., 1996). Cells were stimulated using N-Formyl-L-methionyl-L-leucyl-L-phenylalanine (fMLP) (5 ×10^{-5} M) or an equal volume of PBS as a control. The tubes were incubated for 1 hour at 37ºC, 5% CO_2 with gentle inversion every 15 minutes to prevent sedimentation. The tubes were spun at 500 *g* for 5 minutes to remove the cells. The supernatant was removed and placed in fresh tubes and then centrifuged at 2000 *g* for a further 5 minutes to ensure effective removal of contaminating cells and/or cell debris. The supernatant was placed in fresh tubes and centrifuged for 20,000 *g* for 30 minutes. The pellet was stored at -20ºC until required.

2.3.4 Assessing cellular contamination of neutrophil isolation

Morphological characterisation of isolated cells using Quik-Diff (Merck, UK) was carried out to analyse the purity of the neutrophil isolation. After suspending neutrophils in PBS+ Ca^{2+}+Mg^{2+} (10 million per 1 mL), 10 µl of the suspension (100,000 neutrophils) was diluted in 1% BSA/PBS (1:10). The suspension was transferred onto a coated, charged microscope slide using a Cytospin centrifuge (300 *g* for 4 mins) and fixed using Quik-Diff fixative reagent 1 for 3 minutes. The cells were stained using Quik-Diff reagent 2 for 3 minutes and counterstained in Quik-Diff reagent 3

for 3 minutes. The slides were rinsed in tap water to remove excess stain and left to dry overnight before viewing under a brightfield microscope x10 magnification. Ten random areas on the slide were imaged and quantitative analysis was performed using Image J software by counting the number of different type of cells in each image.

Similarly, after second centrifugation of NMV to remove cells and cellular debris (for detailed description see section 2.3.3), 20 µl of supernatant was added to 80 µl of 1% BSA/PBS and transferred to a microscope slide using the method mentioned above. After drying the slides were analysed under a brightfield microscope for assessing cellular contamination.

2.3.5 Zetaview potential (Nanoparticle tracking analysis)

To assess the sizes of NMVs, Zetaview PMX110 Nanoparticle Tracker Analyzer (Particle Metrix, Germany) was used. This method utilises both Brownian motion to calcite particle size and micro-electrophoresis to calculate zeta potential. NMVs were suspended in milliQ water (diluted 1:50 and 1:200). Videos were recorded and images were taken, and the cycle was repeated 3 times to determine diameter and the range. The frame rate was set to 3.75 frames/second and shutter speed of 70. Measurements were taken at 11 positions in the cell. This allowed to determine distribution of particle size in the sample. The cell chamber was rinsed between samples to ensure it is cleaned and no residue can interfere with the results. Data was analysed using Particle Metrix software (ZetaView 8.03.08.03) and Microsoft 367 Excel 2010 (Microsoft Corp., USA)

2.3.6 Activation assay for isolated neutrophils

To assess the activation status of the neutrophils throughout the isolation process, an activation assay was performed. Neutrophils express various glycoproteins that are differentially expressed during their life span. Changes in expression of these surface receptors can be used to assess the activation status of neutrophils (Fortunati et al., 2009). Upregulation of CD11b, CD18, CD66b and down-regulation of CD62L are markers regularly used to study the activation status of neutrophils (Mann and Chung, 2006). In this study, PE-CD18, FITC- CD66b and CD62L (for details see ***Table 2. 2***) were used. Approximately 1ml of whole blood was removed from the 50 ml tube at the start of the isolation procedure (see section 2.3.2)., and 100 µl of whole blood was placed in sterile 5 mL centrifugation tubes with the appropriate concentration of antibodies (See Table 2.1) and incubated on ice for 30 minutes. 2 ml of 1% BSA/PBS solution was added and the tubes centrifuged at 300 *g* at 4ºC for 6 minutes. To lyse the red blood cells, 2 ml of red blood cell lysis buffer was added and the tubes were incubated at RT for 10 minutes. 6 ml PBS was added and

centrifuged at 500 *g*, 5 mins. The pellet was resuspended in 0.5 ml PBS. Incubation with antibody was repeated before stimulation of neutrophils with fMLP and after 1 hr incubation with fMLP (see section 2.3.3) to demonstrate that neutrophils are stimulated by fMLP.

Table 2. 2 Panel of antibodies and concentration used to characterise neutrophil activation.

Panel of Antibodies	Antibody Supplier	Cat Number	Isotype	Clone	Concentration
PE-anti-human CD18	ThermoFisher Scientific	11-0189-42	Mouse IgG_1	6.7	1 µg/mL
FITC-anti-human CD66b	Biolegend	305103	Mouse IgM	G10F5	0.5 µg/mL
PE-anti-human CD62L	BD Bioscience	555544	Mouse IgG_1	DREG-56	1 µg/mL

2.3.7 Trypan blue exclusion and propidium iodide staining of neutrophils

Trypan blue is a cell impermeable stain, enabling the differentiation between live and dead cells. Live cells exclude the dye, as the dye itself is charged and cannot enter a cell. However, when the cell membrane is compromised the stain is readily taken up, thereby allowing the differentiation between live and dead cells. After stimulation of neutrophils with fMLP for 1h, cells were resuspended to 1×10^7 neutrophils/mL. 10 µl of the sample was added to 90 µl of PBS in a 1.2 ml Eppendorf and 50 µl of this sample was resuspended with 50 µl of 0.4% trypan blue solution and number of trypan blue$^+$ cells counted using a haemocytometer.

An alternative method to assess live/dead cells is using propidium iodide (PI) staining followed by analysis using a flow cytometer. PI is a DNA intercalating dye, and can bind to fragmented DNA, which is one characteristic of an apoptotic cell (Riccardi and Nicoletti, 2006). After stimulation with fMLP for 1h, neutrophils were pelleted and resuspended in 1×10^7 neutrophils/mL. A million neutrophils were resuspended in 100 µl PBS with 1µl PI (1 mg/mL) for 5 minutes in the dark and the viability of neutrophils were analysed using flow cytometry.

2.3.8 Fluorescent Labelling of neutrophil-derived microvesicles

Cell tracker kits with membrane intercalating dyes were used according to manufacturer's instructions (Sigma- Aldrich, USA) to fluorescently label NMVs. Pelleted NMVs were resuspended in 100 µL Diluent C. Ensuring the lights of the laminal hood were turned off, 100 µL of Diluent C was mixed with 1.5 µL of PKH67 or PKH26 in a fresh tube. This mixture was quickly added to vesicles and incubated for 3 minutes at RT. 1% w/v bovine serum albumin was added to stop the reaction. The tubes were centrifuged at 25,000 *g* for 30 minutes at 4°C. The supernatant was discarded, and the pellet protected from direct light by wrapping it in aluminium foil and stored at -20ºC until required.

2.3.9 Quantification of Neutrophil-derived microvesicles by flow cytometry

Flow cytometric analyses were performed with the BD LSRII flow cytometer (BD Biosciences, UK) using settings calibrated with Megamix beads (BioCytex, France), adapted from Robert et al., (2009). To gate out background noise, fluorescently labelled beads of different sizes (3 µm, 0.9 µm and 0.5 µm) were used. Initially, Forward Scatter Area (FSC-A) versus forward Scatter

Width (FSC-W) were used to eliminate the background of the machine and discriminating doublet population.

The first gate was set up to analyse the fluorescence threshold to avoid the machine noise and/or debris and to identify all the bead subsets. (***Figure 2. 1*** **A**). Fluorescence threshold was switched to forward scatter (FS) and the voltage was adjusted such that the ratio between 0.5 um and 0.9 um beads were 50%:50%. The MV gate was defined using 0.9 µm beads as the upper limit for both forward scatter and side scatter (***Figure 2. 1*** **B**). Counting bead population and MVs were gated using FS-Area v SS-A (***Figure 2. 1*** **C**). Finally, the % of labelled versus non-labelled MVs were discriminated using the blue laser (***Figure 2. 1*** **D**).

To count the number of NMVs, the pellet was resuspended in 0.5 mL PBS. In a new tube, 270 µL fresh PBS, 20 µL of resuspended sample and 10 µL of Sphero AccuCount Blank Particles (2.0 µm; Saxon Europe, England) were added. The bead population was gated, and the experiment set up to count 1000 beads. The number of NMVs were calculated using the equation below:

$$\text{No. of MV/ul} = \frac{No.of\ MV\ events}{No.of\ counting\ events\ (1000)} \times \frac{Total\ No.of\ Counting\ beads\ in\ the\ test\ sample}{Final\ volume\ used\ for\ analysis}$$

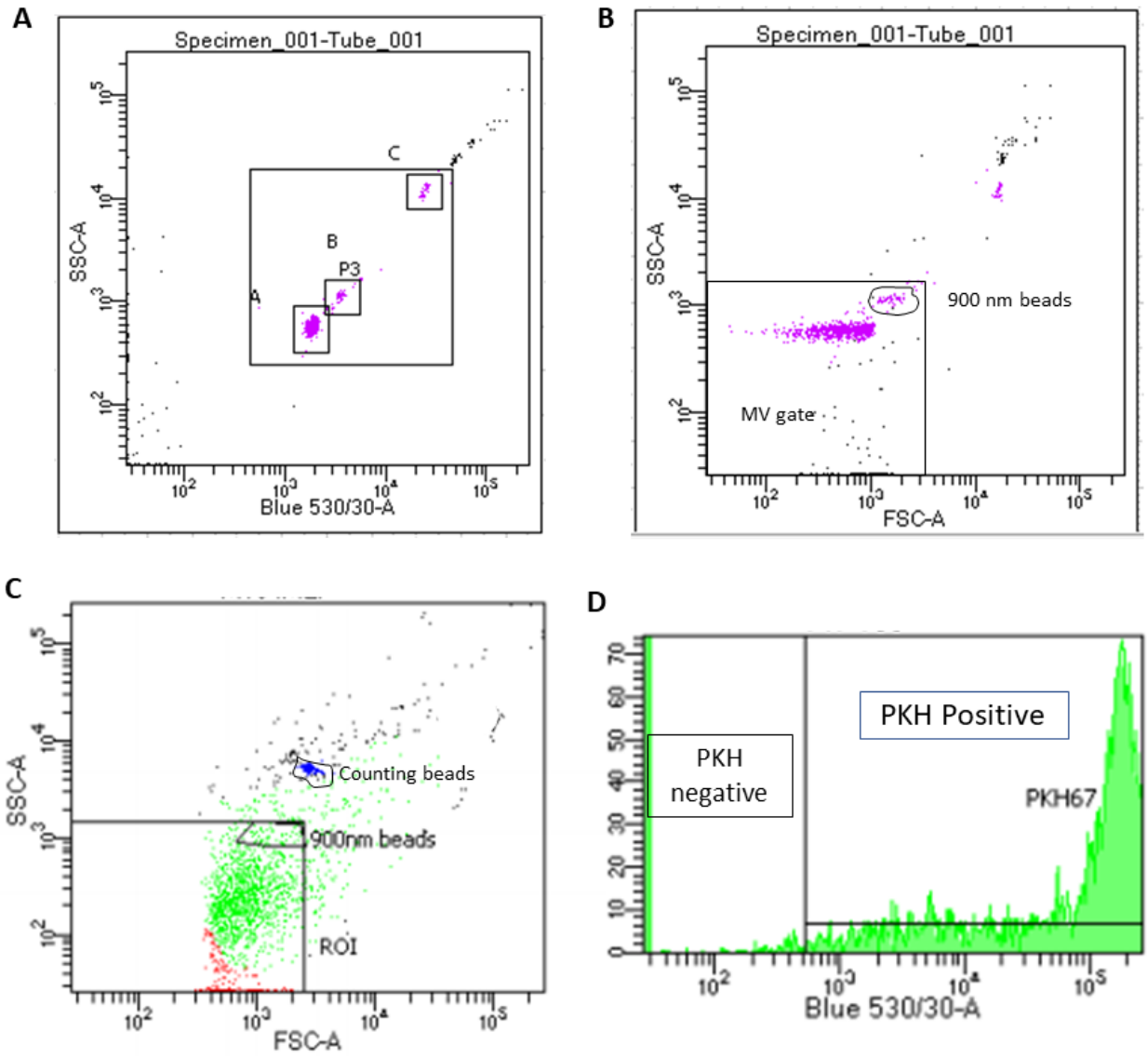

Figure 2. 1 Representative diagram of Megamix bead setup to count NMV using flow cytometry. Megamix beads contains three different bead population, 500 nm , 900 nm and 3 µm. **(A)** Fluorescently labelled bead populations were identified on the flow cytometer using side scatter area. Populations were labelled as A (500 nm), B (900 nm) and C (3 µm). **(B)** MV gate was identified using 900 nm beads, with the events below the 900 nm region representing MVs which range between 100- 1000 nm in diameter. **(C)** For counting MVs, Sphero AccuCount Blank Particles of 2 µm size were gated and 1000 events in this gate counted. **(D)** When MVs were fluorescently labelled, there was a shift in fluorescence, enabling the positive and negative populations to be identified using the gating strategy.

2.3.10 hCMEC/D3 cell culture

The hCMEC/D3 cell line was obtained from Cedarlane, Canada and cultured in EBM-2 medium supplemented with 2.5% FBS, vascular endothelial growth factor (VEGF), insulin-like growth factor-1 (IGF-1) human epidermal growth factor (hEGF), human basic fibroblast growth factor (hFGF), hydrocortisone and ascorbic acid (medium and single supplements -all EGM-2 MV bulletkit, Lonza, Switzerland). All the growth factors (VEGF, IGF-1, hEGF and hFGF) were pooled together and aliquoted into 10 tubes, with each containing 87.5 µl. This was added to 50 ml of aliquoted media as growth factors degrade in the medium. The cells were grown on flasks or plates coated with Collagen- type I from rat tail (150 µg/ml; Sigma, UK). All experiments were performed between passages 26 -35.

2.3.10.1 Sub-culture and Maintenance of hCMEC/D3

When cells reached 80—90% confluency, they were split into new flasks. The media was aspirated and the cells were rinsed with 10 mL of PBS at RT. The cells were incubated at 37ºC with 4 mL of 1× trypsin-EDTA solution (Sigma-Aldrich, USA) for 5 minutes. The flask was examined under the microscope and when ~90% cells were rounded up, the bottom of the flask was tapped gently to detach the cells. The trypsin was neutralised with 6 mL of media. The cells were transferred into a 50 mL centrifuge tube., and the flasks rinsed thoroughly with 10 mL of PBS which was then transferred into the same tube. The tube was centrifuged at 650 *g* for 6 minutes at RT. The supernatant was aspirated and the pellet re-suspended in an appropriate amount of medium ensuring a uniform suspension. 10 µL of resuspended cells were added to a sterile Eppendorf tube containing 90 µL of media, for cell counting. The cell number was determined using a haemocytometer and was calculated using the following formula:

No of cells/mL = Average count from each of the sets of 16 corner squares × 10 (dilution factor) × 10,000

The flasks were split in a 1:3 ratio. The cultures were maintained in an incubator at 37ºC in 5% CO_2 and half media feed was performed every 2 days.

2.3.11 Image Analysis by Confocal Microscopy

hCMEC/D3 (40,000 cells/well) were grown on 13-mm coverslips coated with collagen-I (Sigma-Aldrich, USA) in acetic acid solution (0.05 mg/ml) and were grown to confluence (3-4 days). The cells were incubated with PKH-26 labelled microvesicles for 2h. After the incubation, the cells were fixed with 4% paraformaldehyde (PFA) for 13 minutes and permeabilised using 0.1% Triton-X for 3 minutes. Non-specific binding was blocked by 1% BSA/PBS solution for 30 minutes before staining. The coverslips were incubated with FITC-phalloidin (1:500) for 40 minutes at RT and washed twice with PBS. The nuclei were counterstained using TO-PRO-3 iodide (1:500) for 15 mins at RT. The cover-slips were then washed, patted dry and mounted using Prolong gold mounting media onto a slide before visualisation using a confocal microscope, Inverted Zeiss LSM 510 NLO microscope (Zeiss, Germany).

For co-localisation experiments, hCMEC/D3 were grown as described above and were incubated with PKH-67 labelled microvesicles for 2h. After the incubation, the cells were fixed with 4% paraformaldehyde (PFA) for 15 minutes and permeabilised using 0.1% Triton-X for 3 minutes. Non-specific binding was blocked by 3% BSA/PBS solution for 30 minutes before staining. The coverslips were incubated with EEA-1 antibody (SC-365652; 5µg/ml; SantaCruz Biotechnology) overnight at 4°C. Following 3 washes with PBS to remove unbound antibody, the coverslips were incubated in alexaflour 565 (1:500) for 1h. The coverslips underwent 3 washes with PBS and nuclei were counterstained with Hoescht nuclear dye (1 µg/mL; Sigma). All ICC runs included appropriate controls to confirm the specificity of the staining pattern observed, namely omission of the primary antibody and an isotype control. Localisation of NMV was visualised using a Zeiss LSM 880 with airyscan confocal microscope and images were obtained using Zeiss Leica software.

2.3.12 Analysis of Internalisation of NMVs by hCMEC/D3

To determine if NMVs are internalised by hCMEC/D3, flow cytometric analysis was used. hCMED/D3 were incubated with PKH-67 positive NMVs at various concentrations- 30 NMV/µl, 300 NMV/µl and 3000 NMV/µl for 2h. The cells were detached using trypsin and pelleted at 650g for 6 mins. The pellet was resuspended in 500 µl PBS and kept on ice. Just before the sample was run on the flow cytometer, 100 µl of 0.4% trypan blue (Sigma-Aldrich, USA) was added. Trypan blue quenches fluorescence emitted by green fluorochromes, however all internalised NMVs will not be exposed to the dye and remain green, thereby allowing precise quantitative analysis of NMV

internalisation. This method ensures that any NMVs that adhere to the outside of the cells are not quantified and only the cells that have internalised NMVs will produce a signal and is routinely used to distinguish between internalised and non-internalised particles (Fattorossi et al., 1989). The analysis including gating and sorting were set up using BD FACSDiva software and BD LSRII flow cytometer (BD Bioscience, UK).

2.3.12.1 Internalisation of NMVs by hCMEC/D3

To perform this experiment, 300 NMV/µl was chosen as the concentration for all the experiments henceforth. The cells were treated and collected as described in section 2.3.10.1. The data was analysed using FlowJo software (FlowJo Vx 0.7).

2.3.13 Identification of pathways associated with the internalisation of NMV by hCMEC/D3

To understand if NMV internalisation is energy dependent rather than passive, hCMEC/D3 were co-incubated with NMV (300 NMV/µl) at 4°C for 2h. Furthermore, to determine if the internalisation is through receptor-mediated internalisation, and if this is a calcium dependent process, hCMEC/D3 were incubated with EDTA (Ethane-1,2-diyldinitrilotetraacetic acid), a common calcium chelating agent. To decipher the major pathway of internalisation of NMV by hCMEC/D3, various pharmacological inhibitors were utilised. hCMEC/D3 were cultured in 24 well plate and grown to confluence. The cells were pre-treated with the following inhibitors Monodansylcadaverine (150 µM), Genistein (100 µM), 5-(N-Ethyl-N-isopropyl)amiloride (50 µM), Dynasore (1 µM), Wortmannin (1 µM), Cytochalasin D (10 µM) (for further details see ***Table 2. 3***)

Table 2. 3 Inhibitors used to decipher the pathway of internalisation of NMV by hCMEC/D3.

Inhibitor	Pathway Inhibited	Condition
Monodansylcadaverine (MDC)	Clathrin dependent endocytosis	1 hr pre- incubation and kept in the medium with NMV
5-(N-Ethyl-N-isopropyl) amiloride (EIPA)	Macropinocytosis (Na^+/H^+) exchanger	0.5 hr pre-incubation with serum starvation; kept in the medium with serum along with NMV
Genistein	Caveolae dependent endocytosis	1 hr pre incubation
Wortmannin	PI3- Kinase pathway	1 hr pre- incubation
Cytochalasin D	Actin elongation and polymerisation	0.5 hr pre-incubation and kept in the medium with NMV
Dynasore	Dynamin	1 hr pre-incubation
EDTA	General calcium uptake	2 hrs in the medium with NMV
Proteinase K	General surface interaction	0.5 hr pre-incubation
Incubation at 4°C	Energy-dependent internalisation pathways	N/A

2.3.12.1 Dose-dependent cell viability of pathway inhibitors

Pharmacological inhibitors used are toxic in higher concentrations to the endothelial cells. To determine the safe dose for hCMEC/D3, the cells were treated with various increasing doses for 3 hours. Since the inhibitors were dissolved in DMSO, equal %DMSO (ranging from 0.1% - 1%) was added to the DMSO control as DMSO is toxic to cells. Cell death was analysed using trypan blue method as described in section 2.3.6 after 3 hours.

2.3.13.1 Inhibition of microvesicle internalisation in hCMEC/D3

Each inhibitor dose was selected after analysing cell viability. The dose at which 95% of cells were viable was selected for the inhibition experiments. Since EDTA causes cells to detach and round up, the dose at which the cell shape was not changed was selected. For further details on the conditions and the concentrations under which hCMEC/D3 were treated see ***Table 2. 3***.

2.3.14 Role of Inflammation in internalisation of NMVs

2.3.14.1 Role of pro-inflammatory stimuli on the internalisation of NMV

To understand if inflammation plays a role in the internalisation of NMV, hCMEC/D3 were incubated with pro-inflammatory stimuli including TNF-α or LPS. hCMEC/D3 were pre-incubated with TNF-α (10 ng/ml) or LPS (1 µg/ml) for 16h before adding NMVs for 2h.

2.3.14.2 Time-dependent expression of ICAM-1 by hCMEC/D3 after pro-inflammatory stimuli

Adhesion molecules such as ICAM-1 and VCAM-1 are upregulated by brain endothelial cells following pro-inflammatory activation. To understand the role of adhesion molecules, specifically role of ICAM-1 in the internalisation of NMVs, the optimal expression of ICAM-1 was needed. To induce the expression of ICAM-1, hCMEC/D3 were grown to confluence in 24 well plates and incubated with LPS for 4,6 and 24 h. Since ICAM-1 has surface fractions that are trypsin sensitive, 0.4% trypsin was used to detach the cell. Cells were collected into 1.5 mL Eppendorf tubes and centrifuged at 650 g for 6 mins at 4°C. The pellet was resuspended in PBS and incubated with ICAM-1 antibody. ICAM-1 expression was analysed using BD LSRII flow cytometer and data analysed on FlowJo software.

2.3.14.3 Role of ICAM-1 in internalisation of NMVs

To determine the role of ICAM-1 in the internalisation of NMVs, hCMEC/D3 (40,000 cells/well) were plated in a 24 well plate and grown to confluence. The cells were pre-incubated with LPS (1µg/ml) for 6 h followed by incubation with anti-ICAM-1 (1 µg/ml; 84H10; ThermoFisher) for

1h. The cells were washed with PBS and NMVs (300 NMV/µl) were added for 2 h. Internalisation was measured using flow cytometry, as described in section **2.3.10.**

2.3.15 Statistical Analysis

Statistical analysis was performed using GraphPad Prism analysis software. Each experiment was replicated using a minimum of three independent donors (n=3) to perform statistical analysis. Data is provided in text, tables and figures are presented as mean values and standard deviation (±SD) unless otherwise stated. Data was analysed using the applicable analyse of variance (ANOVA) or t-test. For multiple comparison, paired t-test, and one-way ANOVA with Dunnett's multiple comparison test was performed. P value <0.05 were statistically significant.

2.4 Results

2.4.1 Successful Isolation of neutrophils and microvesicles using density gradient centrifugation

The purity of the isolation of neutrophils using density gradient separation was assessed using cytospin to check for any contamination from monocytes after the lysis step. It was also performed for NMV samples after the two spins to pellet neutrophils to ensure there was no cell contamination. A Qwik-Diff staining protocol was used to distinguish various cell types. Neutrophils were identified by their distinct multilobular nuclei (***Figure 2. 2*** **A**). In the cytospin NMV samples, there were no cells present when imaged under the microscope (***Figure 2. 2*** **B**). Ten images of the slides were taken, and the mean percentage purity was calculated, demonstrating that the neutrophil purity ranged from 95% - 97% (***Figure 2. 2*** **C**).

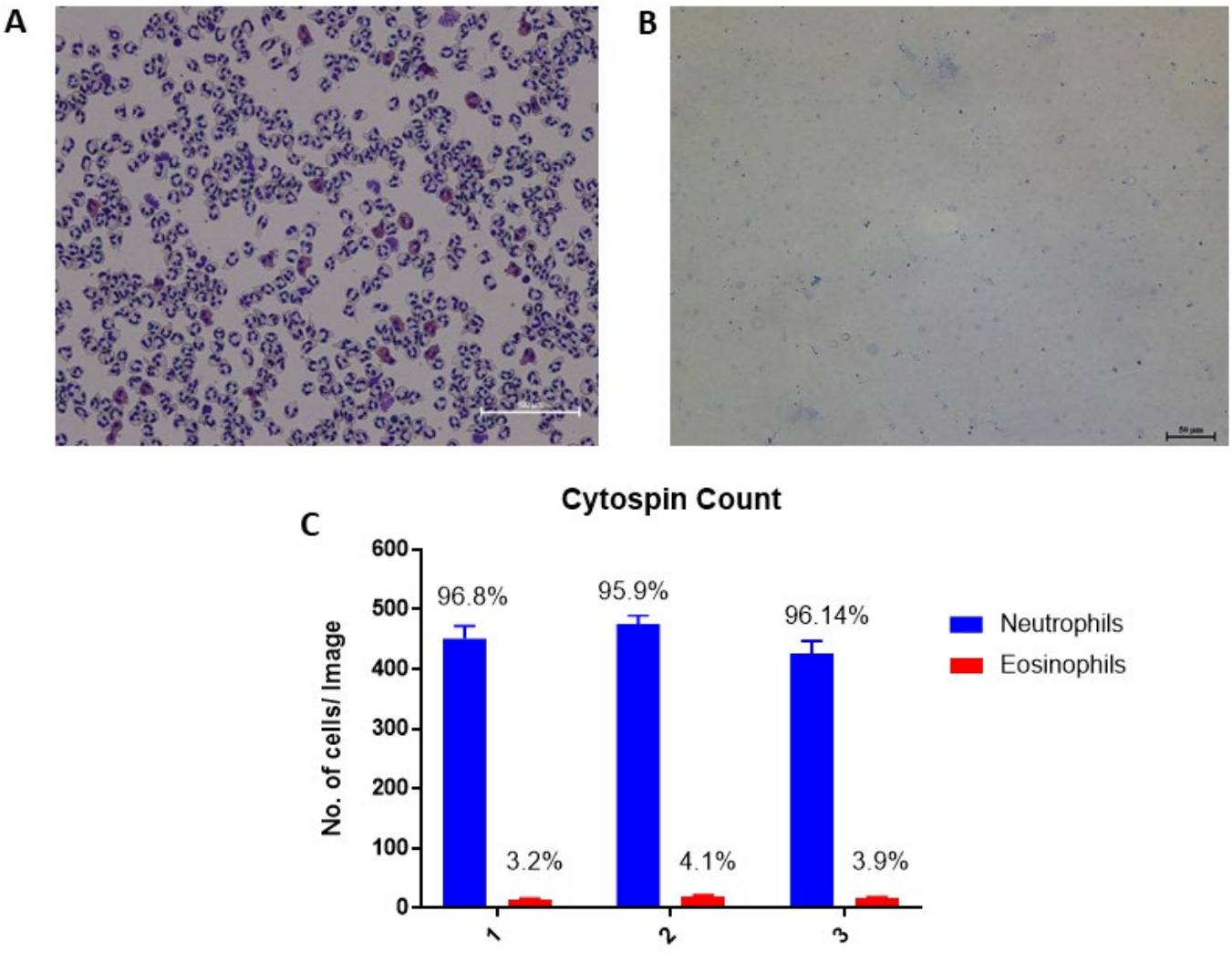

Figure 2. 2 Cytospin sample analysis. (A) Representative image of cytospin sample before activation of neutrophils. Cells were quantified using ImageJ software. **(B)** Representative image of cytospin of NMVs after centrifugation to remove pelleted neutrophils, showing no contamination with cells. **(C)** Total number of cells in 10 images taken at random at x10 magnification of each isolation was quantified and presented as mean ± SEM. 1,2 and 3 represent three independent neutrophil preparations from three independent donors.

2.4.1.1 Activation status of neutrophils throughout the isolation process

To assess the activation status of neutrophils throughout the isolation process fluorescently labelled activation markers, namely CD18 and CD62L were used. CD62L or L-selectin is shed by neutrophils when activated, while CD18 is an adhesion molecule which aids neutrophils to adhere to the endothelium. Throughout the neutrophil isolation process, the activation status of neutrophils gradually increased as demonstrated by the shift in fluorescence of CD62L and CD18 (***Figure 2. 3***). CD62L levels were higher at the start of the isolation process and decreased following activation with fMLP due to L-selectin shedding from the surface, while in contrast the levels of CD18 increased due to increased expression levels.

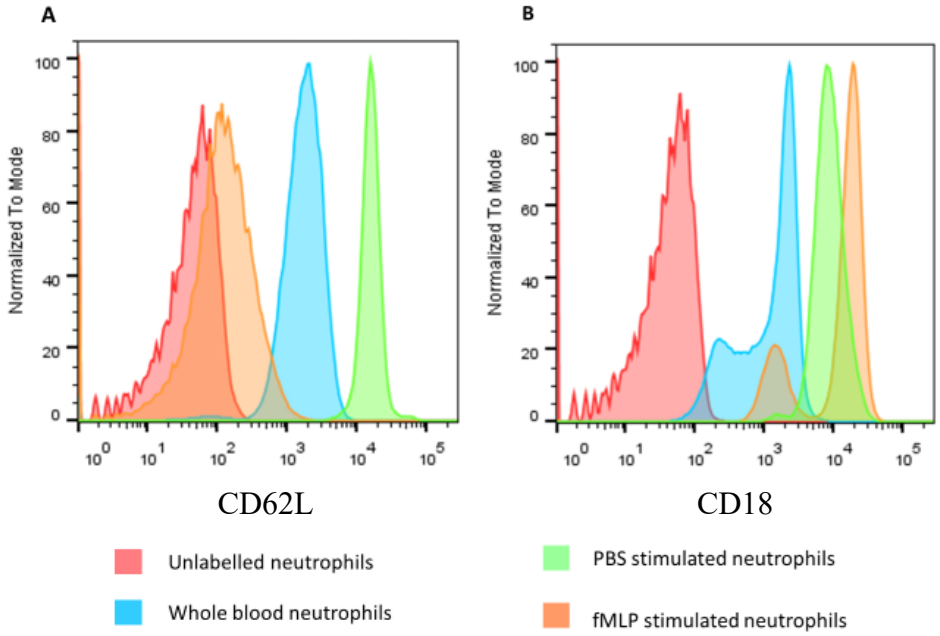

Figure 2. 3 Activation status of neutrophils during the isolation process. (A) CD62L staining of neutrophils throughout the isolation process. The shedding of L-selectin is evident by the fluorescent shifts. **(B)** CD18 staining of neutrophils throughout the isolation process. CD18 expression is increased when neutrophils are activated. Representative diagram of three independent neutrophil isolations.

2.4.1.2 Stimulation of neutrophils by fMLP

Since neutrophils can undergo oxidative burst when activated and give rise to an increase in cell death, the toxicity of fMLP and cell viability was tested using two methods: trypan blue exclusion and flow cytometry. To produce NMVs, neutrophils need to be relatively non-active before stimulation, forcing the potent production of NMVs. After stimulation with fMLP, 95.72% of neutrophils were alive when measured using trypan blue exclusion method (***Figure 2. 4A***). 96.48% of non-stimulated neutrophils (PBS control) were alive after one hour. The percentage of live cells after 1h of fMLP stimulation was statistically greater than that of dead cells ($p < 0.0001$), indicating that neutrophil stimulation with fMLP for 1h does not induce significant cell death. Neutrophil viability after stimulation was also performed using PI staining and the fluorescence was measured using flow cytometry(***Figure 2. 4B***). PI staining confirmed the results that viability of neutrophils was above 90%.

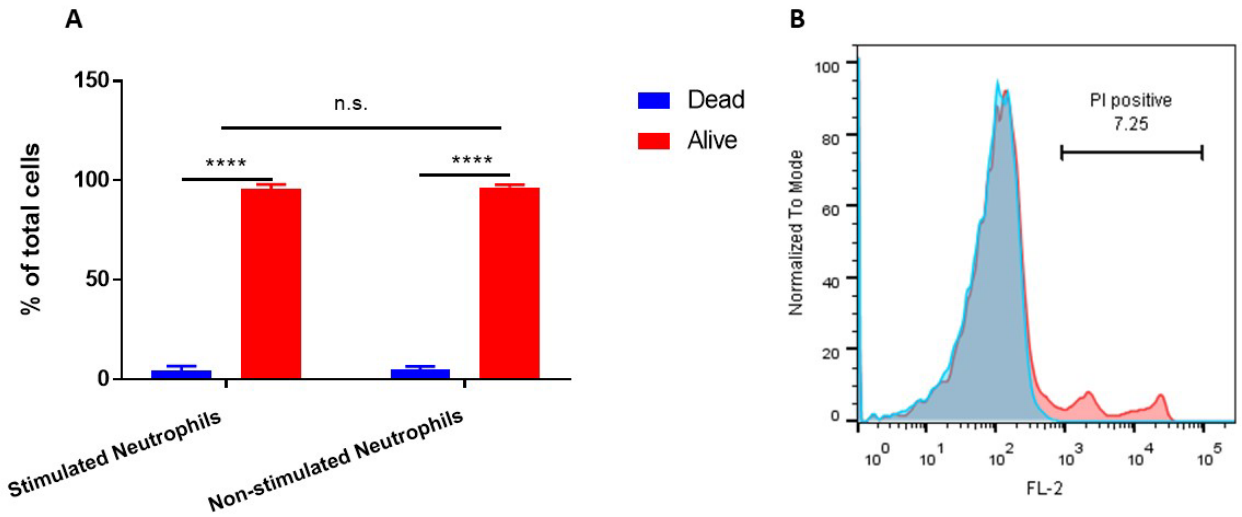

Figure 2. 4 Assessment of viability of neutrophils after fMLP stimulation. Viability of neutrophils were analysed using two methods; trypan blue exclusion and propidium iodide (PI staining). **(A)** After stimulation with fMLP for 1h, neutrophils were resuspended in 0.4% trypan blue and the dead/live cells were counted using a haemocytometer. Data represented as Mean ± SD (n=5) and were analysed for statistical significance using two-way ANOVA with multiple comparisons (**** $p < 0.0001$; n.s.- not significant). **(B)** Neutrophils were resuspended in PI dye and incubated for 15 minutes in the dark and fluorescence was measured using flow cytometry. Representative image of PI gating demonstrating that only 7% of cells took up dye, indicating apoptotic neutrophils.

2.4.1.3 Change in number of NMVs produced after stimulation of neutrophils using fMLP

Isolated neutrophils were either stimulated with fMLP or PBS as a control for 1h at 37°C. PBS acted as a negative control and although it alone cannot activate neutrophils, the isolation process itself can induce low level of activation of the cells. There were large variations in the number of isolated NMVs (for PBS stimulated 7.5 ± 2.9 $x10^9$ NMVs; for fMLP stimulated – 1.2 $x10^{10}$ ± 2.9 $x10^9$ NMVs), likely reflecting the differences in the number of neutrophils isolated from various donors. NMVs released from neutrophils stimulated with fMLP were significantly higher than non-stimulated neutrophils (P=0.02), confirming that fMLP is a potent stimulus for the production of NMVs(**Figure 2. 5**).

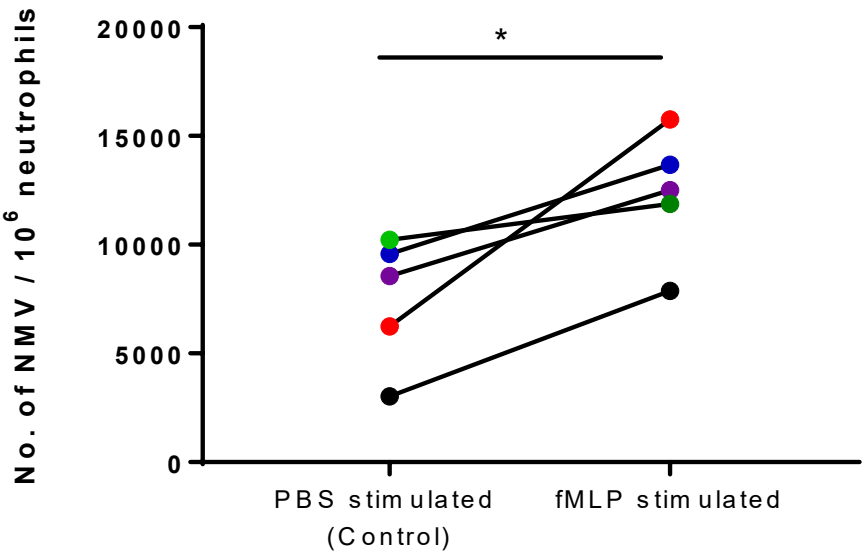

Figure 2. 5 **NMV production of PBS stimulated v fMLP stimulated neutrophils.** Neutrophils were stimulated either using fMLP or PBS as a control for 1h at 37°C. NMVs were quantified using flow cytometry and total number of NMVs were calculated. NMVs from same donors are colour matched. Data are presented as mean ± SD (n =5) and were statistically analysed for significance using a paired t-test (* p =0.0203). The colours represent the same donor.

2.4.1.4 Zeta view potential of isolated NMVs

To characterise the NMVs, Zetaview nanoparticle tracking was used and it revealed that NMV were heterogenous with a mean size of 226 nm. (***Figure 2. 6***), in agreement with the previous finding in our lab (Gomez et al., 2020). Results demonstrated 96% of the NMVs fell within the defined range of 100 – 1000 nm, demonstrating a relative pure population of NMVs. Most of the peaks were between 100 – 300 nm, suggesting that NMVs in our prep mostly range between 100 – 300 nm. This experiment was repeated twice. Furthermore, this result also confirmed that parameters set on flow cytometer agreed with the ranges of NMVs present.

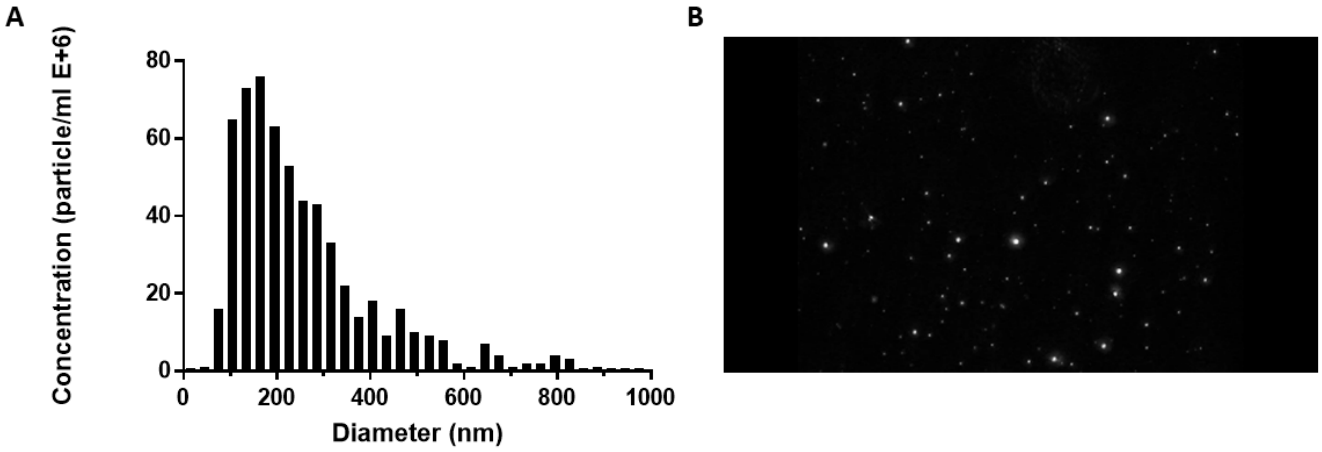

Figure 2. 6 Zetaview potential of NMVs. (A) A histogram demonstrating the range of the sizes distribution of NMVs and the highest number of particle peaks between 100- 300 nm. **(B)** Snapshot of Brownian motion by which Zetaview counts each particle.

2.4.1.5 Surface marker expression of NMVs

To characterise the NMV population, expression of surface markers was analysed using flow cytometry. CD66b is a marker expressed by neutrophils and can be incorporated into NMVs during biogenesis. CD66b expression was analysed using flow cytometer and 57.2 ± 18.87% of NMVs were labelled with CD66b (***Figure 2. 7*A**). During biogenesis of NMVs, phosphatidylserine, a plasma membrane protein found in the inner leaflet of the cell is flipped and are present on MVs. NMVs demonstrated Annexin V positivity demonstrating presence of phosphatidylserine.

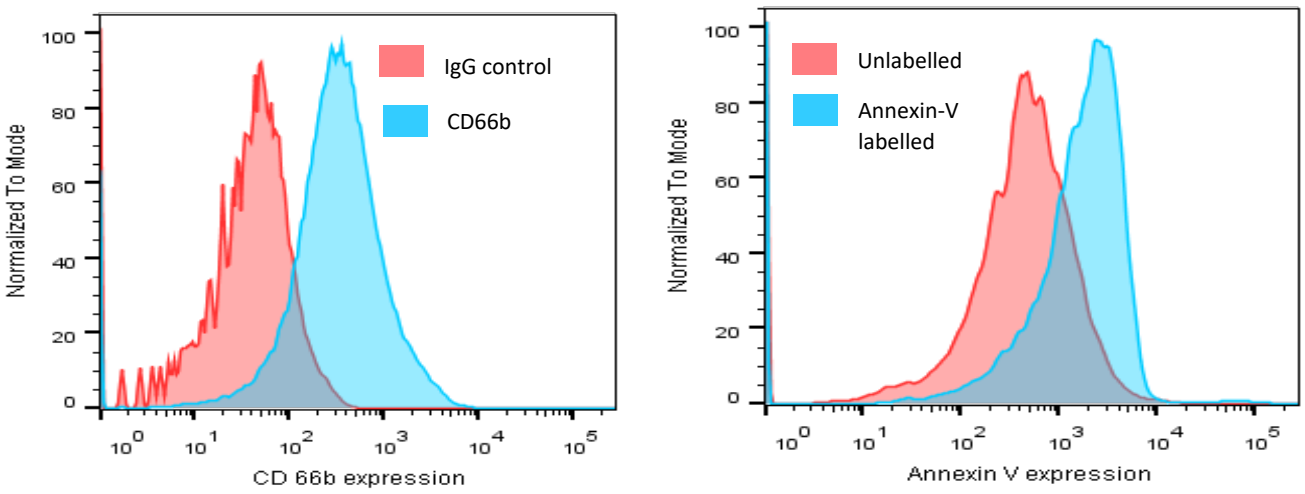

Figure 2. 7 Characterisation of surface markers of NMVs. NMVs were incubated with fluorescently tagged CD66b or Annexin V. Fluorescence was measured by flow cytometry and analysed using FlowJo software. **(A)** Representative histogram of CD66b expression compared to isotype control. **(B)** Representative histogram demonstrating a shift in fluorescence when incubated with Annexin V. Data represent n=3 independent experiments.

2.4.2 Contamination with platelet MVs and monocyte MVs

After pelleting NMVs at 20,000g, the pellets were tested for contamination from MVs produced bymonocytes and platelets using fluorescently labelled markers and analysed using flow cytometry. CD14, is a marker expressed by monocytes and CD41 was used as a marker for platelet contamination. **Figure 2. 8A** demonstrates that there was no detectable contamination by monocyte MV. There was some contamination with platelets (8.16 ± 0.86 %) (**Figure 2. 8B**) but when NMV were double-labelled with CD66b, a neutrophil marker, 8.17 ± 0.89 % MV double-labelled for CD66b and CD41. This was expected as platelets can be very sticky, and some would adhere to NMVs and will pellet at the speed used (***Table 2. 4***).

Table 2. 4 Analysis of Surface marker expression of NMVs.

% CD66b +ve NMVs	% CD41 +ve NMVs	% double positive
78.2	8.45	7.70
72.9	7.23	7.68
81.3	8.90	9.23

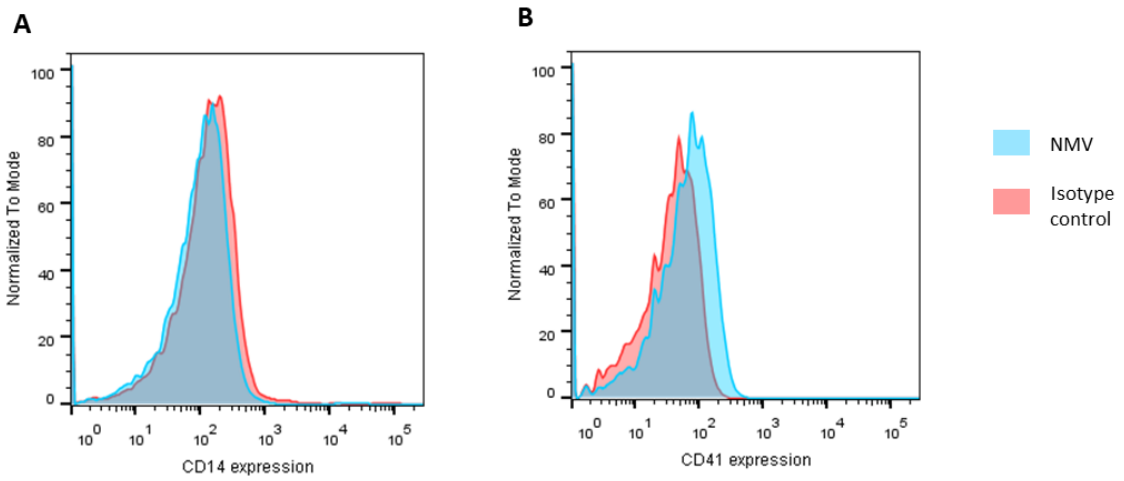

Figure 2. 8 Analysis of contamination by non-neutrophil derived MVs. NMVs were incubated with monocyte markers (CD14) and platelet (CD41) to analyse contamination from other cell types. Fluorescence was measured using flow cytometer. Representative histogram of three independent experiments demonstrating the shift in fluorescence **(A)** NMV with CD14 **(B)** CD41 expression (n=3).

2.4.2 NMVs interact with hCMEC/D3 cells

Confocal imaging revealed that NMVs were internalised by hCMEC/D3 cells after 2 hrs, as shown in ***Figure 2. 9***. Furthermore, Z-stack imaging confirmed the NMVs were located inside the cell and were not solely adhering to the cell surface.

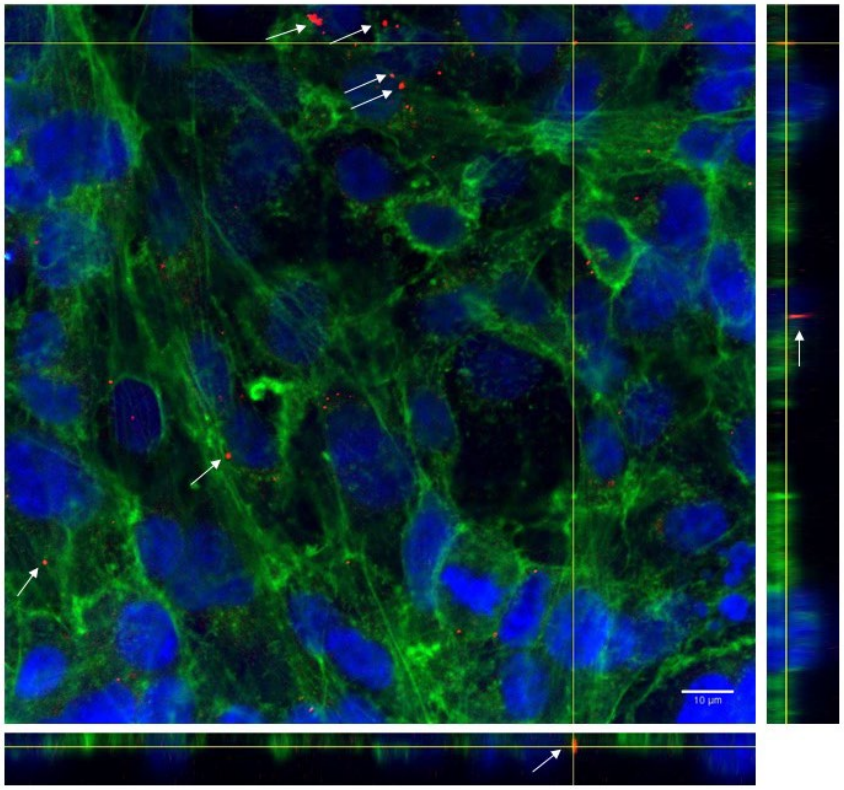

Figure 2. 9 Confocal imaging of interaction of NMVs with hCMEC/D3 cells. hCMEC/D3 cells were incubated with PKH-26 labelled NMVs (300 NMV/µl) for 2h. The coverslips were fixed and stained for FITC-phallodin for actin (green) and counterstained using TOPRO-3-iodide (blue). The white arrow indicates NMV (red). The images were obtained using Nikon confocal microscope (x60 oil immersion) and z-stack was analysed using Image J software. Scale bar represents 10 µm.

2.4.3 NMVs are trafficked into early endosomes after internalisation

Some, but not all, NMVs co-localised with the early endosomal marker EEA-1, demonstrating that NMVs are trafficked into early endosomes (***Figure 2. 10***). Interestingly, most of the NMVs were found near to the endosomes and closer to the nucleus. An IgG control was used to show there was no non-specific binding of EEA-1 antibody (***Figure 2. 10***).

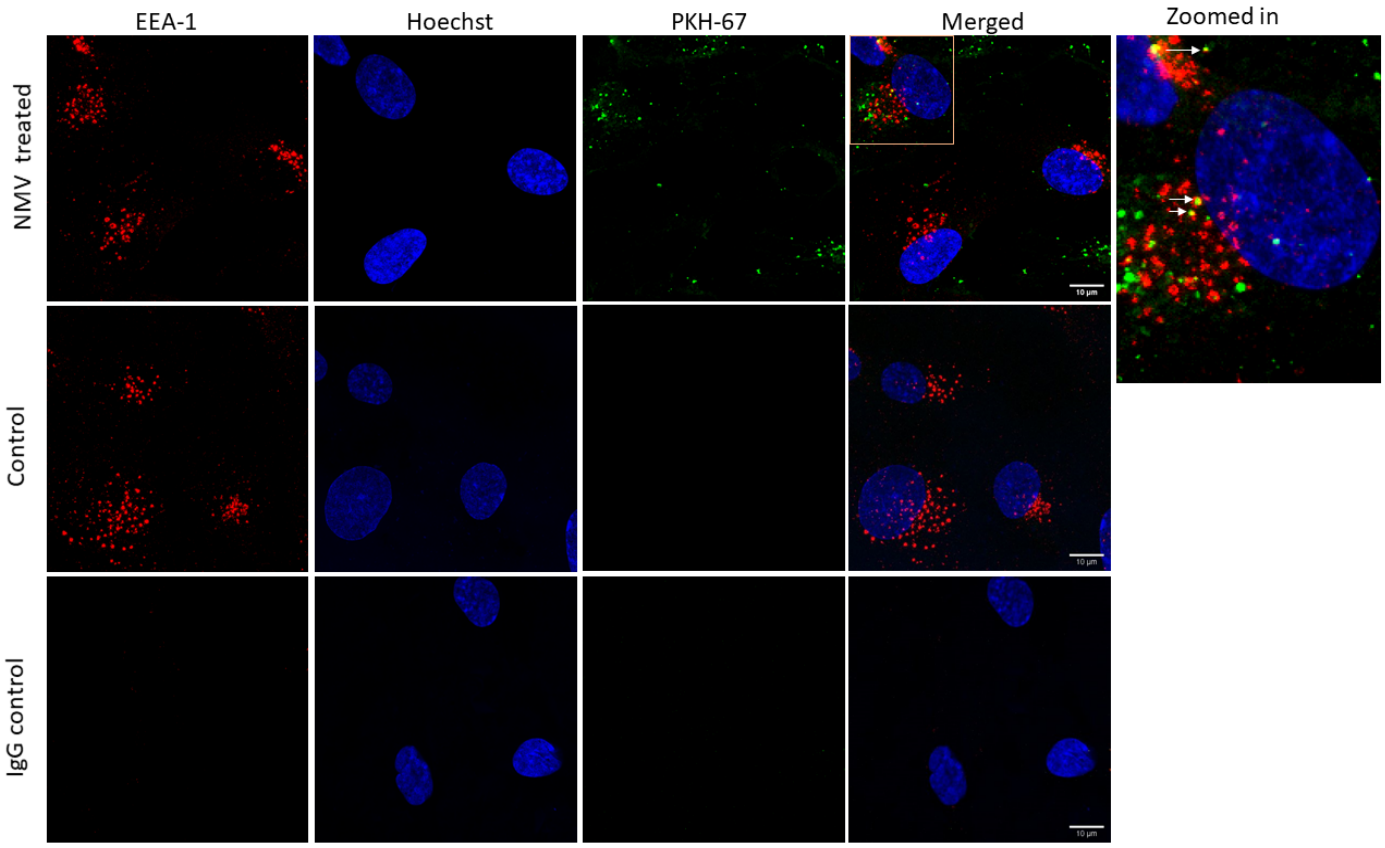

Figure 2. 10 Representative image of EEA-1 staining to visualise co-localisation of NMVs in endosomes. *hCMEC/D3 cells were treated with PKH-67 labelled NMVs and were incubated for 2h. Control was hCMEC/D3 cells without NMVs. The images were obtained using Zeiss KSM 880 with airyscan confocal and images were obtained using Zeiss Leica software. White arrows indicated co-localisation of PKH-26 labelled NMVs (green) with the early endosome marker EEA-1 (red). This is a representative diagram of n=3 independent experiments. Scale bar represents 10 µm.*

2.4.4 hCMEC/D3 internalise PKH-labelled NMVs

Flow cytometry was used to quantitate the number of PKH-labelled NMVs internalised by hCMEC/D3. To exclude any NMVs that were free floating and/or adhered to the outside of the cells, trypan blue quenching was performed were trypan blue was added to the cells before reading it on the flow cytomter. The parameters were adjusted to set the baseline fluorescence intensity before each experiment. Flow cytometric analysis demonstrated that 48.36±11.37% of cells were PKH-67 positive (n=5 independent experiments) (***Figure 2. 11***).

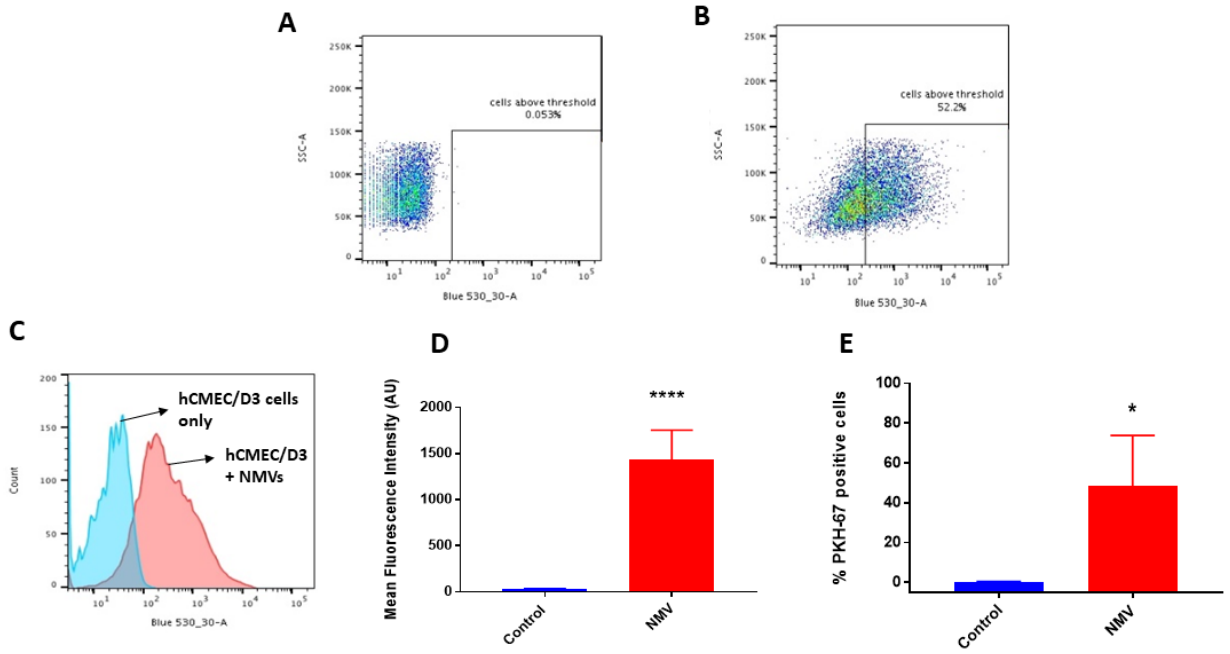

Figure 2. 11 Flow cytometric analysis of internalisation of NMVs by hCMEC/D3. (A) Flow cytometer parameters were adjusted for autofluorescence and a gate set-up for positive fluorescence using hCMEC/D3 cells. **(B)** hCMEC/D3 were incubated with PKH67 labelled NMVs for 2h and the percentage of cells in the positive gate determined. **(C)** Representative histogram indicating an increase in PKH67 positive cells in the NMV treated group. Mean Fluorescence Intensities **(D)** and **(E)** % PKH-67 positive cells of hCMEC/D3 alone (control) or in the presence of NMVs (NMV) are presented as mean ± SD and statistical significance analysed using a paired t-test(*$p<0.05$; **** $p< 0.0001$; n=5)

2.4.5 Investigation of various pathways of NMV internalisation

2.4.5.1 The internalisation of NMVs by hCMEC/D3 is energy-dependent

To investigate the effect of number of NMVs internalised by hCMEC/D3, cells were incubated with increasing numbers of NMVs. ***Figure 2. 12*** (A & B) demonstrates that even with a high number of NMVs (3,000 NMVs/µl), the internalisation of NMVs by hCMEC/D3 did not plateau. However, for the further experiments, 300 NMV/µl were selected as this closely resembles the physiological number of NMVs present in the plasma of patients with systemic inflammation which is in the range of 250-400 NMV/µl (Guervilly et al., 2011; Sellam et al., 2009).

To investigate if the NMV internalisation is calcium dependent, hCMEC/D3 were incubated with EDTA, a calcium chelating agent. Internalisation of NMVs was significantly reduced by 51.51±7.219% ($p = 0.003$) after 2 hours when incubated with EDTA (***Figure 2. 12*****C**).

To investigate the effect of temperature on internalisation, the cells were incubated at 4°C and at 37°C after the addition of NMVs. The internalisation of NMVs by hCMEC/D3 was significantly reduced at 4° C by 94.65±0.81% ($p = 0.0001$), demonstrating this is an energy-dependent process (***Figure 2. 12*****D**).

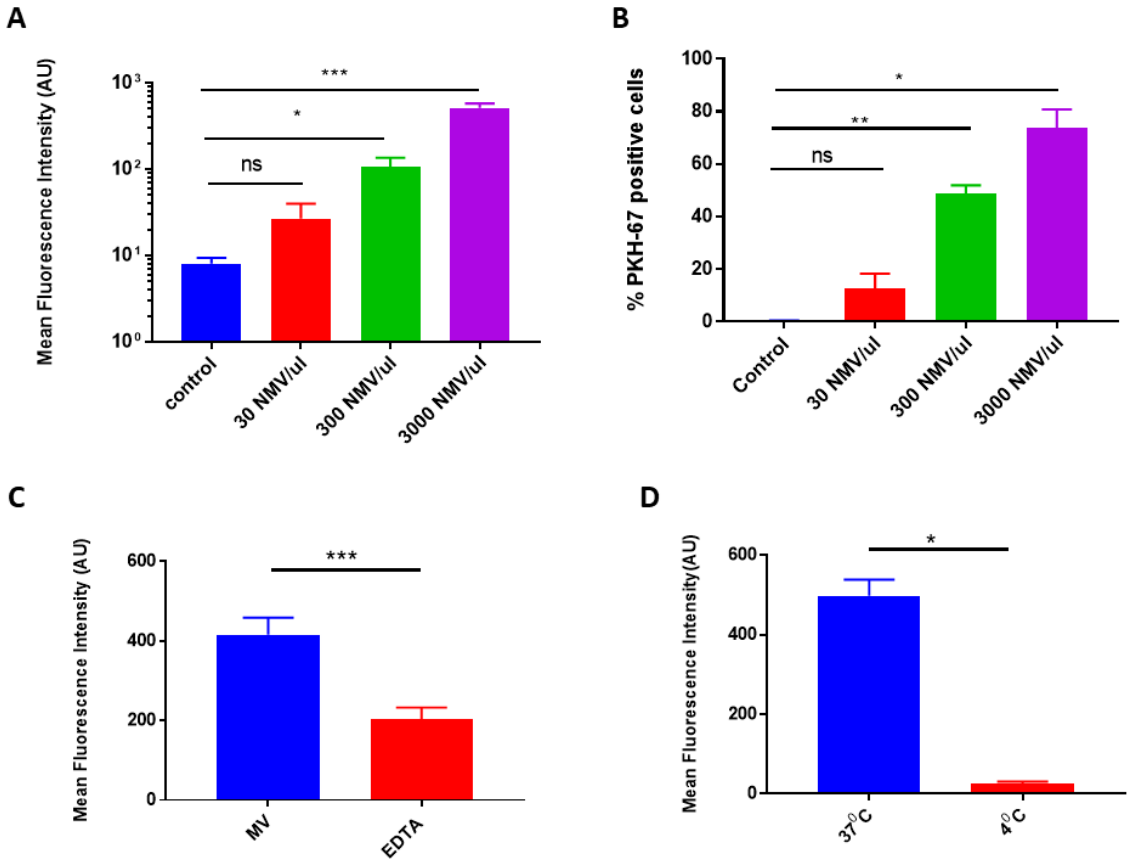

Figure 2. 12 Number, energy and calcium dependent internalisation of NMVs by hCMEC/D3. (A) Quantification as MFI (AU) on effect of PKH-labelled NMVs at various concentrations. **(B)** Data represented as % PKH-positive cells. **(C)** To understand the role of calcium, EDTA was added along with NMV for 2h and MFI was graphed. **(D)** hCMEC/D3 were incubated at 4°C to study the effect of temperature on internalisation and data represent MFI of cells. Data represented as Mean ± SD and statistical analysis was performed using either one-way ANOVA with Dunnett's post test for multiple comparisons (A and B) or a paired t-test (C and D). *p<0.05, **p<0.01,***p<0.001, ns – no significance. The results represent 3-5 experiments.

2.4.5.2 Optimisation of dose-response of various inhibitors on cell viability of hCMEC/D3

To investigate the toxicity of various inhibitors, a dose-dependent toxicity assay was performed. Since internalisation is not passive and is an energy dependent process, various pathways of internalisation were explored. The receptor mediated pathways included clathrin-mediated endocytosis, caveolae-dependent endocytosis and micropinocytosis. Furthermore, the role of actin, dynamin and role of PI3kinase was also explored. To elucidate this, chemical inhibitors were used. Ethyl-isopropyl amiloride or EIPA is an inhibitor or Na^+/H^+ exchanger thereby inhibiting micropinocytosis in the cells. Cytochalasin D inhibits actin polymerisation, thus inhibiting general uptake pathways that involve actin rearrangement. Monodansylcadaverine or MDC can selectively inhibit the clathrin-mediated pathway. Dynasore is a dynamin inhibitor, a protein that is involved in formation of pits during endocytosis. Wortmannin is an inhibitor of phosphatidylinositol 3-kinase, which is involved in various endocytosis pathways.

hCMEC/D3 were incubated with each inhibitor at various doses and the number of live/dead cells were assessed using trypan blue (***Figure 2. 13***). 95% cell viability was selected for the subsequent inhibition experiments. The final doses selected are presented in ***Table 2. 5***.

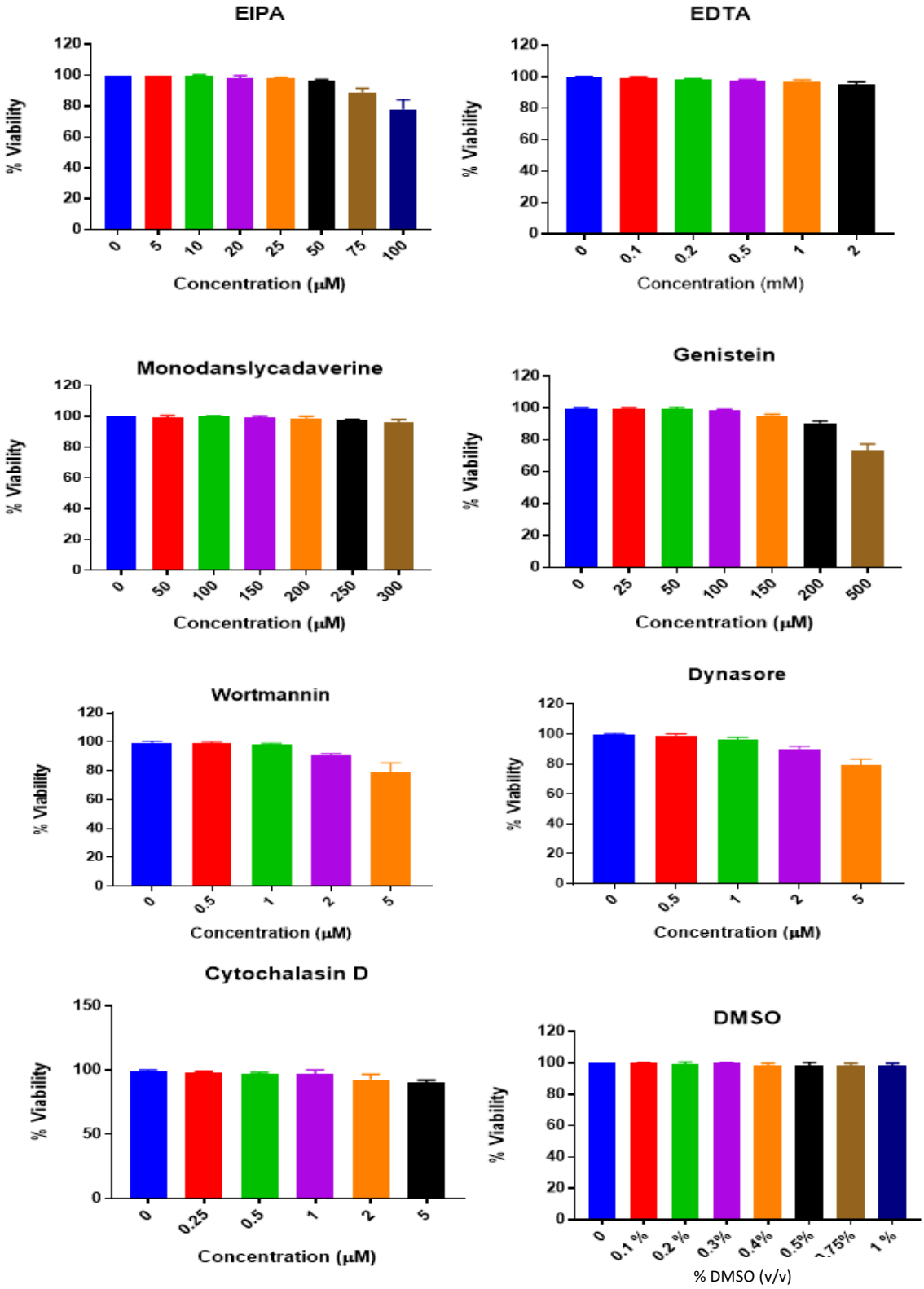

Figure 2. 13 Viability of hCMEC/D3 after pathway-specific pharmacological inhibitors of internalisation. hCMEC/D3 were cultured in a 24 well plate and grown to confluence and were incubated with increasing concentration of pharmacological inhibitors of internalisation

for 1h or 3h at 37°C. Cell viability was determined using trypan exclusion method. Viability of hCMEC/D3 treated with **(A)** EIPA **(B)** EDTA **(C)** Monodansylcadaverine **(D)** genistein **(E)** wortmannin **(F)** Dynasore **(G)** cytochalasin D and **(H)** (0.5%) DMSO control. Data represented as mean ± SD (n=3). Cell viability of 95% and above were considered to be tolerated by hCMEC/D3 and were chosen for the inhibition experiments.

Table 2. 5 Final concentrations of all the inhibitors used

Inhibitor	Final Concentration (µM)
EIPA	50
Cytochalasin D	1
Monodansylcadaverine (MDC)	150
Dynasore	1
Genistein	100
Wortmannin	1
EDTA	0.1

2.4.5.3 Inhibition of NMV internalisation

hCMEC/D3 pre-treated with proteinase K, a broad specificity protease, reduced internalisation by 88.51±3.619% (***Figure 2. 14***), suggesting protein–protein interaction is needed for internalisation of NMVs. To determine other possible cellular mechanisms responsible for NMV internalisation, cells were treated with various pharmacological inhibitors including: dynasore to inhibit the function of dynamin; cytochalasin D to inhibit actin elongation and the formation of microfilaments; EIPA to block the activity of NA^+/H^+ exchangers required for macropinocytosis; MDC to inhibit clathirin-mediated endocytosis; and genistein to inhibit caveole-mediated endocytosis. The largest reduction in internalisation was seen with Dynasore (59.79±5.01%; p =0.0001), followed by cytochalasin D (59.05±13.35%; p =0.0001) and EIPA (49.47±9.908%; p =0.0001)). MDC significantly reduced internalisation by 39.55±17.51% (p-0.0004), while genistein and wortmannin had a moderate effect (25.83±14.08%; p =0.0374 and 25.95±16.61%; p =0.0229, respectively). Varying levels of internalisation inhibition resulting from targeting these differing pathways suggests that NMV uptake occurs via multiple pathways.

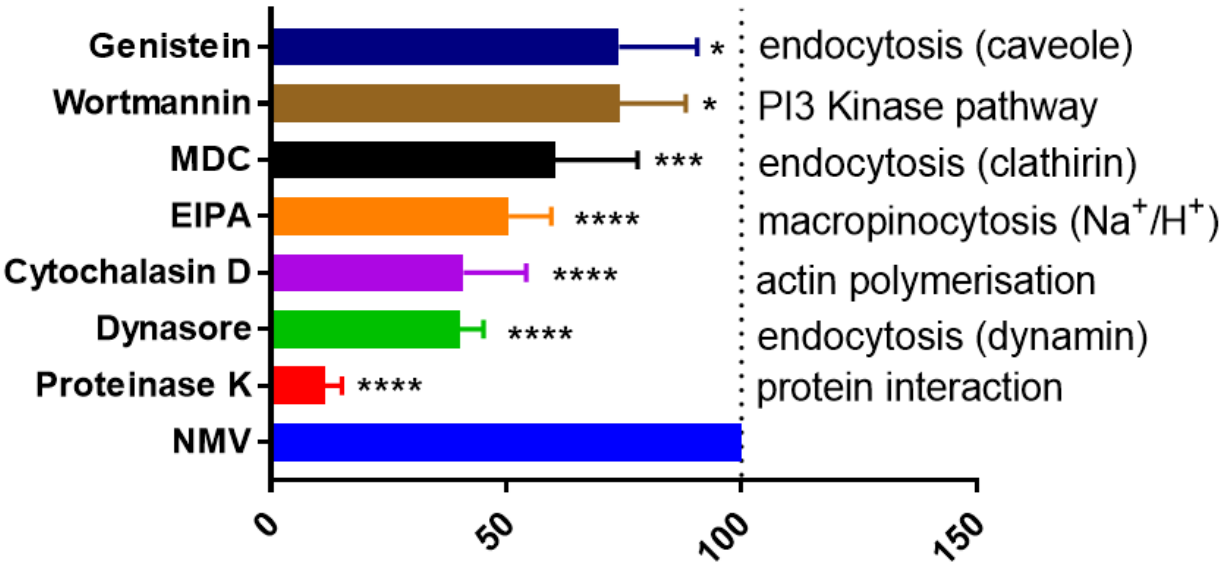

Figure 2. 14 Inhibition of internalisation of NMVs by pharmacological inhibitors. Pharmacological inhibitors were used to inhibit various pathways to elucidate the mechanism of NMV internalisation. hCMEC/D3 were treated with various inhibitors -genistein, wortmannin, MDC, EIPA, cytochalasin D, Dynasore and proteinase K and PKH-67 labelled NMV were added for 2h. Data represent 3-5 independent experiments and are presented as the percentage of NMV uptake compared to the control with no inhibitors present. Data represented as mean ± SD, statistical significance was calculated using one-way ANOVA with Dunnett's multiple comparison test, *p<0.05, ***p<0.001, ****p<0.0001.

2.4.6 Inflammation does not alter rate of internalisation of NMV

2.4.6.1 Optimisation of dose response of ICAM-1 expression

Expression of ICAM-1 by hCMEC/D3 is increased when they are activated by an inflammatory stimulus. hCMEC/D3 were incubated with pro-inflammatory LPS for 4,6 and 24 h and the expression of ICAM-1 was measured using flow cytometry. There was an increase in ICAM-1 expression in hCMEC/D3 after each time point, which is summarised in figure 2.15. The expression of ICAM-1 was significantly increased at 6h (132.3 ± 2.53 %; p-0.0149) and 24h (190.4 ± 11.21%; p-0.0001) when compared to the control. There was slight increase (112.2 ± 2.533%, p-0.4032) in expression of ICAM-1 in cells treated for 4h, compared to the control but was not statistically significant.

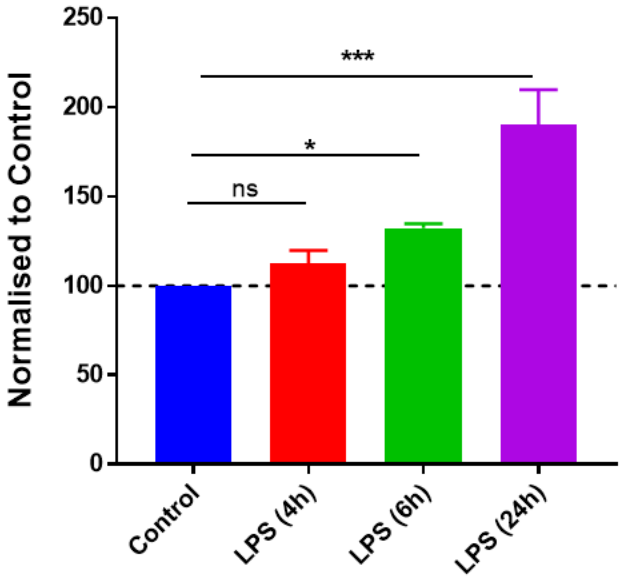

Figure 2. 15 Optimisation of ICAM-1 expression by hCMEC/D3 after LPS treatment. hCMEC/D3 were incubated with LPS (1 µg/ml) for 4,6 and 24 h. ICAM-1 expression of the cells was analysed using flow cytometry and was significantly increased after 6h (p-0.0149) and 24h (p- 0.0001) stimulation with LPS. There was no statistically significant (p- 0.4032) increase in ICAM-1 expression in the cells. MFI was measured and data was normalised to control that did not receive any treatment. Data are presented as mean ± SD (n=3). Statistical significance was analysed using one-way ANOVA with Tukey's multiple comparison test, compared to control *p<0.05, ***p<0.001, ns – no significance.

2.4.6.2 Internalisation of NMVs by hCMEC/D3 is not ICAM-1 dependent and is not affected by the presence of inflammatory stimuli.

To study the role of pro-inflammatory stimuli on the ICAM-1-mediated internalisation of NMVs by hCMEC/D3, cells were pre-incubated with LPS to increase expression of ICAM-1 which was then blocked using anti-ICAM-1 antibody before incubating with NMVs. An isotype control was also used to test the specificity of the result. The data shown in ***Figure 2. 16*** demonstrates that there was a slight increase (118.9 ± 30.22 %) in internalisation of NMV in response to treatment with LPS, but this did not reach significance ($p = 0.5979$). Similarly, after blocking ICAM-1 there was no significant change in the internalisation of NMVs (120.8 ± 23.19%; $p = 0.6029$). Furthermore, pre-incubation with TNF-α, lowered the % of NMV internalisation slightly, but had no significant impact on NMV internalisation (85.85 ± 14.15%; $p = 0.8277$).

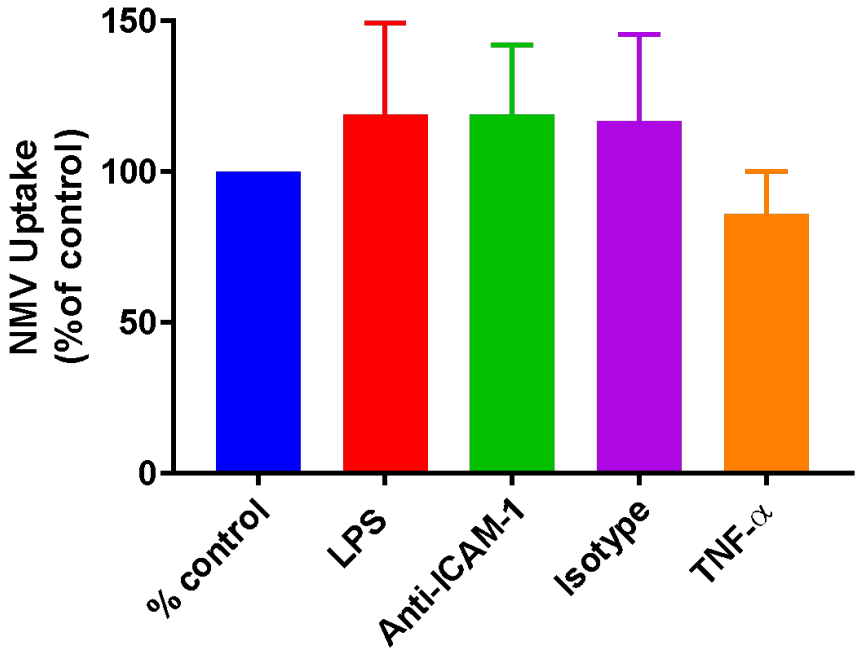

Figure 2. 16 Role of inflammatory stimuli and ICAM-1 in the uptake of NMV. hCMEC/D3 were incubated with LPS for 6h and was incubated with ICAM-1 blocking antibody for 1h, followed by incubation with NMVs for 2h. Additionally, cells were also incubated with TNF-α and incubated with NMVs. MFI was measured using flow cytometer. LPS increased NMV uptake but was not statistically significant. Anti-ICAM-1 did not reduced uptake of PKH-67 labelled NMVs into the cell. Notably, TNF-α reduced NMV uptake slightly but was not statistically significant. Data represented in the graph are normalised to % of control i.e. cells with just NMVs. Data represent mean ± SD (n=3) and statistical significance was measured using one-way ANOVA with Tukey's multiple comparison test.

2.5 Discussion

Neutrophils are key players of the immune response and, in individuals with dementia, they are speculated to contribute to cognitive decline. However, neutrophils are not a prominent feature of dementia neuropathology and they are rarely detected within the brain parenchyma. To understand how peripheral neutrophils can interact with and impact the BBB, the role of NMVs were investigated. We describe a robust protocol for the successful isolation of NMVs from peripheral neutrophils and a detailed characterisation of the interaction between NMVs and human cerebral microvascular endothelial cells. To our knowledge, this is the first study reporting the interaction between NMVs and hCMEC/D3 and the mechanisms involved in the internalisation of NMVs.

2.5.1 Successful isolation of neutrophils and NMVs from human peripheral blood

Neutrophils are the first responders to the site of an infection or inflammation and are the most abundant white blood cell in the body. However, they are also short lived (typically surviving less than 24 hours in the circulation) and are highly susceptible to activation (Athens et al., 1961; Galli et al., 2011). In the current study, neutrophils were isolated from venous blood using density gradient separation. Both the number of neutrophils and NMVs varied considerably from donor to donor, which may reflect differences in age, lifestyle, ethnicity, and genetic variation. Therefore, each set of experiments was repeated with at least three different donors.

To study the effects of NMVs, it is crucial to obtain a relatively pure population of neutrophils so that the samples obtained are not contaminated by MVs from other cell types. Analysis of cytospin preparations revealed a relatively pure population of neutrophils with no significant contamination from other cell types such as monocytes and red blood cells, this is important as monocytes also have the ability to produce microvesicles (Holvoet et al., 2016; Sarkar et al., 2009). The contamination with eosinophils was unavoidable as these granulocytes have a similar size and density to neutrophils, however, using density gradient separation with Histopaque generally achieved >95% of neutrophil purity.

Density gradient separation of neutrophils requires multiple centrifugation steps and has an overall time in excess of 3h, and to isolate NMV requires another 1-2h. As neutrophils are highly sensitive to shear stress and chemical exposure, this technique may alter their activation status and gene expression profile (Freitas et al., 2008). Alternative techniques such as beads

antibody-labelling followed by positive/negative selection dramatically reduces the time and can produce a higher yield of neutrophils. However, this technique is very costly and is not a viable option for large quantities of neutrophil preparations (Hasenberg et al., 2011; Lakschevitz et al., 2015). Another drawback of this alternative technique is that positive selection requires binding to a surface marker, such as CD66b, which may change the phenotype and impact the functional capacity of neutrophils (Zhou et al., 2012). Alternatively, negative selection requires an extensive range of antibodies directed against other cell phenotype markers which increases the cost and is time consuming. Comparison of the gene expression profile of neutrophils isolated using either density gradient isolation or negative selection identified only 25 genes that were significantly differentially expressed between two methods of neutrophil isolation (Thomas et al., 2015). Therefore, the density-gradient isolation technique used in the current study is an appropriate method to isolate a relatively pure population of neutrophils which have low levels of activation.

Neutrophils express a range of surface markers such as CD18, CD66b and CD62L, and changes in expression of these markers are indicative of their activation status. CD18 expression is upregulated in neutrophils when activated by fMLP, while CD62L is constitutively expressed by leukocytes and after activation it is enzymatically cleaved (Gómez-Gaviro et al., 2000; Videm and Strand, 2004). In the current study, neutrophils were minimally activated during the isolation process but showed significant activation when incubated with fMLP, as demonstrated by the increased expression of CD18 and the shedding of CD62L. This agrees with other studies reporting activation of neutrophils with fMLP (Dalli et al., 2013; Gasser and Schifferli, 2004; Slater et al., 2017).

Under normal conditions, most cells produce MVs that are involved in cell-to-cell communication (Raposo and Stoorvogel, 2013). However, when activated, neutrophils produce significantly higher levels of NMVs compared to resting neutrophils. The current study used fMLP to activate neutrophils, however there are alternative methods of stimulating neutrophils to produce microvesicles, including other bacterial by-products, such as latrunculin B, phorbol-12-myristate-13-acetate (PMA), L-NAME and recombinant inflammatory stimuli such as TNF-α and IFNγ (Headland et al., 2015; Nolan et al., 2008; Slater et al., 2017). Although the current study supports the majority of the current literature, it conflicts with the contradictory findings that fMLP, PMA, TNF-α and LPS stimulated neutrophils do not influence NMV number (Timár et al., 2013). Interestingly, that study also used the shortest incubation time of 20 minutes, which likely influenced NMV numbers. Another interesting fact is that the contents

of NMV and their mode of action vary depending on the stimuli. For example, NMVs released from neutrophils stimulated with bacteria or bacterial by-products have the ability to restrict bacterial growth (Timár et al., 2013), demonstrating that NMVs can have an inflammatory effect. However, NMVs from Rheumatoid arthritis patients prevent activation of macrophages thereby exerting an anti-inflammatory effect (Rhys et al., 2018).Dalli et al., (2013) also report that the NMV proteome is distinct depending on the mode of stimulation, suggesting that the mode of neutrophil activation produces functionally distinct NMV contents. However, characterising the content of the NMVs used in the current study is beyond the scope of this project.

ZetaView potential of NMVs demonstrated that they are within the range of 100-1000 nm in diameter, agreeing with other reports (Gomez et al., 2020). To confirm that the MVs originated from neutrophils, expression of the neutrophil marker CD66b was investigated. It should be noted that not all NMVs express CD66b, which may reflect the membrane budding off site (Figure 1.3), and that labelling efficiency varied from donor to donor. Investigation of expression of other cell phenotype markers by the isolated MVs identified negligible contamination with the monocyte marker CD14 and < 10% expression of the platelet marker CD41. However, when dual-labelled with CD66b, most $CD41^+$ MVs were also positive for CD66b. Platelets tend to be extremely sticky, they may adhere either directly to NMV or to the outside of neutrophils were NMV biogenesis is occurring. Complete removal of platelet MVs from the sample is quite difficult to achieve, but overall density-gradient separation is the best technique to obtain a relatively pure population of neutrophils that can be stimulated to produce NMVs.

2.5.2 NMV internalisation by hCMEC/D3

Uptake of MVs originating from other cell types such as monocytes, platelets and cancer cells has been widely reported (Dalli et al., 2013; Faille et al., 2012; Kawamoto et al., 2012; Li et al., 2013; Pitanga et al., 2014), but to our knowledge, this is the first study to report the internalisation of NMVs by human brain microvascular endothelial cells. Confocal imaging of hCMEC/D3 demonstrated that NMVs interact with human brain endothelial cells, with Z-stack imaging demonstrating NMVs are present inside the cell. Flow cytometric analysis confirmed the internalisation of NMVs by hCMEC/D3 and demonstrated that ~50% of hCMEC/D3 contained NMVs. Addition of trypan blue prior to reading the sample on flow cytometer ensured all the external fluorescence was quenched and only the signal from internalised NMVs

were quantitated. It should be noted that while flow cytometry is a standard approach to quantitate the number of cells that have internalised NMVs, it does not discriminate how many NMVs have been internalised by each cell. Moreover, while the PKH-labelling efficiency was checked using flow cytometry and samples were added only if the efficiency was 80% or higher, the actual the number of cells containing NMVs may be an underestimation as the flow cytometry approach cannot differentiate between labelled and non-labelled NMVs internalised by the cells.

NMVs co-localised with the early endosomal marker EEA-1, suggesting that NMVs use endocytosis to enter hCMEC/D3 and are trafficked into early endosomes, supporting previous studies reporting other MVs and other endothelial cells. (Faille et al., 2012; Kawamoto et al., 2012; Kuhn et al., 2014; Schneider et al., 2017). However, not all studies support that endocytosis is the predominant route used by MVs for internalisation, as MVs do not co-localise with early or late endosomal markers in HUVECs (Terrisse et al., 2010), suggesting that pathways processing MVs after their uptake might vary between different endothelial cells. It should be noted that in our samples not all NMVs co-localised with EEA-1, suggesting that not all NMVs are trafficked into endosomes. However, the timing of the cell fixation may have impacted on the location of NMVs. Some studies have reported that MV internalisation is rapid, suggesting that in the current study NMVs may already have moved to late endosomes or fused with lysosomes (Pitanga et al., 2014). Additional co-localisation studies with markers of late endosomes or lysosomes is required to investigate additional endosomal trafficking stages. Furthermore, to understand the precise mechanism, in-depth live cell imaging of NMV trafficking through the cell is needed. However, taken together with confocal imaging and flow cytometry, the current study clearly demonstrates that NMVs interact with and are internalised by hCMEC/D3.

2.5.3 NMV internalisation is through multiple pathways

It was surprising that although the internalisation of NMVs by hCMEC/D3 was dose-dependent, it did not achieve full saturation, suggesting that hCMEC/D3 have the capacity to uptake large numbers of NMVs and process them quickly. There is very little known about actual number of NMV in the circulation during systemic inflammation or infection, so actual numbers of NMVs used *in vitro* and *in vivo* vary extensively in the literature (Dalli et al., 2008; Gomez et al., 2020; Pitanga et al., 2014; Rhys et al., 2018). However, a paper analysing various types of MVs in patients with systemic inflammation reported that NMVs range between 200-

400 NMV/µl (Guervilly et al., 2011). Therefore, for all our experiments we used 300 NMV/µl as this is physiologically relevant.

Many studies have reported that internalisation of MVs is a rapid process, with some suggesting it occurs within 15 minutes (Johnson et al., 2014). In the current study, performing the experiments at 4°C dramatically reduced the internalisation of NMVs, demonstrating that this is not passive but an energy-requiring process. This finding supports other studies that have also reported the uptake of EVs are not passive, demonstrated by addition of EVs to cells fixed in paraformaldehyde (Fitzner et al., 2011). Endocytosis is required by all cells to internalise nutrients, regulate metabolism and transmit information within the cell or between cells. Generally, endocytosis is classified on the basis of size into two mechanisms – phagocytosis and pinocytosis. Phagocytosis is employed for engulfment of larger particles, usually > 1 µm such as bacteria and cellular debris. Although, this is the preferred uptake route for larger particles, it has been shown that particles <0.1 µm can also be internalised though this route (Rudt and Müller, 1993). Pinocytosis involves uptake of smaller sized particles, which can be further divided into macropinocytosis or through receptor mediated pathways.

Internalisation of NMVs require some type of recognition/ docking to the cell surface. Some studies have reported that treating either cells and/or MVs with general proteases significantly reduces internalisation (Baj-Krzyworzeka et al., 2002; Faille et al., 2012; Skliar et al., 2018). The current study confirmed that proteinase K treatment, a general protease, significantly reduces NMV internalisation, and indicates the importance of surface proteins in the recognition and internalisation of NMVs. Other studies have tried to decipher the first stages of recognition and docking, however more in-depth analysis of surface proteins are required to fully understand this mechanism. Another problem that is encountered by researchers is that surface proteins differ depending on the type of MVs and type of stimulation, making it very difficult to exactly pin point the receptors/proteins associated with docking and internalisation. Further in-depth studies are needed in this field to understand how the initial stages of NMV recognition and docking occurs in hCMEC/D3.

Although the current study did not decipher the surface interaction between NMVs and hCMEC/D3, all the evidence points towards NMVs utilising endocytosis internalisation. Since there are several types of endocytosis, pharmacological inhibitors were employed that specifically target various pathways (**see *Figure 2. 17***). The largest reduction in NMV internalisation was seen with the dynamin inhibitor, Dynasore. Dynamin belongs to the GTPase

superfamily, and is essential for clathrin-mediated endocytosis. After invagination, dynamin is recruited to the neck and forms helical structures causing membrane budding (Preta et al., 2015). While Dynasore had the biggest effect on internalisation, the internalisation of NMVs may not be predominantly clathrin–mediated endocytosis, as Dynasore can also disrupt the cholesterol in the plasma membrane, causing changes to lipid raft-mediated MV internalisation (Preta et al., 2015). Therefore, future studies using pharmacological inhibitors targeting lipid raft mediated internalisation need to be investigated to further understand the mechanism of NMV internalisation.

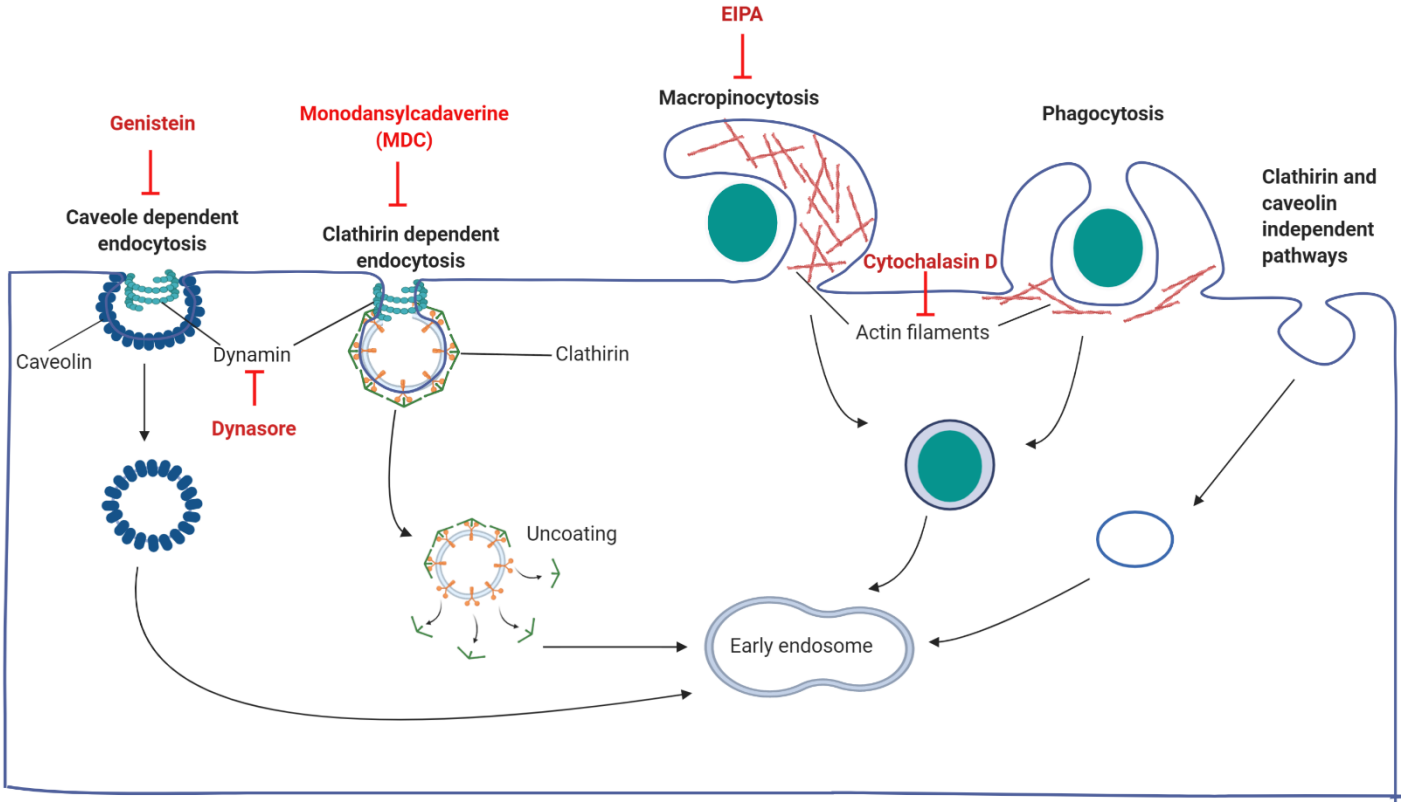

Figure 2. 17 Summary of pathways of internalisation and inhibitors. Cells internalise particles either via phagocytosis or pinocytosis. Pinocytosis is further divided into clathrin mediated endocytosis, caveolae mediated endocytosis, macropinocytosis and clathrin-and caveolae-independent endocytosis. NMVs utilise all of these pathways in varying degrees to be internalised by hCMEC/D3

Interestingly, cytochalasin D also significantly inhibited internalisation, indicating a role of the actin cytoskeleton in this process. Actin polymerisation and cytoskeleton rearrangement is required for macropinocytosis to occur. Furthermore, as cytochalasin D impacts the actincytoskeleton, it can disrupt both macropinocytosis and clathrin-mediated endocytosis as both of these processes require extensive rearrangement of actin. The role of actin is diverse in cells and, as evident in the current study, has a crucial role in the internalisation of NMVs by human brain microvascular endothelial cells.

Macropinocytosis is a process used by cells to uptake large amounts of fluids, is not specific and does not require any additional receptor binding (Swanson, 2008). Another inhibitor that significantly reduced internalisation of NMVs by hCMEC/D3 was EIPA, which is an inhibitor for macropinocytosis. EIPA is an analogue of amiloride, a guanidinium-containing pyrazine derivative, which has the ability to inhibit Na^+/H^+ exchangers (Orlowski and Grinstein, 2004). EIPA lowers submembranous pH, thereby preventing the activation of Rac1, a GTPase involved in actin polymerisation (Koivusalo et al., 2010).

Macropinocytosis requires remodelling of the cytoskeleton, forming cups or protrusions that utilise the activity of phosphatidylinositol-3-kinase (PI3K) (Araki et al., 1996; Lindmo and Stenmark, 2006; Rupper et al., 2001). Activation of PI3K also involves increased Akt signalling, as Akt is a PI3 target kinase (Falcone et al., 2006). Akt is involved in stimulation of membrane ruffling and macropinosome formation during macropinocytosis (Mercer et al., 2010). The fungal metabolite wortmannin inhibits PI3K thus inhibiting fluid phase uptake. There was a significant reduction in the internalisation of NMVs by hCMEC/D3 when treated with wortmannin.

The variety of pathways employed in the internalisation may reflect the wide range of NMV sizes (100-1000 nm), with different sized NMVs being internalised by hCMEC/D3 using different mechanisms. Future studies are required to track different sized NMVs trafficked into hCMEC/D3 and how the cargo is sorted. Furthermore, RNAi mediated knockdown of specific proteins involved in each pathway could be employed to target a single pathway and determine the role each specific pathway plays in the internalisation of NMVs by brain endothelial cells.

2.5.4 Role of inflammation on internalisation of NMVs by brain endothelium

Under normal physiological conditions, low levels of NMVs are present in the circulation (Dalli et al., 2013; Nieuwland et al., 2000; Timár et al., 2013), while under inflammatory

conditions, their levels are elevated (Nieuwland et al., 2000; Timár et al., 2013). To understand the role of inflammation on NMV internalisation by hCMEC/D3, the cells were pre-conditioned with either LPS or TNF-α, both potent pro-inflammatory stimuli. TNF-α impacts the inflammatory profile of hCMEC/D3, while LPS increases permeability and induces activation (Jin et al., 2013; Qin et al., 2015). Interestingly neither inflammatory stimuli impacted the internalisation of NMVs by hCMEC/D3.

After activation neutrophils adhere to endothelium via CD11a/CD18 complex (Li et al., 2018; Tonnesen, 1989; Yang et al., 2005). Previously it was reported that NMVs bind through CD11b/CD18 complex, which binds to endothelium via CD18 (Hong et al., 2012). ICAM-1 is a ligand for CD11a/CD18 complex, and neutrophils are known to utilise this ligand interaction to adhere to endothelium. Although studies have reported that there is an increased ICAM-1 expression in cells after treatment with MVs (Hosseinkhani et al., 2018; Sáez et al., 2019), other studies using brain endothelial cells have reported that blocking ICAM-1 does not decrease internalisation (Faille et al., 2012). The disparity in the results might be due to the high selectivity of brain endothelial cells along with exclusion of blood-derived molecules. It should also be noted that a positive control for the antibody was not performed Another major reason might be due to the antibody used in the experiment, as the ICAM-1 mAb used in these experiments contained sodium azide, which can interfere with binding of the antibody to its site. In future, ideally, mAb without sodium azide should be used to make sure the result obtained is specific and if the interaction between NMVs and brain endothelial cells is ICAM-1 dependent. Additionally, for future experiments, a wider literature search for a neutralising antibody along with a positive control will also aid in the execution of this experiment. However, it should be noted that activation itself may not be enough to drive the internalisation of NMVs by human brain endothelial cells.

2.6 Conclusions

- This study is the first to demonstrate that NMVs are internalised by human brain microvascular endothelial cells *in vitro*, where some co-localise with early endosome markers, suggesting that NMVs are trafficked into endosomes.
- hCMEC/D3 utilise multiple endocytosis pathways to internalise NMVs. Although there was no complete inhibition of internalisation using chemical inhibitors of specific pathways, the results suggest that NMVs utilise multiple pathways which may be dependent on their size.
- Pro-inflammatory stimuli do not impact internalisation of NMVs by hCMEC/D3. Furthermore, blocking of adhesion molecules such as ICAM-1 does not alter the internalisation of NMVs.

Chapter 3: Transcriptomic analysis of the effect of NMV internalisation on hCMEC/D3

3.1 Introduction

The Human Genome Project, formally launched in 1990, identified and mapped around 30,000 genes (Hood and Rowen, 2013). Identifying the functions of the genes and their changes in expression in various diseases has led to a huge drive in genome-based studies. Microarray analysis technology is a very powerful tool to characterise the transcriptomic profile at a certain time point. This microarray approach has enabled the identification of differences in the pattern of gene expression of cells or tissue and has enabled scientists to identify pathways that are disrupted in multiple diseases including cancer (Armstrong et al., 2002; Berchuck et al., 2009; Kumar et al., 2012) and cystic fibrosis (Galvin et al., 2004; Ramachandran et al., 2011). Microarray has enabled researchers to understand pathways that are disrupted in multiple neurodegenerative diseases such as AD (Brooks and Mias, 2019; Guttula et al., 2012), Huntington's Disease (Mina et al., 2016) and MS (Steinman and Zamvil, 2003; Waller et al., 2016).

Primarily there are two types of platform that are used: cDNA microarrays and spotted oligonucleotide microarrays. In a standard cDNA microarray, PCR technology amplifies cDNA introducing a fluorochrome, and the labelled product hybridises to specific probes (Duggan et al., 1999; Govindarajan et al., 2012). In contrast, an oligonucleotide microarray employs single-stranded probes designed using all known genomic sequence information currently deposited in relevant databases (Govindarajan et al., 2012; Murphy, 2002). There are various methods by which an array can be prepared including microspotting onto a glass slide, ink-jet printing using phosphonamidite chemistry and photolithography. One of the leading research tools to characterise the transcriptomic profiles are Affymetrix GeneChips. The Human Genome U133 Plus 2.0 Array (HG-U133 Plus 2.0 Array) is comprised of more than 54,000 probe sets and 1,300,000 distinct oligonucleotide features. The probe sets are selected from various databanks such as GenBank, dbEST and RefSeq, enabling the expression of over 38,000 genes to be assessed. Generally, RNA isolated from the cell-of-interest is converted to cDNA through reverse transcription and then transcribed back to cRNA and labelled with biotin. This labelled cRNA is fragmented (approximately 30-400 base pair fragments),

hybridised to the GeneChips and scanned. The fluorescence intensity of each probe is quantitated as the fluorescence intensity is directly proportional to the starting amount of RNA in the original sample. The high specificity and reproducibility of this method makes it an ideal platform for transcriptomic analysis.

Microarray transcriptomic analysis has been used to characterise the RNA content of extracellular vesicles, such as MVs and exosomes. Garcia-Contreras *et al.*, (2017) reported that patients with type 1 diabetes have a distinct miRNA profile compared to healthy controls. When the transcriptomic profile of cells co-cultured with cancer MVs was compared to the mRNA cargo of the MVs it was revealed that MVs have the ability to transfer oncogenic message(s) to healthy cells (Milani et al., 2017). This further demonstrates that MVs can act as messengers and are likely to be involved in disease progression.

It is only recently that researchers have started exploring the potential role of extracellular vesicles in the pathogenesis of neurodegenerative diseases. The exosomal miRNA profile in the CSF of AD patients has been characterised, and shown to be distinct from Parkinson's disease (Gui et al., 2015), suggesting that miRNA profiles may be a potential biomarker for differentiating between the diseases. Additionally, the altered expression of exosomal miRNA is not restricted to CSF, and has also been reported in the plasma of AD patients (Lugli et al., 2015).

Platelet MVs (PMVs) have also been studied extensively in neurological diseases. These PMVs can induce procoagulant activity and interact with fibrin (Herring et al., 2013), and are elevated in patients with transient ischemic attacks and small vessel disease (Geiser et al., 1998; Lee et al., 1993). They are internalised by brain endothelial cells (Faille et al., 2009), and have the ability to activate endothelial cells (Nomura et al., 2001). Endothelial MVs that are enriched for CD31 and CD61e are elevated in AD compared to age matched controls demonstrating that certain subsets of MVs are associated with cognitive decline in AD (Xue et al., 2012), and could be used as a diagnostic biomarker in the future. Together, these findings demonstrate the potential importance of the MV interaction with brain endothelial cells and how they can be utilised as potential biomarkers.

To date, microarray studies have focused on the content of MVs and exosomes. The majority of these studies have been conducted in the cancer field, as it is already well known that cancer cells utilise MVs for cell-cell communication (Jørgensen et al., 2013; Larrain et al., 2014; Milani et al., 2017; Noerholm et al., 2012). mRNA associated with inflammation, cellular

communication and apoptosis are differentially expressed when compared to healthy controls and the miRNA and/or protein content of these EVs can cause disruption of the BBB (Tominaga et al., 2015). Furthermore, during chronic ischemia, endothelial cell-derived MVs disrupt the BBB and reduce the barrier integrity *in vitro* (Edrissi et al., 2016). All of this suggests that MVs can disrupt cellular communication and can induce variety of pathways in the target cells.

Notably, the least studied of subtypes of MVs are NMVs. Proteomic analysis of NMVs was first performed by Dalli et al. (2010), demonstrating that the NMV content varies depending on the stimuli. This suggests that the role of NMV may vary at different stages of the disease, where the NMV content may be either be pro- or anti-inflammatory. Additionally, NMVs have the ability to modify the gene expression profile of endothelial cells (HUVECs) (Pitanga et al., 2014). This is the only study to our knowledge that has investigated the gene expression changes in endothelial cells after treatment with NMVs. It is important to note at this point that brain endothelial cells have more specialised properties than peripheral endothelial cells. The movement of molecules across the BBB is highly regulated and the rate of diffusion is very low, reflecting that cerebrovascular endothelial cells are highly specialised to protect and maintain brain homeostasis. Further studies are required to elucidate the impact of NMVs on the transcriptomic profile of human brain endothelial cells.

3.2 Aims and Objectives

As demonstrated in Chapter 2, NMVs interact with and are internalised by human brain endothelial cells. We hypothesise that NMVs impact the gene expression profile of the BBB, decreasing the integrity of human cerebrovascular endothelial cells. Identifying key transcriptomic changes in brain endothelial cells in response to NMVs may identify novel therapeutic candidates to modify dysfunction of the BBB in response to systemic infection.

The aim of this chapter was to perform a detailed characterisation of the transcriptomic profile of hCMEC/D3 cells in response to NMV internalisation and identify significantly affected pathways and functional groups.

This chapter specifically aims to:

- Characterise the transcriptomic profile of hCMEC/D3 cells in response to internalisation of NMVs.

- Perform bioinformatic analysis of the datasets generated to identify significantly impacted functional groups and major pathways using a variety of available platforms.

- Validate biologically relevant candidate pathways and functional groups impacted by the internalisation of NMVs.

3.3 Materials and Methods

3.3.1 Transcriptomic analysis of NMV treated hCMEC/D3

To investigate the significant changes in the transcriptomic profile of hCMEC/D3 after treating the cells with NMV (300 NMV/µl) for 24 hours, microarray analysis was performed.

3.3.2 RNA Extraction

hCMEC/D3 (40,000 cells/ well) were plated in 6-well plates and grown to form a confluent monolayer. The cells grown for further 24 hours in the media. The cells were treated with 300 NMV/µl and harvested after 24 hours using 300 µl TRIzol Reagent per well (ThermoFisher Scientific, USA). All conditions were performed in duplicate, so the final volume of TRIzol was 600µl for both control and treated samples. RNA was extracted using the Direct-zol RNA MiniPrep kit (Zymo Research, USA), according to manufacturer's instruction. Equal volumes of ethanol (100%) were added to the TRIzol reagent and mixed thoroughly. The mixture was transferred to a Zymo-Spin IICR column in a collection tube and centrifuged at 16,000 g for 30 seconds. The column was transferred to a new collection tube and the flow-through was discarded. 400 µl of Direct-zol RNA PreWash was added to the column and centrifuged at16,000 g for 30 seconds, this step was repeated. To the column, 700 µl of RNA Wash buffer was added and centrifuged at 16,000 g for 2 minutes. The column was transferred into a RNase-free tube and the RNA eluted in 25 µl of DNase/RNase-free water by centrifuging at 16,000g for 30 seconds. The concentration of the eluted RNA was determined using NanoDrop Spectophotometer (ThermoFisher Scientific) and the quality of RNA was assessed using Agilent RNA 6000 NanoChip (Agilent Technologies INC).

3.3.3 RNA Amplification and Hybridisation

RNA amplification was performed using 3' IVT Pico Reagent kit. All samples were diluted (1:20) prior to amplification. Poly- A RNA controls were used as a positive control for the labelling process. These poly-A controls are exogenous polyadenylated probe set for B. *subtilis* genes (*lys, phe, thr* and *dap*) which are absent from human samples. The pre-synthesized mixture of *lys, phe, thr* and *dap* are present at a final concentration of 1:100,000; 1:50,000; 1:25,000; 1:7,500 respectively. To each sample, 2 µL diluted Poly-A controls were added to make up to a final volume of 5 µL. To amplify the RNA, first strand cDNA was synthesised,

by priming the total RNA with primers containing a T7 protomer sequence at the 5' end. A 3' adaptor was added to the single stranded cDNA with the use of DNA polymerase and RNase H. The single stranded-cDNA acts as a template to synthesise and pre-amplify double stranded-cDNA (ds- cDNA). This new ds-cDNA acts as a template to synthesise antisense RNA or complimentary RNA (cRNA) by a technique known as in vitro transcription (IVT). The resulting cRNA is purified and impurities such as enzymes, salts, inorganic phosphates and unincorporated nucleotides are removed. The yield was quantitated using a Nanodrop spectrophotometer and the quality assessed using the Agilent 6000 NanoChip.

Using the antisense RNA or cRNA as a template, sense-strand cDNA was synthesised by reverse transcription. The complimentary antisense-strand was synthesised by DNA polymerisation using 2nd- cycle primers. Hydrolysis was performed on the resulting ds-cDNA to remove the cRNA template and then purified to remove any impurities such as salts and unincorported dNTPs. The yield was quantitated using a Nanodrop spectrophotometer and quality assessed using the Agilent 6000 Nanochip.

The purified ds-cDNA was fragmented using two specific enzymes: uracil- DNA glycosylase and apurinic/apyrimidic endonuclease1 (APE1). These two enzymes cleave dUTP residues thus breaking the DNA strands. The fragmented cDNA was then labelled by terminal deoxynucleotidyl transferase (TdT) using the Affymetric proprietary DNA labelling reagent which is covalently linked to biotin.

For this gene expression study, Genechip Human Genome U133 Plus 2.0 Arrays were used, which contain 1,300,000 unique oligonucleotides analysing approximately 39,000 human genes. GeneBank, dbEST and RefSeq were used as reference for the design of the probe sets. Sequence clusters for the Genechip were created from Build 159 of UniGene and were refined by analysis and comparison with other publicly available databases including NCBI human genome assembly. The Genechip Human Genome U133 Plus 2.0 array also contain internal housekeeping genes, which have consistent levels of expression in various tissues thereby enabling normalisation of the data.

Before hybridisation, 20X hybridisation controls containing *bioB, bioC, bioD* and *cre* (Affymetrix) were preheated to 65°C for 5 minutes in a thermal cycler. *BioB, bioC* and *bioD* are genes present in the biotin synthesis pathway of *E.Coli* while *cre* is a recombinase gene from P1 bacteriophage. A hybridisation master mix was prepared using hybridisation controls which were added at various concentrations along with a synthetic biotinylated control

oligonucleotide B2 (oligo B2) (to see the final concentration see ***Table 3. 1***. This hybridisation mastermix was added to the biotin-labelled ds-cDNA (160 µL mastermix; 60 µL ds-cDNA) prepared earlier, gently vortexed and incubated for 5 min at 99°C. The tubes were centrifuged briefly and 200 µL of the mix was added to the cartridge and incubated for 16hr at 45°C at a rotation of 60 rpm. The arrays were removed from the oven and each array was washed with Wash Buffer A and placed in the Affymetrix GeneChip Command Console Fluidics Control (ThermoFisher Scientific, USA). Arrays were stained according to Fluidics Protocol FS450_0001.

Table 3. 1 Hybridisation controls and the final concentration used for the microarray

Hybridisation Controls	Final Concentrations
bioB	1.5 pM
bioC	5 pM
bioD	25 pM
cre	100 pM
Oligo B2	3 nM

3.3.4 Microarray quality analysis

Microarray data was analysed using Affymetrix Expression Console 1.4.1.46 and normalised using Robust Multiarray Averaging (RMA), which is a normalisation method that corrects for background levels and summarises the information.

3.3.5 Internal Control Genes

Two internal controls, β-actin and GAPDH, were used as internal controls to assess assay quality. Signals from 3'probe set for each control gene were compared to the corresponding 5' signal values.

3.3.6 Microarray data analysis

The normalised data was analysed using the Qlucore Omics Software (Qlucore, Lund, Sweden). Genes were considered significantly differentially expressed if they had a minimum fold change ≥ 1.2 and $p \leq 0.05$. Online software - DAVID (database for annotation, visualisation and integrated discovery) Tool version 6.7 (Huang et al., 2009) and IMPaLa (Integrated Molecular Pathway Level Analysis) (Kamburov et al., 2011) was used to perform functional grouping and pathway analysis.

3.3.8 Functional Validation

3.3.8.1 Evaluation of Changes in permeability using TEER

Transendothelial electrical resistance (TEER) is a widely used quantitative technique to evaluate the integrity of cell monolayer and tight junctions in endothelial and epithelial barriers (Benson et al., 2013; Srinivasan et al., 2015). TEER was used to study the integrity of the monolayer after the treatment with NMVs over a period of 6 hours. To measure the TEER, the inserts were set up as shown in ***Table 3. 1***. Firstly, the transwells were coated with Collagen-type I from rat tail (150 µg/ml; Sigma, UK) for 1 hour at 37°C and was washed once with PBS. The transwells were returned to 37°C and media was added till the cells were ready to be seeded.The cells were seeded on the transwell membrane in the apical (upper) chamber and media only in the basolateral (lower) chamber. To measure the electrical resistance, one electrode (shorter arm) was placed in the apical chamber and the longer arm placed in the basolateral chamber (***Table 3. 1***). To calculate the TEER for the cells, it was essential to include a blank resistance i.e. the resistance of the transwell membrane without any cells. This technique is based on Ohm's law where the current is directly proportional to the voltage across 2 points (Benson et al., 2013).

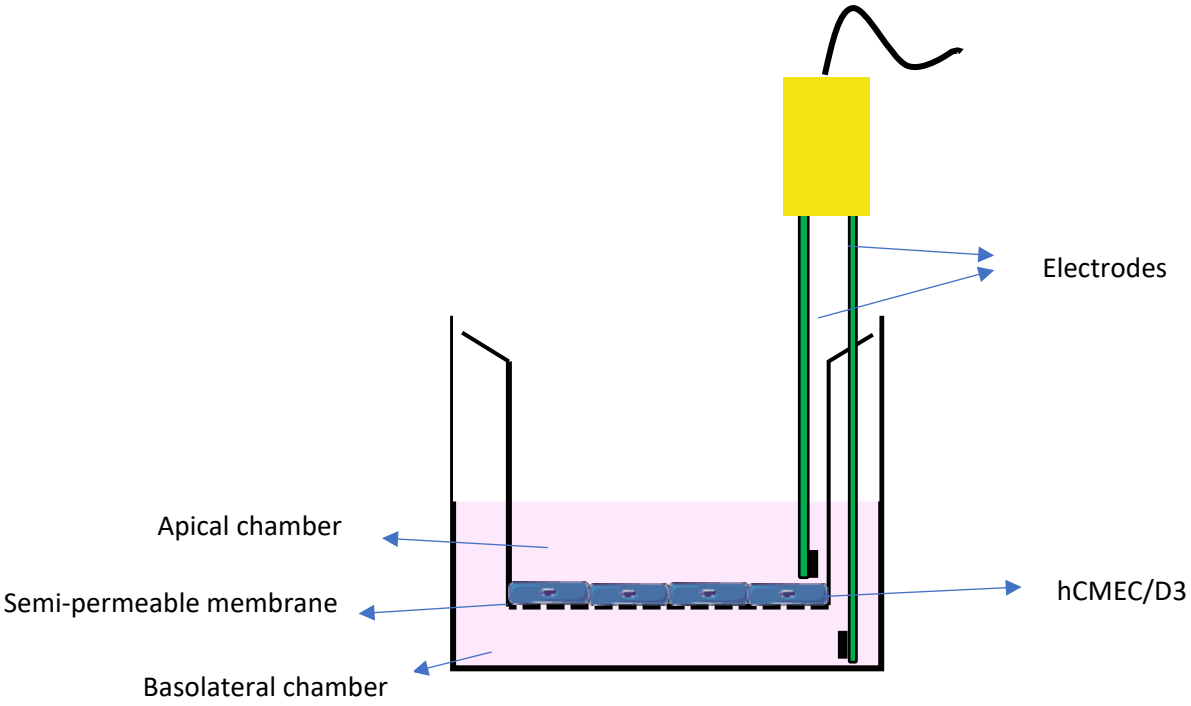

Figure 3. 1 Representative image of transwell setup. The electrodes are used to measure the resistance between the apical chamber with monolayer cells and basolateral chamber.

3.3.8.2 Optimisation of TEER readings

To optimise conditions of growth of hCMEC/D3 on transwells, cells were grown for 5 days and TEER measurement was taken daily. Briefly, transwell inserts (24-well PET membrane, 0.4 µm pore size, diameter (Starstedt, Germany)) were coated with Collagen- type I from rat tail (150 µg/ml; Sigma, UK) for one hr at 37ºC. The excess Collagen-I was aspirated and washed once with PBS. 500 µL of media was added to the bottom chamber and 200 µL to the top chamber and was incubated for one hr at 37ºC. The cells were seeded at a density of 30,000 cells/well (see ***Figure 3. 1***). Three readings were taken per well every day and TEER was monitored for 7 days.

Furthermore, to optimise the cell density needed for TEER readings, inserts were seeded with different concentrations of cells. Cells were seeded (10,000, 20,000, 30,000 and 40,000 cells/well) on inserts, allowed to form a monolayer and TEER was monitored over 7 days.

3.3.8.3 Changes in TEER after NMV treatment

Cells were seeded as descried in 2.3.12.1. An empty well with collagen-I coating was used as a blank control for this experiment. LPS (1 µg/ml; Sigma: L6893) was used as a positive control. An average of 3 TEER readings per well were taken every hour for 6 h and at 24 h (see ***Figure 3. 2*** for experimental setup). The TEER was calculated using the following equation:

$$TEER = (Average\ TEER\ of\ well - Average\ TEER\ blank\ ) * Surface\ Area\ of\ the\ transwell$$

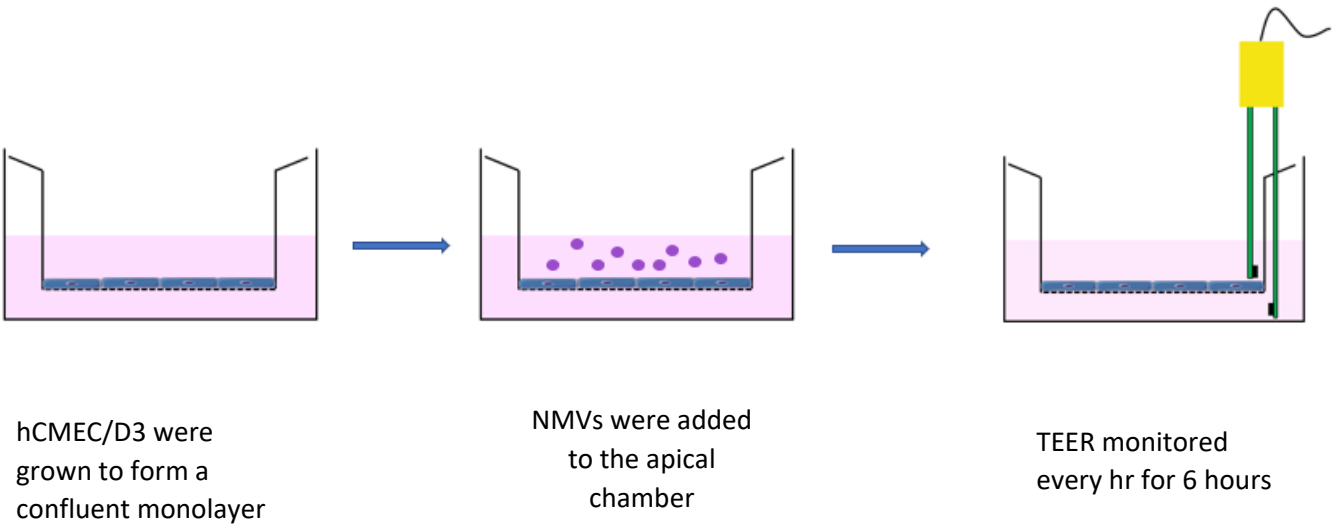

Figure 3. 2 Workflow of TEER measurement. A monolayer of hCMEC/D3 were grown to confluency on transwells and the TEER was monitored. Once they reached confluence, NMVs (or LPS as a positive control) were added to the apical side and TEER was monitored every hour for 6 hours.

3.3.9 Changes in permeability to tracer molecules across a confluent monolayer

3.3.9.1 Optimisation of FITC-Dextran

To measure changes in the flux of macromolecules of various sizes across a confluent monolayer of hCMEC/D3, tracer molecules of various sizes were used (FITC-Dextran, 10 kDa and 70 kDa (Sigma-Aldrich; USA)). Briefly, 30,000 cells were seeded on transwells (Merck-Millipore, Germany) and were grown for confluency for 4 days as described in 2.3.12.1. Cells were treated with either NMVs (200 NMV/ µL or LPS (1µg/mL). FITC-Dextran (1mg/ml) was added to the apical side at the start of the experiment (t=0). 100 µl of media was removed from the lower chamber after 0, 0.5, 1, 1.5, 2, 3, 4, 5 and 6h, and replaced by an equal volume of fresh medium. Fluorescence was measured using a plate-reader at excitation 485 nm and emission 535nm.

3.3.9.2 Change in flux of tracer molecules across a monolayer

After establishing the optimal time, % flux across a confluent hCMEC/D3 monolayer in response to NMV was assessed. The experiment was set up in a similar way as described in 2.3.13.1. After treating the cells with either NMV or LPS and FITC-Dextran, hCMEC/D3 were incubated at 37 °C for 6 hours. 100 µl of media was removed from the lower chamber and fluorescence measured using a plate reader.

3.3.10 Statistical Analysis

Statistical analysis was performed using GraphPad Prism analysis software. Each experiment was replicated using a minimum of three independent donors (n=3) to perform statistical analysis. Data is provided in text, tables and figures are presented as mean values and standard deviation (±SD) unless otherwise stated. Data was analysed using the applicable analyse of variance (ANOVA) or t-test. For multiple comparison, paired t-test, and one-way ANOVA with Dunnett's multiple comparison test was performed. P value <0.05 were statistically significant.

3.4 Results

3.4.1 RNA Integrity of control and treated cells

RNA was collected from 5 untreated and 5 NMV treated (5 different donors) hCMEC/D3 and assessed for both the RNA quality and quantity. On average, 363.0 ± 92.31 ng/µl RNA was eluted in 50 µl nuclease free water (***Table 3. 2***). The RNA integrity was analysed using the Bioanalyzer 2100 and the electropherograms assessed for the presence of two distinct peaks at 18S and 28S (ribosomal peaks), which are an indicator of RNA quality (***Figure 3. 3***).

Table 3. 2 RNA concentration of the samples used for microarray analysis. RNA concentration was measured using a Nanodrop spectrophotometer.

Sample ID	RNA Concentration (ng/µl)	A260/280 Ratio
1C	448.88	1.92
1NMV	465.39	1.98
2C	288.44	2.01
2NMV	305.85	1.89
3C	259.61	2.01
3NMV	249.41	1.85
4C	440.13	1.90
4NMV	284.81	2.00
5C	448.21	1.92
5NMV	447.22	1.97
Mean ± SD	**363.795 ± 92.3079**	**1.945 ±0.056421**

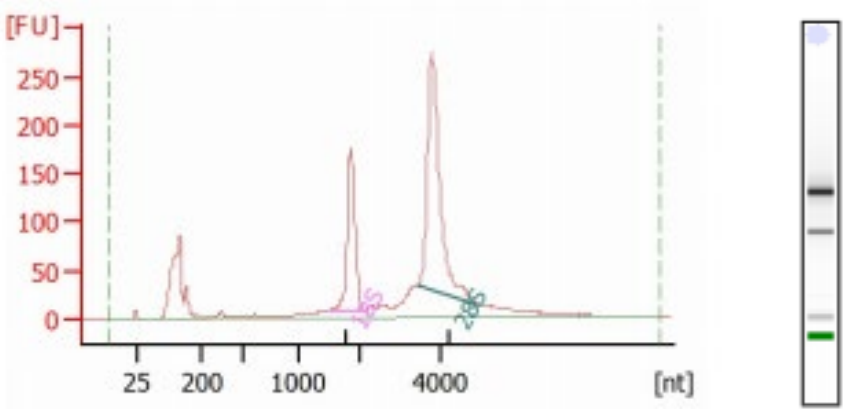

Figure 3. 3 Analysis of RNA integrity using the Agilent 2100 Bioanalyzer. A representative image of an electropherogram of RNA extracted from the cells. The distinct peaks at 18S and 28S rRNA indicate an intact and high-quality RNA. FU: fluorescence unit, nt: nucleotides.

For first strand cDNA synthesis, 10 ng RNA was added to each reaction mixture. The concentration of cRNA was measured using NanoDrop spectrophotometer (***Table 3. 3*** indicates the concentration obtained per sample). For the second cycle ds-cDNA synthesis, 20 µg of cRNA was added to each sample. After purification of ds-cDNA, the concentration of the yield was measured using NanoDrop Spectrophotometer (see ***Table 3. 4***).

Table 3. 3 cRNA concentrations of the samples for microarray measured using NanoDrop Spectrophotometer

Sample ID	cRNA concentration (ng/µl)	260/280 ratio
1C	3629.60	1.74
1NMV	2780.89	2.06
2C	451.93	2.10
2NMV	860.03	2.16
3C	512.60	2.13
3NMV	1158.13	2.16
4C	347.36	2.12
4NMV	1302.91	2.16
5C	2492.99	2.13
5NMV	1558.55	2.13

To fragment and label ds-cDNA, 6.6 µg of ds-cDNA was used to make the final concentration of 143.5 ng/µl. Purified ds-cDNA was fragmented using uracil-DNA glycosylase (UDG) and apurinic/apyrimidinic endonuclease 1 or APE 1. The success of the fragmentation step was assessed using the Agilent 2100 Bioanalyzer. The fragmented cDNA was labelled by TdT, which is linked to a biotin label. Samples were hybridised to the Affymetrix human arrays and analysed as detailed in section 3.3.3.

Table 3. 4 ds-cDNA concentrations of the samples for microarray measured using NanoDrop Spectrophotometer

Sample ID	ds-cDNA concentration (ng/µl)	260/280 ratio
1C	564.67	1.94
1NMV	538.35	1.94
2C	339.78	1.94
2NMV	502.04	1.91
3C	444.05	1.92
3NMV	563.28	1.94
4C	308.80	1.94
4NMV	512.02	1.93
5C	568.81	2.03
5NMV	459.47	1.95

3.4.2 Internal quality control (QC) of microarray samples

Quality control analysis was performed using Affymetrix Expression Console software and all samples were assessed for amplification, hybridisation, housekeeping gene expression and signal intensity. Overall, there were no outliers and clustering analysis demonstrated that samples clustered to two distinct groups (Section 3.4.3.1 ***Figure 3. 11***).

3.4.2.1Amplification Controls

Exogenous RNA controls were added to the samples to act as an independent control for cDNA synthesis and monitor the labelling process. These poly-A controls included probe sets for *subtilis* genes (*lys, phe, thr* and *dap*) and were added at various concentrations (1:100,000, 1:50,000, 1:25,000 and 1:6.667, respectively). They share no known homology to human genes. All the samples demonstrated a similar labelling efficiency (***Figure 3. 4***). However,

sample 2C showed higher signal for all the genes in increasing intensity. Similarly, samples 4C and 3C also displayed similar labelling efficiency. Overall poly-A controls were deemed ‘present’ in increasing signal intensities in respect to their known concentrations.

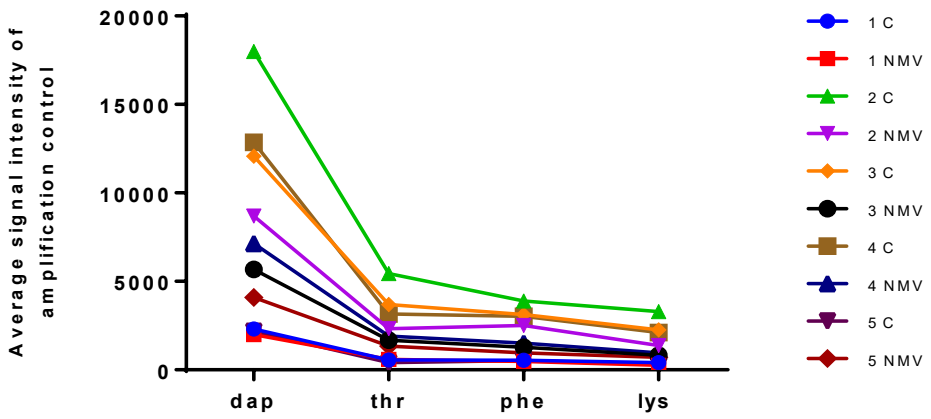

Figure 3. 4 Signal Intensity plots of amplification controls. Signal intensity of Poly-A RNA controls-dap, thr, phe and lys were plotted for all 10 samples. All the samples were deemed 'present' with increasing signal values in the order lys, phe, thr and dap**.**

3.4.2.2 Hybridisation controls

After amplification of cRNA, another set of exogenous RNA controls were added to the samples. These controls originated from *E. coli* bacteria (*bioB, bioC, bioD*) and P1 bacteriophage (*cre*). *BioB, bioC* and *bioD* are genes from the biotin synthesis pathway while *cre* is a recombinase gene. These bacterial spikes acted as hybridisation controls i.e. to normalise the consistency of hybridisation between all the samples present. All samples displayed a similar pattern of hybridisation, with the lowest intensity for *bioB* and the highest for *cre* (see ***Figure 3. 5***). This was expected as all the controls were added at various concentrations (1.5 pM, 5 pM, 25 pM and 100 pM respectively). It is predicted that a detectable signal for *bioB* should be present at least 50% of the time, with other hybridisation controls present with increasing signals in respect to their initial concentrations. Sample 4C had the highest signal but since it also follows the trend, the sample was deemed good. In summary, hybridisation controls were 'present' with increasing intensities with respect to their known concentrations.

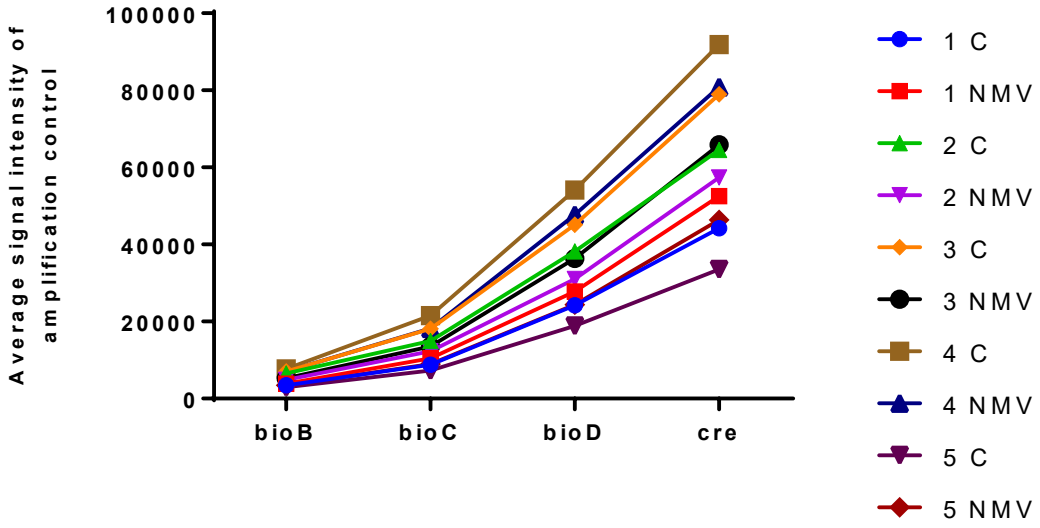

Figure 3. 5 Hybridisation control for control v NMV treated cells. Average signal intensity values of bioB, bioC, bioD and cre were plotted. BioB, bioC, bioD and cre are always 'Present' with increasing signal values, which is reflective of the relative concentrations of amplification controls.

3.4.2.3 Housekeeping controls

Expression of genes for *GAPDH* and *β*-actin were used to assess each RNA sample. The signal intensities of 3' probe sets were compared to 5' signal for both *GAPDH* and *β*-actin, as shown in Figure 3.5. Generally, this value should not exceed 3 for the 1-cycle assay, but the 2-cycle assay can give rise to higher values due to the additional amplification steps. The signal ratios were between 0.52 and 0.77 for *GAPDH* but *β*- actin ratios were quite high (2.49 - 4.2) (***Figure 3. 6***). *GAPDH* and *β*-actin ratio values for control and NMV treated array samples were similar and ratio values for *β*-actin exceeded 3, as expected as it is a 2-cycle assay. This is not unusual and may reflect a specific transcript related or image artefact. All controls were viewed collectively to assess sample/assay quality and deemed appropriate.

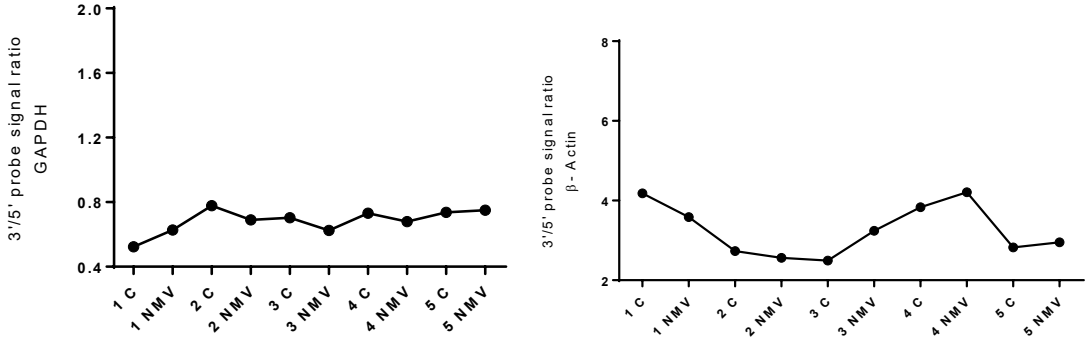

Figure 3. 6 3'-5' probe signal ration for the housekeeping genes. GAPDH and β-actin arrays. GAPDH and β-actin were used as internal controls to assess both the amplification and labelling process. The ratio between the 3' probe to 5' probe ratio is comparable between array samples.

3.4.2.4 Percentage Present

Percentage present (%P) is the number of probe sets called "Present" relative to the total number of probe sets. This was analysed using Affymetrix MAS5 algorithm. Although various things can affect %P value, replicates should have similar % P. Microarray samples reported similar % P values (48.9 – 58.6) across all the samples (***Figure 3. 7***)

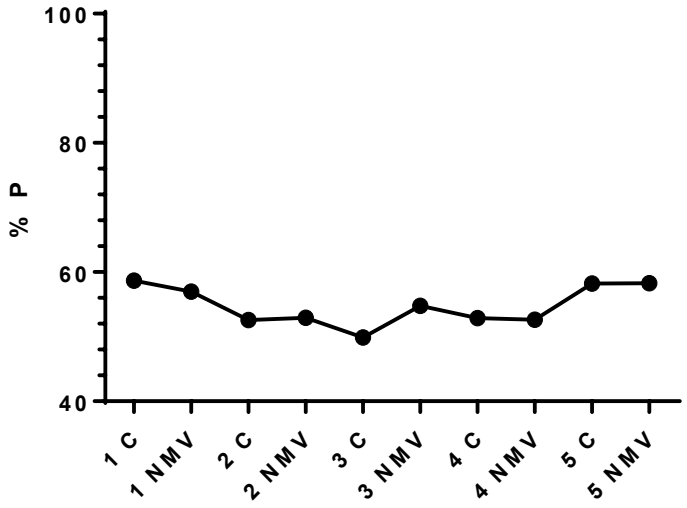

Figure 3. 7 Percentage present in control v NMV treated samples. %P is a value that indicates % of probes that are 'present' in the array. All 10 arrays displayed similar %P profile and were between the range 48.9 – 58.6.

3.4.2.5 Signal Intensity comparison

A histogram of signal intensities for each replicate allows visual comparison between the GeneChip arrays. The signals from the each of the ten arrays were compared in ***Figure 3. 8***. While there was considerable variability in signal intensities across the probe sets, the signal intensity of probes profile was comparable across the samples.

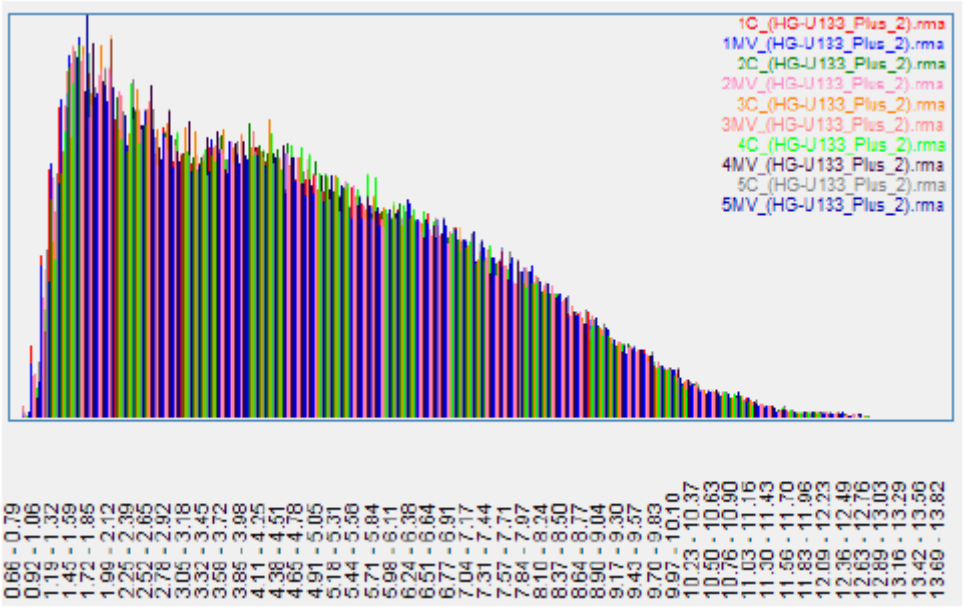

Figure 3. 8 Signal histogram of control v NMV treated arrays. Signal histogram plots the signal intensities of the probes of all the 10 arrays. Intensity of the profile should have comparable intensity across all the arrays. [C denotes control samples, MV denotes NMV treated samples; X axis – Log of signal; Y axis -frequency]

The expression of a probe-set can be compared to the median expression of this probe-set across all arrays, to determine the Relative log expression (RLE). The box plot (***Figure 3. 9***) indicates the RLE across all the arrays. RLE allows visualisation for unwanted variation in the overall data. In an ideal situation, the mean signal value will have box plots centred on zero, with similar size. RLE values for this microarray displays similar spread across all the samples.

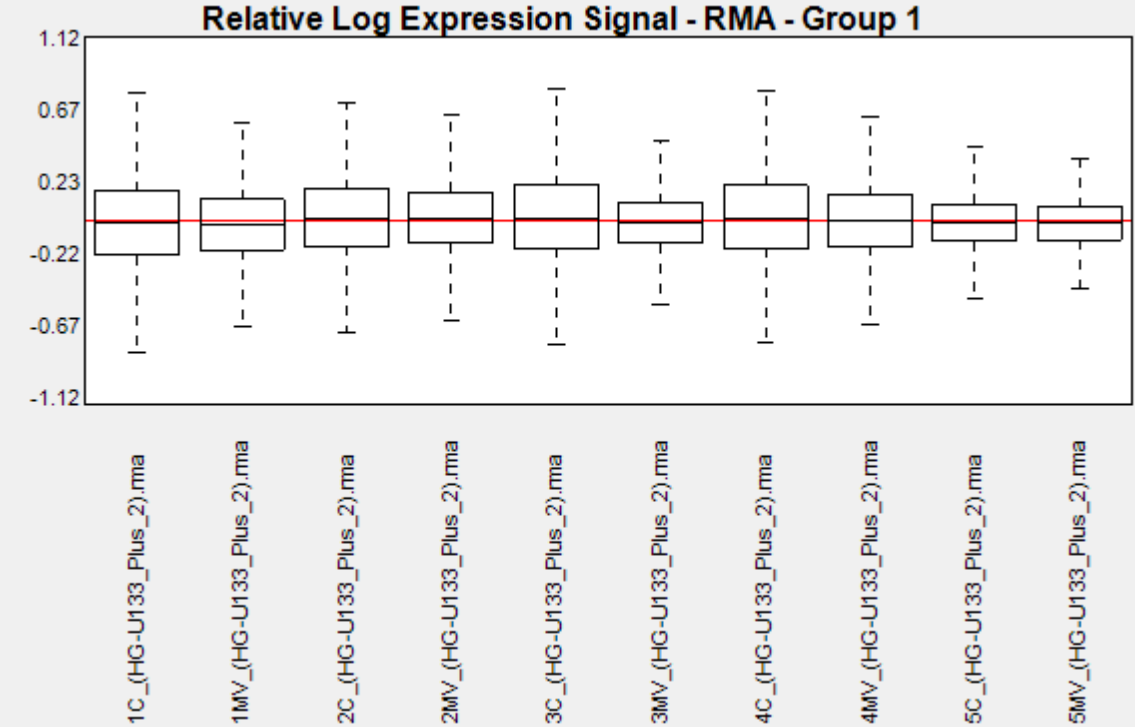

Figure 3. 9 Relative log Expression (RLE) plot for control v NMV treated arrays. RLE values of all 10 arrays demonstrated similar plots.

3.4.3 Correlation of arrays

Pearson's correlation was performed as shown in ***Figure 3. 10***. The minimal coefficient value is a good indicator of homogeneity of the dataset. For this experiment, the lowest coefficient was 0.964, which suggests that the arrays are comparable between each other.

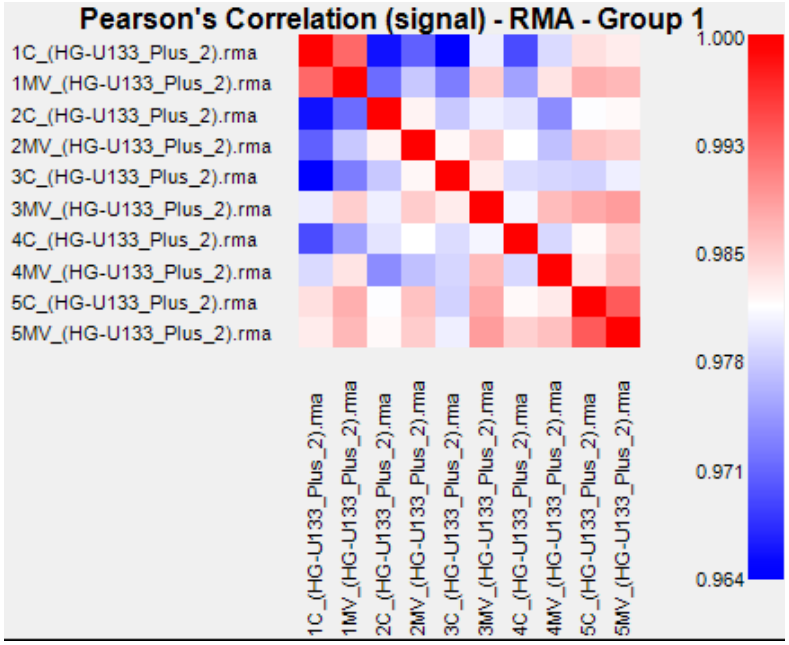

Figure 3. 10 Pearson's Correlation of control v NMV treated cells. Pearson's coefficient (r) measures the strength of the association between two variables. R values ranged between 1 and 0.964 for this set of arrays.

3.4.4 Microarray analysis

3.4.4.1 Clustering Analysis

Qlucore Omics software was used to analyse the changes in the transcriptome of hCMEC/D3 cells in response to NMVs. All the samples were normalised according to RMA method. Genes were considered significantly differentially expressed if they showed a minimum fold change ≥ 1.2 and $p \leq 0.05$. There were 932 genes that were significantly, differentially expressed, of which 363 were upregulated and 569 were down regulated by hCMEC/D3 cells in response to NMV internalisation. PCA was performed to identify the variance in the data sets. The two groups in this study (with and without NMV) clustered as shown in ***Figure 3. 11*A** demonstrating there were no sample outliers. The heat map generated also displayed clear distinction of significantly differentially expressed genes between the two groups in this study (see ***Figure 3. 11*B**). The complete list of significantly differentially expressed genes can be found in the GEO public database accession code GSE137111.

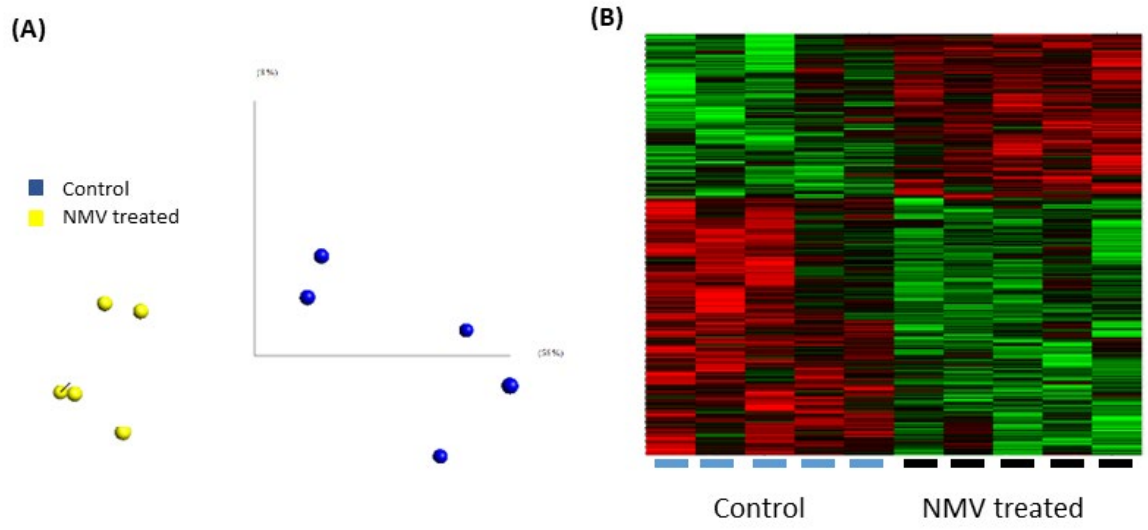

Figure 3. 11 Clustering analysis of control versus NMV treated hCMEC/D3 at 24 hours. **(A)** PCA plot demonstrates that control (blue) and NMV treated (yellow) separate into 2 distinct groups**. (B)** Heat map of control versus NMV treated. There were 932 genes that were significantly differentially expressed (red- up-regulated genes and green- down-regulated genes).

3.4.4.2 Functional group and pathway enrichment analysis

The list of total significantly differentially expressed genes (combining upregulated and downregulated) was analysed using the DAVID, an online software to identify significant changes in pathways and functional groupings within the dataset. Kyoto encyclopaedia of genes and genomes or KEGG pathway analysis identified ubiquitin mediated proteolysis (p - 0.034), SNARE mediated vesicular transport (p- 0.0163) and p38 pathway (p-0.032) (***Table 3. 5***). Functional grouping analysis with the highest stringency setting identified dysregulated genes that were associated with TJ proteins, vesicular transport and metal cluster binding (see ***Table 3. 6***). A list of top 20 upregulated and downregulated genes can be found in Appendix IV.

Table 3. 5 KEGG pathway analysis of significantly differentially expressed genes using DAVID and IMPaLa

Pathway	p-Value
Ubiquitin-mediated proteolysis	0.034
SNARE-mediated vesicular transport	0.0163
P38 pathway/Regulation of SMAD 2/3 signalling	0.0191
Coenzyme B biosynthesis	0.0209
Gap Junction degradation	0.0324

Table 3. 6 Functional grouping analysis of significantly differentially expressed genes

Functional Group	p-value	Number of genes
Tight junction proteins	0.0062	6
Vesicle mediated transport	0.0074	19
Protein transport	0.0019	18
RNA localisation	0.0011	9
Metal cluster binding	0.032	4
FY-rich terminals	0.0043	3

The data was further interrogated, and the upregulated and downregulated genes analysed separately. KEGG pathway analysis revealed that in the upregulated gene lists, the main pathways affected were SNARE interactions (***Figure 3. 12***) and ubiquitin mediated proteolysis (See ***Table 3. 7***). When downregulated gene lists were analysed using DAVID KEGG pathway analysis, there was only one pathway that were significantly dysregulated – pathways in cancer (differentially expressed genes -13; p-0.034).

Table 3. 7 KEGG pathway analysis of upregulated gene list using DAVID

Upreg Pathway Name	Differentially expressed genes	P Value
SNARE interactions in vesicular transport	4	0.029
Ubiquitin mediated proteolysis	7	0.034

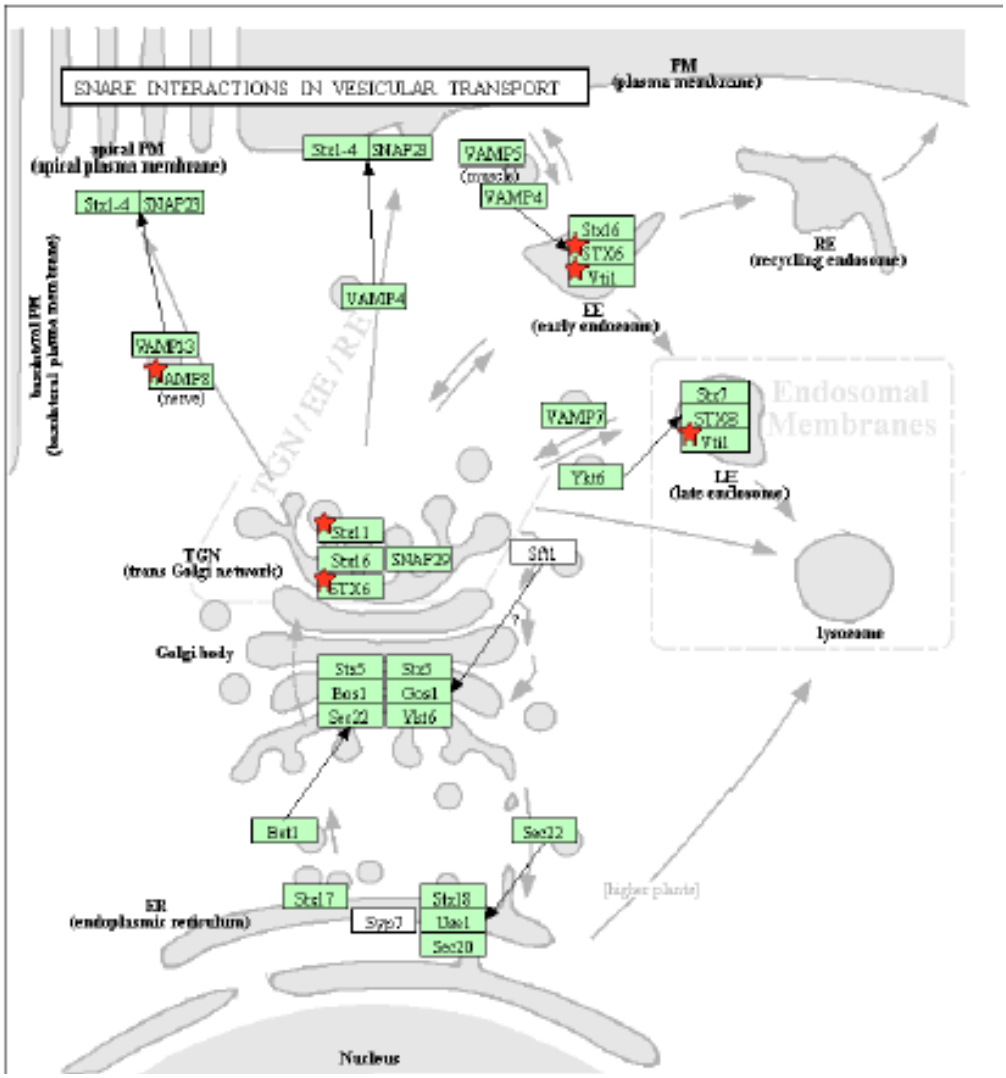

Figure 3. 12 KEGG pathway analysis using DAVID highlighted SNARE interactions in the vesicular transport. The red star indicates the genes that are significantly differentially expressed. Figure produced by DAVID analysis using KEGG pathway analyzer.

3.4.5 Functional Validation

The microarray analysis identified significant dysregulation of genes associated with vascular integrity. To validate this finding, we assessed the effect of NMVs on the permeability of a confluent monolayer of hCMEC/D3.

3.4.5.1 Optimisation of plating density for transwell experiments

To identify the optimal conditions to conduct TEER measurements and to study the flux of FITC-dextran, various conditions were tested. A range of cell densities were plated (two per condition) and the TEER recorded for seven days. The average TEER recorded for each plating density is summarised in ***Table 3. 8***.

A plating density of 10,000 cells/well showed a slow increase in TEER over 7 days, with the average highest TEER recorded at 18 $\Omega.cm^2$. A plating density of 30,000 cells per well displayed the highest TEER at 28 $\Omega.cm^2$. Although 40,000 cells/well also has displayed a similar TEER at 25 Ωcm^2., the cells quickly became confluent and there was substantial cell death.

For experiments hereafter, a plating density of 30,000 cells/well were used and TEER time course experiments were performed on day 4.

Table 3. 8 Average TEER measurements over 7 day period.

Plating Density	Day 1	Day 2	Day 3	Day 4	Day 5	Day 6	Day 7
	TEER ($\Omega.cm^2$)						
10,000	7	8	9	12	15	18	17
20,000	11	13	15	18	21	21	19
30,000	12	15	22	28	27	24	20
40,000	13	19	25	24	18	13	14

3.4.5.2 NMVs significantly reduce TEER of a confluent monolayer

To investigate if NMVs have an effect on the TEER of a confluent monolayer of hCMEC/D3, a transwell system was utilised. NMVs were added to the apical chamber (top) and TEER was measured for 6h. NMVs significantly reduced the TEER of the monolayer after 3h ($p=0.0083$) and maintained the reduction after 4h ($p= 0.0234$), 5h ($p= 0.0042$) and 6h ($p= 0.0001$). LPS was used as a positive control, as it is known to decrease TEER of a monolayer (Dohgu and Banks, 2008; Hu et al., 2019), however a significant reduction in TEER ($p= 0.0193$) was only detected after 6h incubation with LPS (***Figure 3. 13***). Each experiment was performed in duplicates and was repeated with three independent donors.

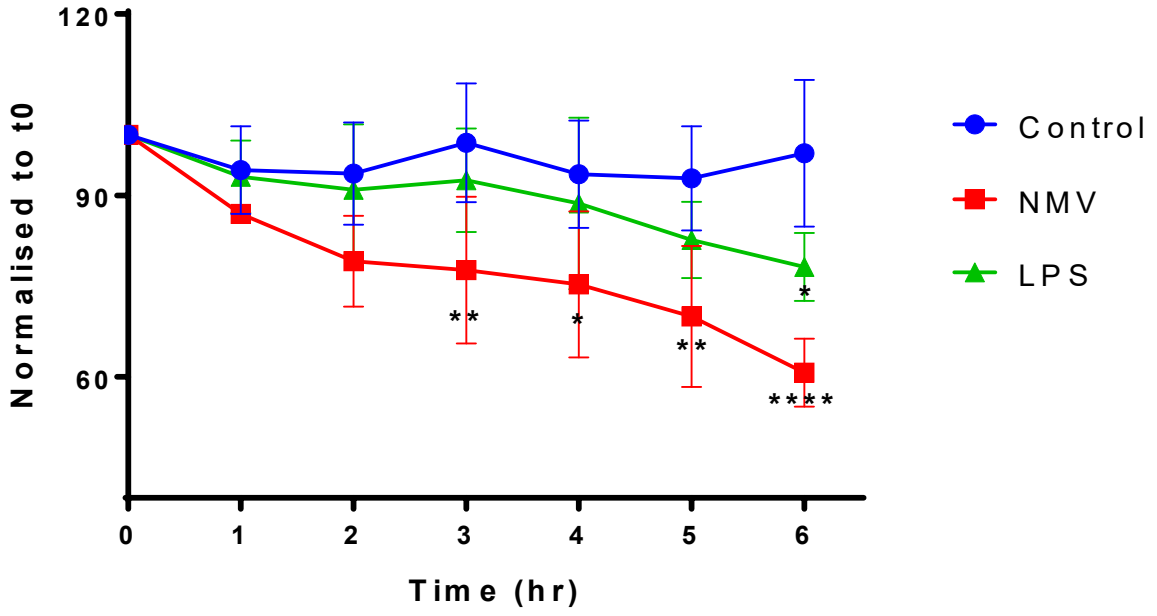

Figure 3. 13 NMV significantly decrease the TEER of a confluent monolayer of hCMEC/D3. A confluent monolayer of hCMEC/D3 on transwells were either treated with NMVs or LPS and TEER was measured every hour for 6h. NMV significantly reduced TEER within 3 hours. Data represent three independent experiments, expressed as mean ± SD. Statistical significance was measured using one-way ANOVA with Dunnett's multiple comparison test, *p<0.05, **p<0.01, **** p<0.0001.

3.4.5.4 Optimisation of time course of flux of FITC- Dextran

The flux of FITC-dextran (70 kDa) increased in the control transwell system over time (see ***Figure 3. 14***). In response to NMV internalisation, there was a significant increase in the flux of FITC-dextran across a confluent monolayer of hCMEC/D3 over the 6h ($p<0.0001$). LPS also induced a significant increase in the flux of FITC-dextran across a confluent monolayer over the 6h ($p=0.0011$). While the amount of FITC-dextran crossing the monolayer was greater in the NMV-treated group compared to the LPS-treated positive control group at all time points, it was not significantly different ($p=0.0685$).

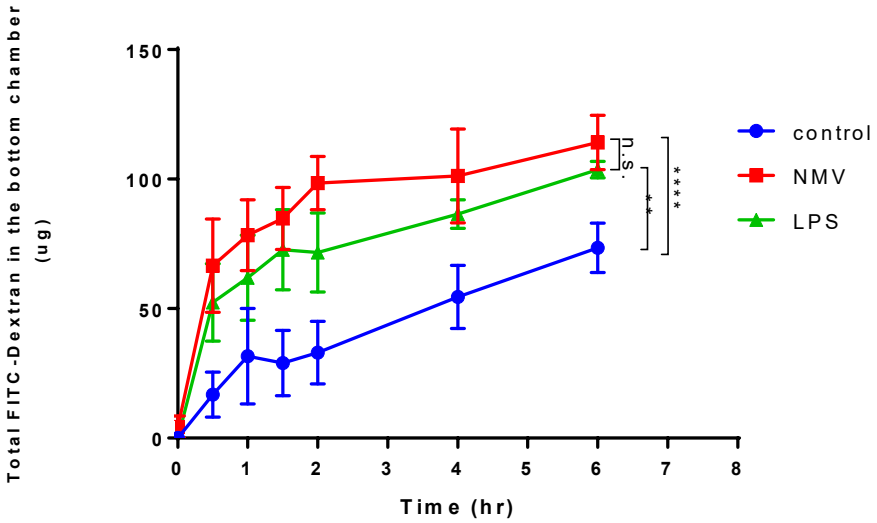

Figure 3. 14 NMV increases permeability to FITC-dextran of a confluent hCMEC/D3 monolayer. To a confluent monolayer grown on a transwell, either NMV or LPS was added with FITC-Dextran and the flux was measured for 6h. Flux of FITC-dextran increased significantly after 6h. NMV caused increased permeability than LPS. Statistical different was measured using a two-way ANOVA with Tukey's multiple comparison test. Data represent three independent experiments, expressed as mean ± SD. **p<0.01, ****p<0.0001, n.s. – not significant.

3.4.5.5 Change in permeability of monolayer

To assess NMV-induced differences in the flux of differing sized molecules, the permeability of a confluent monolayer for different size of FITC-dextran (10 kDa and 70 kDa) was assessed. As demonstrated in ***Figure 3. 15*** **A&B** the flux of 10 kDa FITC-dextran is greater than the flux of 70kDa FITC-dextran, in response to NMV internalisation. There was a 40.8 ± 3.3% increase in flux of 10kDa FITC-dextran to the basolateral chamber in response to NMV (p=0.0024). Similarly, paracellular flux of 70kDa FITC-dextran was also significantly increased when NMV were present (20.93± 4.794%; p=-0.0272). LPS was used as a positive control and significantly increased the flux of 10kDa FITC-Dextran (36.6±5.298%; p=0.0034) (***Figure 3. 14***) but not 70kDa FITC-dextran (p=0.093). No cell detachment was observed during the 6 hours of this experiment.

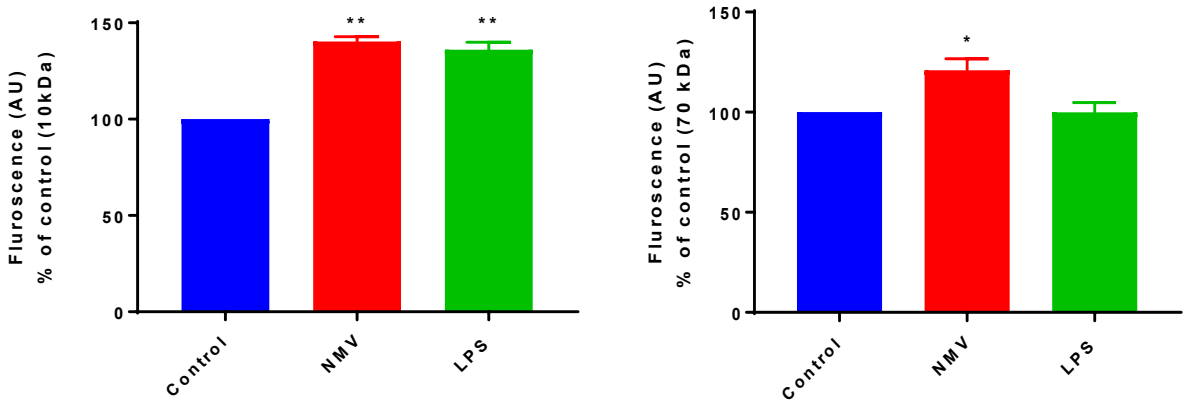

Figure 3. 15 NMV significantly increase the permeability of hCMEC/D3. NMV significantly increase the flux of **(A)** 10 kDA dextran and **(B)** 70 kDa dextran across a confluent monolayer of hCMEC/D3. Data represent 3 independent experiments, expressed as mean ± SD. Statistical significance was measured using one-way ANOVA with Dunnett's multiple comparison test, *p<0.05, **p<0.01.

3.5 Discussion

In this chapter we demonstrate that the internalisation of NMV impacts the transcriptomic profile of hCMEC/D3, significantly increasing the permeability and reducing the integrity of human brain endothelial cells. This is the first study to report the impact of NMV on human brain endothelial cells (Ajikumar et al., 2019), as to date, NMV have only been reported to significantly impact the gene expression profile of HUVECs (Dalli et al., 2013).

3.5.1 Functional Validation

As NMV-induced dysregulation in the expression of tight junction proteins was identified in the array analysis, we performed functional validation using a transwell system. In support of our transcriptomic data, the functional studies confirmed that NMV significantly increased the permeability of a confluent monolayer of hCMEC/D3. When the BBB is disturbed, the flux of tracer molecules increases across the endothelial cell monolayer (Tai et al., 2010), allowing us to utilise this effect to study changes at the BBB. In the current study we used tracer molecules of two different sizes (10 kDa and 70 kDa) to represent different sizes of molecules present in the blood. NMV significantly increased the flux of FITC-dextran (both 10 kDa and 70 kDa) across a confluent monolayer of hCMEC/D3. Notably, flux of 10 kDa molecules were higher compared to 70kDa, suggesting that NMV have a greater effect on the flux of smaller molecules through the monolayer. Notably, most cytokines have smaller molecular weights (Akdis et al., 2016) and increased flux of cytokines across the BBB can modulate the neuroinflammatory response (Biesmans et al., 2013; Henry et al., 2009).

Another approach to assessing the permeability of an endothelial barrier is by measuring the TEER of a confluent monolayer. Our study has confirmed that NMV significantly decrease the integrity and significantly increase the permeability of a confluent monolayer of hCMEC/D3. This supports other studies that have demonstrated increased BBB disruption by MV isolated from plasma *in vitro* (Edrissi et al., 2016) and exosomes *in vivo* (Yang et al., 2015). While our results confirm previous findings that hCMEC/D3 have a TEER ranging from 20 to 30 Ωcm^2 (Eigenmann et al., 2013; Weksler et al., 2013) it should be noted that this does not reflect the TEER of the BBB *in vivo* (Butt et al., 1990). Even with these study limitations, we demonstrate

that NMV cause dysfunction of the BBB resulting in increased permeability and reduced vascular integrity.

3.5.2 Internalisation of NMV is associated with increased vesicular transport

Unsurprisingly, NMV induced an increased upregulation of soluble *N*-ethylmaleimide-sensitive factor attachment protein receptor (SNARE) pathway genes in human brain endothelial cells, reinforcing the findings of Chapter 2 that NMV require some type of docking mechanism for their internalisation. Generally, fusion of EVs with plasma membrane is Ca^{2+} -dependent, and acidic conditions are also known to enhance their binding (Parolini et al., 2009). As the endosomes are known to be slightly acidic, it may enhance the binding of EVs once they are internalised.

SNARE proteins have been studied extensively at synapses as neurons use vesicles for neurotransmission (Han et al., 2017; Ulloa et al., 2018). There are around 40 SNAREs identified in mammalian cells (Jahn and Scheller, 2006). Transport of MVs once internalised is still much debated. SNARE proteins are involved in intracellular vesicular traffic and can be found on endosomes and the plasma membrane. SNAREs are also implicated in MV biogenesis and release (Beer and Wehman, 2017). Some of the group of proteins that make SNARE complexes include VAMP and syntaxin of which six transcripts were up-regulated in NMV treated hCMEC/D3. It is only recently that scientists have started exploring the role of SNARE protein complexes with EVs after internalisation. It was recently reported that distinct SNAREs are recruited during the budding of a vesicle and this can determine the target cell (Koike and Jahn, 2019). This demonstrates that SNARE proteins are crucial for fusion with the target cell and the up-regulation of SNARE pathway indicates that some of these proteins might be upregulated after the initial fusion to help sort out the cargo. Further experiments are required to address the role of SNARE protein complexes in the context of NMVs and how they can be implicated in BBB disruption. To date, no studies have reported the role of vesicular transport proteins in the intracellular sorting of NMVs, despite being an integral part of how they may impact gene expression.

3.5.2 NMV impact signalling pathways

The internalisation of NMVs significantly impacted the transcriptomic profile of several key pathways, including p38 MAPK pathway in hCMEC/D3. The p38 MAPK mediates the inflammatory response by upregulating pro-inflammatory cytokine production (Schieven,

2005). Increased immunoreactivity of MAPK is present in Aβ plaques and NFT in AD, and is associated with the earlier stages of plaque development (Hensley et al., 1999; Pei et al., 2001; Sun et al., 2003). Moreover, MAPK activation and downstream phosphorylation is reduced in the later stages of AD (higher Braak stages)(Rosenberger et al., 2016). Activation of MAPK can lead to microglial activation (Bhat et al., 1998)(Culbert et al., 2006; Giovannini et al., 2002). Although p38 MAPK pathways are involved in the pathogenesis of AD (Lee and Kim, 2017; Zhu et al., 2002), it is only recently its activation in endothelial cells has been studied in depth. Activation of MAPK signalling leads to increased transcytosis in brain endothelial cells *in vitro* (Miller et al., 2005). Furthermore, monocyte EVs can activate MAPK signalling thereby activating endothelial cells, and preventing the release of EVs from activated monocytes can inhibit inflammation in brain endothelial cells (Dalvi et al., 2017). Other studies have shown that activation of MAPK signalling in brain endothelial cells can induce dysregulation of TJ proteins, thereby leading to BBB dysfunction (Qin et al., 2015). Together with the present study these findings suggest that NMVs activate MAPK, which contributes to BBB dysfunction thereby causing increased influx into the brain, leading to the activation of microglia and an increased neuroinflammatory response.

Most therapeutic inhibitors of MAPK kinases have been developed to treat peripheral inflammatory conditions, such as rheumatoid arthritis, and are intentionally made to not be able to cross BBB (Munoz and Ammit, 2010; Peifer et al., 2006). However, in more recent times, studies have focussed on small molecules that can cross the BBB and target MAPK in the CNS, as reviewed in detail (Lee and Kim, 2017). Although MAPK signalling is a complex pathway interconnected with many other kinases, we need to understand it fully as it is emerging as a therapeutic target for neurodegeneration.

Genes directly or indirectly affected by the p38 MAPK pathway include *TGFBR1*. NMVs contain TGF-β (Pitanga et al., 2014), a pleiotropic cytokine that is released in response to various insults, including stroke, hypoxia and Aβ plaques (Caraci et al., 2008; Dobolyi et al., 2012; Doyle et al., 2010). TGF-β binds to TGFBR (there are two types – type I and II), forming a receptor complex that can activate Smads which translocate into the nucleus and regulate the gene expression (Derynck and Zhang, 2003). TGFBR1 expression in endothelial cells is reported to mediate vessel permeability (Lebrin et al., 2005), by regulating TJPs and thus indirectly controlling paracellular permeability *in vitro* (Ishihara et al., 2008). Activation of this pathway has also been shown to increase substrate permeability into the brain *in vivo* by mediating changes in expression of TJPs in rat brain endothelial cells (Ronaldson et al., 2009).

All of this evidence points towards a role of TGFBR1 in regulating cerebrovascular permeability. The finding of the present study suggests that during systemic inflammation the internalisation of NMV impacts TGFBR1 expression which may result in BBB dysfunction.

Tumour Protein P53 Inducible Nuclear Protein 1 (*TP53INP1*) is a susceptibility gene for AD identified through GWAS analysis (Escott-Price et al., 2014), and was identified as significantly differentially expressed in the current study. *TP31INP1* is a p53 target gene that promotes cell growth and is a tumour suppressor (Wei et al., 2012). *TP53INP1* is also one of the highly conserved genes among mammals and is overexpressed during the inflammatory response both *in vitro* and *in vivo* (Jiang et al., 2004; Seillier et al., 2015; Tomasini et al., 2001). It is also a downstream target of miR-155 (Zhang et al., 2015), a miRNA that is known to be enriched in NMVs (Gomez et al., 2020). MiR-155 has the ability to alter brain endothelial cell permeability *in vitro* by targeting TJ proteins and focal adhesions (Lopez-Ramirez et al., 2014). Furthermore, miR-155 is altered in post mortem samples of AD patients (Culpan et al., 2011). Together these findings suggest that NMVs can exert their effect on BBB through various mechanisms, one of which is through miR-155.

Similarly, another candidate gene identified in the microarray analysis was mitogen activated protein kinase (*MAP3K1*), which has the ability to activate ERK pathway, and which in turn has an anti-apoptotic effect (Yujiri et al., 1998). Although there are limited studies of the role of MAP3K1 in relation to AD, its role in induction of inflammation is crucial, as it may induce inflammation at BBB, causing further release of cytokines and changes in brain homeostasis (Derada Troletti et al., 2019; Wu et al., 2017).

NIMA related kinase 1 *(NEK1*) is a member of a highly conserved kinase family. This serine/threonine kinase has various roles including cell-cycle regulation and DNA damage repair (Chen et al., 2009; Pelegrini et al., 2010). Similarly, BH3 interacting domain death agonist (*BID1*) is a B-cell lymphoma 2 (BCL2) protein and has a role in regulation of inflammatory response to injury or stress. *BID1* can interact with downstream targets of MAP3K1, mainly IKK complex (Yeretssian et al., 2011). Both of these genes can feed into p38 pathway and can regulate inflammation and DNA repair. As, discussed earlier, this can intensify *MAP3K1* response i.e., increase inflammation, causing dysregulation at BBB.

BH3 interacting domain death agonist (BID-1), is a member of the BCL-2 family, which plays a crucial rule in the inflammatory process. BID can modulate NOD1, which can ultimately impact NF-κB signalling (Yeretssian et al., 2011). Interestingly, caspase-8, a pro-apoptotic

protease also interacts with BID-1, initiating intrinsic pathways (Van Herreweghe et al., 2010). However, not much research has focused on BID-1 interaction in the context of neurodegeneration. More detailed research is needed to understand how this pro-apoptotic protein can drive changes in the brain endothelium.

Finally, one of the major functional pathways that was identified by the microarray analysis was ubiquitin mediated proteolysis. Ubiquitination is a process in which proteins are labelled for proteasomal degradation. This process is crucial as it helps in clearing damaged and aggregated proteins (Vilchez et al., 2014). In AD, this process can be disrupted (Ciechanover and Kwon, 2015), leading to aggregation of misfolded proteins. Matrix metalloproteinases, such as MMP-9, are significantly higher in NMV released from activated neutrophils (Long et al., 2019). MMPs can impact the BBB by either cleaving junctional proteins or by proteolysation of junctional proteins. Two of the major substrates of MMP2/9 are occludin and claudin-5, which are major junctional proteins at BBB (Stamatovic et al., 2016). Since proteolysis is crucial for changes at the BBB, dysregulation of this pathway can lead to the breakdown of BBB. Although this process is dynamic, and depending on the duration of the stimulus, proteins could be degraded for a longer timer, leading to a severe barrier dysfunction. More studies are needed to understand how NMV can cause changes to the proteolytic pathway in the BBB.

3.6 Conclusion & major findings

- This is the first study to detail the transcriptomic changes of human brain microvascular endothelial cells in response to NMV internalisation *in vitro*.
- Bioinformatic analysis of the array datasets implicate NMV induced changes in gene expression affecting multiple pathways and functional groups, including tight junction proteins, p38 MAPK pathways and proteolysis.
- Functional validation of changes in vascular integrity using a transwell system demonstrated that the internalisation of NMVs significantly increases the permeability and decreases the electrical resistance of a confluent monolayer of hCMEC/D3.

Chapter 4: Transcriptomic profiling of cerebral microvessels in age-associated white matter lesions

4.1 Introduction

To date, most of the research into dementia has focused on the changes in the cortex, but post-mortem tissue studies have highlighted that white matter pathology is also a key contributor to disease that can develop independently of cortical pathology, and is associated with co-morbidity pathologies including diabetes, vascular diseases and hypertension (Bronge et al., 2002; Brun and Englund, 1986; Kalaria, 2002, 2000).

Cerebral white matter is an area rich in neuronal connections that are essential for processing information (Vernooij et al., 2008). It is enriched with fibre pathways that connect cortical and subcortical structures (Schmahmann et al., 2008) and is responsible for effective cognition and behaviour (Madden et al., 2009). Lesions in this region, often referred to as white matter lesions (WML), present as high signal intensity areas in T_2- weighted and diffusion tensor magnetic resonance imaging (MRI) (Ovbiagele and Saver, 2006). WML, also known as white matter hyperintensities, are a common feature of the ageing brain (over 65 years) (Knopman et al., 2003; Wharton et al., 2011) and are considered to be a part of normal ageing (Ylikoski et al., 1995). WML are neuropathologically characterised by extensive degradation of myelin and axonal loss, which is associated with widespread gliosis along with extensive microglial activation (Simpson et al., 2007; Tomimoto, 2015). Systematic reviews and meta-analyses have demonstrated the association between WML formation and rapid cognitive decline (Debette and Markus, 2010; Gunning-Dixon and Raz, 2000), and have revealed that subjects with WML have a higher risk of stroke, dementia and death. Furthermore, population representative studies have indicated that WML are an independent risk factor for dementia (Fernando et al., 2006; Prins et al., 2004). Changes in WM volume has detrimental effects on the structure and function of the brain, even in healthy individuals (DeCarli et al., 1995). These microstructural changes play a key role in cognition, as demonstrated in patients with traumatic brain injury (Kinnunen et al., 2011). WML are often observed more frequently in patients with mild cognitive impairment (MCI) and early AD compared to age-matched healthy controls,

suggesting WM damage is an early event contributing to the progression of dementia (Medina et al., 2006; Strozyk et al., 2017), and are a risk factor for progression of MCI to AD (Clerici et al., 2012). WML also play a role in progression of AD and correlate significantly with cognitive dysfunction (O'Brien et al., 2003; Peters and Sethares, 2002), suggesting that loss of WM integrity is an important factor in driving the disease.

WML can be classified by their neuroanatomical location: deep subcortical lesions (DSCL) – lesions in the deep white matter and periventricular lesions (PVL) – located immediately adjacent to the ventricles. Histological examination of both lesion subtypes indicates many similarities such as myelin loss, astrogliosis and increased microglial reactivity, but there are differences in the microglial phenotype depending on the location of the lesion: DSCL contain high levels of microglial with a phagocytic phenotype while PVL contain higher levels of microglia with an immune activated phenotype (Simpson *et al.*, 2007; Boche, Perry and Nicoll, 2013; Waller *et al.*, 2019). This chapter will focus on vascular transcriptomic changes associated with DSCL.

There are several causes attributed to the formation of WML, including (i) cortical pathology resulting in axonal loss, (ii) cerebral hypoperfusion and a resulting hypoxic environment and (iii) dysfunction of the blood brain barrier (BBB) (Fernando et al., 2006, 2004; Simpson et al., 2007, 2010; Wharton et al., 2011). There are excellent reviews of (i) and (ii) (Wharton et al., 2011), but this chapter focuses on the hypothesis that BBB dysfunction contributes to the pathogenesis of WML formation and cognitive impairment.

Although there is extensive research on BBB dysfunction in ageing and dementia, the pathological mechanisms underlying disruption of the barrier are poorly understood. In the ageing brain, there are reports of increased presence of serum proteins which are normally excluded from the CNS, such as albumin or fibrinogen (Farrall and Wardlaw, 2009; Simpson et al., 2010). In ageing mice, there is increased IgG extravasation into the brain, which is associated with increased neuroinflammation, astrogliosis and a significant reduction in occludin expression (Elahy et al., 2015; Goodall et al., 2018). Post-mortem analysis of WML indicates evidence of BBB dysfunction which is associated with the increased immunoreactivity of serum proteins, such as fibrinogen and albumin (Hainsworth et al., 2017; Simpson et al., 2010). The presence of serum protein immunoreactive clasmatodendritic astrocytes within WML also demonstrates that astrocytes have the ability to uptake serum

proteins, which may modulate their function and enhance neuroinflammation. Several MRI studies also support that extravasation of serum proteins is common in the ageing brain (Huisa et al., 2015; Topakian et al., 2010; Wardlaw et al., 2009; Zhang et al., 2017), and this BBB dysfunction in WML is associated with dementia (Hainsworth et al., 2017). Together these studies demonstrate that while dysfunction of the BBB occurs during normal ageing, it is also a prevalent feature of WML. However, the contribution of this vascular dysfunction to the pathogenesis of WML, and mechanism(s) underlying BBB damage is currently unknown.

One of the most powerful tools in the recent times is the advancement in the technologies that can be employed to characterise transcriptomic changes between healthy and disease status. Transcriptomic profiling enables scientists to identify and target molecular pathways related to disease and enables the identification of novel therapeutic targets. Microarray analysis is a powerful platform to characterise the changes in gene expression in relation to disease. In most cases, complex interactions with multiple pathways significantly contribute to the progression of the disease. To date there are only a few studies reporting microarray analysis of ageing WM in humans in the context of dementia (Ritz et al., 2016; Simpson et al., 2009; Wang et al., 2011). While these studies have identified transcriptomic changes in WML and identified potential mechanisms underlying pathology, these studies were performed on a heterogeneous population of cells from total tissue extracts and did not exclusively focus on the gene expression changes associated with cerebral endothelial cells.

Identifying transcriptomic changes associated with the BBB in WML will enable key gene expression changes associated with vascular pathology to be determined. In addition to studying established WML, it is also important to study the radiologically normal appearing white matter (NAWM) surrounding lesions as this approach will determine if the transcriptomic changes are confined to the lesion or extend beyond it.

The current study was performed on well-characterised cases from the Cognitive Function and Ageing Study (CFAS) neuropathology cohort. CFAS is an ageing population-representative study of individuals in UK over the age of 65. Over 18,000 individuals were invited to participate in the study, selected from the GP register based solely on their age and not on any clinical information, making this a true ageing population-representative study. The cohort underwent regular cognitive testing approximately every 5 years, and completed questionnaires to enable data on lifestyle, medication and general health to be collected. A sub-group of

approximately 550 respondents donated their brain to the CFAS neuropathology study, enabling pathological changes to be assessed in relation to dementia status (Neuropathology, 2001).

A previous study assessed the transcriptomic profile of age-associated WML in the CFAS cohort, identifying significant increases in genes associated with tissue remodelling, the immune response and apoptosis (Simpson et al., 2009). However, this study examined the gene expression profile of whole tissue extracts which may have masked specific changes at the BBB. To limit the interference due to whole tissue sampling, a technique called immuno-Laser Capture Microdissection (LCM) was used in the current study to isolate cerebral endothelial cells from the tissue. This method combines two techniques to isolate an enriched population of interest. Firstly, a modified immunostaining protocol is employed to visualise specific cells of interest, and this is then combined with standard LCM. This involves firing a laser over the immunopositive cells causing the cell to adhere to the film, which can be then removed from the tissue. LCM has allowed scientists to study specific cell populations isolated from post-mortem tissue, including astrocytes (Garwood et al., 2015; Waller et al., 2016) and neurones (Simpson et al., 2016). When combined with microarray analysis this technique allows transcriptomic profiling of the cells of interest. LCM allows researchers to identify gene expression changes between normal physiological conditions versus disease status, thereby enabling potential biologically relevant gene expression changes to be identified.

To date, only a few studies have reported employing both LCM and microarray analysis to understand the gene expression changes associated with neurological disease (Cunnea et al., 2010; Jin and Xia, 2010; Mycko et al., 2012; Waller et al., 2016). Enrichment of a specific cell population of interest by LCM allows accurate cell-specific gene expression profiling and provides higher specificity of differentially expressed genes compared to transcriptomic analysis of bulk tissue selection (Klee et al., 2009). Therefore, the current study utilised immuno-LCM to isolate endothelial vessels from DSCL, NAWM from lesional cases and control WM from non-lesional cases and performed microarray analysis to analyse transcriptomic changes in the endothelial cells in these three groups. This approach enables the elucidation of transcriptomic changes associated with microvessels in age-associated WML and may identify novel candidate genes for therapeutic targeting.

4.2 Aims and Objectives

While WML are a common feature of the ageing brain, their presence is a significant risk factor for dementia. Histological characterisation of WML has demonstrated they are associated with BBB dysfunction, which may drive the neuroinflammatory response and impact on cognition. Previous studies have assessed the transcriptomic profile of WML but these whole tissue studies may have masked BBB-specific gene expression changes. Therefore, this study aimed to test the hypothesis that BBB dysfunction contributes to the pathogenesis of WML formation and cognitive impairment. Specifically, this chapter aims to:

- Isolate microvessels from DSCL, radiologically normal appearing WM (NAWM) from lesional cases and NAWM from non-lesional (control) cases using LCM

- Assess the transcriptomic profile of the microvessels to identify specific BBB-associated gene expression changes which may contribute to lesion pathogenesis.

4.3 Materials and Methods

4.3.1 White Matter Sampling and Case Selection

Frozen brain tissue samples were obtained from the Cognitive Function And Ageing Study (CFAS) neuropathology cohort (Ethical Committee Approval REC Reference 15/SW/0246; Appendix II). CFAS is a multi-centred, population-based study of the ageing population (> 65y). Upon brain donation, one hemisphere was fixed in formalin and coronal slices underwent T2 magnetic resonance imaging (MRI). The contralateral hemisphere was coronally sliced and snap frozen. Two independent radiologists who were blinded to any clinical information scored MRI scans of the formalin-fixed samples, and based on these scores, the cases were classified into lesional and non-lesional control cases. For this project, matched CNS areas from 5 non-lesional control cases, 5 lesional cases and 5 radiologically normal appearing white matter (NAWM) from lesional cases were used. The MRI scans of the formalin-fixed hemisphere were used to guide sampling of the contralateral frozen hemisphere, as reports suggest WML are symmetrical (Wardlaw et al., 2013b), and then underwent histological characterisation to confirm whether a lesion was present or not (***Figure 4. 1***).

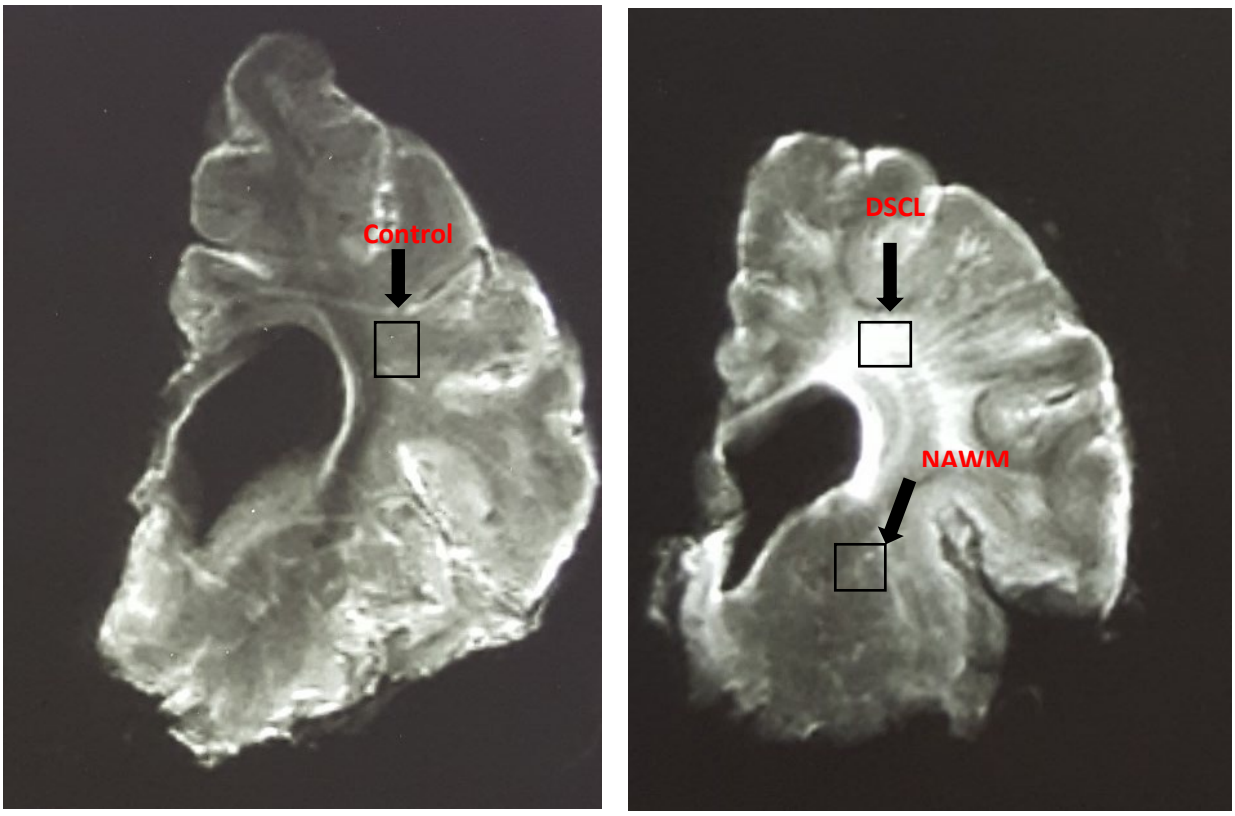

Figure 4. 1 MRI Scan of post-mortem WM: (A) Representative MRI scans of non-lesional control and **(B)** deep subcortical lesion and normal appearing white matter.

4.3.2 Histological characterisation

All the sampled blocks were histologically characterised using the standard histological stains luxol fast blue (LFB), haematoxylin and eosin (H&E) and CD68 immunohistochemistry (IHC). LFB stain was used to visualise the demyelinated WML using a simple acid—base reaction where luxol, an alcohol soluble substance, is attracted to the lipoproteins of the myelin, which are basic. The reaction happens when the lipoprotein is replaced by the dye allowing visualisation of myelin in the tissue. H&E is one of the most common stains routinely used in neuropathology and has been used for at least a century (Fischer et al., 2008). Haematoxylin stains nucleic acids deep blue—purple and eosin stains proteins non-specifically and has a pinkish colour (Fischer et al., 2008). CD68 is a protein that is widely expressed on intracellular lysosomal membrane. Microglia with a phagocytic phenotype express high levels of CD68 (Hendrickx et al., 2017).

4.3.2.1 Luxol Fast Blue (LFB) stain

Tissue sections (5µm) from frozen samples were collected onto poly-L-lysine-coated slides and warmed to RT prior to staining. The sections were fixed in 95% alcohol (Fischer, UK) for 5 minutes and then submerged in LFB solution for 2 hours at 60°C. The sections were rinsed in 70% alcohol to remove any excess stain, followed by rinsing in tap water. Sections were differentiated in 0.5% lithium carbonate for 30 seconds and differentiated in 95% alcohol until grey and WM were clearly distinguished. The sections were washed in tap water, dehydrated in a graded series of alcohol [75%, 95%, 100%, 100%] and cleared in xylene (Fisher Scientific, UK) for 5 minutes before being mounted using DPX mountant (Leica, UK) and covered with a glass cover slips. The slides were left to dry overnight in the oven.

4.3.2.2 Haematoxylin and Eosin (H&E) Stain

The sections (5µm) from frozen samples were warmed to room temperature (RT) before fixing in ice-cold acetone at 4ºC for 3 minutes and were then immediately transferred into Harris' haematoxylin for 3 minutes. The sections were rinsed in tap water and then blued in Scott's tap water for 2 minutes and placed in 1% eosin for 5 minutes. The sections were washed in tap water and dehydrated through a graded series of alcohols [70%, 90%, 100% and 100%], cleared in xylene (Fischer Scientific, UK) for 5 minutes and mounted using DPX mountant (Leica, UK). The sections were covered with glass cover slips and left to dry overnight in the oven at 60^0C before being viewed under the microscope.

4.3.3 CD68 Immunohistochemistry (IHC)

Sections (5µm) from frozen samples were collected onto poly-L-lysine-coated microscope slides, warmed to RT and fixed in ice-cold acetone for 3 minutes. Sections were air dried for 30 seconds, ensuring the acetone was fully evaporated. All steps were carried out at room temperature (RT) unless otherwise stated. The sections were completely covered with 1.5% blocking solution (VECTASATIN Elite ABC-HRP kit, Vector Laboratories UK) and incubated for 30 minutes. The blocking solution was removed by tapping the slides and sections were incubated with CD68 antibody (1:100 dilution) (Dako, Denmark) for 60 minutes. The sections were washed with tris-buffered saline (TBS) for 5 mins and incubated with 0.5% biotinylated secondary antibody for 30 minutes. The sections were rinsed in TBS for 5 minsand incubated with 2% horseradish peroxidase-conjugated avidin-biotin complex (ABC-HRP) reagent (Vectastain Elite ABC-HRP kit, Vector Laboratories, UK) for 30 minutes. The ABC-HRP reagent was made 30 minutes prior to use. The sections were washed in TBS for 5 mins. The substrate 4,4'-diaminodenzedine tetrahydrochloride (DAB) (Vector laboratories, UK) was added and the reaction was visualised using a microscope. When the stain had developed sufficiently to visualise the cells, the enzymatic reaction was quenched by rinsing in d.H_2O for 30 seconds, followed by tap water. Sections were counterstained using Harris' haematoxylin for 30—60 seconds and rinsed in tap water. They were submerged in Scott's tap water for 30 seconds before being dehydrated through graded alcohol [70%, 95%, 100%, 100%] for 30 seconds each. The sections were cleared in xylene for 5 minutes, mounted using DPX mountant (Leica, UK) and covered with glass cover slips. The slides were left to dry overnight in the oven.

4.3.4 RNA Integrity Analysis- Pre LCM

The RNA quality of the starting material was analysed to ensure the cases selected were of sufficient starting RNA quality. A thick section (20µm) of each sampled frozen block was collected into a sterile 1.5-mL Eppendorf and RNA extraction was carried out using the standard Trizol method. One ml of Trizol reagent was added slowly into the tube and the cells were lysed using a handheld homogeniser. 200 µl Chloroform was added, vortexed briefly and incubated at RT for 3 minutes. The sample was centrifuged at 12000 *g* for 15 minutes at 4°C. The upper aqueous phase was removed and transferred to a new sterile tube. 500 µl isopropanol was added and incubated at RT for 10 minutes. The sample was centrifuged at 12000 *g* for 10 minutes at 4ºC. The supernatant was discarded, and the pellet was washed in 1 mL of 75%

ethanol. The sample was vortexed briefly before centrifuging at 7500 *g* for 5 minutes at 4ºC. The supernatant was removed, and the sample was left to air dry for 10 minutes. The pellet, resuspended in 20 µl RNASe free water, was incubated for 10 minutes at 55ºC. Both the quality and quantity of RNA in the samples were analysed using a bioanalyzer (Agilent, UK) and NanoDrop Spectrophotometer (Thermo Scientific, UK), respectively. All the samples were stored at −80ºC.

4.3.5 Laser Capture Microdissection (LCM) of Vessels from WM

4.3.5.1 Modified Rapid IHC

Collagen IV is the most abundant type of collagen in the basement membrane (Xu et al., 2018) and can be used to identify capillaries in the frozen tissue sections. Freshly prepared, 6µm cryosections from frozen WM tissue were collected onto uncharged glass slides. The sections were warmed to RT, ensuring all the condensation had completely evaporated, and were fixed in ice-cold acetone for 3 minutes, briefly air-dried and immunostained using a modified rapid ABC staining technique (VECTASTAIN Elite ABC kit, Vector laboratories, UK). All steps were carried out using sterile equipment and reagents and were performed at RT unless otherwise stated.

Sections were air dried for 30seconds, ensuring the acetone was fully evaporated. The sections were completely covered and blocked with 2% normal serum for 3 minutes at RT. The blocking solution was removed from the sections which were then incubated at RT with anti-Collagen IV (Abcam, UK) primary antibody (1:50 dilution) for 3 minutes. The sections were rinsed with TBS for 30 seconds and incubated with 5% biotinylated secondary antibody (VECTASTAIN Elite ABC-HRP Kit) for 3 minutes. The sections were washed with TBS and incubated with 4% ABC-HRP reagent for 3 minutes (ABC-HRP reagent was made 30 minutes and incubated at RT prior to use). The sections were washed in TBS prior to incubation with the peroxidase substrate DAB for 3 minutes. The enzymatic reaction was quenched by covering the sections in d.H_2O for 30 seconds. The sections were dehydrated through a series of graded alcohol [70%, 95%, 100%, 100%] for 15 seconds each before clearing in xylene for 5 minutes. They were then placed in a laminar flow hood to air dry for approximately 60 minutes before proceeding to the LCM step.

4.3.5.2 Laser Capture Microdissection (LCM)

LCM of microvessels was performed using the PixCell II laser-capture microdissection system (Arcturus Engineering, Mountain View, USA). The immunostained slides (ensuring the slides were completely dry) were mounted onto the stage and a CapSure Macro LCM cap (Arcturus Engineering, Mountain View, USA) was placed over the sample. Using the monitor as a guide, the Coll-IV immunopositive capillaries were identified and the infrared laser was fired causing the film to melt and the vessel of interest to adhere to the cap. LCM power was set at 45—50 mW and roughly an hour was spent on each case. After LCM, the film from the cap was removed using sterile forceps and placed in a sterile 0.2 mL Eppendorf that contained 50 µl of extraction buffer from the PicoPure RNA isolation kit. All the samples were stored at -80ºC before proceeding to RNA extraction.

4.3.5.3 RNA Extraction

All the extractions were carried out using the RNA PicoPure Isolation kit (Applied Biosystems, UK). The Eppendorf containing the film suspended in extraction buffer was incubated at 42ºC for 30 minutes on the thermo cycler (MJ Research, Canada). The extraction columns were conditioned by adding 250 µl conditioning buffer and were incubated at RT for 5 minutes. Columns were centrifuged at 16,000 *g* for 1 minute and the flow through was discarded. 50 µl of 70% ethanol was added to the sample and mixed thoroughly. The solution was transferred to the centre of the column and was centrifuged at low speed (100 *g*) for 2 minutes, followed by a high-speed centrifugation (16,000 *g*) for 1 minute. 100 µl wash buffer 1 was added and centrifuged at 8000 *g* for 1 minute. 100 µl wash buffer 2 was added and centrifuged at 8,000 *g* for 1 minute. The sample was again washed with 100-µl wash buffer 2 and centrifuged at 16,000 *g* for 1 minute. The column was transferred to a sterile 1.5 ml Eppendorf. 11 µl of elution buffer was added to the column and incubated for 1 minute. It was centrifuged at 1,000 *g* for 1 minute followed by 16,000 *g* for 1 minute. The eluent was collected, which contained the RNA from cells isolated by LCM. The quality of the RNA sample was analysed using bioanalyzer (Agilent, UK) and quantity was measured using Nanodrop spectrophotometer. All the extracted RNA was stored at -80ºC until required.

4.3.6 Confirmation of endothelial cell enrichment

To confirm the cell population isolated by LCM was an enriched population of endothelial cells, RT- PCR was performed. Specific primers for vessels - von willebrand factor (vWF); astrocytes - GFAP; microglia- CD68; neurones/axons - NeuN; oligodendrocytes - OLIG2 were used along with β-actin as the housekeeping gene (Primer sequence: ***Table 4. 1***).

Table 4. 1 Gene specific primer sequences used for confirmation of enriched population of endothelial cells.

Gene	Primer Sequence	Product Size (bp)
CD68	F: 5'- CGA GCA TCA TTC TTT CAC CAG CT R: 5'- ATG AGA GGC AGC AAG ATG GAC C	135
GFAP	F: 5'-GCA GAA GCT CCA GGA TGA AAC R: 5' TCC ACA TGG ACC TGC TGT C	213
NeuN	F: 5'-ACG ATG GTA GAG GGA CGG AA R: 5'-AAT TCA GGC CCG TAG ACT GC	84
OLIG2	F: 5'-CCC TGA GGC TTT TCG GAG CG R: 5'-GCG GCT GTT GAT CTT AGA CGG	474
vWF	F: 5'-GTG TGT CCG AGT GAA GGA GG R: 5'-CAG CAC GCT GAG GTC TTA CA	116
Beta- Actin	F: 5'- TCC CCC AAC TTG AGA TGT AAG R: 5'- AAC TGG TCT CAA GTC AGT GTA CAG G	100

4.3.6.1 cDNA Synthesis

To a sterile 0.2 ml Eppendorf, 2 µl of qScript (Quanta, UK), 3 µl of RNAse free water and 5 µl of sample were added. The tube was placed in the thermo cycler and the sample was run through the following thermal cycles: 25ºC for 5 minutes, 42ºC for 30 minutes, 85ºC for 5 minutes and then holding at 4ºC. At this stage, the cDNA was removed and was stored at −20ºC until required.

4.3.6.2 DNA Amplification

To make the PCR reaction mix, 1 µl of cDNA, 4 µl 5x Firepol Green (Solis Biodyne, UK) and 1 µl forward and reverse primers (5pM/µl) and 13 µl sterile d.H_2O were added into a sterile 0.2 µl Eppendorf. A no template control (NTC) was included for each specific primer, which was identical to the PCR reaction mix, but replaced 1 µl cDNA with 1 µl sterile d.H_2O. The tubes were vortexed briefly and placed in the thermo cycler for denaturation at 95ºC for 10 minutes. The PCR products were amplified using the following thermal cycle: for GFAP, vWF, Neu and β-actin (40 cycles at 95ºC for 15 seconds and 60ºC for 60 seconds, 72ºC for 10 minutes and holding at 10ºC) and for CD68 and OLIG2 (2 cycles at 94ºC, 35 cycles at 94ºC for 30 seconds, 58ºC for 45 seconds and 72ºC for 1 minute, 72ºC for 15 minutes and 15ºC for holding).

4.3.6.3 Agarose Gel Electrophoresis

To visualise the PCR products, a 3% agarose gel was made by dissolving 3 g of agarose in 100 ml TAE. The gel was heated in the microwave on full power until all the agarose dissolved. The gel was cooled to RT by running the flask under cold tap water. 1 µl of ethidium bromide (ThermoFisher, UK) was added to the cooled gel mix and poured into the casting tray with the comb in position. The gel was left to set at RT for approximately 30mins. 3 µl of Hyperladder, 25 bp (Bioline, UK) was added and 10µl samples or NTC were loaded into the gel which was run at 100 V for 1 hour. The product was visualised using G-box.

4.3.9 Transcriptomic Analysis of WM cases

4.3.9.1 RNA Amplification and hybridisation

RNA extracted from LCM-ed endothelial cells was used to characterise the transcriptomic profile of microvessels in 5 non-lesional control cases and 5 lesional cases (both WML and NAWM). Extracted RNA samples were amplified using a 3' IVT Pico Reagent Kit

(ThermoFisher Scientific, USA). The process of amplification and hybridisation was carried out exactly as described in Chapter 2, section 2.8.9.1.

4.3.9.2 Microarray quality control analysis

The quality control analysis was performed as described in **section 3.3.4** and normalised using robust multi-array analysis.

4.3.9.3 Microarray data analysis

The data was analysed using the Qlucore Omics Explorer software (Qlucore, Lund, Sweden). Two and three group comparisons were performed with parameters set as $p \leq 0.05$ and fold change ≥ 1.2. DAVID Bioinformatics resources version 6.8 (NIAID, NIH, USA) and IMPaLA were used to analyse the functional groupings and pathways with stringency levels set as highest.

4.4 Results

4.4.1 Histological characterisation of control, WML and NAWM cases

Frozen WM blocks were sampled from the CFAS cohort, using MRI of the contralateral formalin-fixed hemisphere as a guide, and were histologically assessed to confirm the WM classification. Histological assessment was performed to visualise demyelination and to assess the presence of amoeboid $CD68^+$ microglia in the WM. Radiologically and histologically confirmed control cases were characterised by minimal evidence of demyelination and the presence and regular distribution of resting microglia with a ramified morphology throughout the WM (***Figure 4. 2***). Some of the radiologically classified control cases were histologically abnormal, containing moderate levels of $CD68^+$ ameboid microglia. Deep subcortical lesional cases displayed an abundance of $CD68^+$ microglia with a large, round cell body with retracted processes There was also evidence of demyelination indicated by reduced LFB staining, indicating loss of myelin (figure 4.1). NAWM cases were radiological normal regions from cases which had a WML elsewhere in the tissue slice. In contrast to WML, NAWM contained lower levels of $CD68^+$ phagocytic microglia and had a predominantly bipolar morphology, histologically more similar to control WM (***Figure 4. 1***). Initial studies prepared and assessed 29 WM blocks and categorised these blocks into control, NAWM and WML according to their histological profile.

After analysing all the cases, suitable cases were selected (see ***Table 4. 2***) and the RNA profile was assessed prior to LCM. New label for the selected cases can be found in ***Table 4. 3***. Demographic information for the selected cases is listed in ***Table 4. 4***.

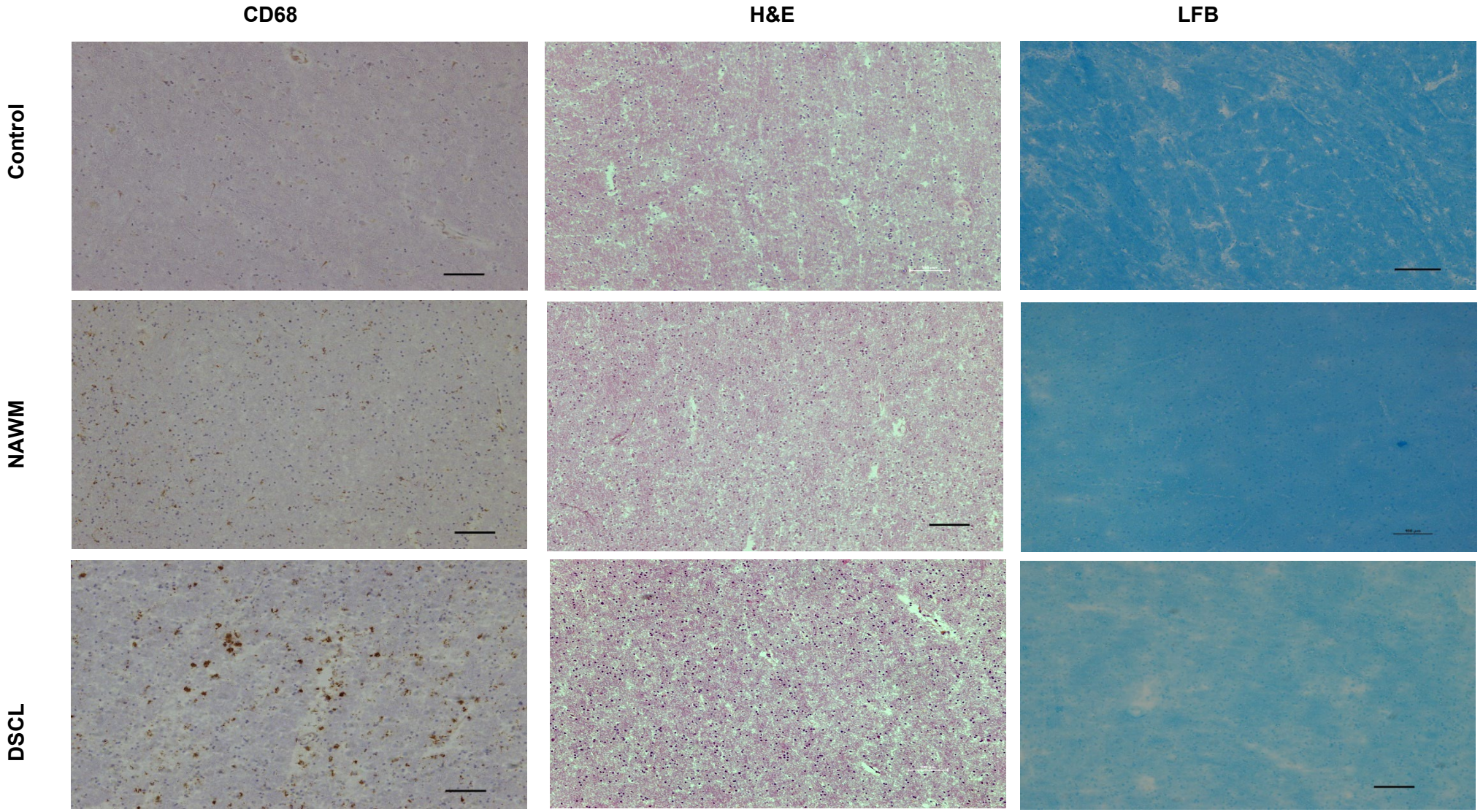

Figure 4. 2 Histological characterisation of WM. Both Control WM and NAWM contained low levels of $CD68^{+}$ microglia, predominantly with a bipolar morphology. In contrast DSCL contain high levels of large microglia with a round, amoeboid morphology, demonstrating a classic phagocytic phenotype. H&E stains nuclei a deep purple while staining cytoplasm a light pinkish colour. Both control and NAWM displayed a regular distribution of cells through the WM area. In contrast, a greater number of nuclei is observed in DSCL representing hypercellularity in the area. LFB stains myelin, both control and NAWM display intact myelin while DSCL display loss of myelin. Scale bar represents 100 µm

Table 4. 2 MRI and histological classification of WM blocks. Each MRI-guided sample was histologically characterised and classified. The cases in red were selected to take forward for RNA analysis and LCM. Some cases were excluded (highlighted in yellow) as there was evidence of extensive freeze- thaw artefacts throughout the tissue.

CASE No	MRI Classification	Histological Classification
RH6 (H6)	Control	Control
23/94 (11)	Control	Control
100/00 (8)	Control	Control
201/95 (9)	Control	Excluded
11/98 (11)	DSCL	NAWM
178/96(8)	DSCL	NAWM
105/94 (10)	DSCL	NAWM
31/00 (8)	DSCL	NAWM
47/97 (13)	DSCL	NAWM
31/00 (9)	DSCL	Lesion
121/96(10)	DSCL	NAWM
105/94 (11)	DSCL	NAWM
178/96 (10)	DSCL	Lesion
11/98 (9)	NAWM	Lesion
47/97 (10)	NAWM	NAWM
67/94(14)	NAWM	NAWM
178/96 (12)	NAWM	NAWM
63/98 (7)	NAWM	NAWM
47/97 (14)	NAWM	NAWM
121/96 (11)	NAWM	NAWM
106/94(25)	DSCL	NAWM
68/94(10)	DSCL	NAWM
127/94(9)	DSCL	NAWM
RH03 (H4)	DSCL	Lesion
RH11 (H5)	control	Excluded
RH04 (H4)	Control	Control
RH23(H5)	Control	Control
RH37(H4)	Control	Excluded
RH69(H7)	DSCL	Lesion

Table 4. 3 Cases that were selected for the microarray and the new labels used in the study

Name of the cases	New label
RH3-L	L-1
RH69-L	L-2
31/00(9)	L-3
178/96(10)	L-4
11/98(9)	L-5
RH3-N	N-1
RH69-N	N-2
11/98(11)	N-3
198/96(12)	N-4
31/00(8)	N-5
RH6	C-1
23/94(11)	C-2
100/00(8)	C-3
RH23	C-4
RH04	C-5

Table 4. 4 Demographic information for cases used in microarray analysis. Age, gender, post-mortem delay (PMD) and pH of cases; N/A indicates unavailable data.

Cases	Age at death	Gender	Post-mortem delay (PMD) (hours)	pH of brain
C-1	89	M	11	6.69
C-2	93	M	33	N/A
C-3	78	F	79	N/A
C-4	N/A	N/A	N/A	N/A
C-5	85	F	N/A	7.02
L-1	82	F	N/A	6.47
L-2	95	f	35	6.43
L-3	90	M	79	N/A
L-4	N/A	N/A	N/A	N/A
L-5	75	M	20	N/A
N-1	82	F	N/A	6.47
N-2	95	f	35	6.43
N-3	75	M	20	N/A
N-4	N/A	N/A	N/A	N/A
N-5	90	M	79	N/A

4.4.2 Laser Capture Microdissection (LCM) of vessels from WM

All the suitable cases identified in the histological characterisation were taken forward for assessment of RNA integrity and, if appropriate, LCM isolation of Collagen-IV^{+} vessels. A modified IHC protocol for Collagen- IV allowed detection of the vessels, which appeared string- like or rounded depending on their orientation within the tissue section. LCM allowed isolation of these Collagen-IV^{+} cells (***Figure 4. 3***). Approximately 1.5 hr was spent on each section to generate an enriched population of vessel-associated cells. The RIN values and RNA profiles were assessed for all the cases post-LCM.

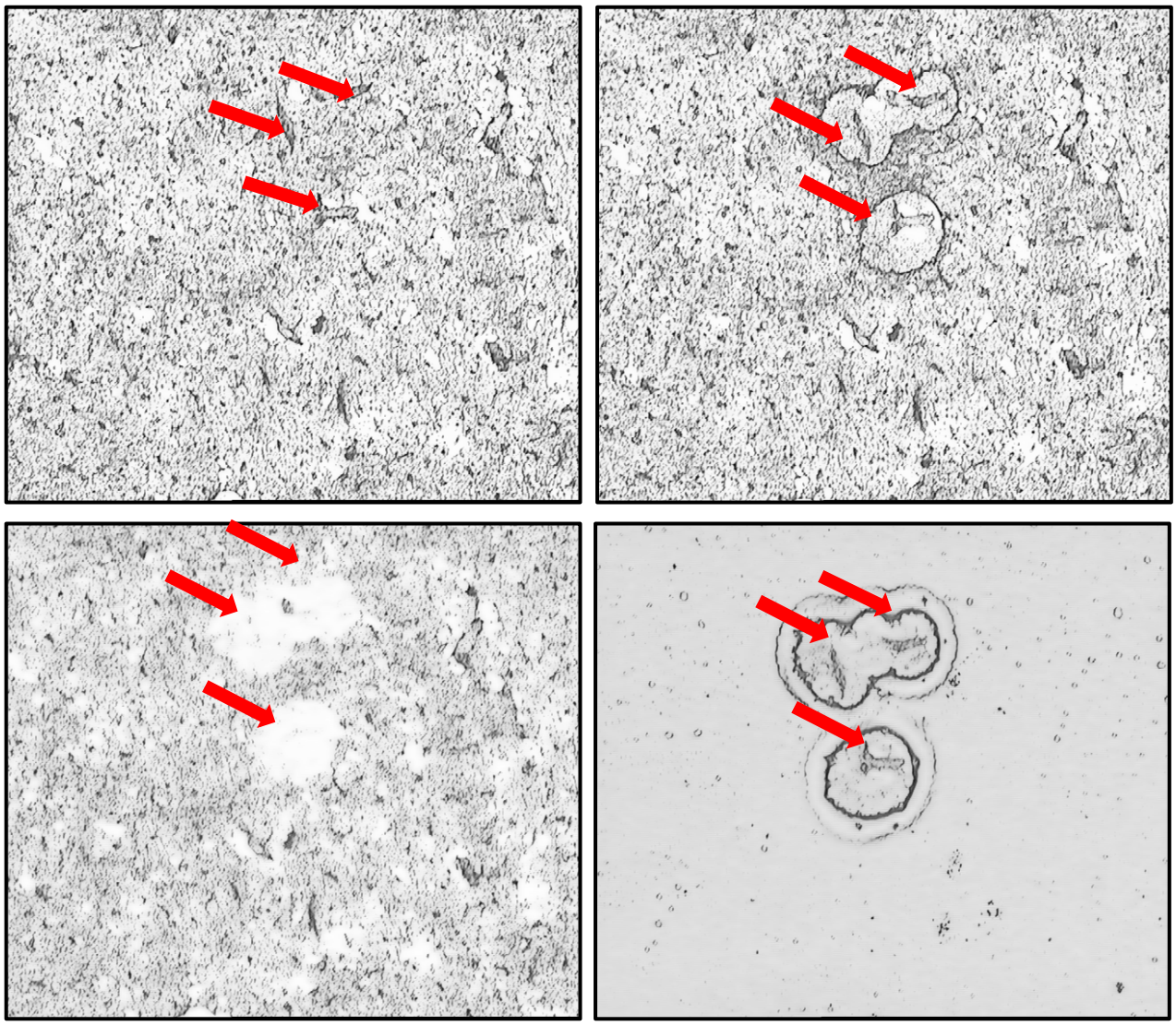

Figure 4. 3 LCM of collagen-IV positive vessels. (A) Blood vessels were immunolabelled with collagen-IV. **(B)** A cap was placed on the section and the laser was fired, melting the film and attaching the cells of interest to the LCM cap. **(C)** The remaining tissue where the vessels were removed and (D) microdissected vessels from the tissue on the cap.

4.4.3 RNA Integrity of frozen samples

4.4.3 Confirmation of enriched endothelial cell population

To confirm an enriched population of endothelial cells, RT- PCR was performed. Expression of the endothelial cell marker von Willebrand factor (vWF) was used to assess the enrichment. As endothelial cells are in close proximity to astrocytes, axons, microglia and oligodendrocytes, PCR was also performed for: astrocyte (GFAP), axons (NeuN), microglia (CD68), oligodendrocyte (Olig2) to assess any contamination from other cell types and confirm endothelial cell enrichment. β-actin was used as a housekeeping gene and the presence of an intense band at ~ 100 bp also confirmed successful cDNA synthesis. Expression of vWF (110bp) in the sample confirmed the enrichment of the sample (***Figure 4. 4***). No product was observed in the NTC, confirming the specificity of the reaction.

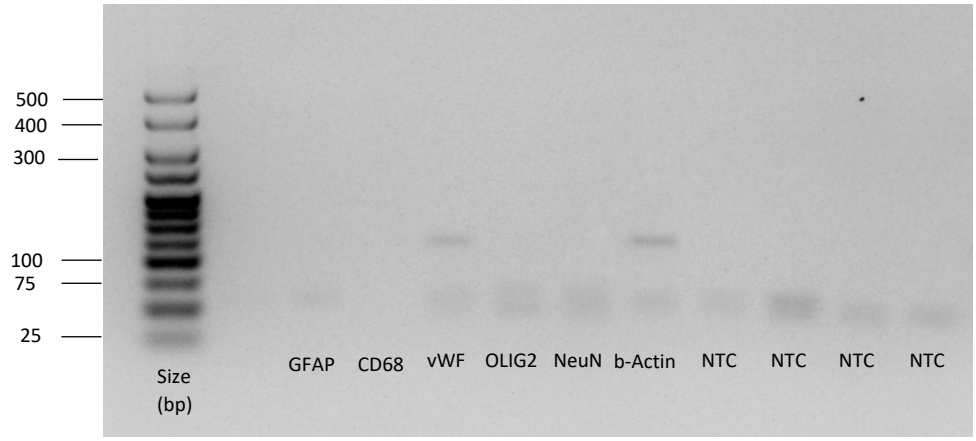

Figure 4. 4 Confirmation of enrichment of endothelial cells in LCM-ed sample. PCR for specific cell phenotypes was performed on LCM-ed samples following RNA extraction. vWF expression confirmed that the sample is enriched for endothelial cells and an intense band at β-Actin confirmed that it was a successful cDNA synthesis. There was no GFAP, CD68, OLIG2 and NeuN products detected. (bp- base pairs).

4.4.4 RNA Integrity of frozen samples

The quality of the RNA isolated from the frozen samples was analysed using Picochip Analysis (see ***Table 4. 5***). RNA integrity analysis of the cases was also performed after LCM. Since most cases did not have a RIN, the RNA profile was examined before the cases were taken forward for microarray analysis (see ***Figure 4. 5***).

Table 4. 5 RNA concentrations and RIN Values of the samples. The RNA concentration was obtained using a Nanodrop spectrophotometer and RIN values were obtained using a bioanlayzer. RIN values were not available for some of the cases (N/A: not available.)

Cases	RNA Concentration (µg/mL)	RIN Values before LCM	RIN Values after LCM
L-1	9.5	1.1	N/A
L-2	9.54	2	1
L-3	14.4	N/A	N/A
L-4	3.09	N/A	N/A
L-5	6.03	1	N/A
N-1	9.2	N/A	N/A
N-2	2.39	1.3	N/A
N-3	4.67	3	1.9
N-4	5.63	N/A	N/A
N-5	6.59	2.3	1.6
C-1	10.15	2	N/A
C-2	5.20	N/A	N/A
C-3	6.56	1.6	N/A
C-4	21.86	N/A	N/A
C-5	5.16	N/A	N/A

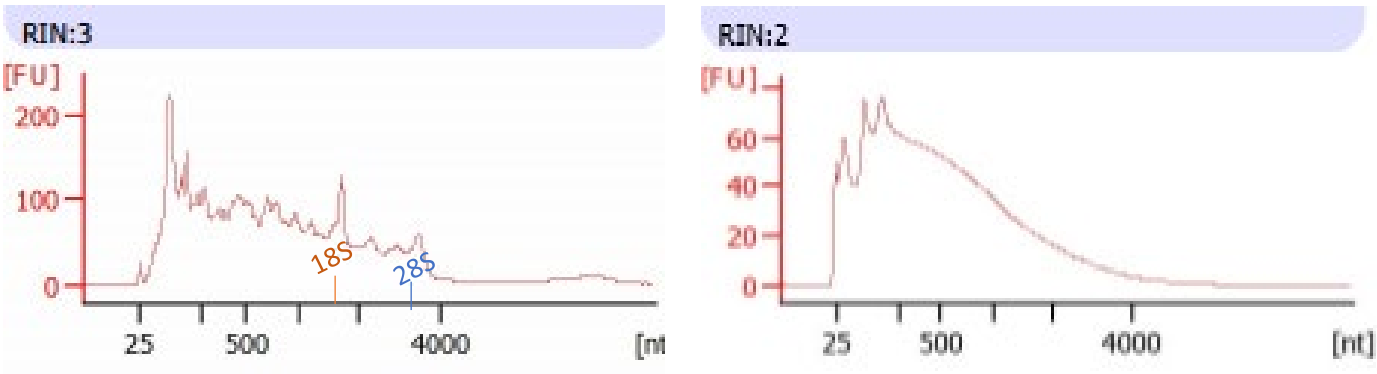

Figure 4. 5 Representative Image of the RNA profile of a case pre- and post-LCM obtained using the Agilent Bioanalyzer. (Left) Electropherogram of RNA extracted before LCM. The RIN profile was used to assess RNA integrity pre- and post-LCM. 18S and 28S peaks represent ribosomal RNA. The presence of two ribosomal peaks demonstrates that RNA is not fully degraded and can be used for further applications downstream. (Right) Electropherogram of RNA extracted after LCM. The RIN profile shifted largely towards the left, indicating presence of short RNA strands. Some of the degradation during LCM is unavoidable. (FU: fluorescence unit; nt: nucleotide).

4.4.4 Internal Quality Control of microarray analysis

Quality control analysis was performed using Affymetrix Expression Console software (as described in Chapter 3, section 3.3.4). The samples were all analysed for amplification, hybridisation, housekeeping genes and signal intensity. A control sample (C-5) and a NAWM samples (N-5) were identified as outliers as their arrays did not produce signal, and so were removed from subsequent downstream analysis.

4.4.4.1 Amplification Controls

A poly-A RNA control provided by Affymetrix was used in the microarray analysis to monitor the labelling efficiency. Poly-A controls, derived from B. *subtilis* bacterial genes *lys, phe, thr* and *dap*, were added to each of the samples at decreasing concentrations (1:100,000, 1:50,000, 1:25,000 and 1:6,667 respectively). N-2 demonstrated a greater labelling efficiency for all four poly-A-controls when compared to other samples. All other samples had poly-A controls present in decreasing concentration as shown in ***Figure 4. 6***).

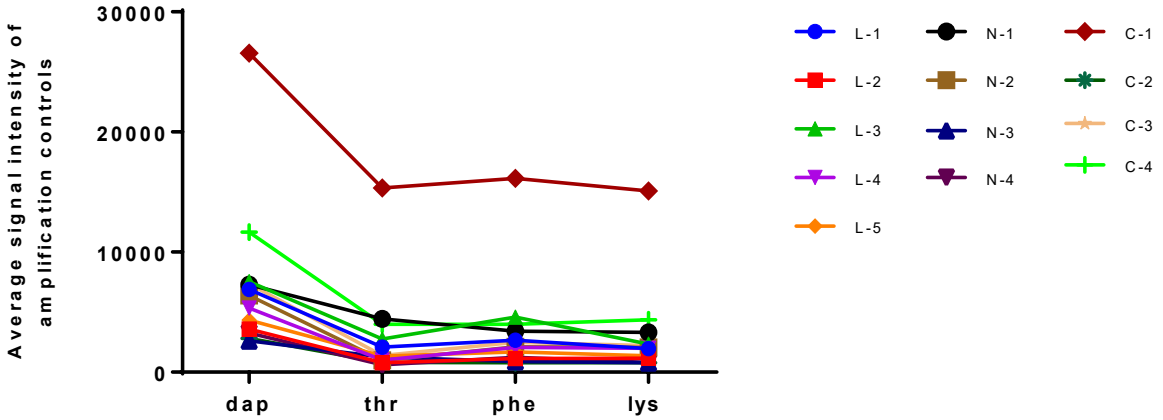

Figure 4. 6 Amplification controls for endothelial enriched RNA samples from control, lesional and NAWM cases. Average signal intensity of poly- A controls *dap, thr, phe* and *lys* was plotted for the 13 samples. Sample C-1 had the highest signal intensity for all the poly-A controls, but it followed a similar trend to the other samples.

4.4.4.2 Hybridisation Controls

Another set of exogenous RNA controls were added to the samples. These controls originated from *E.Coli* bacteria (*bioB, bioC, bioD)* and P1 bacteriophage (Cre), and monitor how consistent the hybridisation was across all the arrays. All 13 array samples followed a similar signalling pattern. All four controls were present in increasing concentrations, as expected. The sensitivity of the array was measured by looking at bioB as it should be present at least 50% of the time (***Figure 4. 7***). In summary, hybridisation controls are 'present' across all the samples with increasing intensities with respect to their concentrations.

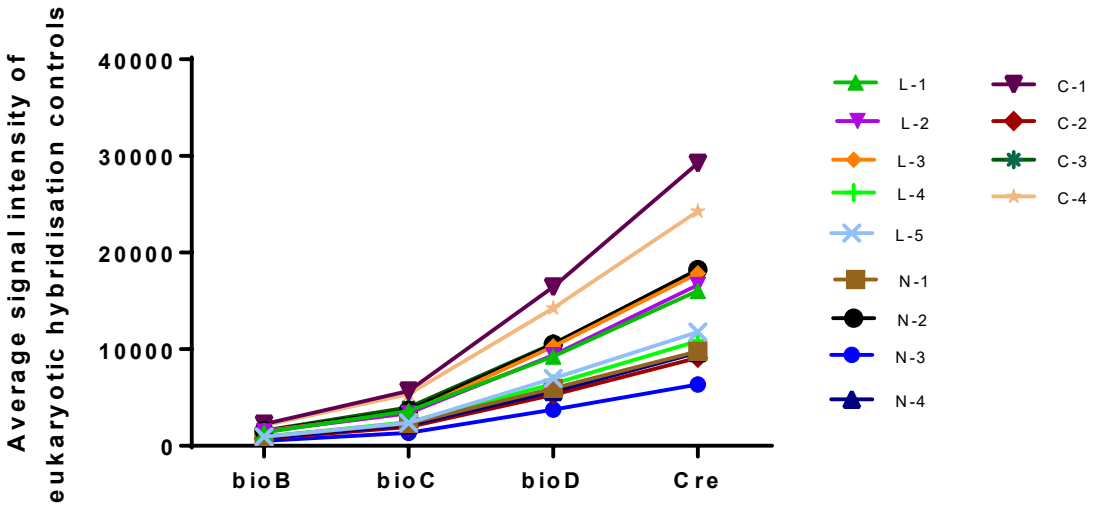

Figure 4. 7 Hybridisation controls for endothelial RNA enriched sample from controls, lesional and NAWM cases. The average signal intensity of eukaryotic hybridisation controls, bioB, bioC, bioD and cre was plotted for each of the 13 cases. The highest signal intensity was recorded by Control-1, but it followed a similar trend to the other samples.

4.4.4.2 Housekeeping and Signal Quality

Housekeeping genes such as *GAPDH*, *tubulin*, *PDHX* and *Actin* are widely used as internal controls. In this microarray, *GAPDH* and *β-actin* were utilised to assess the expression of housekeeping genes. The signal intensities of 3' probe sets were compared to 5' signal for both genes for 13 arrays as shown in ***Figure 4. 8***. For *GAPDH*, the signal ratios were between 0.26 and 0.63, but *β-actin* ratios for all the 13 arrays were between 1.35 and 1.40. Although the ratio for *β-actin* is higher than for *GAPDH*, this is not unusual as the 2-cycle assay can give rise to higher values due to additional amplification cycles. Overall, this does not impact the array quality.

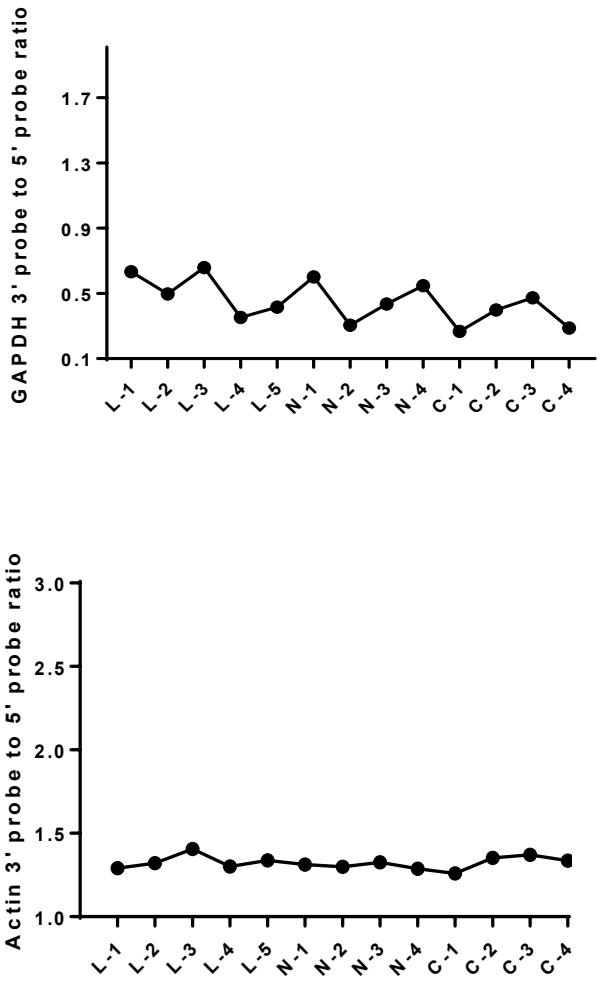

Figure 4. 8 Housekeeping controls for endothelial RNA enriched samples from control, lesional and NAWM cases. 3' to 5' probe ratio of *GAPDH* and *β-actin* was used as internal controls. The ratio varied between 0. 0.26 and 0.63 for *GAPDH* and *β-actin* ratios for all the arrays were between 1.35 and 1.40.

4.4.4 Signal Intensity

Figure 4. 9 summarises the signal intensity profile of all the 13 samples. All the samples in this microarray analysis displayed comparable signal intensity.

Relative log expression (RLE) is another method that is used to compare the expression of a probe set to the median expression of this probe set across all arrays. The results are expressed as a box plot (***Figure 4.10*****).** In an ideal plot, box plots are centred on zero, with all the plots having a similar size. Two samples- C-1 and L-3 have higher values and box plots, but all other samples have similar plots.

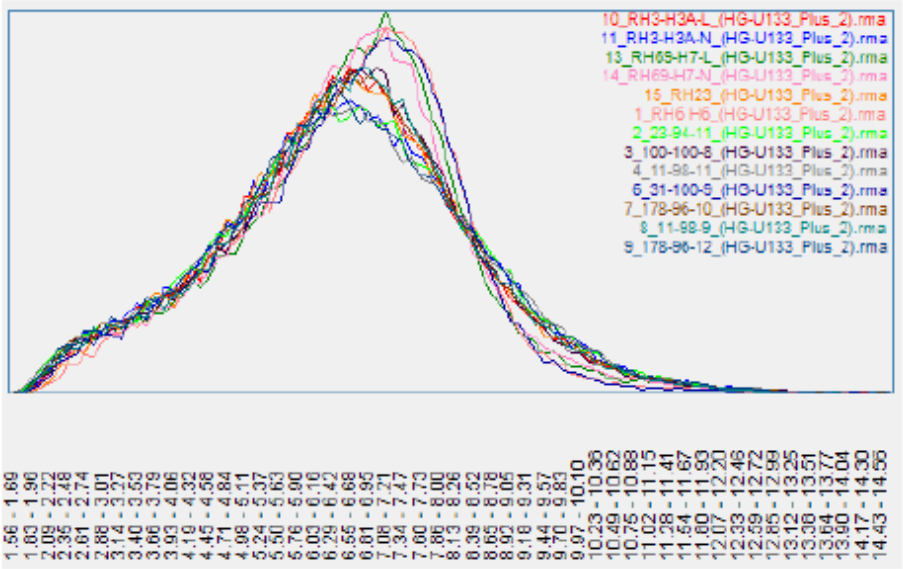

Figure 4. 9 Histogram of endothelial RNA enriched samples from controls lesional and NAWM cases. The histogram of signal intensities of each probe sets across the 13 samples were analysed. All the samples displayed comparable signal intensities across the probe sets. [X axis – Log of signal; Y axis -frequency]

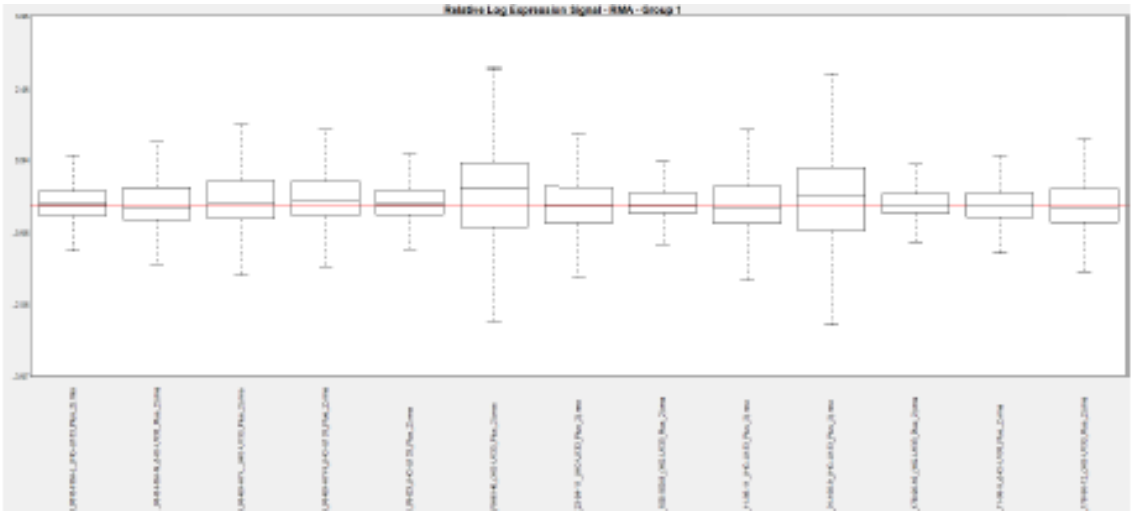

Figure 4. 10 *:* Relative Log Expression plots for all the 13 samples. The RLE values of all the cases except for samples C-1 and L-3 are all close to zero and have similar sized plots.

4.4.6 Data Analysis

4.4.5.1 Clustering Analysis

Having removed any outliers identified in the study, Qlucore Omics Explorer was used to analyse the transcriptomic profile of LCM-ed vessels from DSCL, NAWM and control cases. All the samples were normalised according to RMA method before the analysis was done. After normalising, genes were considered significantly differentially expressed if they showed a minimal fold change ≥ 1.2 (either upregulated or downregulated) and $p \leq 0.05$. Initially three-way comparison was performed, with the PCA plot demonstrating a clear separation between all the three groups, as shown in ***Figure 4. 11***).

To further visualise the differences in the transcriptomic profile of the samples, two- group analysis was also performed i.e. control v DSCL, control v NAWM and NAWM v DSCL. PCA plots of the three comparison groups further shows the differential gene expression profile (***Figure 4. 12***). Clustering analysis demonstrates that all three groups are clustered neatly and show a clear separation (***Figure 4. 11***)

The greatest number of dysregulated genes (2830 genes: 1566 genes upregulated and 1264 genes downregulated) were found when the transcriptomic profile of DSCL was compared to NAWM. There were 1206 genes (288 genes upregulated and 918 genes downregulated) significantly differentially expressed in DSCL compared to control WM. Furthermore, when the transcriptomic profile of NAWM was compared to non-lesional control WM, 1113 genes were significantly differentially expressed (426 upregulated and 687 downregulated) (for a detailed breakdown, please refer to ***Table 4. 6***). A complete set of genes that were significantly, differentially expressed can be found in Appendix III). A list of top 20 upregulated and downregulated genes can be found in Appendix IV.

Table 4. 6 Number of genes dysregulated in two-group analysis. After the samples were normalised according to RMA method, the datasets were analysed with the stringency settings: minimal fold change ≥ 1.2 (either upregulated or downregulated) and p ≤ 0.05**.**

Two group Comparison	No. of Upregulated Genes	No. of Downregulated genes
DSCL v control	288	918
NAWM v Control	426	687
DSCL v NAWM	1566	1264

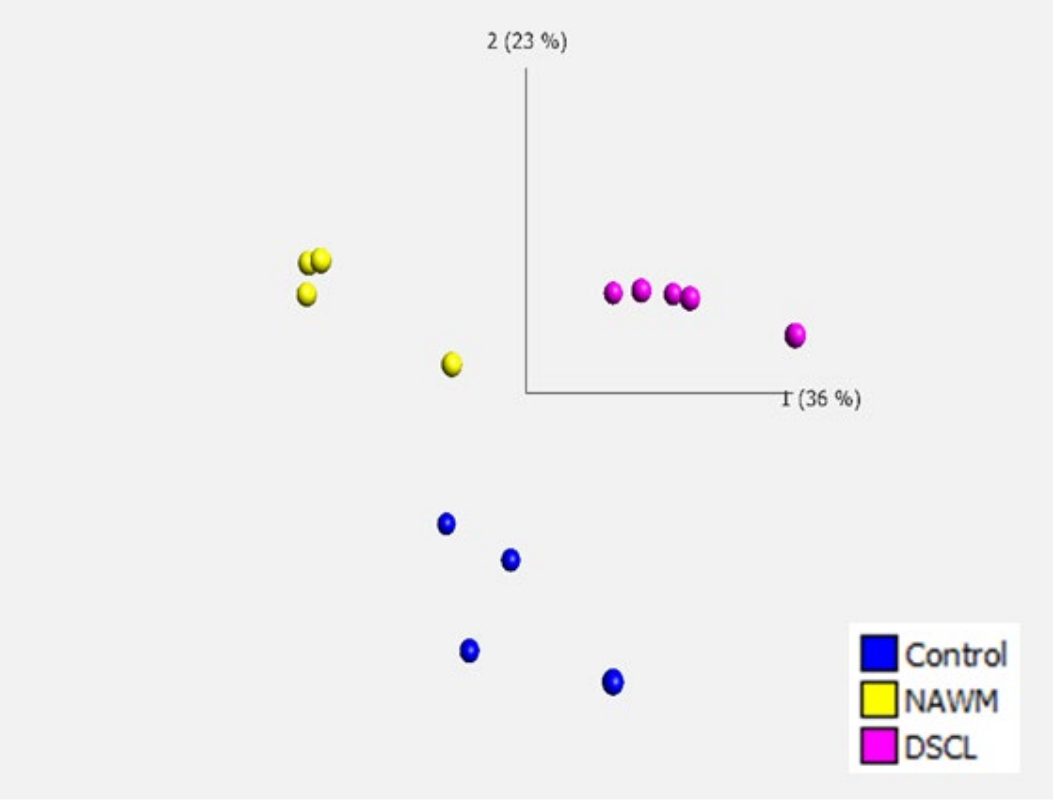

Figure 4. 11 PCA plot of control, lesional and NAWM cases. PCA plot of the transcriptomic profile of endothelial cells from control, NAWM and DSCL, cases were analysed using Qlucore Omics software (parameters: fold change ≥1.2; p≤ 0.05). All three groups displayed a clear separation suggesting distinct transcriptomic variation between all 3 groups and the similarity of samples within each group. (Control -blue, NAWM- yellow and DSCL -red).

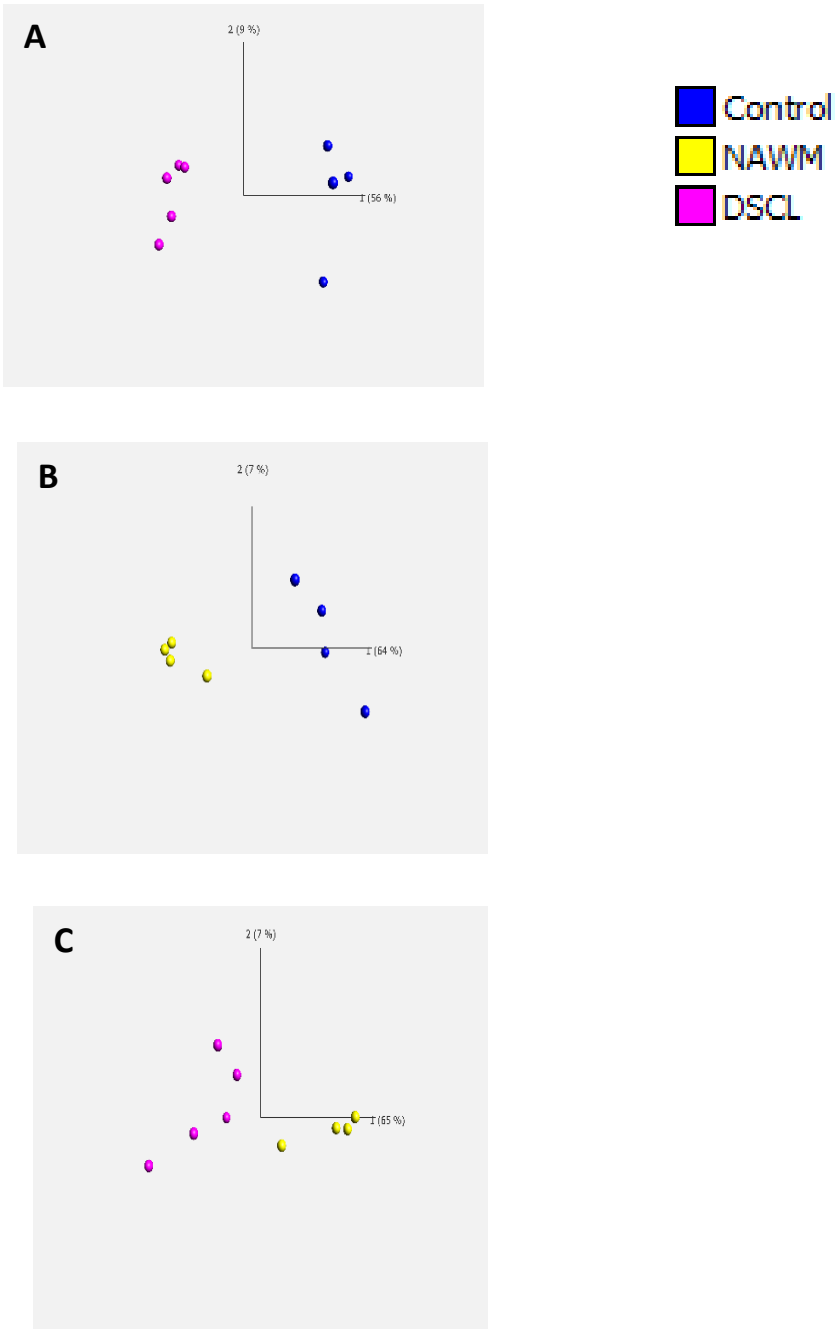

Figure 4. 12 Clustering analysis of control, lesional and NAWM cases. A PCA plot was generated using Qlucore Omics software to look at group comparisons separately. **(A)** PCA plot of control v DSCL, showing clear separation between the two groups. **(B)** PCA plot of control v NAWM demonstrating separation between the two groups. **(C)** PCA plot of NAWM and DSCL showing the clear separation between the groups.

To determine if there were any overlapping dysregulated genes between the three groups, the date was analysed using Venny (Version 2.1.0). As seen in ***Figure 4.12***, there were 6 transcripts common between the three groups (Table 4.5). Only five transcripts could be identified out of six, as shown in Table 4.5, and they did not belong to any common pathway.

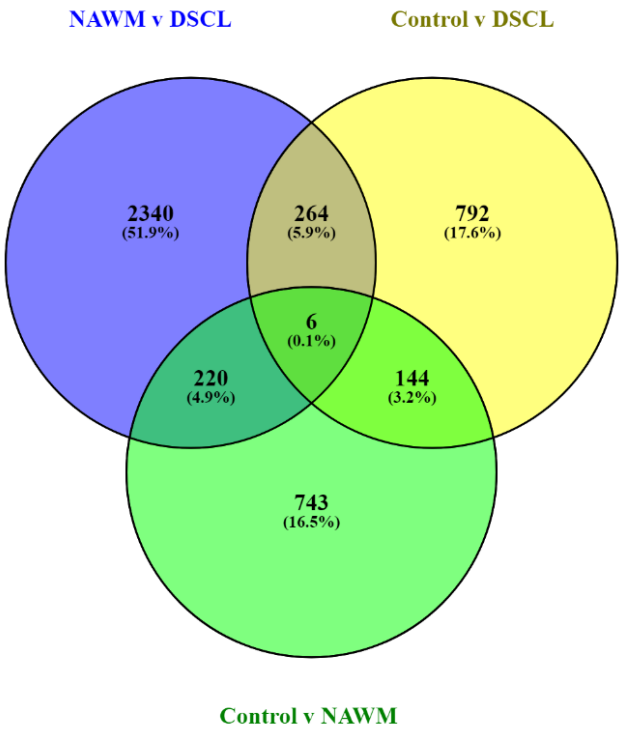

Figure 4. 13 Venn diagram identifying overlapping genes between three groups. Significantly differentially expressed genes were plotted in a Venn diagram using Venny (Version 2.1.0) to map the % of genes that were overlapping between the groups. There were only 0.1% (6 transcripts) that overlapped in the three-group analysis.

Table 4. 7 Common genes dysregulated in the three group comparison – control, NAWM and DSCL. The gene lists were analysed using Venny (version 2.1.0) to identify any common genes between the three two-group analysis. Venny identified six transcripts, only 5 of which were known.

Gene Name	Gene Symbol
Ring finger protein	*RNF8*
Vesicle- trafficking protein	*SEC22b*
Sphingomyelin phosphodiesterase acid like 3A	*SMPDL3A*
Arsenite methyltransferase (AS3MT)	*AS3MT*
Proteasome inhibitor subunit	*PSMF1*

4.4.5.2 Functional groupings and pathway analysis

4.4.5.2.1 Functional grouping analysis

Functional grouping analysis was performed using the DAVID Functional Annotation tool (Version 6.8) using the gene list obtained from Qlucore Omics. The significantly dysregulated gene list was analysed for each of the three groups. When DSCL versus NAWM was analysed, dysregulated genes included those associated with metal binding, nucleus and transcription regulation (p-values ≤0.05; ***Table 4. 8***).

Table 4. 8 Functional grouping analysis of DSCL versus NAWM. Functional grouping analysis was performed using DAVID Functional Annotation Tool with stringency setting set to 'High'.

Functional Groupings	Gene Count	P-Value
Metal binding	207	0.00025
Nucleus and transcription regulation	261	0.0019
Nucleotide-binding	207	0.00034
Phosphotyrosine interaction domain	10	0.0014
Spectrin repeats	7	0.0035

When DSCL versus control cases were analysed, functional groups that were dysregulated included ubiquitin-associated domain, microtubule, DNA damage response and regulation of apoptotic process (p-values ≤ 0.05; ***Table 4. 9***).

Table 4. 9 Functional grouping analysis of DSCL versus control. Functional grouping analysis was performed using DAVID Functional Annotation Tool with stringency setting set to 'High'.

Functional Groupings	Gene Count	P-Value
Ubiquitin-associated domain	3	0.038
Microtubule	8	0.013
DNA damage response and regulation of apoptotic process	5	0.0024
Metal ion binding	43	0.044
Transcription factor binding	8	0.018

Finally, when NAWM versus control group was analysed using DAVID, the main groups identified included transcription, metal ion binding proteins and nuclear membrane associated proteins (p-values ≤0.05; ***Table 4. 9***).

Table 4. 10 Functional grouping analysis of NAWM versus control. Functional grouping analysis was performed using DAVID Functional Annotation Tool with stringency setting set to 'High'.

Functional Groupings	Gene Count	P-Value
Transcription	114	0.01
Metal ion binding proteins	3	0.018
Nuclear membrane associated proteins	3	0.018
Collagen triple helix repeats	9	0.011

4.4.5.2.2 Pathway analysis

To identify if significant differentially expressed genes related to specific pathways the gene list obtained from Qlucore Omics (fold change ≥1.2; p-values ≤0.05) were analysed using the DAVID bioinformatic tool (version 6.8). The three two-group analysis datasets were analysed individually. Furthermore, to tease out the small but significant changes, up-regulated and down-regulated gene lists were analysed separately. The pathway analyses are summarised in ***Table 4.10-4.12.***

The dysregulated pathways identified by DAVID analysis in the DSCL vs non-lesional control WM group included endocytosis, ubiquitin mediated proteolysis and antigen processing and presentation (***Table 4. 11***). The highest number of dysregulated pathways occurred in the DSCL vs NAWM group comparison which included endocytosis, ras signalling pathway and FOXO signalling pathways (***Table 4. 12***). Interestingly, a pathway related to endocytosis was also enriched in NAWM vs control WM comparison (***Table 4. 13***).

Table 4. 11 KEGG pathway analysis of significantly differentially expressed genes in DSCL versus non-lesional control WM. KEGG pathway analysis was performed using the DAVID Functional Annotation Tool (Version 6.8).

Pathway	Gene Count	P value
Endocytosis	22	0.0019
Ubiquitin mediated proteolysis	15	0.0026
Proteoglycans in cancer	19	0.0028
Glioma	8	0.023
Viral carcinogenesis	16	0.035
Endocrine and other factor-regulated calcium reabsorption	6	0.045
Antigen processing and presentation	8	0.048

Table 4. 12 KEGG pathway analysis of significantly differentially expressed genes in DSCL versus NAWM from lesional cases. KEGG pathway analysis was performed using the DAVID Functional Annotation Tool (Version 6.8).

Pathway	Gene Count	P value
Endocytosis	39	0.0015
Ras signalling pathway	36	0.0031
Ubiquitin mediated proteolysis	24	0.0057
Proteoglycans in cancer	31	0.0094
Glycosphingolipid biosynthesis - ganglion series	6	0.011
FoxO signalling pathway	22	0.017
Hypertrophic cardiomyopathy	14	0.035
Glycosphingolipid biosynthesis - globo series	5	0.039
Prostate cancer	15	0.041

Table 4. 13 KEGG pathway analysis of significantly differentially expressed genes in NAWM versus non-lesional control WM. KEGG pathway analysis was performed using the DAVID Functional Annotation Tool (Version 6.8).

Pathway	Gene Count	P value
Axon guidance	10	0.0028
Butanoate metabolism	5	0.017
beta-Alanine metabolism	4	0.027
p53 signalling pathway	5	0.039
Alanine, aspartate and glutamate metabolism	9	0.041

When downregulated and upregulated gene lists were analysed separately, it identified many important pathways that can attribute to changes in WM. When DAVID analysis of down-regulated and up-regulated lists were analysed separately in DSCL versus NAWM, it identified downregulation of endocytosis, ubiquitin-mediated pathways and FoxO signalling pathways (p values < 0.05; ***Table 4. 14***). The pathways that were upregulated in DSCL versus NAWM included Ras signalling pathway, focal adhesion, calcium signalling and MAPK signalling (p values <0.05; ***Table 4. 15***).

Table 4. 14 KEGG pathway analysis of downregulated and upregulated genes in DSCL versus NAWM. KEGG pathway analysis was performed using the DAVID Functional Annotation Tool (Version 6.8).

Pathways	Up/Down Regulated	Gene Count	P-Value
Endocytosis	Down	27	0.00025
Ras signalling pathway	Up	22	0.0016
Basal cell carcinoma	Up	9	0.003
Ubiquitin mediated proteolysis	Down	16	0.0044
Proteoglycans in cancer	Up	19	0.0048
Pyrimidine metabolism	Down	12	0.014
ErbB signalling pathway	Up	10	0.018
FoxO signaling pathway	Down	14	0.02
P53 signalling pathway	Down	9	0.021
Cell Cycle	Down	13	0.025
Protein processing in ER	Down	16	0.027
PI3K-Akt signalling pathway	Up	25	0.028
Focal Adhesion	Up	17	0.028
Calcium signalling	Up	15	0.036
MAPK signalling pathway	Up	19	0.043
Chemokine signalling pathway	Up	15	0.048

Similarly, when KEGG pathway analysis was performed on downregulated and upregulated gene lists in control versus DSCL groups, pathways including ubiquitin mediated proteolysis, hippo signalling pathway and endocytosis were upregulated (p values <0.05; ***Table 4. 15***). However, there were no significantly downregulated genes identified using the DAVID KEGG pathway analysis.

Table 4. 15 KEGG pathway analysis of downregulated and upregulated genes in DSCL versus NAWM. KEGG pathway analysis was performed using the DAVID Functional Annotation Tool (Version 6.8).

Pathway	Up/Down Regulated	P-Value
Ubiquitin mediated proteolysis	Up	0.0014
Hippo signalling pathway	Up	0.0048
Endocytosis	Up	0.014
Antigen processing and presentation	Up	0.02
Glioma	Up	0.03

When NAWM versus non-lesional control downregulated and upregulated gene list was analysed using DAVID, one of the main pathways identified was axon guidance and cell adhesion molecules (p values <0.05; ***Table 4. 16***). There were no significantly up-regulated pathways when genes from this two-group comparison.

Table 4. 16 KEGG pathway analysis of downregulated and upregulated genes in NAWM versus non-lesional controls. KEGG pathway analysis was performed using the DAVID Functional Annotation Tool (Version 6.8). There were no statistically significant upregulated pathways identified in the DAVID analysis.

Pathway	UP/Down Regulated	P-Value
Axon guidance	Down	0.0026
Butanoate metabolism	Down	0.0032
Cell adhesion molecules (CAMs)	Down	0.046

Overall, the endocytic pathway was upregulated in control versus DSCL and downregulated in DSCL versus NAWM group. Similarly, ubiquitin mediated proteolysis pathway was upregulated in non-lesional control versus DSCL group but was downregulated in DSCL versus NAWM group. There was no pathway that overlapped in the three-group comparison.

4.4.5.4 Summary of Microarray analysis

In summary, the data presented demonstrates that microvessels in DSCL are associated with significant dysregulation of genes associated with endocytosis and ubiquitin-mediated proteolysis compared to both control WM and NAWM. Furthermore, there is dysregulation in immune response-related genes in the DSCL compared to non-lesional control WM, and in FOXO signalling associated genes compared to NAWM. Interestingly, the transcriptomic profile of NAWM from lesional cases was significantly different compared to the control WM from non-lesional cases and was associated with dysregulation of genes related to p53 signalling.

4.5 Discussion

WML are an independent risk factor for dementia and their presence is associated with the acceleration of mild cognitive impairment to AD. While the precise mechanism underlying their pathogenesis is currently unknown, they have been suggested to arise as a result of disruption to the BBB. Histological characterisation of age associated WML has demonstrated that these lesions show evidence of disruption of the BBB, which may result in the accumulation of serum proteins within the CNS and the activation of a neuroinflammatory response (Huang et al., 2010; Simpson et al., 2010) . Previous studies have characterised the transcriptomic profile of WML but have examined whole tissue extracts which likely masked vessel-specific changes (Ritz et al., 2016; Simpson et al., 2009) . Therefore, the current study used LCM to isolate microvessels from WML and compared their gene expression profile to vessels isolated from the NAWM of lesional cases and control WM from non-lesional cases. The transcriptomic signatures identified in this study elucidate gene expression changes which may underlie lesion formation in the ageing brain.

The highest number of significantly differentially expressed genes were detected in the NAWM versus DSCL comparison. When the transcriptomic profile of vessels in the NAWM was compared to control cases, over 1000 genes were significantly differentially expressed, providing further evidence that transcriptomic changes are not restricted to the lesion and that WML arise in a field effect of gene expression changes. Transcriptomic changes in the NAWM identified pathways including endocytosis, proteolysis and antigen presentation, which indicate that gene expression changes are not limited to the focal lesion and suggest potential mechanisms which may underlie lesion spread. Although the NAWM appears radiologically normal under MRI examination, newer techniques such as diffusion tensor imaging (DTI) and magnetic resonance spectroscopy (MRS) are more sensitive to microstructural changes (O'Donnell and Westin, 2011; Wen et al., 2019; Wozniak and Lim, 2006). In future, these techniques might allow clinicians to detect the small early subclinical lesions which may develop into WML. Overall, the findings of the current study indicate that WML arise in a background of gene expression changes, and these changes in the NAWM may give rise to lesion spread.

4.5.1 Dysregulation of proteolysis and endocytosis as a mechanism for lesion formation

One of the major pathways identified by the microarray analysis was dysregulation of proteolysis, corroborating the findings of a previous study which investigated transcriptomic

changes in total extracts from WML versus control (Simpson et al., 2009). Intracellular proteolytic activation is important for the maintenance of the vasculature, however dysregulation of this pathway can lead to cerebral ischemia (Asahi et al., 2001; Gingrich and Traynelis, 2000). Extracellular proteolysis may contribute to the tissue damage seen in WML and may give rise to an ischemic environment by impacting vascular integrity (Asahi et al., 2001). Proteolysis of the cerebrovascular basal lamina and junctional proteins, specifically ZO-1 and occludin, can impact BBB function leading to local neuroinflammatory responses (Kniesel and Wolburg, 2000).

Another major finding was the differential expression of genes associated with endocytosis, indicating that the potential uptake and/or transport of molecules by the endothelial cells are disrupted. Unlike other barrier endothelial cells, brain endothelial cells are highly regulated (Tuma and Hubbard, 2003). Endocytosis is a pathway utilised by brain endothelial cells for the transport of macromolecules such as proteins and peptides. This tight regulation of movement of molecules across the barrier means the endothelial transcriptome is highly enriched in genes coding for transporters (11% of all the genes) (Enerson and Drewes, 2006). Since this process is highly regulated in the cerebral endothelial cells and the rate of uptake changes according to the needs of the neighbouring neurons/axons, dysfunction of this biological pathway would potentially severely impact the normal brain function.

4.5.2 Role of ubiquitin-mediated proteolysis in BBB dysfunction

Another major pathway identified in the current study was ubiquitin-mediated proteolysis. This pathway, commonly known as the ubiquitin-proteasome system plays a central role in the clearance of damaged and mis-folded proteins from the nucleus and cytoplasm of the cell (Kleiger and Mayor, 2014). In addition, this system also degrades normal proteins and helps to recycle amino acids thereby maintaining proteostasis by preventing protein aggregation in the body. Interestingly, ubiquitin-mediated proteolysis is studied extensively in AD as protein aggregation of amyloid-β is one of the major features of AD neuropathology. In fact, the role of ubiquitin-mediated proteolysis was first reported in the 1980's when polyclonal antibodies against conjugated ubiquitin intensely stained the neurofibrillary tangles in AD (Lowe et al., 1988; Mori et al., 1987). In contrast, fewer studies have investigated the role of ubiquitin-mediated proteolysis in the pathogenesis of age-associated WML.

One of the most prominent chaperons, heat shock protein 70 (HSP70) family is responsible for the folding of proteins as well transport of misfolded proteins for degradation (Hartl et al.,

2011). Heat shock 70kDa protein 4 *(HSPA4)* was significantly differentially expressed (downregulated) in DSCL when compared to non-lesional control cases. Interestingly this gene was also downregulated in DSCL when compared to NAWM, suggesting that this molecule chaperon system and ubiquitin mediated proteolysis play an important role in lesion formation. Downregulation of genes in this pathway may lead to accumulation of misfolded proteins, leading to cellular stress which can eventually cause apoptosis (Stone and Lin, 2015). Interestingly, *HSPA4* was also reported to be downregulated in AD, when post-mortem tissue of cortex and hippocampus was analysed using microarray analysis (Liang et al., 2008). *HSPA4* is also an important component of the molecular chaperon system that can disassemble tau fibrils (Nachman et al., 2020), which can eventually lead to NFT formation.

Ubiquitin specific ligases such as E3 ligases can affect cell-cell contacts such as VE-cadherin by controlling its expression levels and localisation at cell-junctions (Orsenigo et al., 2012). The TJ protein occludin can be affected by ubiquitination, thereby affecting junctional stability (Murakami et al., 2012, 2009). Animal model studies have added more insight into how the ubiquitin pathway can play a role in junctional stability, for example ubiquitination of occludin leads to a decrease in vascular integrity in an ischemic rat model (Zhang et al., 2013). This paper also demonstrated that targeting ubiquitination and degradation of occludin reduces the leakage of Evan's blue into the brain parenchyma, further demonstrating the role of ubiquitination in the regulation of junctional stability. Targeting of the MARCH family of E3 ligases in brain endothelial cells by siRNA results in the upregulated expression of claudin-5 and occludin, both junctional proteins (Leclair et al., 2016). Interestingly, this pathway is different to ubiquitination and degradation of claudin-5 in human brain endothelial cells by HECT domain E3 ligases (Rui et al., 2018). Together with the results of the current study, these findings suggest a role for the ubiquitin pathway in regulating the vascular integrity which is crucial for maintaining the normal function of the BBB. Disruption of the pathway may underlie the vascular pathology seen in WML and contribute to lesion pathogenesis.

Another dysregulated pathway was adhesion molecules, which play a role in maintaining BBB integrity through their interaction with TJ proteins, supporting previous reports of tight junction protein loss in WML (Hawkins and Davis, 2005; Simpson et al., 2010; Takechi et al., 2017). The actin cytoskeleton of endothelial cells can influence the spatial arrangements of TJ proteins and AJ proteins (Tietz and Engelhardt, 2015). This close association is responsible for remodelling in response to an injury, allowing disassembly of the barrier and recruitment of immune cells and plasma proteins that will effectively allow for tissue repair (Tietz and

Engelhardt, 2015). In patients with dementia, brain endothelial cells release significantly higher levels of proteases such as thrombin and MMPs which have the ability to remodel the BBB (Thirumangalakudi et al., 2006). Systemic inflammation and oxidative stress also increase the proteolysis of TJ proteins which may exacerbate BBB dysfunction (Cipolla et al., 2011; Kamada et al., 2007).

Cerebrovascular dysfunction is an early event and precedes cognitive decline in AD (Bell and Zlokovic, 2009; de la Torre, 2004). Studies of BBB function in patients with DSCL using traceable dyes, indicate increased BBB permeability compared to non-neurological controls (Topakian et al., 2010). This loss of BBB integrity and associated leakage increases as the lesion load increases (Farrall and Wardlaw, 2009; Skoog et al., 1998). Furthermore, patients with a higher lesion load also have increased BBB leakage in the NAWM (Wardlaw et al., 2013a). Together with the current study, these findings indicate that BBB dysfunction is a feature of age-associated WML and impaired vascular integrity in the NAWM may contribute to lesion spread.

4.5.3 p53 dysregulation may underlie the loss of BBB integrity in WML

The current study demonstrates dysregulation of the p53 signalling pathway is a feature of the endothelial cells in the NAWM, supporting previous histological studies of ageing white matter pathology (Al-Mashhadi et al., 2015). Under normal conditions, p53 is activated in response to cellular stress, for example oxidative-stress induced DNA damage. If this repair mechanism fails to completely repair the DNA damage, it can lead to p53-mediated apoptosis. Since p53 plays a key role in maintaining genomic stability its role is crucial for maintaining homeostasis within the CNS. P53 can also be activated by hypoxia, which is a feature of DSCL and the surrounding NAWM (Fernando et al., 2004) . Together these findings suggest dysregulation of p53 signalling may contribute to the loss of BBB integrity in the NAWM.

P53 has been extensively studied in the cancer field, and how it can impact the immune response (Blagih et al., 2020). It is only recently that the role of p53 is starting to be elucidated in the development of dementia. Fibroblasts from sporadic AD patients exhibit impaired p53 signalling resulting in an impaired DNA damage response (Uberti et al., 2002). Furthermore, levels of conformationally altered p53 are statistically higher in patients with dementia compared to age matched controls, suggesting their use as a novel biomarker candidate (Lanni

et al., 2008). While these studies indicate a role for p53 in AD, more research is needed to understand if this is true for all types of dementia.

Interestingly, the ubiquitin-mediated proteolysis system also plays a crucial role in regulating p53 (Yang et al., 2004), an unstable protein with a short half-life (Oren et al., 1981; Pant et al., 2011). Under normal conditions, p53 levels are tightly controlled by ubiquitination (Querido et al., 2001). The major E3 ligase for p53 is Mdm2 (Haupt et al., 1997; Michael and Oren, 2003; Pant et al., 2011), and under stress or DNA damage, Mdm2 undergoes phosphorylation and is degraded (Horn and Vousden, 2007), leading to p53 stabilisation. In the current study, *MDM2* is downregulated in DSCL when compared to both control and NAWM, indicating that proteolysis pathway itself is dysregulated leading to activation and stabilisation of p53, which can result in apoptosis.

Together, all this evidence suggests a role of p53 in the vascular pathology associated with ageing WM pathology, one which is very complex with interplay between several pathways. Our findings suggest endothelial cell death due to activation of p53 is not just a feature of established lesions, it is also upregulated in NAWM, indicating WML arise in a field effect of vascular pathology.

4.5.4 Microarray is a powerful platform to study transcriptomic changes in ageing WM

Microarray technologies provide an excellent opportunity to look beyond individual gene candidates and identify novel pathways that can be targeted for potential new therapeutics. To date there are few studies that have combined laser capture microdissection with microarray analysis to investigate transcriptomic changes in a specific cell type in the brain. Previous microarray analysis of ageing WM pathology has been performed on whole tissue extracts. To our knowledge, this study is the first one to report microarray analysis performed on isolated endothelial cells from ageing WM. Although the previous studies performed microarray analysis of whole tissue extracts, it should be noted that they identified dysregulation of inflammation and apoptosis in WML (Ritz et al., 2016; Simpson et al., 2009), supporting the findings of the current study. However, the current study also identified dysregulation of other biologically relevant candidates, including tight junction proteins and endocytosis. Using LCM to isolate an enriched population enables the identification of cell-specific transcriptomic changes which are likely masked when analysing whole tissue extracts.

Although WML are an independent risk factor for dementia, to date most studies have focused on cortical changes. Transcriptomic profiling of WM has mostly been performed on other WM diseases, such as multiple sclerosis (MS). While MS is a distinct disease, the WML observed in MS do share some similarities to age associated WML, including demyelination and BBB dysfunction (Lock et al., 2002; Melief et al., 2019; Mycko et al., 2003; Waller et al., 2016; Whitney et al., 2001), and recent transcriptomic profiling of the NAWM in MS indicates that gene expression changes extend beyond the MS lesion into the surrounding radiologically normal appearing white matter (Waller et al., 2016). Even though there are more studies performed on WML in MS diseases, not many have utilised LCM combined with transcriptomic profiling to interrogate gene expression changes related to disease (Kinnecom and Pachter, 2005; Kirk et al., 2003; Mojsilovic-Petrovic et al., 2004). Combining LCM with transcriptomic profiling is a valuable tool to identify potential mechanisms underlying pathology.

LCM was first developed by Emmert-Buck et al. and has effectively transformed the study of individual cell populations (Emmert-Buck et al., 1996), including the isolation of cerebral endothelial cells (Cunnea et al., 2010; Macdonald et al., 2008). It allows isolation of mRNA, RNA and proteins from an enriched cell population, and can be coupled with microarray analysis to understand cell-associated changes in the transcriptome (Bernard et al., 2009; Harris et al., 2008). However, it should be acknowledged that LCM does not isolate a pure population, rather it isolates an enriched cell population. As the astrocyte endfeet are in intimate contact with the BBB, contamination of the LCM-ed endothelial cells with astrocyte transcripts is unavoidable (Ball et al., 2002; Mojsilovic-Petrovic et al., 2004), however PCR analysis of the RNA extracted from LCM-ed cerebral microvessels in the current study indicates that the population is enriched for endothelial cells.

Various factors such as the agonal state of the patient, post-mortem delay, storage and sectioning can affect the quality of the RNA (Ferreira et al., 2018)(Koppelkamm et al., 2011; Preece and Cairns, 2003). The process of immunostaining, even with a rapid protocol, and LCM is lengthy, and can further impact the RNA quality. However, human post-mortem transcriptomic studies are immensely valuable for identifying disease-associated gene expression changes and are a valuable hypothesis generating tool.

Initial comparison between microarray analysis from chapter 3 and post-mortem analysis was performed, showing that there were no overlapping pathway changes between endothelial cells

in WM in post mortem tissue and NMV treated endothelial cells. However in-depth analysis is required and since WM was not from patients who had peripheral inflammation, it would be hard to predict if any changes were induced due to NMVs.

4.6 Conclusions & major findings

- LCM can be employed to isolate an enriched endothelial population from post-mortem tissue.
- While the NAWM is radiologically normal, transcriptomic analysis suggest WML arise in a field effect of transcriptomic changes.
- Dysregulation of p53 signalling may contribute to the loss of BBB integrity in the NAWM.
- Ubiquitin-mediated proteolysis may underlie BBB dysfunction in WML.
- Dysregulation of endocytosis is associated with endothelial cells in both the NAWM and DSCL and may impact the movement of molecules across the BBB.

Chapter 5: General Conclusion

5.1 Major findings and limitations of this study

Dysfunction of the BBB is a major feature of various neurodegenerative diseases, but the mechanisms underlying this dysfunction remain poorly understood. The BBB is a dynamic barrier that controls the movement of molecules between the circulation and the CNS. This tightly controlled barrier is crucial to protect the CNS from the harmful substances that can be found in the blood, which may be toxic to neurons. As we age, our immune system is repeatedly challenged causing it to be primed. Repeated peripheral challenge to the immune system can exaggerate and prolong CNS inflammation (Godbout et al., 2005; Li et al., 2012). Furthermore, systemic inflammation can exacerbate dementia (Fong et al., 2015; Girard et al., 2010). Additionally microstructural changes in the endothelium are associated with peripheral inflammation in AD patients (Swardfager et al., 2017), demonstrating a role of peripheral inflammation in the activation and dysfunction of the BBB.

Neutrophils play a role in driving cognitive impairment in animal model of AD and depletion of neutrophils improves cognition in the early stages of AD (Zenaro et al., 2015), suggesting that neutrophils contribute to cognitive dysfunction. Since neutrophils are not a feature of dementia neuropathology, the current study hypothesised that neutrophils contribute to BBB dysfunction through their release of NMVs. There is mounting evidence that NMVs target other peripheral endothelial cells thereby contributing to the disease pathogenesis (Gomez et al., 2020; Pitanga et al., 2014). Therefore, this study aimed to determine if brain microvascular endothelial cells interact with NMVS *in vitro* and if that interaction caused transcriptomic changes in the endothelial cells. At the same time, evidence of BBB dysfunction and potential mechanisms underlying this dysfunction was studied *in vivo*, in WML tissue.

The first part of this study aimed to develop an *in vitro* model to investigate the interactions between NMVs and the BBB (see ***Figure 5. 1***) To model the BBB, the human cerebral microvessel endothelial cell line hCMEC/D3 was used. There are many advantages of using this cell line over primary endothelial cells. These cells have the ability to form a contact-inhibited monolayer, express junctional proteins and display restricted permeability to tracer molecules such as lucifer yellow (Weksler et al., 2013). Additionally, this cell line is used in many drug transport studies, is commercially available and relatively easy to culture, all making this cell line a great resource to study the BBB. Nevertheless, hCMEC/D3 also have some disadvantages which should be acknowledged, for example they do not develop a high

TEER, which can be used as an indicator for barrier integrity. Under physiological conditions *in vivo* TEER values can range between 1500-2000 Ωcm^2 (Butt et al., 1990). This study confirmed the previous finding that hCMEC/D3 have a TEER ranging from 20-30 Ωcm^2 (Eigenmann et al., 2013; Weksler et al., 2013). Although hCMEC/D3 are a robust cell model for studying the BBB, it should be acknowledged that the BBB comprises more than endothelial cells and also contains astrocytic endfeet and pericytes. However, to understand how NMVs interact with cerebral endothelial cells using this monoculture enabled us to determine how endothelial cells interact with and internalise NMVs. This preliminary work informs how NMVs may work in complex *in vitro* models of the BBB.

Incubation of NMVs with hCMEC/D3 initiated internalisation of NMV via multiple energy dependent endocytosis pathways. To our knowledge, this is the first study to report the internalisation of NMV by human brain microvascular endothelial cells. Internalisation of NMVs was confirmed using two different techniques – confocal microscopy and flow cytometry. Although this study reported that internalisation of NMVs by hCMEC/D3 was dose-dependent, it should be noted that full saturation was not observed. There is very little knowledge about the actual concentration of NMVs found in the circulation during inflammation/an infection. Several *in vivo* and *in vitro* studies have used various concentrations (Dalli et al., 2008; Gomez et al., 2020; Pitanga et al., 2014; Rhys et al., 2018). This study opted to use 300 NMV/μL as the final concentration, guided by the findings of a paper analysing various MVs in blood in patients with systemic inflammation which reported that NMV ranged between 200- 400 concentration NMV/μL (Guervilly et al., 2011). However, it should be noted that this makes it harder to compare this study's findings to other *in vitro* studies as the concentration differs between them.

One of the major limitations of this study was using NMVs from young control participants. The average age of the participants was 25 years; however it should be noted that the immune system of younger participants is robust and may react differently to older participants. Neutrophils from elderly patients can be primed, leading to constituent activation (Hazeldine et al., 2014), which may affect the contents of NMVs and the differential expression of genes in their target cells. However, investigating NMVs from control participants enabled this study to investigate how the NMVs are internalised and which genes could be targeted in the brain microvascular endothelial cells.

Transcriptomic profiling of hCMEC/D3 cells treated with NMVs revealed that NMVs induce dysregulation in the expression of tight junction proteins, p38 pathway and SNARE-mediated vesicular transport. It should be noted that these changes were present after 24h incubation with one dose of NMV at the start of the experiment and may not reflect physiological conditions. During systemic inflammation, neutrophils are activated and release NMVs into the bloodstream. It is surprising that although this was a one-off challenge, it elicited dysregulation of genes involved in cellular apoptosis, inflammation and vascular integrity. These findings have potential implications *in vivo* as it suggests that persistent challenge by NMVs in the circulation may impact cerebrovascular integrity and elicit a neuroinflammatory response.

The second part of this study aimed to characterise the gene expression changes associated with cerebral microvessels in ageing WM (see summary ***Figure 5. 2***). Transcriptomic profiling of isolated endothelial cells suggest that BBB dysfunction underlies the pathogenesis of age associated WML. One of the main pathways identified was cell adhesion, supporting previous reports. Another important pathway highlighted was proteolysis. Interestingly this pathway was upregulated in the vessels in the NAWM versus DSCL and downregulated in the DSCL versus control WM, suggesting that increased proteolysis is an early feature of lesion pathogenesis which decreases when the lesion is established. A major finding of the current study was the large number of significant gene expression changes in the radiologically NAWM surrounding WML, compared to both the lesion and control WM from non-lesional cases. This finding indicates that transcriptomic changes are not isolated to vessels in established WML but extend beyond the lesion into the radiologically NAWM giving rise to a field-effect.

There are some limitations to this *in vivo* study which should be acknowledged. Although LCM is now widely used to isolate various cell populations, including endothelial cells, it does not isolate a pure endothelial population. A small level of contamination with glial cells was observed, though this is not surprising given the intimate proximity of astrocyte endfeet to endothelial cells. However, this technique superior to studying whole tissue extracts which likely mask specific transcriptomic changes associated with endothelial cells. Nevertheless, LCM enabled an enriched population to be isolated which enabled the transcriptomic profile of endothelial cells to be determined.

In our study, we were blinded to any clinical information to avoid potential bias and only MRI scans were available. After radiologically identifying the cases, they were histologically

characterised to confirm the presence/absence of a lesion. It should be noted that not all post-mortem tissue could be used for LCM, as some cases were considered unsuitable due to the presence of freeze-thaw artefacts making it difficult to identify vessels for LCM. Furthermore, post-mortem tissue often represents end-stage of a disease and the gene expression changes detected could also be attributed to ageing, making it difficult to decipher pathogenic mechanisms relating to WML formation. Despite all these limitations, post-mortem tissue is a valuable resource to identify changes in the transcriptome of endothelial cells in age associated WML.

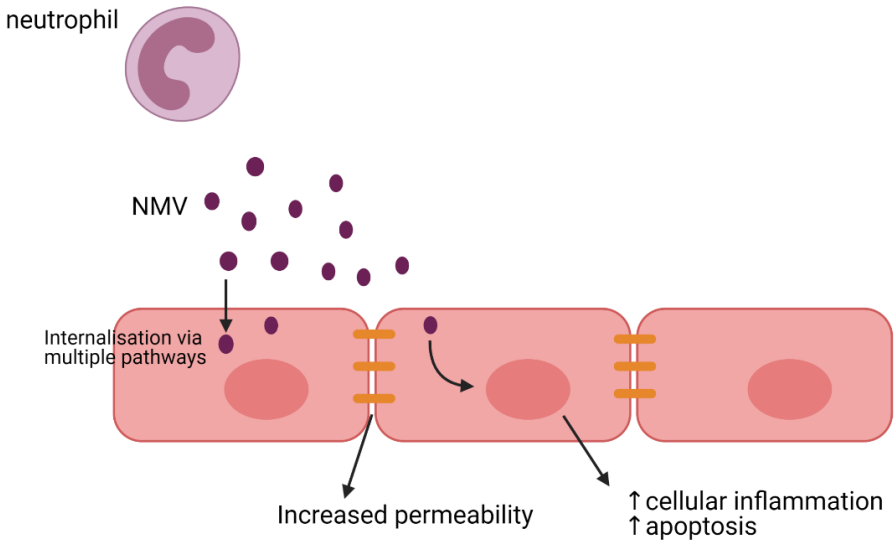

Figure 5. 1- Summary diagram 1: Neutrophils release neutrophil derived microvesicles (NMV) into circulation in response to peripheral inflammation. NMV interact with brain endothelial cells by internalisation via various energy dependent pathways. Internalisation may deliver neutrophil specific cargo to these cells causing increased permeability at blood brain barrier, increased inflammation, and apoptosis. These findings indicate that NMV can interact with and affect gene expression of brain endothelial cells affecting their integrity.

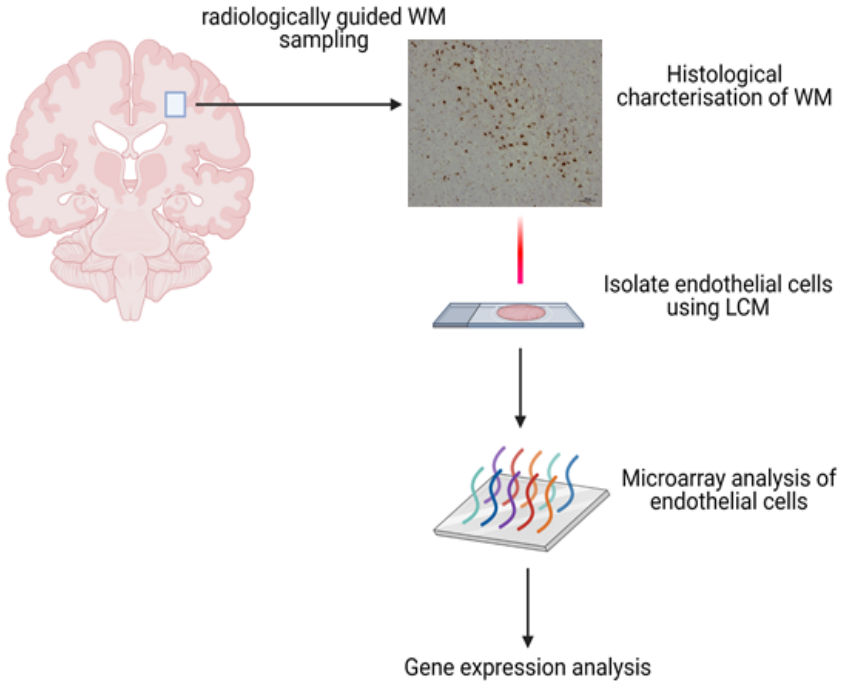

Figure 5. 2- Summary diagram 2: MRI guided sampling was performed on post-mortem tissue to guide WM sampling. After identifying control and lesional cases, each case was histologically charcaterised using CD68 and luxol fast blue to confirm the presence/absence of the lesion. After identifying 5 controls, 5 lesional (DSCL) and 5 radiological normal appearing white matter areas around the lesion (NAWM), endothelial cells were isolated by LCM. RNA was extracted from the LCM-ed capillaries and gene expression analysis performed using microarray analysis. Transcriptomic profiling indicates dysfunction of endothelial cells in both DSCL and NAWM, including dysregulation of genes associated with proteolysis and inflammation. A large number of significant gene expression changes were found in NAWM suggesting lesions arise in a field effect of white matter abnormality.

5.2 Future Work

5.2.1 Characterisation of NMV interaction with co-culture models

The BBB is not just brain microvascular endothelial cells in isolation, but is a complex unit comprising endothelial cells, astrocytic endfeet and pericytes. Future studies investigating the NMV interaction with this complex system will allow us to understand how the peripheral immune system may impact the BBB through MVs. Future studies should aim to investigate the interaction between NMVs and a co-culture model of the BBB comprising astrocytes and pericytes along with endothelial cells. Additionally, co-culture methods should be employed which allow separation of the individual cell type to enable cell-specific changes in gene expression to be measured, thereby enabling a comprehensive understanding of the interaction between NMVs and all components of the BBB.

Additionally, to mimic physiological conditions future studies should aim to employ primary endothelial cells or induced pluripotent stem cells, as they are known to achieve higher TEER values, ensuring the tight junctions between the endothelial cells are fully formed. This approach will also provide a more biologically relevant TEER reading. Furthermore, measuring TEER over a longer time course will enable NMV-induced long-term changes to the permeability of the barrier to be determined.

5.2.2 Investigating how NMV differs in dementia patients with and without infection

The current study demonstrates the impact of NMVs from control participants has a significant impact on the integrity of healthy endothelial cells. However, many studies have demonstrated that the immune system is primed in dementia patients, and after an infection their cognitive status does not return to previous levels. It is highly likely that the NMVs from dementia patients may differ to non-dementia patients. Therefore, future studies should aim to repeat the current study in age and gender matched controls and dementia patients, both with and without infections. This approach would determine if NMVs from dementia patients (both with and without infection) have a more significant impact on vascular integrity *in vitro*. This could be further interrogated by assessing the transcriptomic profile of hCMEC/D3 in response to internalisation of NMVs from dementia patients (with and without an infection). By doing this, it would allow us to compare the results obtained from this study using healthy donors to that of dementia patients, allowing an in depth understanding of the changes in the transcriptome.

5.2.3 Characterisation of the contents of NMV

Although this study has focused on the effects of NMVs on brain microvascular endothelial cells, it did not characterise the contents of NMVs. NMVs are a source of miRNAs, which are known to regulate the transcription of many genes in the target cells, therefore profiling the miRNA content of NMVs from dementia patients may indicate how NMVs impact their target cell(s), and could also be characterised in dementia patients with and without an infection.

5.2.4 Validation of microarray findings

The enrichment analysis using DAVID highlighted dysregulation of genes involved in ubiquitin mediated proteolysis, SNARE mediated vesicular transport and p38 pathway, demonstrating NMVs significantly affect the gene expression of major pathways involved in cellular functions in brain endothelial cells. Ubiquitination plays a key role in clearing damaged and aggregated proteins from the cell. Proteolysis is also important to the regulation of BBB integrity and dysregulation of this pathway may lead to the breakdown of BBB. SNARE proteins are also involved in intracellular traffic and may a role in the vesicular transport of MVs. P38 is a major pathway which can regulate inflammation and DNA repair. Due to limited time, validation of key genes of interest from pathways and functional groups was not conducted. Validation of a panel of candidate gene expression changes should be performed at both the gene and protein level, by qPCR and western blotting respectively, to understand if key gene expression changes are translated to changes in protein levels. Validation of these pathways and functional groups will aid in understanding how NMVs exert their effect on BBB, leading to its dysfunction.

5.2.5 Animal model studies to investigate the NMV interaction with the BBB

Previous studies have shown that NMVs injected in the periphery can be detected in the aorta of the mice (Gomez et al., 2020). This approach could be applied to study the interaction between NMVs and the BBB *in vivo* in an animal model of dementia and determine if NMVs are transcytosed across the BBB. Administration of LPS to this model, to mimic peripheral infection, would also enable the impact of systemic inflammation on NMV internalisation by the BBB to be assessed. In addition, the permeability of BBB using tracer molecules could be measured at various time points. This approach would extend the current study and enable NMV-induced BBB dysfunction to be determined in a relevant model of dementia.

5.2.6 Validation of the post-mortem microarray findings

Due to limited time, validation of the candidates identified in the microarray analysis of endothelial cells in WML were not conducted. Validation of the key transcriptomic changes should be performed on an extended cohort, using both qPCR to assess key gene expression changes and immunohistochemistry or western blotting to determine if gene expression changes are reflected at the protein level. Using these approaches to study a panel of candidates would enable key differences in the gene expression of vessels to be validated and may identify biologically relevant mechanisms underlying BBB dysfunction and the pathogenesis of age associated WML.

5.2.7 Post-mortem tissue analysis

Transcriptomic analysis of endothelial cells from control, DSCL and NAWM samples revealed many changes linked to BBB dysfunction. A better way to analyse and understand if these changes are directly linked to infection is to utilise post-mortem tissue of patients who died with and without an infection. Transcriptomic profiling of endothelial cells from patients with and without an infection may identify BBB changes directly linked to an infection. Data obtained from this proposed research could be compared to the data obtained in this study, allowing a deeper understanding of the changes in endothelium related to infection.

References

Abi Abdallah, D.S., Egan, C.E., Butcher, B.A., Denkers, E.Y., 2011. Mouse neutrophils are professional antigen-presenting cells programmed to instruct Th1 and Th17 T-cell differentiation. Int. Immunol. 23, 317–326.

Abraham, H.M.A., Wolfson, L., Moscufo, N., Guttmann, C.R.G., Kaplan, R.F., White, W.B., 2016. Cardiovascular risk factors and small vessel disease of the brain: Blood pressure, white matter lesions, and functional decline in older persons. J. Cereb. Blood Flow Metab. 36, 132–142. doi:10.1038/jcbfm.2015.121

Aisen, P.S., Schafer, K.A., Grundman, M., Pfeiffer, E., Sano, M., Davis, K.L., Farlow, M.R., Jin, S., Thomas, R.G., Thal, L.J., Study, for the A.D.C., 2003. Effects of Rofecoxib or Naproxen vs Placebo on Alzheimer Disease ProgressionA Randomized Controlled Trial. JAMA 289, 2819–2826. doi:10.1001/jama.289.21.2819

Ajikumar, A., Long, M.B., Heath, P.R., Wharton, S.B., Ince, P.G., Ridger, V.C., Simpson, J.E., 2019. Neutrophil-Derived Microvesicle Induced Dysfunction of Brain Microvascular Endothelial Cells In Vitro. Int. J. Mol. Sci. . doi:10.3390/ijms20205227

Akdis, M., Aab, A., Altunbulakli, C., Azkur, K., Costa, R.A., Crameri, R., Duan, S., Eiwegger, T., Eljaszewicz, A., Ferstl, R., Frei, R., Garbani, M., Globinska, A., Hess, L., Huitema, C., Kubo, T., Komlosi, Z., Konieczna, P., Kovacs, N., Kucuksezer, U.C., Meyer, N., Morita, H., Olzhausen, J., O'Mahony, L., Pezer, M., Prati, M., Rebane, A., Rhyner, C., Rinaldi, A., Sokolowska, M., Stanic, B., Sugita, K., Treis, A., van de Veen, W., Wanke, K., Wawrzyniak, M., Wawrzyniak, P., Wirz, O.F., Zakzuk, J.S., Akdis, C.A., 2016. Interleukins (from IL-1 to IL-38), interferons, transforming growth factor beta, and TNF-alpha: Receptors, functions, and roles in diseases. J. Allergy Clin. Immunol. 138, 984–1010. doi:10.1016/j.jaci.2016.06.033

Al-Mashhadi, S., Simpson, J.E., Heath, P.R., Dickman, M., Forster, G., Matthews, F.E., Brayne, C., Ince, P.G., Wharton, S.B., Medical Research Council Cognitive Function and Ageing Study, 2015. Oxidative glial cell damage associated with white matter lesions in the aging human brain. Brain Pathol. 25, 565–74. doi:10.1111/bpa.12216

Amulic, B., Cazalet, C., Hayes, G.L., Metzler, K.D., Zychlinsky, A., 2012. Neutrophil function: from mechanisms to disease. Annu. Rev. Immunol. 30, 459–489. doi:10.1146/annurev-immunol-020711-074942

Anblagan, D., Pataky, R., Evans, M.J., Telford, E.J., Serag, A., Sparrow, S., Piyasena, C., Semple, S.I., Wilkinson, A.G., Bastin, M.E., Boardman, J.P., 2016. Association between preterm brain injury and exposure to chorioamnionitis during fetal life. Sci. Rep. 6, 37932. doi:10.1038/srep37932

Armstrong, S.A., Staunton, J.E., Silverman, L.B., Pieters, R., den Boer, M.L., Minden, M.D., Sallan, S.E., Lander, E.S., Golub, T.R., Korsmeyer, S.J., 2002. MLL translocations specify a distinct gene expression profile that distinguishes a unique leukemia. Nat. Genet. 30, 41–47. doi:10.1038/ng765

Asahi, M., Wang, X., Mori, T., Sumii, T., Jung, J.C., Moskowitz, M.A., Fini, M.E., Lo, E.H., 2001. Effects of matrix metalloproteinase-9 gene knock-out on the proteolysis of blood-brain barrier and white matter components after cerebral ischemia. J. Neurosci. 21, 7724–7732. doi:10.1523/JNEUROSCI.21-19-07724.2001

Athens, J.W., Haab, O.P., Raab, S.O., Mauer, A.M., Ashenbrucker, H., Caerwright, G.E., Wintrobe, M.M., 1961. Leukokinetic studies. IV. The total blood, circulating and marginal granulocyte pools and the granulocyte turnover rate in normal subjects. J. Clin. Invest. 40, 989–995. doi:10.1172/JCI104338

Atwood, D., A., W.P., L., H.-C.N., M., M.J., Alexa, B., B., D.R., Charles, D., 2004. Genetic Variation

in White Matter Hyperintensity Volume in the Framingham Study. Stroke 35, 1609–1613. doi:10.1161/01.STR.0000129643.77045.10

Auerbach, S.D., Yang, L., Luscinskas, F.W., 2007. Endothelial ICAM-1 functions in adhesion and signaling during leukocyte recruitment, in: Adhesion Molecules: Function and Inhibition. Springer, pp. 99–116.

Avramopoulos, D., Szymanski, M., Wang, R., Bassett, S., 2011. Gene expression reveals overlap between normal aging and Alzheimer's disease genes. Neurobiol. Aging 32, 2319-e27.

Ball, H.J., McParland, B., Driussi, C., Hunt, N.H., 2002. Isolating vessels from the mouse brain for gene expression analysis using laser capture microdissection. Brain Res. Protoc. 9, 206–213.

Barkovich, A.J., Kjos, B.O., Jackson, D.E.J., Norman, D., 1988. Normal maturation of the neonatal and infant brain: MR imaging at 1.5 T. Radiology 166, 173–180. doi:10.1148/radiology.166.1.3336675

Barry, O.P., FitzGerald, G.A., 1999. Mechanisms of cellular activation by platelet microparticles. Thromb. Haemost. 82, 794–800.

Bartzokis, G., Sultzer, D., Lu, P.H., Nuechterlein, K.H., Mintz, J., Cummings, J.L., 2004. Heterogeneous age-related breakdown of white matter structural integrity: implications for cortical "disconnection" in aging and Alzheimer's disease. Neurobiol. Aging 25, 843–851. doi:10.1016/j.neurobiolaging.2003.09.005

Beach, T.G., Wilson, J.R., Sue, L.I., Newell, A., Poston, M., Cisneros, R., Pandya, Y., Esh, C., Connor, D.J., Sabbagh, M., Walker, D.G., Roher, A.E., 2007. Circle of Willis atherosclerosis: association with Alzheimer's disease, neuritic plaques and neurofibrillary tangles. Acta Neuropathol. 113, 13–21. doi:10.1007/s00401-006-0136-y

Beckett, N.S., Peters, R., Fletcher, A.E., Staessen, J.A., Liu, L., Dumitrascu, D., Stoyanovsky, V., Antikainen, R.L., Nikitin, Y., Anderson, C., Belhani, A., Forette, F., Rajkumar, C., Thijs, L., Banya, W., Bulpitt, C.J., 2008. Treatment of hypertension in patients 80 years of age or older. N. Engl. J. Med. 358, 1887–1898. doi:10.1056/NEJMoa0801369

Beer, K.B., Wehman, A.M., 2017. Mechanisms and functions of extracellular vesicle release in vivo-What we can learn from flies and worms. Cell Adh. Migr. 11, 135–150. doi:10.1080/19336918.2016.1236899

Bell, R.D., Winkler, E.A., Sagare, A.P., Singh, I., LaRue, B., Deane, R., Zlokovic, B. V, 2010. Pericytes control key neurovascular functions and neuronal phenotype in the adult brain and during brain aging. Neuron 68, 409–427. doi:10.1016/j.neuron.2010.09.043

Bell, R.D., Zlokovic, B. V, 2009. Neurovascular mechanisms and blood-brain barrier disorder in Alzheimer's disease. Acta Neuropathol. 118, 103–113. doi:10.1007/s00401-009-0522-3

Benros, M.E., Sorensen, H.J., Nielsen, P.R., Nordentoft, M., Mortensen, P.B., Petersen, L., 2015. The Association between Infections and General Cognitive Ability in Young Men - A Nationwide Study. PLoS One 10, e0124005. doi:10.1371/journal.pone.0124005

Benson, K., Cramer, S., Galla, H.-J., 2013. Impedance-based cell monitoring: barrier properties and beyond. Fluids Barriers CNS 10, 5. doi:10.1186/2045-8118-10-5

Berchuck, A., Iversen, E.S., Luo, J., Clarke, J.P., Horne, H., Levine, D.A., Boyd, J., Alonso, M.A., Secord, A.A., Bernardini, M.Q., Barnett, J.C., Boren, T., Murphy, S.K., Dressman, H.K., Marks, J.R., Lancaster, J.M., 2009. Microarray Analysis of Early Stage Serous Ovarian Cancers Shows Profiles Predictive of Favorable Outcome. Clin. Cancer Res. 15, 2448 LP – 2455. doi:10.1158/1078-0432.CCR-08-2430

Berckmans, R.J., Nieuwland, R., Kraan, M.C., Schaap, M.C.L., Pots, D., Smeets, T.J.M., Sturk, A.,

Tak, P.P., 2005. Synovial microparticles from arthritic patients modulate chemokine and cytokine release by synoviocytes. Arthritis Res. Ther. 7, R536. doi:10.1186/ar1706

Bernard, R., Kerman, I.A., Meng, F., Evans, S.J., Amrein, I., Jones, E.G., Bunney, W.E., Akil, H., Watson, S.J., Thompson, R.C., 2009. Gene expression profiling of neurochemically defined regions of the human brain by in situ hybridization-guided laser capture microdissection. J. Neurosci. Methods 178, 46–54.

Bhat, N.R., Zhang, P., Lee, J.C., Hogan, E.L., 1998. Extracellular signal-regulated kinase and p38 subgroups of mitogen-activated protein kinases regulate inducible nitric oxide synthase and tumor necrosis factor-α gene expression in endotoxin-stimulated primary glial cultures. J. Neurosci. 18, 1633–1641.

Biesmans, S., Meert, T.F., Bouwknecht, J.A., Acton, P.D., Davoodi, N., De Haes, P., Kuijlaars, J., Langlois, X., Matthews, L.J.R., Ver Donck, L., 2013. Systemic immune activation leads to neuroinflammation and sickness behavior in mice. Mediators Inflamm. 2013.

Black, S., Gao, F., Bilbao, J., 2009. Understanding white matter disease: imaging-pathological correlations in vascular cognitive impairment. Stroke 40, S48-52. doi:10.1161/STROKEAHA.108.537704

Blagih, J., Buck, M.D., Vousden, K.H., 2020. p53, cancer and the immune response. J. Cell Sci. 133, jcs237453. doi:10.1242/jcs.237453

Block, M.L., Zecca, L., Hong, J.-S., 2007. Microglia-mediated neurotoxicity: uncovering the molecular mechanisms. Nat. Rev. Neurosci. 8, 57–69. doi:10.1038/nrn2038

Boche, D., Perry, V.H., Nicoll, J.A.R., 2013. Review: activation patterns of microglia and their identification in the human brain. Neuropathol. Appl. Neurobiol. 39, 3–18. doi:10.1111/nan.12011

Bonestroo, H.J.C., Heijnen, C.J., Groenendaal, F., van Bel, F., Nijboer, C.H., 2015. Development of Cerebral Gray and White Matter Injury and Cerebral Inflammation over Time after Inflammatory Perinatal Asphyxia. Dev. Neurosci. 37, 78–94. doi:10.1159/000368770

Borregaard, N., Sorensen, O.E., Theilgaard-Monch, K., 2007. Neutrophil granules: a library of innate immunity proteins. Trends Immunol. 28, 340–345. doi:10.1016/j.it.2007.06.002

Breitner, J.C.S., Haneuse, S.J.P.A., Walker, R., Dublin, S., Crane, P.K., Gray, S.L., Larson, E.B., 2009. Risk of dementia and AD with prior exposure to NSAIDs in an elderly community-based cohort. Neurology 72, 1899–1905. doi:10.1212/WNL.0b013e3181a18691

Brickman, A.M., Provenzano, F.A., Muraskin, J., Manly, J.J., Blum, S., Apa, Z., Stern, Y., Brown, T.R., Luchsinger, J.A., Mayeux, R., 2012. Regional White Matter Hyperintensity Volume, Not Hippocampal Atrophy, Predicts Incident Alzheimer Disease in the CommunityWhite Matter Hyperintensity and Alzheimer Disease. JAMA Neurol. 69, 1621–1627. doi:10.1001/archneurol.2012.1527

Brinkmann, V., Reichard, U., Goosmann, C., Fauler, B., Uhlemann, Y., Weiss, D.S., Weinrauch, Y., Zychlinsky, A., 2004. Neutrophil extracellular traps kill bacteria. Science 303, 1532–1535. doi:10.1126/science.1092385

Broe, G.A., Grayson, D.A., Creasey, H.M., Waite, L.M., Casey, B.J., Bennett, H.P., Brooks, W.S., Halliday, G.M., 2000. Anti-inflammatory Drugs Protect Against Alzheimer Disease at Low Doses. JAMA Neurol. 57, 1586–1591. doi:10.1001/archneur.57.11.1586

Bronge, L., Bogdanovic, N., Wahlund, L.O., 2002. Postmortem MRI and histopathology of white matter changes in Alzheimer brains: A quantitative, comparative study. Dement. Geriatr. Cogn. Disord. 13, 205–212. doi:10.1159/000057698

Brooks, L.R.K., Mias, G.I., 2019. Data-Driven Analysis of Age, Sex, and Tissue Effects on Gene Expression Variability in Alzheimer's Disease . Front. Neurosci. .

Brown, W.R., Thore, C.R., 2011. Review: cerebral microvascular pathology in ageing and neurodegeneration. Neuropathol. Appl. Neurobiol. 37, 56–74. doi:10.1111/j.1365-2990.2010.01139.x

Brun, A., Englund, E., 1986. A white matter disorder in dementia of the Alzheimer type: a pathoanatomical study. Ann. Neurol. 19, 253–262. doi:10.1002/ana.410190306

Brydon, L., Harrison, N.A., Walker, C., Steptoe, A., Critchley, H.D., 2008. Peripheral inflammation is associated with altered substantia nigra activity and psychomotor slowing in humans. Biol. Psychiatry 63, 1022–1029. doi:10.1016/j.biopsych.2007.12.007

Bucks, R.S., Gidron, Y., Harris, P., Teeling, J., Wesnes, K.A., Perry, V.H., 2008. Selective effects of upper respiratory tract infection on cognition, mood and emotion processing: A prospective study. Brain. Behav. Immun. 22, 399–407. doi:10.1016/j.bbi.2007.09.005

Butt, A.M., Jones, H.C., Abbott, N.J., 1990. Electrical resistance across the blood-brain barrier in anaesthetized rats: a developmental study. J. Physiol. 429, 47–62. doi:10.1113/jphysiol.1990.sp018243

Caraci, F., Battaglia, G., Busceti, C., Biagioni, F., Mastroiacovo, F., Bosco, P., Drago, F., Nicoletti, F., Sortino, M.A., Copani, A., 2008. TGF-beta 1 protects against Abeta-neurotoxicity via the phosphatidylinositol-3-kinase pathway. Neurobiol. Dis. 30, 234–242. doi:10.1016/j.nbd.2008.01.007

Chang, A., Staugaitis, S.M., Dutta, R., Batt, C.E., Easley, K.E., Chomyk, A.M., Yong, V.W., Fox, R.J., Kidd, G.J., Trapp, B.D., 2012. Cortical remyelination: a new target for repair therapies in multiple sclerosis. Ann. Neurol. 72, 918–926.

Chang, C.-W., Horng, J.-T., Hsu, C.-C., Chen, J.-M., 2016. Mean Daily Dosage of Aspirin and the Risk of Incident Alzheimer's Dementia in Patients with Type 2 Diabetes Mellitus: A Nationwide Retrospective Cohort Study in Taiwan. J. Diabetes Res. 2016, 9027484. doi:10.1155/2016/9027484

Chargaff, E., West, R., 1946. The biological significance of the thromboplastic protein of blood. J. Biol. Chem. 166, 189–197.

Chen, Y., Craigen, W.J., Riley, D.J., 2009. Nek1 regulates cell death and mitochondrial membrane permeability through phosphorylation of VDAC1. Cell Cycle 8, 257–267.

Cheslow, L., Alvarez, J.I., 2016. Glial-endothelial crosstalk regulates blood–brain barrier function. Curr. Opin. Pharmacol. 26, 39–46. doi:https://doi.org/10.1016/j.coph.2015.09.010

Choi, J.Y., Cui, Y., Kim, B.G., 2015. Interaction between hypertension and cerebral hypoperfusion in the development of cognitive dysfunction and white matter pathology in rats. Neuroscience 303, 115–125. doi:https://doi.org/10.1016/j.neuroscience.2015.06.056

Ciardiello, C., Cavallini, L., Spinelli, C., Yang, J., Reis-Sobreiro, M., de Candia, P., Minciacchi, V.R., Di Vizio, D., 2016. Focus on extracellular vesicles: New frontiers of cell-to-cell communication in cancer. Int. J. Mol. Sci. 17, 175.

Ciechanover, A., Kwon, Y.T., 2015. Degradation of misfolded proteins in neurodegenerative diseases: therapeutic targets and strategies. Exp. Mol. Med. 47, e147–e147. doi:10.1038/emm.2014.117

Cipolla, M.J., Huang, Q., Sweet, J.G., 2011. Inhibition of protein kinase Cbeta reverses increased blood-brain barrier permeability during hyperglycemic stroke and prevents edema formation in vivo. Stroke 42, 3252–3257. doi:10.1161/STROKEAHA.111.623991

Clerici, F., Caracciolo, B., Cova, I., Fusari Imperatori, S., Maggiore, L., Galimberti, D., Scarpini, E.,

Mariani, C., Fratiglioni, L., 2012. Does Vascular Burden Contribute to the Progression of Mild Cognitive Impairment to Dementia? Dement. Geriatr. Cogn. Disord. 34, 235–243.

Collino, F., Deregibus, M.C., Bruno, S., Sterpone, L., Aghemo, G., Viltono, L., Tetta, C., Camussi, G., 2010. Microvesicles derived from adult human bone marrow and tissue specific mesenchymal stem cells shuttle selected pattern of miRNAs. PLoS One 5, e11803–e11803. doi:10.1371/journal.pone.0011803

Cote, S., Carmichael, P.-H., Verreault, R., Lindsay, J., Lefebvre, J., Laurin, D., 2012. Nonsteroidal anti-inflammatory drug use and the risk of cognitive impairment and Alzheimer's disease. Alzheimers. Dement. 8, 219–226. doi:10.1016/j.jalz.2011.03.012

Cox, S.R., Ritchie, S.J., Tucker-Drob, E.M., Liewald, D.C., Hagenaars, S.P., Davies, G., Wardlaw, J.M., Gale, C.R., Bastin, M.E., Deary, I.J., 2016. Ageing and brain white matter structure in 3,513 UK Biobank participants. Nat. Commun. 7, 13629.

Cribbs, D.H., Berchtold, N.C., Perreau, V., Coleman, P.D., Rogers, J., Tenner, A.J., Cotman, C.W., 2012. Extensive innate immune gene activation accompanies brain aging, increasing vulnerability to cognitive decline and neurodegeneration: a microarray study. J. Neuroinflammation 9, 1.

Cukierman-Yaffe, T., Gerstein, H.C., Williamson, J.D., Lazar, R.M., Lovato, L., Miller, M.E., Coker, L.H., Murray, A., Sullivan, M.D., Marcovina, S.M., Launer, L.J., 2009. Relationship between baseline glycemic control and cognitive function in individuals with type 2 diabetes and other cardiovascular risk factors: the action to control cardiovascular risk in diabetes-memory in diabetes (ACCORD-MIND) trial. Diabetes Care 32, 221–226. doi:10.2337/dc08-1153

Culbert, A.A., Skaper, S.D., Howlett, D.R., Evans, N.A., Facci, L., Soden, P.E., Seymour, Z.M., Guillot, F., Gaestel, M., Richardson, J.C., 2006. MAPK-activated Protein Kinase 2 Deficiency in Microglia Inhibits Pro-inflammatory Mediator Release and Resultant Neurotoxicity RELEVANCE TO NEUROINFLAMMATION IN A TRANSGENIC MOUSE MODEL OF ALZHEIMER DISEASE. J. Biol. Chem. 281, 23658–23667.

Culpan, D., Kehoe, P.G., Love, S., 2011. Tumour necrosis factor-α (TNF-α) and miRNA expression in frontal and temporal neocortex in Alzheimer's disease and the effect of TNF-α on miRNA expression in vitro. Int. J. Mol. Epidemiol. Genet. 2, 156–162.

Culshaw, S., Millington, O.R., Brewer, J.M., McInnes, I.B., 2008. Murine neutrophils present Class II restricted antigen. Immunol. Lett. 118, 49–54. doi:10.1016/j.imlet.2008.02.008

Cunnea, P., McMahon, J., O'Connell, E., Mashayekhi, K., Fitzgerald, U., McQuaid, S., 2010. Gene expression analysis of the microvascular compartment in multiple sclerosis using laser microdissected blood vessels. Acta Neuropathol. 119, 601–615. doi:10.1007/s00401-009-0618-9

Cunningham, C., 2013. Microglia and neurodegeneration: the role of systemic inflammation. Glia 61, 71–90.

D'Souza-Schorey, C., Clancy, J.W., 2012. Tumor-derived microvesicles: shedding light on novel microenvironment modulators and prospective cancer biomarkers. Genes Dev. 26, 1287–1299. doi:10.1101/gad.192351.112

Dalli, J., Montero-Melendez, T., Norling, L. V, Yin, X., Hinds, C., Haskard, D., Mayr, M., Perretti, M., 2013. Heterogeneity in neutrophil microparticles reveals distinct proteome and functional properties. Mol. Cell. Proteomics 12, 2205–2219.

Dalli, J., Norling, L. V, Renshaw, D., Cooper, D., Leung, K.-Y., Perretti, M., 2008. Annexin 1 mediates the rapid anti-inflammatory effects of neutrophil-derived microparticles. Blood 112, 2512 LP – 2519.

Dalvi, P., Sun, B., Tang, N., Pulliam, L., 2017. Immune activated monocyte exosomes alter

microRNAs in brain endothelial cells and initiate an inflammatory response through the TLR4/MyD88 pathway. Sci. Rep. 7, 9954. doi:10.1038/s41598-017-10449-0

Daneman, R., Engelhardt, B., 2017. Brain barriers in health and disease. Neurobiol. Dis. 107, 1–3.

De Groot, J.C., De Leeuw, F., Oudkerk, M., Van Gijn, J., Hofman, A., Jolles, J., Breteler, M.M.B., 2002. Periventricular cerebral white matter lesions predict rate of cognitive decline. Ann. Neurol. 52, 335–341.

de Groot, M., Verhaaren, B.F.J., de Boer, R., Klein, S., Hofman, A., van der Lugt, A., Ikram, M.A., Niessen, W.J., Vernooij, M.W., 2013. Changes in normal appearing white matter precede development of white matter lesions. Stroke 44, 1037–1042.

de la Torre, J.C., 2004. Is Alzheimer's disease a neurodegenerative or a vascular disorder? Data, dogma, and dialectics. Lancet. Neurol. 3, 184–190. doi:10.1016/S1474-4422(04)00683-0

De Magalhães, J.P., Curado, J., Church, G.M., 2009. Meta-analysis of age-related gene expression profiles identifies common signatures of aging. Bioinformatics 25, 875–881.

Debette, S., Markus, H.S., 2010. The clinical importance of white matter hyperintensities on brain magnetic resonance imaging: systematic review and meta-analysis. Bmj 341, 1–9. doi:10.1136/bmj.c3666

DeCarli, C., Murphy, D.G., Tranh, M., Grady, C.L., Haxby, J. V, Gillette, J.A., Salerno, J.A., Gonzales-Aviles, A., Horwitz, B., Rapoport, S.I., 1995. The effect of white matter hyperintensity volume on brain structure, cognitive performance, and cerebral metabolism of glucose in 51 healthy adults. Neurology 45, 2077–2084.

Derada Troletti, C., Fontijn, R.D., Gowing, E., Charabati, M., van Het Hof, B., Didouh, I., van der Pol, S.M.A., Geerts, D., Prat, A., van Horssen, J., Kooij, G., de Vries, H.E., 2019. Inflammation-induced endothelial to mesenchymal transition promotes brain endothelial cell dysfunction and occurs during multiple sclerosis pathophysiology. Cell Death Dis. 10, 45. doi:10.1038/s41419-018-1294-2

Deregibus, M.C., Cantaluppi, V., Calogero, R., Lo Iacono, M., Tetta, C., Biancone, L., Bruno, S., Bussolati, B., Camussi, G., 2007. Endothelial progenitor cell derived microvesicles activate an angiogenic program in endothelial cells by a horizontal transfer of mRNA. Blood 110, 2440–2448. doi:10.1182/blood-2007-03-078709

Derynck, R., Zhang, Y.E., 2003. Smad-dependent and Smad-independent pathways in TGF-beta family signalling. Nature 425, 577–584. doi:10.1038/nature02006

Devine, M.E., Fonseca, J.A.S., Walker, Z., 2013. Do cerebral white matter lesions influence the rate of progression from mild cognitive impairment to dementia? Int. psychogeriatrics 25, 120–127.

Diehl, P., Fricke, A., Sander, L., Stamm, J., Bassler, N., Htun, N., Ziemann, M., Helbing, T., El-Osta, A., Jowett, J.B.M., 2012. Microparticles: major transport vehicles for distinct microRNAs in circulation. Cardiovasc. Res. 93, 633–644.

Dimopoulos, N., Piperi, C., Salonicioti, A., Mitropoulos, P., Kallai, E., Liappas, I., Lea, R.W., Kalofoutis, A., 2006. Indices of low-grade chronic inflammation correlate with early cognitive deterioration in an elderly Greek population. Neurosci. Lett. 398, 118–123.

DiStasi, M.R., Ley, K., 2009. Opening the flood-gates: how neutrophil-endothelial interactions regulate permeability. Trends Immunol. 30, 547–556. doi:10.1016/j.it.2009.07.012

Dobolyi, A., Vincze, C., Pal, G., Lovas, G., 2012. The neuroprotective functions of transforming growth factor beta proteins. Int. J. Mol. Sci. 13, 8219–8258. doi:10.3390/ijms13078219

Dohgu, S., Banks, W.A., 2008. Lipopolysaccharide-enhanced transcellular transport of HIV-1 across the blood-brain barrier is mediated by the p38 mitogen-activated protein kinase pathway. Exp.

Neurol. 210, 740–749.

Doyle, K.P., Cekanaviciute, E., Mamer, L.E., Buckwalter, M.S., 2010. TGFβ signaling in the brain increases with aging and signals to astrocytes and innate immune cells in the weeks after stroke. J. Neuroinflammation 7, 62. doi:10.1186/1742-2094-7-62

Duggan, D.J., Bittner, M., Chen, Y., Meltzer, P., Trent, J.M., 1999. Expression profiling using cDNA microarrays. Nat. Genet. 21, 10–14. doi:10.1038/4434

Duncan, J.R., Cock, M.L., Scheerlinck, J.-P.Y., Westcott, K.T., McLean, C., Harding, R., Rees, S.M., 2002. White matter injury after repeated endotoxin exposure in the preterm ovine fetus. Pediatr. Res. 52, 941–949.

Dupont, R.M., Jernigan, T.L., Butters, N., Delis, D., Hesselink, J.R., Heindel, W., Gillin, J.C., 1990. Subcortical abnormalities detected in bipolar affective disorder using magnetic resonance imaging. Clinical and neuropsychological significance. Arch. Gen. Psychiatry 47, 55–59. doi:10.1001/archpsyc.1990.01810130057008

Edrissi, H., Schock, S.C., Hakim, A.M., Thompson, C.S., 2016. Microparticles generated during chronic cerebral ischemia increase the permeability of microvascular endothelial barriers in vitro. Brain Res. 1634, 83–93. doi:https://doi.org/10.1016/j.brainres.2015.12.032

Eigenmann, D.E., Xue, G., Kim, K.S., Moses, A. V, Hamburger, M., Oufir, M., 2013. Comparative study of four immortalized human brain capillary endothelial cell lines, hCMEC/D3, hBMEC, TY10, and BB19, and optimization of culture conditions, for an in vitro blood-brain barrier model for drug permeability studies. Fluids Barriers CNS 10, 33. doi:10.1186/2045-8118-10-33

Eken, C., Gasser, O., Zenhaeusern, G., Oehri, I., Hess, C., Schifferli, J.A., 2008. Polymorphonuclear Neutrophil-Derived Ectosomes Interfere with the Maturation of Monocyte-Derived Dendritic Cells. J. Immunol. 180, 817 LP – 824. doi:10.4049/jimmunol.180.2.817

Elahy, M., Jackaman, C., Mamo, J.C.L., Lam, V., Dhaliwal, S.S., Giles, C., Nelson, D., Takechi, R., 2015. Blood–brain barrier dysfunction developed during normal aging is associated with inflammation and loss of tight junctions but not with leukocyte recruitment. Immun. Ageing 12, 2.

Emmert-Buck, M.R., Bonner, R.F., Smith, P.D., Chuaqui, R.F., Zhuang, Z., Goldstein, S.R., Weiss, R.A., Liotta, L.A., 1996. Laser capture microdissection. Science (80-.). 274, 998–1001.

Enerson, B.E., Drewes, L.R., 2006. The rat blood-brain barrier transcriptome. J. Cereb. blood flow Metab. Off. J. Int. Soc. Cereb. Blood Flow Metab. 26, 959–973. doi:10.1038/sj.jcbfm.9600249

Enzinger, C., Smith, S., Fazekas, F., Drevin, G., Ropele, S., Nichols, T., Behrens, T., Schmidt, R., Matthews, P.M., 2006. Lesion probability maps of white matter hyperintensities in elderly individuals: results of the Austrian stroke prevention study. J. Neurol. 253, 1064–1070. doi:10.1007/s00415-006-0164-5

Escott-Price, V., Bellenguez, C., Wang, L.-S., Choi, S.-H., Harold, D., Jones, L., Holmans, P., Gerrish, A., Vedernikov, A., Richards, A., DeStefano, A.L., Lambert, J.-C., Ibrahim-Verbaas, C.A., Naj, A.C., Sims, R., Jun, G., Bis, J.C., Beecham, G.W., Grenier-Boley, B., Russo, G., Thornton-Wells, T.A., Denning, N., Smith, A. V, Chouraki, V., Thomas, C., Ikram, M.A., Zelenika, D., Vardarajan, B.N., Kamatani, Y., Lin, C.-F., Schmidt, H., Kunkle, B., Dunstan, M.L., Vronskaya, M., Consortium, U.K.B.E., Johnson, A.D., Ruiz, A., Bihoreau, M.-T., Reitz, C., Pasquier, F., Hollingworth, P., Hanon, O., Fitzpatrick, A.L., Buxbaum, J.D., Campion, D., Crane, P.K., Baldwin, C., Becker, T., Gudnason, V., Cruchaga, C., Craig, D., Amin, N., Berr, C., Lopez, O.L., De Jager, P.L., Deramecourt, V., Johnston, J.A., Evans, D., Lovestone, S., Letenneur, L., Hernández, I., Rubinsztein, D.C., Eiriksdottir, G., Sleegers, K., Goate, A.M., Fiévet, N., Huentelman, M.J., Gill, M., Brown, K., Kamboh, M.I., Keller, L., Barberger-Gateau, P., McGuinness, B., Larson, E.B., Myers, A.J., Dufouil, C., Todd, S., Wallon, D., Love, S.,

Rogaeva, E., Gallacher, J., George-Hyslop, P.S., Clarimon, J., Lleo, A., Bayer, A., Tsuang, D.W., Yu, L., Tsolaki, M., Bossù, P., Spalletta, G., Proitsi, P., Collinge, J., Sorbi, S., Garcia, F.S., Fox, N.C., Hardy, J., Naranjo, M.C.D., Bosco, P., Clarke, R., Brayne, C., Galimberti, D., Scarpini, E., Bonuccelli, U., Mancuso, M., Siciliano, G., Moebus, S., Mecocci, P., Zompo, M. Del, Maier, W., Hampel, H., Pilotto, A., Frank-García, A., Panza, F., Solfrizzi, V., Caffarra, P., Nacmias, B., Perry, W., Mayhaus, M., Lannfelt, L., Hakonarson, H., Pichler, S., Carrasquillo, M.M., Ingelsson, M., Beekly, D., Alvarez, V., Zou, F., Valladares, O., Younkin, S.G., Coto, E., Hamilton-Nelson, K.L., Gu, W., Razquin, C., Pastor, P., Mateo, I., Owen, M.J., Faber, K.M., Jonsson, P. V, Combarros, O., O'Donovan, M.C., Cantwell, L.B., Soininen, H., Blacker, D., Mead, S., Mosley Jr, T.H., Bennett, D.A., Harris, T.B., Fratiglioni, L., Holmes, C., de Bruijn, R.F.A.G., Passmore, P., Montine, T.J., Bettens, K., Rotter, J.I., Brice, A., Morgan, K., Foroud, T.M., Kukull, W.A., Hannequin, D., Powell, J.F., Nalls, M.A., Ritchie, K., Lunetta, K.L., Kauwe, J.S.K., Boerwinkle, E., Riemenschneider, M., Boada, M., Hiltunen, M., Martin, E.R., Schmidt, R., Rujescu, D., Dartigues, J.-F., Mayeux, R., Tzourio, C., Hofman, A., Nöthen, M.M., Graff, C., Psaty, B.M., Haines, J.L., Lathrop, M., Pericak-Vance, M.A., Launer, L.J., Van Broeckhoven, C., Farrer, L.A., van Duijn, C.M., Ramirez, A., Seshadri, S., Schellenberg, G.D., Amouyel, P., Williams, J., (CHS), C.H.S., 2014. Gene-wide analysis detects two new susceptibility genes for Alzheimer's disease. PLoS One 9, e94661–e94661. doi:10.1371/journal.pone.0094661

Etminan, M., Gill, S., Samii, A., 2003. Effect of non-steroidal anti-inflammatory drugs on risk of Alzheimer's disease: systematic review and meta-analysis of observational studies. BMJ 327, 128. doi:10.1136/bmj.327.7407.128

Fabene, P.F., Navarro Mora, G., Martinello, M., Rossi, B., Merigo, F., Ottoboni, L., Bach, S., Angiari, S., Benati, D., Chakir, A., Zanetti, L., Schio, F., Osculati, A., Marzola, P., Nicolato, E., Homeister, J.W., Xia, L., Lowe, J.B., McEver, R.P., Osculati, F., Sbarbati, A., Butcher, E.C., Constantin, G., 2008. A role for leukocyte-endothelial adhesion mechanisms in epilepsy. Nat. Med. 14, 1377–1383. doi:10.1038/nm.1878

Faille, D., Combes, V., Mitchell, A.J., Fontaine, A., Juhan-Vague, I., Alessi, M.-C., Chimini, G., Fusai, T., Grau, G.E., 2009. Platelet microparticles: a new player in malaria parasite cytoadherence to human brain endothelium. FASEB J. Off. Publ. Fed. Am. Soc. Exp. Biol. 23, 3449–3458. doi:10.1096/fj.09-135822

Fan, Y., Yang, X., Tao, Y., Lan, L., Zheng, L., Sun, J., 2015. Tight junction disruption of blood-brain barrier in white matter lesions in chronic hypertensive rats. Neuroreport 26, 1039–1043. doi:10.1097/WNR.0000000000000464

Farrall, A.J., Wardlaw, J.M., 2009. Blood-brain barrier: ageing and microvascular disease - systematic review and meta-analysis. Neurobiol.Aging 30, 337–352.

Favrais, G., Van De Looij, Y., Fleiss, B., Ramanantsoa, N., Bonnin, P., Stoltenburg-Didinger, G., Lacaud, A., Saliba, E., Dammann, O., Gallego, J., 2011. Systemic inflammation disrupts the developmental program of white matter. Ann. Neurol. 70, 550–565.

Fazekas, F., Kleinert, R., Offenbacher, H., Schmidt, R., Kleinert, G., Payer, F., Radner, H., Lechner, H., 1993. Pathologic correlates of incidental MRI white matter signal hyperintensities. Neurology 43, 1683–1689. doi:10.1212/WNL.43.9.1683

Fernandez-Cadenas, I., Mendioroz, M., Domingues-Montanari, S., Del Rio-Espinola, A., Delgado, P., Ruiz, A., Hernandez-Guillamon, M., Giralt, D., Chacon, P., Navarro-Sobrino, M., Ribo, M., Molina, C.A., Alvarez-Sabin, J., Rosell, A., Montaner, J., 2011. Leukoaraiosis is associated with genes regulating blood-brain barrier homeostasis in ischaemic stroke patients. Eur. J. Neurol. 18, 826–835. doi:10.1111/j.1468-1331.2010.03243.x

Fernando, M.S., O'Brien, J.T., Perry, R.H., English, P., Forster, G., McMeekin, W., Slade, J.Y., Golkhar, A., Matthews, F.E., Barber, R., Kalaria, R.N., Ince, P.G., 2004. Comparison of the

pathology of cerebral white matter with post-mortem magnetic resonance imaging (MRI) in the elderly brain. Neuropathol. Appl. Neurobiol. 30, 385–395. doi:10.1111/j.1365-2990.2004.00550.x

Fernando, M.S., Simpson, J.E., Matthews, F., Brayne, C., Lewis, C.E., Barber, R., Kalaria, R.N., Forster, G., Esteves, F., Wharton, S.B., Shaw, P.J., O'Brien, J.T., Ince, P.G., 2006. White matter lesions in an unselected cohort of the elderly: Molecular pathology suggests origin from chronic hypoperfusion injury. Stroke 37, 1391–1398. doi:10.1161/01.STR.0000221308.94473.14

Ferreira, P.G., Muñoz-Aguirre, M., Reverter, F., Sá Godinho, C.P., Sousa, A., Amadoz, A., Sodaei, R., Hidalgo, M.R., Pervouchine, D., Carbonell-Caballero, J., Nurtdinov, R., Breschi, A., Amador, R., Oliveira, P., Çubuk, C., Curado, J., Aguet, F., Oliveira, C., Dopazo, J., Sammeth, M., Ardlie, K.G., Guigó, R., 2018. The effects of death and post-mortem cold ischemia on human tissue transcriptomes. Nat. Commun. 9, 490. doi:10.1038/s41467-017-02772-x

Fischer, A.H., Jacobson, K.A., Rose, J., Zeller, R., 2008. Hematoxylin and eosin staining of tissue and cell sections. CSH Protoc. 2008, pdb.prot4986. doi:10.1101/pdb.prot4986

Fitzner, D., Schnaars, M., van Rossum, D., Krishnamoorthy, G., Dibaj, P., Bakhti, M., Regen, T., Hanisch, U.-K., Simons, M., 2011. Selective transfer of exosomes from oligodendrocytes to microglia by macropinocytosis. J. Cell Sci. 124, 447–458. doi:10.1242/jcs.074088

Fong, T.G., Davis, D., Growdon, M.E., Albuquerque, A., Inouye, S.K., 2015. The interface between delirium and dementia in elderly adults. Lancet Neurol. 14, 823–832.

Fong, T.G., Jones, R.N., Shi, P., Marcantonio, E.R., Yap, L., Rudolph, J.L., Yang, F.M., Kiely, D.K., Inouye, S.K., 2009. Delirium accelerates cognitive decline in Alzheimer disease. Neurology 72, 1570–1575.

Franklin, R.J.M., Ffrench-Constant, C., 2008. Remyelination in the CNS: from biology to therapy. Nat. Rev. Neurosci. 9, 839–855. doi:10.1038/nrn2480

Frischer, J.M., Weigand, S.D., Guo, Y., Kale, N., Parisi, J.E., Pirko, I., Mandrekar, J., Bramow, S., Metz, I., Brück, W., Lassmann, H., Lucchinetti, C.F., 2015. Clinical and pathological insights into the dynamic nature of the white matter multiple sclerosis plaque. Ann. Neurol. 78, 710–721. doi:10.1002/ana.24497

Fujimi, S., Ogura, H., Tanaka, H., Koh, T., Hosotsubo, H., Nakamori, Y., Kuwagata, Y., Shimazu, T., Sugimoto, H., 2003. Increased production of leukocyte microparticles with enhanced expression of adhesion molecules from activated polymorphonuclear leukocytes in severely injured patients. J. Trauma 54, 114–120. doi:10.1097/01.ta.0000046317.49507.f2

Fujimi, S., Ogura, H., Tanaka, H., Koh, T., Hosotsubo, H., Nakamori, Y., Kuwagata, Y., Shimazu, T., Sugimoto, H., 2002. Activated polymorphonuclear leukocytes enhance production of leukocyte microparticles with increased adhesion molecules in patients with sepsis. J. Trauma 52, 443–448. doi:10.1097/00005373-200203000-00005

Galea, I., Bechmann, I., Perry, V.H., 2007. What is immune privilege (not)? Trends Immunol. 28, 12–18. doi:10.1016/j.it.2006.11.004

Galli, S.J., Borregaard, N., Wynn, T.A., 2011. Phenotypic and functional plasticity of cells of innate immunity: macrophages, mast cells and neutrophils. Nat. Immunol. 12, 1035–1044. doi:10.1038/ni.2109

Galvin, P., Clarke, L.A., Harvey, S., Amaral, M.D., 2004. Microarray analysis in cystic fibrosis. J. Cyst. Fibros. 3 Suppl 2, 29–33. doi:10.1016/j.jcf.2004.05.006

Garcia-Contreras, M., Shah, S.H., Tamayo, A., Robbins, P.D., Golberg, R.B., Mendez, A.J., Ricordi, C., 2017. Plasma-derived exosome characterization reveals a distinct microRNA signature in long duration Type 1 diabetes. Sci. Rep. 7, 5998. doi:10.1038/s41598-017-05787-y

Garwood, C.J., Ratcliffe, L.E., Morgan, S. V, Simpson, J.E., Owens, H., Vazquez-Villasenor, I., Heath, P.R., Romero, I.A., Ince, P.G., Wharton, S.B., 2015. Insulin and IGF1 signalling pathways in human astrocytes in vitro and in vivo; characterisation, subcellular localisation and modulation of the receptors. Mol. Brain 8, 51. doi:10.1186/s13041-015-0138-6

Gasser, O., Schifferli, J.A., 2004. Activated polymorphonuclear neutrophils disseminate anti-inflammatory microparticles by ectocytosis. Blood 104, 2543–2548.

Gauley, J., Pisetsky, D.S., 2010. The release of microparticles by RAW 264.7 macrophage cells stimulated with TLR ligands. J. Leukoc. Biol. 87, 1115–1123. doi:10.1189/jlb.0709465

Geiser, T., Sturzenegger, M., Genewein, U., Haeberli, A., Beer, J.H., 1998. Mechanisms of cerebrovascular events as assessed by procoagulant activity, cerebral microemboli, and platelet microparticles in patients with prosthetic heart valves. Stroke 29, 1770–1777. doi:10.1161/01.str.29.9.1770

Gensert, J.M., Goldman, J.E., 1997. Endogenous Progenitors Remyelinate Demyelinated Axons in the Adult CNS. Neuron 19, 197–203. doi:https://doi.org/10.1016/S0896-6273(00)80359-1

Ginestra, A., La Placa, M.D., Saladino, F., Cassara, D., Nagase, H., Vittorelli, M.L., 1998. The amount and proteolytic content of vesicles shed by human cancer cell lines correlates with their in vitro invasiveness. Anticancer Res. 18, 3433–3437.

Gingrich, M.B., Traynelis, S.F., 2000. Serine proteases and brain damage - is there a link? Trends Neurosci. 23, 399–407. doi:10.1016/s0166-2236(00)01617-9

Giovannini, M.G., Scali, C., Prosperi, C., Bellucci, A., Vannucchi, M.G., Rosi, S., Pepeu, G., Casamenti, F., 2002. β-Amyloid-induced inflammation and cholinergic hypofunction in the rat brain in vivo: involvement of the p38MAPK pathway. Neurobiol. Dis. 11, 257–274.

Girard, T.D., Jackson, J.C., Pandharipande, P.P., Pun, B.T., Thompson, J.L., Shintani, A.K., Gordon, S.M., Canonico, A.E., Dittus, R.S., Bernard, G.R., Ely, E.W., 2010. Delirium as a predictor of long-term cognitive impairment in survivors of critical illness. Crit. Care Med. 38, 1513–1520. doi:10.1097/CCM.0b013e3181e47be1

Godbout, J.P., Chen, J., Abraham, J., Richwine, a F., Berg, B.M., Kelley, K.W., Johnson, R.W., 2005. Exaggerated neuroinflammation and sickness behavior in aged mice following activation of the peripheral innate immune system. FASEB J. 19, 1329–1331. doi:10.1096/fj.05-3776fje

Goldmann, E.E., 1909. Die äussere und innere Sekretion des gesunden Organismus im Lichte der" vitalen Färbung": Mit 15 farb. lithogr. Tafeln. H. Laupp.

Gomez, I., Ward, B., Souilhol, C., Recarti, C., Ariaans, M., Johnston, J., Burnett, A., Mahmoud, M., Luong, L.A., West, L., Long, M., Parry, S., Woods, R., Hulston, C., Benedikter, B., Niespolo, C., Bazaz, R., Francis, S., Kiss-Toth, E., van Zandvoort, M., Schober, A., Hellewell, P., Evans, P.C., Ridger, V., 2020. Neutrophil microvesicles drive atherosclerosis by delivering miR-155 to atheroprone endothelium. Nat. Commun. 11, 214. doi:10.1038/s41467-019-14043-y

Gooch, J., Wilcock, D.M., 2016. Animal Models of Vascular Cognitive Impairment and Dementia (VCID). Cell. Mol. Neurobiol. 36, 233–239. doi:10.1007/s10571-015-0286-3

Goodall, E.F., Wang, C., Simpson, J.E., Baker, D.J., Drew, D.R., Heath, P.R., Saffrey, M.J., Romero, I.A., Wharton, S.B., 2018. Age-associated changes in the blood-brain barrier: comparative studies in human and mouse. Neuropathol. Appl. Neurobiol. 44, 328–340. doi:10.1111/nan.12408

Gouw, A.A., Seewann, A., van der Flier, W.M., Barkhof, F., Rozemuller, A.M., Scheltens, P., Geurts, J.J.G., 2011. Heterogeneity of small vessel disease: a systematic review of MRI and histopathology correlations. J. Neurol. Neurosurg. Psychiatry 82, 126–135. doi:10.1136/jnnp.2009.204685

Govindarajan, R., Duraiyan, J., Kaliyappan, K., Palanisamy, M., 2012. Microarray and its applications. J. Pharm. Bioallied Sci. 4, S310–S312. doi:10.4103/0975-7406.100283

Grammas, P., Martinez, J., Miller, B., 2011. Cerebral microvascular endothelium and the pathogenesis of neurodegenerative diseases. Expert Rev. Mol. Med. 13, e19. doi:10.1017/S1462399411001918

Greenwalt, T.J., 2006. The how and why of exocytic vesicles. Transfusion 46, 143–152. doi:10.1111/j.1537-2995.2006.00692.x

Gross, A.L., Jones, R.N., Habtemariam, D.A., Fong, T.G., Tommet, D., Quach, L., Schmitt, E., Yap, L., Inouye, S.K., 2012. Delirium and Long-term Cognitive Trajectory Among Persons With Dementia. Arch. Intern. Med. 172, 1324–1331. doi:10.1001/archinternmed.2012.3203

Guerra, C., Linde-Zwirble, W.T., Wunsch, H., 2012. Risk factors for dementia after critical illness in elderly Medicare beneficiaries. Crit. Care 16, R233. doi:10.1186/cc11901

Guervilly, C., Lacroix, R., Forel, J.-M., Roch, A., Camoin-Jau, L., Papazian, L., Dignat-George, F., 2011. High levels of circulating leukocyte microparticles are associated with better outcome in acute respiratory distress syndrome. Crit. Care 15, R31. doi:10.1186/cc9978

Gui, Y., Liu, H., Zhang, L., Lv, W., Hu, X., 2015. Altered microRNA profiles in cerebrospinal fluid exosome in Parkinson disease and Alzheimer disease. Oncotarget 6, 37043–37053. doi:10.18632/oncotarget.6158

Gunning-Dixon, F.M., Raz, N., 2000. The cognitive correlates of white matter abnormalities in normal aging: a quantitative review. Neuropsychology 14, 224–32. doi:10.1037//0894-4105.14.2.224

Gurol, M.E., Viswanathan, A., Gidicsin, C., Hedden, T., Martinez-Ramirez, S., Dumas, A., Vashkevich, A., Ayres, A.M., Auriel, E., van Etten, E., Becker, A., Carmasin, J., Schwab, K., Rosand, J., Johnson, K.A., Greenberg, S.M., 2013. Cerebral amyloid angiopathy burden associated with leukoaraiosis: a positron emission tomography/magnetic resonance imaging study. Ann. Neurol. 73, 529–536. doi:10.1002/ana.23830

Guttula, S.V., Allam, A., Gumpeny, R.S., 2012. Analyzing microarray data of Alzheimer's using cluster analysis to identify the biomarker genes. Int. J. Alzheimers. Dis. 2012, 649456. doi:10.1155/2012/649456

Guzman-Martinez, L., Maccioni, R.B., Andrade, V., Navarrete, L.P., Pastor, M.G., Ramos-Escobar, N., 2019. Neuroinflammation as a Common Feature of Neurodegenerative Disorders . Front. Pharmacol. .

Gyorgy, B., Szabo, T.G., Turiak, L., Wright, M., Herczeg, P., Ledeczi, Z., Kittel, A., Polgar, A., Toth, K., Derfalvi, B., Zelenak, G., Borocz, I., Carr, B., Nagy, G., Vekey, K., Gay, S., Falus, A., Buzas, E.I., 2012. Improved flow cytometric assessment reveals distinct microvesicle (cell-derived microparticle) signatures in joint diseases. PLoS One 7, e49726. doi:10.1371/journal.pone.0049726

Hafezi-Moghadam, A., Thomas, K.L., Wagner, D.D., 2007. ApoE deficiency leads to a progressive age-dependent blood-brain barrier leakage. Am. J. Physiol. Cell Physiol. 292, C1256-62. doi:10.1152/ajpcell.00563.2005

Hainsworth, A.H., Minett, T., Andoh, J., Forster, G., Bhide, I., Barrick, T.R., Elderfield, K., Jeevahan, J., Markus, H.S., Bridges, L.R., 2017. Neuropathology of White Matter Lesions, Blood-Brain Barrier Dysfunction, and Dementia. Stroke 48, 2799–2804. doi:10.1161/STROKEAHA.117.018101

Hakim, A.M., 2019. Small Vessel Disease . Front. Neurol. .

Han, J., Pluhackova, K., Böckmann, R.A., 2017. The Multifaceted Role of SNARE Proteins in Membrane Fusion . Front. Physiol. .

Hannestad, J., Gallezot, J.-D., Schafbauer, T., Lim, K., Kloczynski, T., Morris, E.D., Carson, R.E., Ding, Y.-S., Cosgrove, K.P., 2012. Endotoxin-induced systemic inflammation activates microglia: [(1)(1)C]PBR28 positron emission tomography in nonhuman primates. Neuroimage 63, 232–239. doi:10.1016/j.neuroimage.2012.06.055

Harris, L.W., Wayland, M., Lan, M., Ryan, M., Giger, T., Lockstone, H., Wuethrich, I., Mimmack, M., Wang, L., Kotter, M., 2008. The cerebral microvasculature in schizophrenia: a laser capture microdissection study. PLoS One 3.

Harrison, N.A., Brydon, L., Walker, C., Gray, M.A., Steptoe, A., Critchley, H.D., 2009. Inflammation causes mood changes through alterations in subgenual cingulate activity and mesolimbic connectivity. Biol. Psychiatry 66, 407–414. doi:10.1016/j.biopsych.2009.03.015

Hartl, F.U., Bracher, A., Hayer-Hartl, M., 2011. Molecular chaperones in protein folding and proteostasis. Nature 475, 324–332. doi:10.1038/nature10317

Hassan, A., Hunt, B.J., O'Sullivan, M., Parmar, K., Bamford, J.M., Briley, D., Brown, M.M., Thomas, D.J., Markus, H.S., 2003. Markers of endothelial dysfunction in lacunar infarction and ischaemic leukoaraiosis. Brain 126, 424–432. doi:10.1093/brain/awg040

Haupt, Y., Maya, R., Kazaz, A., Oren, M., 1997. Mdm2 promotes the rapid degradation of p53. Nature 387, 296–299.

Hawkins, B.T., Davis, T.P., 2005. The Blood-Brain Barrier / Neurovascular Unit in Health and Disease. Pharmacol. Rev. 57, 173–185. doi:10.1124/pr.57.2.4.173

Hazeldine, J., Harris, P., Chapple, I.L., Grant, M., Greenwood, H., Livesey, A., Sapey, E., Lord, J.M., 2014. Impaired neutrophil extracellular trap formation: a novel defect in the innate immune system of aged individuals. Aging Cell 13, 690–698. doi:10.1111/acel.12222

Hendrickx, D.A.E., van Eden, C.G., Schuurman, K.G., Hamann, J., Huitinga, I., 2017. Staining of HLA-DR, Iba1 and CD68 in human microglia reveals partially overlapping expression depending on cellular morphology and pathology. J. Neuroimmunol. 309, 12–22. doi:10.1016/j.jneuroim.2017.04.007

Henry, C.J., Huang, Y., Wynne, A.M., Godbout, J.P., 2009. Peripheral Lipopolysaccharide (LPS) challenge promotes microglial hyperactivity in aged mice that is associated with exaggerated induction of both pro-inflammatory IL-1β and anti-inflammatory IL-10 cytokines. Brain. Behav. Immun. 23, 309–317. doi:10.1016/j.bbi.2008.09.002

Hensley, K., Floyd, R.A., Zheng, N., Nael, R., Robinson, K.A., Nguyen, X., Pye, Q.N., Stewart, C.A., Geddes, J., Markesbery, W.R., 1999. p38 kinase is activated in the Alzheimer's disease brain. J. Neurochem. 72, 2053–2058.

Heppner, F.L., Ransohoff, R.M., Becher, B., 2015. Immune attack: the role of inflammation in Alzheimer disease. Nat. Rev. Neurosci. 16, 358–372. doi:10.1038/nrn3880

Herring, J.M., McMichael, M.A., Smith, S.A., 2013. Microparticles in health and disease. J. Vet. Intern. Med. 27, 1020–1033. doi:10.1111/jvim.12128

Hess, C., Sadallah, S., Hefti, A., Landmann, R., Schifferdi, J.A., 1998. Ectosomes released by human neutrophils are specialized functional units. Mol. Immunol. 6, 354.

Ho, K.L., Garcia, J.H., Pantoni, L., Inzitari, D., Wallin, A., 2000. The matter of white matter.

Holder, B.S., Tower, C.L., Jones, C.J.P., Aplin, J.D., Abrahams, V.M., 2012. Heightened Pro-Inflammatory Effect of Preeclamptic Placental Microvesicles on Peripheral Blood Immune Cells in Humans1. Biol. Reprod. 86. doi:10.1095/biolreprod.111.097014

Holland, C.M., Smith, E.E., Csapo, I., Gurol, M.E., Brylka, D.A., Killiany, R.J., Blacker, D., Albert, M.S., Guttmann, C.R.G., Greenberg, S.M., 2008. Spatial distribution of white-matter hyperintensities in Alzheimer disease, cerebral amyloid angiopathy, and healthy aging. Stroke 39, 1127–1133. doi:10.1161/STROKEAHA.107.497438

Holmes, C., Cunningham, C., Zotova, E., Woolford, J., Dean, C., Kerr, S., Culliford, D., Perry, V.H., 2009. Systemic inflammation and disease progression in Alzheimer disease. Neurology 73. doi:10.1212/WNL.0b013e3181b6bb95

Hong, Y., Eleftheriou, D., Hussain, A.A.K., Price-Kuehne, F.E., Savage, C.O., Jayne, D., Little, M.A., Salama, A.D., Klein, N.J., Brogan, P.A., 2012. Anti-neutrophil cytoplasmic antibodies stimulate release of neutrophil microparticles. J. Am. Soc. Nephrol. 23, 49–62.

Hood, L., Rowen, L., 2013. The Human Genome Project: big science transforms biology and medicine. Genome Med. 5, 79. doi:10.1186/gm483

Hopperton, K.E., Mohammad, D., Trépanier, M.O., Giuliano, V., Bazinet, R.P., 2018. Markers of microglia in post-mortem brain samples from patients with Alzheimer's disease: a systematic review. Mol. Psychiatry 23, 177–198. doi:10.1038/mp.2017.246

Horn, H.F., Vousden, K.H., 2007. Coping with stress: multiple ways to activate p53. Oncogene 26, 1306–1316.

Hosokawa, M., Ueno, M., 1999. Aging of blood-brain barrier and neuronal cells of eye and ear in SAM mice. Neurobiol. Aging 20, 117–123.

Hu, Y., Bi, Y., Yao, D., Wang, P., Li, Y., 2019. Omi/HtrA2 Protease Associated Cell Apoptosis Participates in Blood-Brain Barrier Dysfunction. Front. Mol. Neurosci. 12, 48. doi:10.3389/fnmol.2019.00048

Huang, C.-W., Tsai, M.-H., Chen, N.-C., Chen, W.-H., Lu, Y.-T., Lui, C.-C., Chang, Y.-T., Chang, W.-N., Chang, A.Y.W., Chang, C.-C., 2015. Clinical significance of circulating vascular cell adhesion molecule-1 to white matter disintegrity in Alzheimer's dementia. Thromb. Haemost. 114, 1230–1240.

Huang, D.W., Sherman, B.T., Lempicki, R.A., 2009. Systematic and integrative analysis of large gene lists using DAVID bioinformatics resources. Nat. Protoc. 4, 44–57. doi:10.1038/nprot.2008.211

Huang, W., Chen, W., Zhang, X., 2017. Multiple sclerosis: Pathology, diagnosis and treatments (Review). Exp Ther Med 13, 3163–3166. doi:10.3892/etm.2017.4410

Huang, Y., Zhang, W., Lin, L., Feng, J., Chen, F., Wei, W., Zhao, X., Guo, W., Li, J., Yin, W., Li, L., 2010. Is endothelial dysfunction of cerebral small vessel responsible for white matter lesions after chronic cerebral hypoperfusion in rats? J. Neurol. Sci. 299, 72–80. doi:10.1016/j.jns.2010.08.035

Hugel, B., Martinez, M.C., Kunzelmann, C., Freyssinet, J.-M., 2005. Membrane microparticles: two sides of the coin. Physiology (Bethesda). 20, 22–27. doi:10.1152/physiol.00029.2004

Hugh Perry, V., 1998. A revised view of the central nervous system microenvironment and major histocompatibility complex class II antigen presentation. J. Neuroimmunol. 90, 113–121. doi:10.1016/S0165-5728(98)00145-3

Huisa, B.N., Caprihan, A., Thompson, J., Prestopnik, J., Qualls, C.R., Rosenberg, G.A., 2015. Long-term blood–brain barrier permeability changes in Binswanger disease. Stroke 46, 2413–2418.

Hulsmans, M., Holvoet, P., 2013. MicroRNA-containing microvesicles regulating inflammation in association with atherosclerotic disease. Cardiovasc. Res. 100, 7–18. doi:10.1093/cvr/cvt161

Ide, M., Harris, M., Stevens, A., Sussams, R., Hopkins, V., Culliford, D., Fuller, J., Ibbett, P., Raybould, R., Thomas, R., 2016. Periodontitis and Cognitive Decline in Alzheimer's Disease.

PLoS One 11, e0151081.

Inouye, S.K., Charpentier, P.A., 1996. Precipitating factors for delirium in hospitalized elderly persons: predictive model and interrelationship with baseline vulnerability. Jama 275, 852–857.

Ishihara, H., Kubota, H., Lindberg, R.L.P., Leppert, D., Gloor, S.M., Errede, M., Virgintino, D., Fontana, A., Yonekawa, Y., Frei, K., 2008. Endothelial cell barrier impairment induced by glioblastomas and transforming growth factor beta2 involves matrix metalloproteinases and tight junction proteins. J. Neuropathol. Exp. Neurol. 67, 435–448. doi:10.1097/NEN.0b013e31816fd622

Iturria-Medina, Y., Sotero, R.C., Toussaint, P.J., Mateos-Pérez, J.M., Evans, A.C., Weiner, M.W., Aisen, P., Petersen, R., Jack, C.R., Jagust, W., Trojanowki, J.Q., Toga, A.W., Beckett, L., Green, R.C., Saykin, A.J., Morris, J., Shaw, L.M., Khachaturian, Z., Sorensen, G., Kuller, L., Raichle, M., Paul, S., Davies, P., Fillit, H., Hefti, F., Holtzman, D., Mesulam, M.M., Potter, W., Snyder, P., Schwartz, A., Montine, T., Thomas, R.G., Donohue, M., Walter, S., Gessert, D., Sather, T., Jiminez, G., Harvey, D., Bernstein, M., Fox, N., Thompson, P., Schuff, N., Borowski, B., Gunter, J., Senjem, M., Vemuri, P., Jones, D., Kantarci, K., Ward, C., Koeppe, R.A., Foster, N., Reiman, E.M., Chen, K., Mathis, C., Landau, S., Cairns, N.J., Householder, E., Taylor-Reinwald, L., Lee, V., Korecka, M., Figurski, M., Crawford, K., Neu, S., Foroud, T.M., Potkin, S., Shen, L., Faber, K., Kim, S., Nho, K., Thal, L., Buckholtz, N., Albert, Marylyn, Frank, R., Hsiao, J., Kaye, J., Quinn, J., Lind, B., Carter, R., Dolen, S., Schneider, L.S., Pawluczyk, S., Beccera, M., Teodoro, L., Spann, B.M., Brewer, J., Vanderswag, H., Fleisher, A., Heidebrink, J.L., Lord, J.L., Mason, S.S., Albers, C.S., Knopman, D., Johnson, Kris, Doody, R.S., Villanueva-Meyer, J., Chowdhury, M., Rountree, S., Dang, M., Stern, Y., Honig, L.S., Bell, K.L., Ances, B., Carroll, M., Leon, S., Mintun, M.A., Schneider, S., Oliver, A., Marson, D., Griffith, R., Clark, D., Geldmacher, D., Brockington, J., Roberson, E., Grossman, H., Mitsis, E., de Toledo-Morrell, L., Shah, R.C., Duara, R., Varon, D., Greig, M.T., Roberts, P., Albert, Marilyn, Onyike, C., D'Agostino, D., Kielb, S., Galvin, J.E., Cerbone, B., Michel, C.A., Rusinek, H., de Leon, M.J., Glodzik, L., De Santi, S., Doraiswamy, P.M., Petrella, J.R., Wong, T.Z., Arnold, S.E., Karlawish, J.H., Wolk, D., Smith, C.D., Jicha, G., Hardy, P., Sinha, P., Oates, E., Conrad, G., Lopez, O.L., Oakley, M., Simpson, D.M., Porsteinsson, A.P., Goldstein, B.S., Martin, K., Makino, K.M., Ismail, M.S., Brand, C., Mulnard, R.A., Thai, G., Mc-Adams-Ortiz, C., Womack, K., Mathews, D., Quiceno, M., Diaz-Arrastia, R., King, R., Weiner, M., Martin-Cook, K., DeVous, M., Levey, A.I., Lah, J.J., Cellar, J.S., Burns, J.M., Anderson, H.S., Swerdlow, R.H., Apostolova, L., Tingus, K., Woo, E., Silverman, D.H.S., Lu, P.H., Bartzokis, G., Graff-Radford, N.R., Parfitt, F., Kendall, T., Johnson, H., Farlow, M.R., Hake, A., Matthews, B.R., Herring, S., Hunt, C., van Dyck, C.H., Carson, R.E., MacAvoy, M.G., Chertkow, H., Bergman, H., Hosein, C., Black, S., Stefanovic, B., Caldwell, C., Hsiung, G.-Y.R., Feldman, H., Mudge, B., Assaly, M., Kertesz, A., Rogers, J., Bernick, C., Munic, D., Kerwin, D., Mesulam, M.-M., Lipowski, K., Wu, C.-K., Johnson, N., Sadowsky, C., Martinez, W., Villena, T., Turner, R.S., Johnson, Kathleen, Reynolds, B., Sperling, R.A., Johnson, K.A., Marshall, G., Frey, M., Lane, B., Rosen, A., Tinklenberg, J., Sabbagh, M.N., Belden, C.M., Jacobson, S.A., Sirrel, S.A., Kowall, N., Killiany, R., Budson, A.E., Norbash, A., Johnson, P.L., Allard, J., Lerner, A., Ogrocki, P., Hudson, L., Fletcher, E., Carmichael, O., Olichney, J., DeCarli, C., Kittur, S., Borrie, M., Lee, T.-Y., Bartha, R., Johnson, S., Asthana, S., Carlsson, C.M., Potkin, S.G., Preda, A., Nguyen, D., Tariot, P., Reeder, S., Bates, V., Capote, H., Rainka, M., Scharre, D.W., Kataki, M., Adeli, A., Zimmerman, E.A., Celmins, D., Brown, A.D., Pearlson, G.D., Blank, K., Anderson, K., Santulli, R.B., Kitzmiller, T.J., Schwartz, E.S., Sink, K.M., Williamson, J.D., Garg, P., Watkins, F., Ott, B.R., Querfurth, H., Tremont, G., Salloway, S., Malloy, P., Correia, S., Rosen, H.J., Miller, B.L., Mintzer, J., Spicer, K., Bachman, D., Finger, E., Pasternak, S., Rachinsky, I., Drost, D., Pomara, N., Hernando, R., Sarrael, A., Schultz, S.K., Ponto, L.L.B., Shim, H., Smith, K.E., Relkin, N., Chaing, G., Raudin, L., Smith, A., Fargher, K., Raj, B.A., Neylan, T., Grafman, J., Davis, M., Initiative, T.A.D.N., 2016. Early role of vascular dysregulation on late-onset Alzheimer's disease based on multifactorial data-driven analysis. Nat. Commun. 7, 11934. doi:10.1038/ncomms11934

Iwashyna, T.J., Ely, E.W., Smith, D.M., Langa, K.M., 2010. Long-term Cognitive Impairment and Functional Disability Among Survivors of Severe Sepsis. JAMA 304, 1787–1794. doi:10.1001/jama.2010.1553

Jackson, J.C., Gordon, S.M., Hart, R.P., Hopkins, R.O., Ely, E.W., 2004. The association between delirium and cognitive decline: a review of the empirical literature. Neuropsychol. Rev. 14, 87–98.

Jaffe, E.A., Nachman, R.L., Becker, C.G., Minick, C.R., 1973. Culture of Human Endothelial Cells Derived from Umbilical Veins. IDENTIFICATION BY MORPHOLOGIC AND IMMUNOLOGIC CRITERIA. J. Clin. Invest. 52, 2745–2756.

Jahn, R., Scheller, R.H., 2006. SNAREs—engines for membrane fusion. Nat. Rev. Mol. cell Biol. 7, 631–643.

Janota, C.S., Brites, D., Lemere, C.A., Brito, M.A., 2015. Glio-vascular changes during ageing in wild-type and Alzheimer's disease-like APP/PS1 mice. Brain Res. 1620, 153–168. doi:10.1016/j.brainres.2015.04.056

Jenne, C.N., Wong, C.H.Y., Zemp, F.J., McDonald, B., Rahman, M.M., Forsyth, P.A., McFadden, G., Kubes, P., 2013. Neutrophils recruited to sites of infection protect from virus challenge by releasing neutrophil extracellular traps. Cell Host Microbe 13, 169–180. doi:10.1016/j.chom.2013.01.005

Ji, K., Akgul, G., Wollmuth, L.P., Tsirka, S.E., 2013. Microglia Actively Regulate the Number of Functional Synapses. PLoS One 8, e56293.

Jiang, P.-H., Motoo, Y., Iovanna, J.L., Pebusque, M.-J., Xie, M.-J., Okada, G., Sawabu, N., 2004. Tumor protein p53-induced nuclear protein 1 (TP53INP1) in spontaneous chronic pancreatitis in the WBN/Kob rat: drug effects on its expression in the pancreas. JOP 5, 205–216.

Jin, C., Xia, Y., 2010. Using Laser Capture Microdissection and cDNA Microarray to Elucidate the Molecular Signatures of Ocular Surface Development. Invest. Ophthalmol. Vis. Sci. 51, 1648.

Jin, L., Nation, R.L., Li, J., Nicolazzo, J.A., 2013. Species-Dependent Blood-Brain Barrier Disruption of Lipopolysaccharide: Amelioration by Colistin In Vitro and In Vivo. Antimicrob. Agents Chemother. 57, 4336 LP – 4342. doi:10.1128/AAC.00765-13

Johnson, B.L., Kuethe, J.W., Caldwell, C.C., 2014. Neutrophil Derived Microvesicles: Emerging Role of a Key Mediator to the Immune Response. Endocr. Metab. Immune Disord. Drug Targets 14, 210–217.

Jørgensen, M., Bæk, R., Pedersen, S., Søndergaard, E.K.L., Kristensen, S.R., Varming, K., 2013. Extracellular Vesicle (EV) Array: microarray capturing of exosomes and other extracellular vesicles for multiplexed phenotyping. J. Extracell. Vesicles 2, 20920. doi:10.3402/jev.v2i0.20920

Kadhim, H., Tabarki, B., Verellen, G., De Prez, C., Rona, A.-M., Sebire, G., 2001. Inflammatory cytokines in the pathogenesis of periventricular leukomalacia. Neurology 56, 1278–1284.

Kalaria, R.N., 2002. Small vessel disease and Alzheimer's dementia: pathological considerations. Cerebrovasc. Dis. 13 Suppl 2, 48–52. doi:49150

Kalaria, R.N., 2000. The role of cerebral ischemia in Alzheimer's disease. Neurobiol. Aging 21, 321–330.

Kalaria, R.N., Erkinjuntti, T., 2006. Small vessel disease and subcortical vascular dementia. J. Clin. Neurol. 2, 1–11. doi:10.3988/jcn.2006.2.1.1

Kamada, H., Yu, F., Nito, C., Chan, P.H., 2007. Influence of hyperglycemia on oxidative stress and matrix metalloproteinase-9 activation after focal cerebral ischemia/reperfusion in rats: relation to

blood-brain barrier dysfunction. Stroke 38, 1044–1049.

Kamburov, A., Cavill, R., Ebbels, T.M.D., Herwig, R., Keun, H.C., 2011. Integrated pathway-level analysis of transcriptomics and metabolomics data with IMPaLA. Bioinformatics 27, 2917–2918. doi:10.1093/bioinformatics/btr499

King, K.S., Peshock, R.M., Rossetti, H.C., McColl, R.W., Ayers, C.R., Hulsey, K.M., Das, S.R., 2014. Effect of normal aging versus hypertension, abnormal body mass index, and diabetes mellitus on white matter hyperintensity volume. Stroke 45, 255–257. doi:10.1161/STROKEAHA.113.003602

Kinnecom, K., Pachter, J.S., 2005. Selective capture of endothelial and perivascular cells from brain microvessels using laser capture microdissection. Brain Res. Protoc. 16, 1–9. doi:https://doi.org/10.1016/j.brainresprot.2005.08.002

Kinnunen, K.M., Greenwood, R., Powell, J.H., Leech, R., Hawkins, P.C., Bonnelle, V., Patel, M.C., Counsell, S.J., Sharp, D.J., 2011. White matter damage and cognitive impairment after traumatic brain injury. Brain 134, 449–463.

Kirk, J., Plumb, J., Mirakhur, M., McQuaid, S., 2003. Tight junctional abnormality in multiple sclerosis white matter affects all calibres of vessel and is associated with blood–brain barrier leakage and active demyelination. J. Pathol. 201, 319–327. doi:10.1002/path.1434

Kivipelto, M., Helkala, E.-L., Laakso, M.P., Hänninen, T., Hallikainen, M., Alhainen, K., Iivonen, S., Mannermaa, A., Tuomilehto, J., Nissinen, A., Soininen, H., 2002. Apolipoprotein E ϵ4 Allele, Elevated Midlife Total Cholesterol Level, and High Midlife Systolic Blood Pressure Are Independent Risk Factors for Late-Life Alzheimer Disease. Ann. Intern. Med. 137, 149–155. doi:10.7326/0003-4819-137-3-200208060-00006

Klee, E.W., Erdogan, S., Tillmans, L., Kosari, F., Sun, Z., Wigle, D.A., Yang, P., Aubry, M.C., Vasmatzis, G., 2009. Impact of sample acquisition and linear amplification on gene expression profiling of lung adenocarcinoma: laser capture micro-dissection cell-sampling versus bulk tissue-sampling. BMC Med. Genomics 2, 13. doi:10.1186/1755-8794-2-13

Kleiger, G., Mayor, T., 2014. Perilous journey: a tour of the ubiquitin-proteasome system. Trends Cell Biol. 24, 352–359. doi:10.1016/j.tcb.2013.12.003

Kniesel, U., Wolburg, H., 2000. Tight junctions of the blood-brain barrier. Cell. Mol. Neurobiol. 20, 57–76. doi:10.1023/a:1006995910836

Knijff-Dutmer, E.A.J., Koerts, J., Nieuwland, R., Kalsbeek-Batenburg, E.M., van de Laar, M.A.F.J., 2002. Elevated levels of platelet microparticles are associated with disease activity in rheumatoid arthritis. Arthritis Rheum. 46, 1498–1503. doi:10.1002/art.10312

Knopman, D.S., Parisi, J.E., Salviati, A., Floriach-Robert, M., Boeve, B.F., Ivnik, R.J., Smith, G.E., Dickson, D.W., Johnson, K.A., Petersen, L.E., McDonald, W.C., Braak, H., Petersen, R.C., 2003. Neuropathology of cognitively normal elderly. J. Neuropathol. Exp. Neurol. 62, 1087–1095.

Koike, S., Jahn, R., 2019. SNAREs define targeting specificity of trafficking vesicles by combinatorial interaction with tethering factors. Nat. Commun. 10, 1608. doi:10.1038/s41467-019-09617-9

Komulainen, P., Lakka, T.A., Kivipelto, M., Hassinen, M., Penttilä, I.M., Helkala, E.-L., Gylling, H., Nissinen, A., Rauramaa, R., 2007. Serum high sensitivity C-reactive protein and cognitive function in elderly women. Age Ageing 36, 443–448.

Koppelkamm, A., Vennemann, B., Lutz-Bonengel, S., Fracasso, T., Vennemann, M., 2011. RNA integrity in post-mortem samples: influencing parameters and implications on RT-qPCR assays. Int. J. Legal Med. 125, 573–580. doi:10.1007/s00414-011-0578-1

Kotter, M.R., Li, W.-W., Zhao, C., Franklin, R.J.M., 2006. Myelin impairs CNS remyelination by inhibiting oligodendrocyte precursor cell differentiation. J. Neurosci. 26, 328–332. doi:10.1523/JNEUROSCI.2615-05.2006

Kreutzberg, G.W., 1996. Microglia: a sensor for pathological events in the CNS. Trends Neurosci. 19, 312–318. doi:10.1016/0166-2236(96)10049-7

Krishnan, K.R., Goli, V., Ellinwood, E.H., France, R.D., Blazer, D.G., Nemeroff, C.B., 1988. Leukoencephalopathy in patients diagnosed as major depressive. Biol. Psychiatry 23, 519–522. doi:10.1016/0006-3223(88)90025-x

Krstic, D., Knuesel, I., 2013. Deciphering the mechanism underlying late-onset Alzheimer disease. Nat. Rev. Neurol. 9, 25–34. doi:10.1038/nrneurol.2012.236

Kubicki, M., McCarley, R.W., Shenton, M.E., 2005. Evidence for white matter abnormalities in schizophrenia. Curr. Opin. Psychiatry 18, 121–134.

Kumar, R., Sharma, A., Tiwari, R.K., 2012. Application of microarray in breast cancer: An overview. J. Pharm. Bioallied Sci. 4, 21–26. doi:10.4103/0975-7406.92726

Kuyumcu, M.E., Yesil, Y., Ozturk, Z.A., Kizilarslanoglu, C., Etgul, S., Halil, M., Ulger, Z., Cankurtaran, M., Ariogul, S., 2012. The evaluation of neutrophil-lymphocyte ratio in Alzheimer's disease. Dement. Geriatr. Cogn. Disord. 34, 69–74. doi:10.1159/000341583

Lan, L.-F., Zheng, L., Yang, X., Ji, X.-T., Fan, Y.-H., Zeng, J.-S., 2015. Peroxisome proliferator-activated receptor-γ agonist pioglitazone ameliorates white matter lesion and cognitive impairment in hypertensive rats. CNS Neurosci. Ther. 21, 410–416. doi:10.1111/cns.12374

Lanni, C., Racchi, M., Mazzini, G., Ranzenigo, A., Polotti, R., Sinforiani, E., Olivari, L., Barcikowska, M., Styczynska, M., Kuznicki, J., Szybinska, A., Govoni, S., Memo, M., Uberti, D., 2008. Conformationally altered p53: a novel Alzheimer's disease marker? Mol. Psychiatry 13, 641–647. doi:10.1038/sj.mp.4002060

Larrain, M.T.I., Rabassa, M.E., Lacunza, E., Barbera, A., Creton, A., Segal-Eiras, A., Croce, M.V., 2014. IDO is highly expressed in breast cancer and breast cancer-derived circulating microvesicles and associated to aggressive types of tumors by in silico analysis. Tumor Biol. 35, 6511–6519.

Lebrin, F., Deckers, M., Bertolino, P., Ten Dijke, P., 2005. TGF-β receptor function in the endothelium. Cardiovasc. Res. 65, 599–608.

Leclair, H.M., André-Grégoire, G., Treps, L., Azzi, S., Bidère, N., Gavard, J., 2016. The E3 ubiquitin ligase MARCH3 controls the endothelial barrier. FEBS Lett. 590, 3660–3668. doi:10.1002/1873-3468.12417

Lee, C.-K., Weindruch, R., Prolla, T.A., 2000. Gene-expression profile of the ageing brain in mice. Nat. Genet. 25, 294–297.

Lee, J.K., Kim, N.-J., 2017. Recent Advances in the Inhibition of p38 MAPK as a Potential Strategy for the Treatment of Alzheimer's Disease. Molecules 22, 1287. doi:10.3390/molecules22081287

Lee, S.-J., Kim, J.-S., Chung, S.-W., Kim, B.-S., Ahn, K.-J., Lee, K.-S., 2011. White matter hyperintensities (WMH) are associated with intracranial atherosclerosis rather than extracranial atherosclerosis. Arch. Gerontol. Geriatr. 53, e129–e132. doi:https://doi.org/10.1016/j.archger.2010.07.008

Lee, S., Viqar, F., Zimmerman, M.E., Narkhede, A., Tosto, G., Benzinger, T.L.S., Marcus, D.S., Fagan, A.M., Goate, A., Fox, N.C., Cairns, N.J., Holtzman, D.M., Buckles, V., Ghetti, B., McDade, E., Martins, R.N., Saykin, A.J., Masters, C.L., Ringman, J.M., Ryan, N.S., Forster, S., Laske, C., Schofield, P.R., Sperling, R.A., Salloway, S., Correia, S., Jack, C.J., Weiner, M.,

Bateman, R.J., Morris, J.C., Mayeux, R., Brickman, A.M., 2016. White matter hyperintensities are a core feature of Alzheimer's disease: Evidence from the dominantly inherited Alzheimer network. Ann. Neurol. 79, 929–939. doi:10.1002/ana.24647

Lee, Y.-L., Hu, H.-Y., Huang, L.-Y., Chou, P., Chu, D., 2017. Periodontal Disease Associated with Higher Risk of Dementia: Population-Based Cohort Study in Taiwan. J. Am. Geriatr. Soc. 65, 1975–1980. doi:10.1111/jgs.14944

Lee, Y.J., Jy, W., Horstman, L.L., Janania, J., Reyes, Y., Kelley, R.E., Ahn, Y.S., 1993. Elevated platelet microparticles in transient ischemic attacks, lacunar infarcts, and multiinfarct dementias. Thromb. Res. 72, 295–304. doi:10.1016/0049-3848(93)90138-e

Lehnardt, S., Lachance, C., Patrizi, S., Lefebvre, S., Follett, P.L., Jensen, F.E., Rosenberg, P.A., Volpe, J.J., Vartanian, T., 2002. The toll-like receptor TLR4 is necessary for lipopolysaccharide-induced oligodendrocyte injury in the CNS. J. Neurosci. 22, 2478–2486.

Leliefeld, P.H.C., Wessels, C.M., Leenen, L.P.H., Koenderman, L., Pillay, J., 2016. The role of neutrophils in immune dysfunction during severe inflammation. Crit. Care 20, 1.

Li, J., Wang, Y.J., Zhang, M., Xu, Z.Q., Gao, C.Y., Fang, C.Q., Yan, J.C., Zhou, H.D., 2011. Vascular risk factors promote conversion from mild cognitive impairment to Alzheimer disease. Neurology 76, 1485–1491.

Li, J., Ye, L., Wang, X., Liu, J., Wang, Y., Zhou, Y., Ho, W., 2012. (−)-Epigallocatechin gallate inhibits endotoxin-induced expression of inflammatory cytokines in human cerebral microvascular endothelial cells. J. Neuroinflammation 9, 161. doi:10.1186/1742-2094-9-161

Liang, W.S., Dunckley, T., Beach, T.G., Grover, A., Mastroeni, D., Ramsey, K., Caselli, R.J., Kukull, W.A., McKeel, D., Morris, J.C., Hulette, C.M., Schmechel, D., Reiman, E.M., Rogers, J., Stephan, D.A., 2008. Altered neuronal gene expression in brain regions differentially affected by Alzheimer's disease: a reference data set. Physiol. Genomics 33, 240–256. doi:10.1152/physiolgenomics.00242.2007

Licastro, F., Morini, M.C., Davis, L.J., Malpassi, P., Cucinotta, D., Parente, R., Melotti, C., Savorani, G., 1994. Increased chemiluminescence response of neutrophils from the peripheral blood of patients with senile dementia of the Alzheimer's type. J. Neuroimmunol. 51, 21–26. doi:https://doi.org/10.1016/0165-5728(94)90124-4

Lim, K., Sumagin, R., Hyun, Y.-M., 2013. Extravasating Neutrophil-derived Microparticles Preserve Vascular Barrier Function in Inflamed Tissue. Immune Netw. 13, 102–106. doi:10.4110/in.2013.13.3.102

Lock, C., Hermans, G., Pedotti, R., Brendolan, A., Schadt, E., Garren, H., Langer-Gould, A., Strober, S., Cannella, B., Allard, J., Klonowski, P., Austin, A., Lad, N., Kaminski, N., Galli, S.J., Oksenberg, J.R., Raine, C.S., Heller, R., Steinman, L., 2002. Gene-microarray analysis of multiple sclerosis lesions yields new targets validated in autoimmune encephalomyelitis. Nat. Med. 8, 500–508. doi:10.1038/nm0502-500

Long, M.B., Ajikumar, A., Lodge, K., Condliffe, A., Ridger, V., 2019. Neutrophil-derived microvesicles are internalised by lung epithelial cells and induce inflammatory activation. ERJ Open Res. 5, PP203. doi:10.1183/23120541.lungscienceconference-2019.PP203

Lopez-Ramirez, M.A., Wu, D., Pryce, G., Simpson, J.E., Reijerkerk, A., King-Robson, J., Kay, O., de Vries, H.E., Hirst, M.C., Sharrack, B., 2014. MicroRNA-155 negatively affects blood–brain barrier function during neuroinflammation. FASEB J. 28, 2551–2565.

Lowe, J., Blanchard, A., Morrell, K., Lennox, G., Reynolds, L., Billett, M., Landon, M., Mayer, R.J., 1988. Ubiquitin is a common factor in intermediate filament inclusion bodies of diverse type in man, including those of Parkinson's disease, Pick's disease, and Alzheimer's disease, as well as

Rosenthal fibres in cerebellar astrocytomas, cytoplasmic bodies in m. J. Pathol. 155, 9–15. doi:10.1002/path.1711550105

Lugli, G., Cohen, A.M., Bennett, D.A., Shah, R.C., Fields, C.J., Hernandez, A.G., Smalheiser, N.R., 2015. Plasma Exosomal miRNAs in Persons with and without Alzheimer Disease: Altered Expression and Prospects for Biomarkers. PLoS One 10, e0139233.

Macdonald, J.A., Murugesan, N., Pachter, J.S., 2008. Validation of immuno-laser capture microdissection coupled with quantitative RT-PCR to probe blood–brain barrier gene expression in situ. J. Neurosci. Methods 174, 219–226.

Macfarlane, L.-A., Murphy, P.R., 2010. MicroRNA: Biogenesis, Function and Role in Cancer. Curr. Genomics 11, 537–561. doi:10.2174/138920210793175895

Madden, D.J., Bennett, I.J., Song, A.W., 2009. Cerebral white matter integrity and cognitive aging: Contributions from diffusion tensor imaging. Neuropsychol. Rev. doi:10.1007/s11065-009-9113-2

Mallat, Z., Hugel, B., Ohan, J., Leseche, G., Freyssinet, J.-M., Tedgui, A., 1999. Shed membrane microparticles with procoagulant potential in human atherosclerotic plaques: a role for apoptosis in plaque thrombogenicity. Circulation 99, 348–353.

Marcos-Ramiro, B., Nacarino, P.O., Serrano-Pertierra, E., Blanco-Gelaz, M.Á., Weksler, B.B., Romero, I.A., Couraud, P.O., Tuñón, A., López-Larrea, C., Millán, J., 2014. Microparticles in multiple sclerosis and clinically isolated syndrome: effect on endothelial barrier function. BMC Neurosci. 15, 110.

Marioni, R.E., Stewart, M.C., Murray, G.D., Deary, I.J., Fowkes, F.G.R., Lowe, G.D.O., Rumley, A., Price, J.F., 2009. Peripheral levels of fibrinogen, C-reactive protein, and plasma viscosity predict future cognitive decline in individuals without dementia. Psychosom. Med. 71, 901.

Markus, H.S., Hunt, B., Palmer, K., Enzinger, C., Schmidt, H., Schmidt, R., 2005. Markers of endothelial and hemostatic activation and progression of cerebral white matter hyperintensities longitudinal results of the Austrian Stroke Prevention Study. Stroke 36, 1410–1414.

Martin, B.K., Szekely, C., Brandt, J., Piantadosi, S., Breitner, J.C.S., Craft, S., Evans, D., Green, R., Mullan, M., 2008. Cognitive function over time in the Alzheimer's Disease Anti-inflammatory Prevention Trial (ADAPT): results of a randomized, controlled trial of naproxen and celecoxib. Arch. Neurol. 65, 896–905. doi:10.1001/archneur.2008.65.7.nct70006

McAleese, K.E., Alafuzoff, I., Charidimou, A., De Reuck, J., Grinberg, L.T., Hainsworth, A.H., Hortobagyi, T., Ince, P., Jellinger, K., Gao, J., Kalaria, R.N., Kovacs, G.G., Kövari, E., Love, S., Popovic, M., Skrobot, O., Taipa, R., Thal, D.R., Werring, D., Wharton, S.B., Attems, J., 2016. Post-mortem assessment in vascular dementia: advances and aspirations. BMC Med. 14, 129. doi:10.1186/s12916-016-0676-5

Medina, D., DeToledo-Morrell, L., Urresta, F., Gabrieli, J.D., Moseley, M., Fleischman, D., Bennett, D.A., Leurgans, S., Turner, D.A., Stebbins, G.T., 2006. White matter changes in mild cognitive impairment and AD: A diffusion tensor imaging study. Neurobiol Aging 27, 663–672. doi:S0197-4580(05)00142-9 [pii]\r10.1016/j.neurobiolaging.2005.03.026

Melief, J., Orre, M., Bossers, K., van Eden, C.G., Schuurman, K.G., Mason, M.R.J., Verhaagen, J., Hamann, J., Huitinga, I., 2019. Transcriptome analysis of normal-appearing white matter reveals cortisol- and disease-associated gene expression profiles in multiple sclerosis. Acta Neuropathol. Commun. 7, 60. doi:10.1186/s40478-019-0705-7

Merten, M., Pakala, R., Thiagarajan, P., Benedict, C.R., 1999. Platelet microparticles promote platelet interaction with subendothelial matrix in a glycoprotein IIb/IIIa–dependent mechanism. Circulation 99, 2577–2582.

Mesri, M., Altieri, D.C., 1999. Leukocyte microparticles stimulate endothelial cell cytokine release and tissue factor induction in a JNK1 signaling pathway. J. Biol. Chem. 274, 23111–23118.

Mesri, M., Altieri, D.C., 1998. Endothelial cell activation by leukocyte microparticles. J. Immunol. 161, 4382–4387.

Messerli, M., May, K., Hansson, S.R., Schneider, H., Holzgreve, W., Hahn, S., Rusterholz, C., 2010. Feto-maternal interactions in pregnancies: Placental microparticles activate peripheral blood monocytes. Placenta 31, 106–112. doi:https://doi.org/10.1016/j.placenta.2009.11.011

Michael, D., Oren, M., 2003. The p53–Mdm2 module and the ubiquitin system, in: Seminars in Cancer Biology. Elsevier, pp. 49–58.

Milani, G., Lana, T., Bresolin, S., Aveic, S., Pastò, A., Frasson, C., te Kronnie, G., 2017. Expression Profiling of Circulating Microvesicles Reveals Intercellular Transmission of Oncogenic Pathways. Mol. Cancer Res. 15, 683 LP – 695. doi:10.1158/1541-7786.MCR-16-0307

Miller, F., Fenart, L., Landry, V., Coisne, C., Cecchelli, R., Dehouck, M.-P., Buée-Scherrer, V., 2005. The MAP kinase pathway mediates transcytosis induced by TNF-alpha in an in vitro blood-brain barrier model. Eur. J. Neurosci. 22, 835–844. doi:10.1111/j.1460-9568.2005.04273.x

Mina, E., van Roon-Mom, W., Hettne, K., van Zwet, E., Goeman, J., Neri, C., A.C. 't Hoen, P., Mons, B., Roos, M., 2016. Common disease signatures from gene expression analysis in Huntington's disease human blood and brain. Orphanet J. Rare Dis. 11, 97. doi:10.1186/s13023-016-0475-2

Mojsilovic-Petrovic, J., Nesic, M., Pen, A., Zhang, W., Stanimirovic, D., 2004. Development of rapid staining protocols for laser-capture microdissection of brain vessels from human and rat coupled to gene expression analyses. J. Neurosci. Methods 133, 39–48. doi:https://doi.org/10.1016/j.jneumeth.2003.09.026

Mooradian, A.D., McCuskey, R.S., 1992. In vivo microscopic studies of age-related changes in the structure and the reactivity of cerebral microvessels. Mech. Ageing Dev. 64, 247–254.

Morandi, A., Davis, D., Bellelli, G., Arora, R.C., Caplan, G.A., Kamholz, B., Kolanowski, A., Fick, D.M., Kreisel, S., MacLullich, A., Meagher, D., Neufeld, K., Pandharipande, P.P., Richardson, S., Slooter, A.J.C., Taylor, J.P., Thomas, C., Tieges, Z., Teodorczuk, A., Voyer, P., Rudolph, J.L., 2017. The Diagnosis of Delirium Superimposed on Dementia: An Emerging Challenge. J. Am. Med. Dir. Assoc. 18, 12–18. doi:https://doi.org/10.1016/j.jamda.2016.07.014

Mori, H., Kondo, J., Ihara, Y., 1987. Ubiquitin is a component of paired helical filaments in Alzheimer's disease. Science (80-.). 235, 1641 LP – 1644. doi:10.1126/science.3029875

Mount, C., Downton, C., 2006. Alzheimer disease: progress or profit? Nat Med 12, 780–784.

Munoz, L., Ammit, A.J., 2010. Targeting p38 MAPK pathway for the treatment of Alzheimer's disease. Neuropharmacology 58, 561–568.

Murakami, T., Felinski, E.A., Antonetti, D.A., 2009. Occludin Phosphorylation and Ubiquitination Regulate Tight Junction Trafficking and Vascular Endothelial Growth Factor-induced Permeability. J. Biol. Chem. 284, 21036–21046. doi:10.1074/jbc.M109.016766

Murakami, T., Frey, T., Lin, C., Antonetti, D.A., 2012. Protein Kinase Cβ Phosphorylates Occludin Regulating Tight Junction Trafficking in Vascular Endothelial Growth Factor–Induced Permeability In Vivo. Diabetes 61, 1573 LP – 1583. doi:10.2337/db11-1367

Murphy, D., 2002. GENE EXPRESSION STUDIES USING MICROARRAYS: PRINCIPLES, PROBLEMS, AND PROSPECTS. Adv. Physiol. Educ. 26, 256–270. doi:10.1152/advan.00043.2002

Mycko, M.P., Brosnan, C.F., Raine, C.S., Fendler, W., Selmaj, K.W., 2012. Transcriptional profiling of microdissected areas of active multiple sclerosis lesions reveals activation of heat shock

protein genes. J. Neurosci. Res. 90, 1941–1948. doi:10.1002/jnr.23079

Mycko, M.P., Papoian, R., Boschert, U., Raine, C.S., Selmaj, K.W., 2003. cDNA microarray analysis in multiple sclerosis lesions: detection of genes associated with disease activity. Brain 126, 1048–1057. doi:10.1093/brain/awg107

Nachman, E., Wentink, A.S., Madiona, K., Bousset, L., Katsinelos, T., Allinson, K., Kampinga, H., McEwan, W.A., Jahn, T.R., Melki, R., Mogk, A., Bukau, B., Nussbaum-Krammer, C., 2020. Disassembly of Tau fibrils by the human Hsp70 disaggregation machinery generates small seeding-competent species. J. Biol. Chem. 295, 9676–9690. doi:10.1074/jbc.RA120.013478

Nebes, R.D., Vora, I.J., Meltzer, C.C., Fukui, M.B., Williams, R.L., Kamboh, M.I., Saxton, J., Houck, P.R., DeKosky, S.T., Reynolds, C.F. 3rd, 2001. Relationship of deep white matter hyperintensities and apolipoprotein E genotype to depressive symptoms in older adults without clinical depression. Am. J. Psychiatry 158, 878–884. doi:10.1176/appi.ajp.158.6.878

Neuropathology, G., 2001. Pathological correlates of late-onset dementia in a multicentre, community-based population in England and Wales. Neuropathology Group of the Medical Research Council Cognitive Function and Ageing Study (MRC CFAS). Lancet (London, England) 357, 169.

Noerholm, M., Balaj, L., Limperg, T., Salehi, A., Zhu, L.D., Hochberg, F.H., Breakefield, X.O., Carter, B.S., Skog, J., 2012. RNA expression patterns in serum microvesicles from patients with glioblastoma multiforme and controls. BMC Cancer 12, 22.

Nomura, S., Tandon, N.N., Nakamura, T., Cone, J., Fukuhara, S., Kambayashi, J., 2001. High-shear-stress-induced activation of platelets and microparticles enhances expression of cell adhesion molecules in THP-1 and endothelial cells. Atherosclerosis 158, 277–287. doi:10.1016/s0021-9150(01)00433-6

O'brien, J., Desmond, P., Ames, D., Schweitzer, I., Harrigan, S., Tress, B., 1996. A magnetic resonance imaging study of white matter lesions in depression and Alzheimer's disease. Br. J. Psychiatry 168, 477–485.

O'Brien, J.T., Erkinjuntti, T., Reisberg, B., Roman, G., Sawada, T., Pantoni, L., Bowler, J. V, Ballard, C., DeCarli, C., Gorelick, P.B., Rockwood, K., Burns, A., Gauthier, S., DeKosky, S.T., 2003. Vascular cognitive impairment. Lancet Neurol. 2, 89–98. doi:http://dx.doi.org/10.1016/S1474-4422(03)00305-3

O'Donnell, L.J., Westin, C.-F., 2011. An introduction to diffusion tensor image analysis. Neurosurg. Clin. 22, 185–196.

O'Donnell, M.J., Xavier, D., Liu, L., Zhang, H., Chin, S.L., Rao-Melacini, P., Rangarajan, S., Islam, S., Pais, P., McQueen, M.J., Mondo, C., Damasceno, A., Lopez-Jaramillo, P., Hankey, G.J., Dans, A.L., Yusoff, K., Truelsen, T., Diener, H.-C., Sacco, R.L., Ryglewicz, D., Czlonkowska, A., Weimar, C., Wang, X., Yusuf, S., 2010. Risk factors for ischaemic and intracerebral haemorrhagic stroke in 22 countries (the INTERSTROKE study): a case-control study. Lancet (London, England) 376, 112–123. doi:10.1016/S0140-6736(10)60834-3

O'Sullivan, M., Jones, D.K., Summers, P.E., Morris, R.G., Williams, S.C., Markus, H.S., 2001. Evidence for cortical "disconnection" as a mechanism of age-related cognitive decline. Neurology 57, 632–638. doi:10.1212/wnl.57.4.632

Obermeier, B., Daneman, R., Ransohoff, R.M., 2013. Development, maintenance and disruption of the blood-brain barrier. Nat. Med. 19, 1584.

Office of National Statistics, 2018. National population based projections: 2018 -based statisical bulletin.

Olivier, M., Laurence, J., Jean-Marie, F., Florence, T., 2011. Cellular Mechanisms Underlying the

Formation of Circulating Microparticles. Arterioscler. Thromb. Vasc. Biol. 31, 15–26. doi:10.1161/ATVBAHA.109.200956

Opal, S.M., 2003. Severe sepsis and septic shock: defining the clinical problem. Scand. J. Infect. Dis. 35, 529–534. doi:10.1080/00365540310015917

Oren, M., Maltzman, W., Levine, A.J., 1981. Post-translational regulation of the 54K cellular tumor antigen in normal and transformed cells. Mol. Cell. Biol. 1, 101–110. doi:10.1128/mcb.1.2.101

Orihuela, R., McPherson, C.A., Harry, G.J., 2016. Microglial M1/M2 polarization and metabolic states. Br. J. Pharmacol. 173, 649–665. doi:10.1111/bph.13139

Orsenigo, F., Giampietro, C., Ferrari, A., Corada, M., Galaup, A., Sigismund, S., Ristagno, G., Maddaluno, L., Young Koh, G., Franco, D., Kurtcuoglu, V., Poulikakos, D., Baluk, P., McDonald, D., Grazia Lampugnani, M., Dejana, E., 2012. Phosphorylation of VE-cadherin is modulated by haemodynamic forces and contributes to the regulation of vascular permeability in vivo. Nat. Commun. 3, 1208. doi:10.1038/ncomms2199

Ovbiagele, B., Saver, J.L., 2006. Cerebral white matter hyperintensities on MRI: Current concepts and therapeutic implications. Cerebrovasc. Dis. 22, 83–90. doi:10.1159/000093235

Pang, Y., Cai, Z., Rhodes, P.G., 2003. Disturbance of oligodendrocyte development, hypomyelination and white matter injury in the neonatal rat brain after intracerebral injection of lipopolysaccharide. Dev. Brain Res. 140, 205–214.

Pant, V., Xiong, S., Iwakuma, T., Quintás-Cardama, A., Lozano, G., 2011. Heterodimerization of Mdm2 and Mdm4 is critical for regulating p53 activity during embryogenesis but dispensable for p53 and Mdm2 stability. Proc. Natl. Acad. Sci. U. S. A. 108, 11995–12000. doi:10.1073/pnas.1102241108

Pantoni, L., 2010. Cerebral small vessel disease: from pathogenesis and clinical characteristics to therapeutic challenges. Lancet. Neurol. 9, 689–701. doi:10.1016/S1474-4422(10)70104-6

Parolini, I., Federici, C., Raggi, C., Lugini, L., Palleschi, S., De Milito, A., Coscia, C., Iessi, E., Logozzi, M., Molinari, A., Colone, M., Tatti, M., Sargiacomo, M., Fais, S., 2009. Microenvironmental pH is a key factor for exosome traffic in tumor cells. J. Biol. Chem. 284, 34211–34222. doi:10.1074/jbc.M109.041152

Pasquet, J.-M., Dachary-Prigent, J., Nurden, A.T., 1996. Calcium Influx is a Determining Factor of Calpain Activation and Microparticle Formation in Platelets. Eur. J. Biochem. 239, 647–654. doi:10.1111/j.1432-1033.1996.0647u.x

Pedditzi, E., Peters, R., Beckett, N., 2016. Corrigenda: Corrigendum to 'The risk of overweight/obesity in mid-life and late life for the development of dementia: a systematic review and meta-analysis of longitudinal studies.' Age Ageing 45, 740.

Pei, J.-J., Braak, E., Braak, H., Grundke-Iqbal, I., Iqbal, K., Winblad, B., Cowburn, R.F., 2001. Localization of active forms of C-jun kinase (JNK) and p38 kinase in Alzheimer's disease brains at different stages of neurofibrillary degeneration. J. Alzheimer's Dis. 3, 41–48.

Peifer, C., Wagner, G., Laufer, S., 2006. New approaches to the treatment of inflammatory disorders small molecule inhibitors of p38 MAP kinase. Curr. Top. Med. Chem. 6, 113–149.

Pelegrini, A.L., Moura, D.J., Brenner, B.L., Ledur, P.F., Maques, G.P., Henriques, J.A.P., Saffi, J., Lenz, G., 2010. Nek1 silencing slows down DNA repair and blocks DNA damage-induced cell cycle arrest. Mutagenesis 25, 447–454.

Perry, V Hugh, Andersson, P.B., Gordon, S., 1993. Macrophages and inflammation in the central nervous system. Trends Neurosci. 16, 268–73. doi:10.1016/0166-2236(93)90180-T

Perry, V.H., Holmes, C., 2014. Microglial priming in neurodegenerative disease. Nat Rev Neurol 10.

doi:10.1038/nrneurol.2014.38

Perry, V H, Matyszak, M.K., Fearn, S., 1993. Altered antigen expression of microglia in the aged rodent CNS. Glia 7, 60–67. doi:10.1002/glia.440070111

Peters, A., Sethares, C., 2002. Aging and the myelinated fibers in prefrontal cortex and corpus callosum of the monkey. J. Comp. Neurol. 442, 277–291. doi:10.1002/cne.10099

Piaton, G., Aigrot, M.-S., Williams, A., Moyon, S., Tepavcevic, V., Moutkine, I., Gras, J., Matho, K.S., Schmitt, A., Soellner, H., Huber, A.B., Ravassard, P., Lubetzki, C., 2011. Class 3 semaphorins influence oligodendrocyte precursor recruitment and remyelination in adult central nervous system. Brain 134, 1156–1167. doi:10.1093/brain/awr022

Pitanga, T.N., de Aragão França, L., Rocha, V.C.J., Meirelles, T., Borges, V.M., Gonçalves, M.S., Pontes-de-Carvalho, L.C., Noronha-Dutra, A.A., dos-Santos, W.L.C., 2014. Neutrophil-derived microparticles induce myeloperoxidase-mediated damage of vascular endothelial cells. BMC Cell Biol. 15, 1.

Poggesi, A., Salvadori, E., Pantoni, L., Pracucci, G., Cesari, F., Chiti, A., Ciolli, L., Cosottini, M., Del Bene, A., De Stefano, N., 2012. Risk and determinants of dementia in patients with mild cognitive impairment and brain subcortical vascular changes: A study of clinical, neuroimaging, and biological markers—The VMCI-Tuscany study: Rationale, design, and methodology. Int. J. Alzheimer's Dis. 2012.

Posner, H.B., Tang, M.-X., Luchsinger, J., Lantigua, R., Stern, Y., Mayeux, R., 2002. The relationship of hypertension in the elderly to AD, vascular dementia, and cognitive function. Neurology 58, 1175–1181. doi:10.1212/wnl.58.8.1175

Prakash, P.S., Caldwell, C.C., Lentsch, A.B., Pritts, T.A., Robinson, B.R.H., 2012. Human microparticles generated during sepsis in patients with critical illness are neutrophil-derived and modulate the immune response. J. Trauma Acute Care Surg. 73, 401–407. doi:10.1097/TA.0b013e31825a776d

Preece, P., Cairns, N.J., 2003. Quantifying mRNA in postmortem human brain: influence of gender, age at death, postmortem interval, brain pH, agonal state and inter-lobe mRNA variance. Brain Res. Mol. Brain Res. 118, 60–71. doi:10.1016/s0169-328x(03)00337-1

Prins, N.D., van Dijk, E.J., den Heijer, T., Vermeer, S.E., Koudstaal, P.J., Oudkerk, M., Hofman, A., Breteler, M.M.B., 2004. Cerebral white matter lesions and the risk of dementia.[see comment]. Arch. Neurol. 61, 1531–1534.

Puddu, P., Puddu, G.M., Cravero, E., Muscari, S., Muscari, A., 2010. The involvement of circulating microparticles in inflammation, coagulation and cardiovascular diseases. Can. J. Cardiol. 26, e140–e145.

Qin, L., Huang, W., Mo, X., Chen, Y., Wu, X., 2015. LPS induces occludin dysregulation in cerebral microvascular endothelial cells via MAPK signaling and augmenting MMP-2 levels. Oxid. Med. Cell. Longev. 2015.

Querido, E., Blanchette, P., Yan, Q., Kamura, T., Morrison, M., Boivin, D., Kaelin, W.G., Conaway, R.C., Conaway, J.W., Branton, P.E., 2001. Degradation of p53 by adenovirus E4orf6 and E1B55K proteins occurs via a novel mechanism involving a Cullin-containing complex. Genes Dev. 15, 3104–3117. doi:10.1101/gad.926401

Rai, B., Kaur, J., Anand, S.C., 2012. Possible relationship between periodontitis and dementia in a North Indian old age population: a pilot study. Gerodontology 29, e200–e205. doi:10.1111/j.1741-2358.2010.00441.x

Ramachandran, S., Clarke, L.A., Scheetz, T.E., Amaral, M.D., McCray, P.B.J., 2011. Microarray mRNA expression profiling to study cystic fibrosis. Methods Mol. Biol. 742, 193–212.

doi:10.1007/978-1-61779-120-8_12

Ratajczak, J., Wysoczynski, M., Hayek, F., Janowska-Wieczorek, A., Ratajczak, M.Z., 2006. Membrane-derived microvesicles: important and underappreciated mediators of cell-to-cell communication. Leukemia 20, 1487–1495.

Raz, N., Yang, Y., Dahle, C.L., Land, S., 2012. Volume of white matter hyperintensities in healthy adults: contribution of age, vascular risk factors, and inflammation-related genetic variants. Biochim. Biophys. Acta 1822, 361–369. doi:10.1016/j.bbadis.2011.08.007

Reichenberg, A., Yirmiya, R., Schuld, A., Kraus, T., Haack, M., Morag, A., Pollmächer, T., 2001. Cytokine-associated emotional and cognitive disturbances in humans. Arch. Gen. Psychiatry 58, 445–452.

Reijmer, Y.D., van Veluw, S.J., Greenberg, S.M., 2016. Ischemic brain injury in cerebral amyloid angiopathy. J. Cereb. Blood Flow Metab. 36, 40–54. doi:10.1038/jcbfm.2015.88

Rezaie, P., Dean, A., 2002. Periventricular leukomalacia, inflammation and white matter lesions within the developing nervous system. Neuropathology 22, 106–132.

Rhys, H.I., Dell'Accio, F., Pitzalis, C., Moore, A., Norling, L. V, Perretti, M., 2018. Neutrophil Microvesicles from Healthy Control and Rheumatoid Arthritis Patients Prevent the Inflammatory Activation of Macrophages. EBioMedicine 29, 60–69. doi:10.1016/j.ebiom.2018.02.003

Ridger, V.C., Boulanger, C.M., Angelillo-Scherrer, A., Badimon, L., Blanc-Brude, O., Bochaton-Piallat, M.-L., Boilard, E., Buzas, E.I., Caporali, A., Dignat-George, F., Evans, P.C., Lacroix, R., Lutgens, E., Ketelhuth, D.F.J., Nieuwland, R., Toti, F., Tunon, J., Weber, C., Hoefer, I.E., 2017. Microvesicles in vascular homeostasis and diseases. Position Paper of the European Society of Cardiology (ESC) Working Group on Atherosclerosis and Vascular Biology. Thromb. Haemost. 117, 1296–1316. doi:10.1160/TH16-12-0943

Ritz, M.-F., Grond-Ginsbach, C., Kloss, M., Tolnay, M., Fluri, F., Bonati, L.H., Traenka, C., Zeis, T., Schaeren-Wiemers, N., Peters, N., Engelter, S.T., Lyrer, P.A., 2016. Identification of Inflammatory, Metabolic, and Cell Survival Pathways Contributing to Cerebral Small Vessel Disease by Postmortem Gene Expression Microarray. Curr. Neurovasc. Res. 13, 58–67. doi:10.2174/1567202612666151027151025

Ronaldson, P.T., Demarco, K.M., Sanchez-Covarrubias, L., Solinsky, C.M., Davis, T.P., 2009. Transforming growth factor-beta signaling alters substrate permeability and tight junction protein expression at the blood-brain barrier during inflammatory pain. J. Cereb. Blood Flow Metab. 29, 1084–1098. doi:10.1038/jcbfm.2009.32

Rosenberg, G.A., 2009. Inflammation and white matter damage in vascular cognitive impairment. Stroke 40, S20–S23.

Rosenberger, A.F.N., Hilhorst, R., Coart, E., García Barrado, L., Naji, F., Rozemuller, A.J.M., Van der Flier, W.M., Scheltens, P., Hoozemans, J.J.M., Van der Vies, S.M., 2016. Protein kinase activity decreases with higher Braak stages of Alzheimer's disease pathology. J. Alzheimer's Dis. 49, 927–943.

Rostrup, E., Gouw, A.A., Vrenken, H., van Straaten, E.C.W., Ropele, S., Pantoni, L., Inzitari, D., Barkhof, F., Waldemar, G., 2012. The spatial distribution of age-related white matter changes as a function of vascular risk factors--results from the LADIS study. Neuroimage 60, 1597–1607. doi:10.1016/j.neuroimage.2012.01.106

Rui, L., Weiyi, L., Yu, M., Hong, Z., Jiao, Y., Zhe, M., Hongjie, F., 2018. The serine/threonine protein kinase of Streptococcus suis serotype 2 affects the ability of the pathogen to penetrate the blood–brain barrier. Cell. Microbiol. 20, e12862. doi:10.1111/cmi.12862

Russell, J.A., 2006. Management of sepsis. N. Engl. J. Med. 355, 1699–1713. doi:10.1056/NEJMra043632

Sachdev, P.S., Zhuang, L., Braidy, N., Wen, W., 2013. Is Alzheimer's a disease of the white matter? Curr. Opin. Psychiatry 26, 244–251. doi:10.1097/YCO.0b013e32835ed6e8

Saczynski, J.S., Marcantonio, E.R., Quach, L., Fong, T.G., Gross, A., Inouye, S.K., Jones, R.N., 2012. Cognitive trajectories after postoperative delirium. N. Engl. J. Med. 367, 30–39. doi:10.1056/NEJMoa1112923

Safaei, R., Larson, B.J., Cheng, T.C., Gibson, M.A., Otani, S., Naerdemann, W., Howell, S.B., 2005. Abnormal lysosomal trafficking and enhanced exosomal export of cisplatin in drug-resistant human ovarian carcinoma cells. Mol. Cancer Ther. 4, 1595–1604. doi:10.1158/1535-7163.MCT-05-0102

Saitoh, T., Komano, J., Saitoh, Y., Misawa, T., Takahama, M., Kozaki, T., Uehata, T., Iwasaki, H., Omori, H., Yamaoka, S., Yamamoto, N., Akira, S., 2012. Neutrophil extracellular traps mediate a host defense response to human immunodeficiency virus-1. Cell Host Microbe 12, 109–116. doi:10.1016/j.chom.2012.05.015

Schieven, G.L., 2005. The biology of p38 kinase: a central role in inflammation. Curr. Top. Med. Chem. 5, 921–928.

Schmahmann, J.D., Smith, E.E., Eichler, F.S., Filley, C.M., 2008. Cerebral white matter: Neuroanatomy, clinical neurology, and neurobehavioral correlates. Ann. N. Y. Acad. Sci. doi:10.1196/annals.1444.017

Scott, J.A., Braskie, M.N., Tosun, D., Thompson, P.M., Weiner, M., DeCarli, C., Carmichael, O.T., 2015. Cerebral Amyloid and Hypertension are Independently Associated with White Matter Lesions in Elderly . Front. Aging Neurosci. .

Seillier, M., Pouyet, L., N'Guessan, P., Nollet, M., Capo, F., Guillaumond, F., Peyta, L., Dumas, J.-F., Varrault, A., Bertrand, G., Bonnafous, S., Tran, A., Meur, G., Marchetti, P., Ravier, M.A., Dalle, S., Gual, P., Muller, D., Rutter, G.A., Servais, S., Iovanna, J.L., Carrier, A., 2015. Defects in mitophagy promote redox-driven metabolic syndrome in the absence of TP53INP1. EMBO Mol. Med. 7, 802–818. doi:10.15252/emmm.201404318

Sellam, J., Proulle, V., Jüngel, A., Ittah, M., Miceli Richard, C., Gottenberg, J.-E., Toti, F., Benessiano, J., Gay, S., Freyssinet, J.-M., Mariette, X., 2009. Increased levels of circulating microparticles in primary Sjögren's syndrome, systemic lupus erythematosus and rheumatoid arthritis and relation with disease activity. Arthritis Res. Ther. 11, R156. doi:10.1186/ar2833

Shad, K.F., Aghazadeh, Y., Ahmad, S., Kress, B., 2013. Peripheral markers of Alzheimer's disease: Surveillance of white blood cells. Synapse 67, 541–543.

Shalev, D., Arbuckle, M.R., 2017. Metabolism and Memory: Obesity, Diabetes, and Dementia. Biol. Psychiatry 82, e81–e83. doi:10.1016/j.biopsych.2017.09.025

Shedden, K., Xie, X.T., Chandaroy, P., Chang, Y.T., Rosania, G.R., 2003. Expulsion of small molecules in vesicles shed by cancer cells: association with gene expression and chemosensitivity profiles. Cancer Res. 63, 4331–4337.

Simpson, Fernando, M.S., Clark, L., Ince, P.G., Matthews, F., Forster, G., O'Brien, J.T., Barber, R., Kalaria, R.N., Brayne, C., Shaw, P.J., Lewis, C.E., Wharton, S.B., 2007. White matter lesions in an unselected cohort of the elderly: Astrocytic, microglial and oligodendrocyte precursor cell responses. Neuropathol. Appl. Neurobiol. 33, 410–419. doi:10.1111/j.1365-2990.2007.00828.x

Simpson, J., Ince, P.G., Higham, C.E., Gelsthorpe, C.H., Fernando, M.S., Matthews, F., Forster, G., O'Brien, J.T., Barber, R., Kalaria, R.N., Brayne, C., Shaw, P.J., Stoeber, K., Williams, G.H., Lewis, C.E., Wharton, S.B., 2007. Microglial activation in white matter lesions and nonlesional

white matter of ageing brains. Neuropathol. Appl. Neurobiol. 33, 670–683. doi:10.1111/j.1365-2990.2007.00890.x

Simpson, J.E., Hosny, O., Wharton, S.B., Heath, P.R., Holden, H., Fernando, M.S., Matthews, F., Forster, G., O'Brien, J.T., Barber, R., Kalaria, R.N., Brayne, C., Shaw, P.J., Lewis, C.E., Ince, P.G., 2009. Microarray RNA Expression Analysis of Cerebral White Matter Lesions Reveals Changes in Multiple Functional Pathways. Stroke 40, 369 LP – 375.

Simpson, J.E., Ince, P.G., Minett, T., Matthews, F.E., Heath, P.R., Shaw, P.J., Goodall, E., Garwood, C.J., Ratcliffe, L.E., Brayne, C., 2016. Neuronal DNA damage response-associated dysregulation of signalling pathways and cholesterol metabolism at the earliest stages of A lzheimer-type pathology. Neuropathol. Appl. Neurobiol. 42, 167–179.

Simpson, J.E., Wharton, S.B., Cooper, J., Gelsthorpe, C., Baxter, L., Forster, G., Shaw, P.J., Savva, G., Matthews, F.E., Brayne, C., Ince, P.G., 2010. Alterations of the blood-brain barrier in cerebral white matter lesions in the ageing brain. Neurosci. Lett. 486, 246–251. doi:10.1016/j.neulet.2010.09.063

Skoog, I., Wallin, A., Fredman, P., Hesse, C., Aevarsson, O., Karlsson, I., Gottfries, C.G., Blennow, K., 1998. A population study on blood-brain barrier function in 85-year-olds: relation to Alzheimer's disease and vascular dementia. Neurology 50, 966–971. doi:10.1212/wnl.50.4.966

Smith, J.A., Turner, S.T., Sun, Y. V, Fornage, M., Kelly, R.J., Mosley, T.H., Jack, C.R., Kullo, I.J., Kardia, S.L.R., 2009. Complexity in the genetic architecture of leukoaraiosis in hypertensive sibships from the GENOA Study. BMC Med. Genomics 2, 16. doi:10.1186/1755-8794-2-16

Snyder, H.M., Corriveau, R.A., Craft, S., Faber, J.E., Greenberg, S.M., Knopman, D., Lamb, B.T., Montine, T.J., Nedergaard, M., Schaffer, C.B., Schneider, J.A., Wellington, C., Wilcock, D.M., Zipfel, G.J., Zlokovic, B., Bain, L.J., Bosetti, F., Galis, Z.S., Koroshetz, W., Carrillo, M.C., 2015. Vascular contributions to cognitive impairment and dementia including Alzheimer's disease. Alzheimer's Dement. 11, 710–717. doi:https://doi.org/10.1016/j.jalz.2014.10.008

Spauwen, P.J.J., Kohler, S., Verhey, F.R.J., Stehouwer, C.D.A., van Boxtel, M.P.J., 2013. Effects of type 2 diabetes on 12-year cognitive change: results from the Maastricht Aging Study. Diabetes Care 36, 1554–1561. doi:10.2337/dc12-0746

Spilt, A., Goekoop, R., Westendorp, R.G.J., Blauw, G.J., de Craen, A.J.M., van Buchem, M.A., 2006. Not all age-related white matter hyperintensities are the same: a magnetization transfer imaging study. AJNR. Am. J. Neuroradiol. 27, 1964–1968.

Srinivasan, B., Kolli, A.R., Esch, M.B., Abaci, H.E., Shuler, M.L., Hickman, J.J., 2015. TEER measurement techniques for in vitro barrier model systems. J. Lab. Autom. 20, 107–126. doi:10.1177/2211068214561025

Stamatovic, S.M., Johnson, A.M., Keep, R.F., Andjelkovic, A. V, 2016. Junctional proteins of the blood-brain barrier: New insights into function and dysfunction. Tissue Barriers 4, e1154641. doi:10.1080/21688370.2016.1154641

Steinman, L., Zamvil, S., 2003. Transcriptional analysis of targets in multiple sclerosis. Nat. Rev. Immunol. 3, 483–492. doi:10.1038/nri1108

Stewart, P.A., Hayakawa, K., Akers, M.A., Vinters, H. V, 1992. A morphometric study of the blood-brain barrier in Alzheimer's disease. Lab. Invest. 67, 734–742.

Stewart, W.F., Kawas, C., Corrada, M., Metter, E.J., 1997. Risk of Alzheimer's disease and duration of NSAID use. Neurology 48, 626–632. doi:10.1212/wnl.48.3.626

Stolp, H.B., Dziegielewska, K.M., 2009. Review: Role of developmental inflammation and blood–brain barrier dysfunction in neurodevelopmental and neurodegenerative diseases. Neuropathol. Appl. Neurobiol. 35, 132–146. doi:10.1111/j.1365-2990.2008.01005.x

Stolp, H.B., Dziegielewska, K.M., Ek, C.J., Potter, A.M., Saunders, N.R., 2005. Long-term changes in blood–brain barrier permeability and white matter following prolonged systemic inflammation in early development in the rat. Eur. J. Neurosci. 22, 2805–2816.

Stolp, H.B., Ek, C.J., Johansson, P.A., Dziegielewska, K.M., Bethge, N., Wheaton, B.J., Potter, A.M., Saunders, N.R., 2009. Factors involved in inflammation-induced developmental white matter damage. Neurosci. Lett. 451, 232–236. doi:10.1016/j.neulet.2009.01.021

Stone, S., Lin, W., 2015. The unfolded protein response in multiple sclerosis. Front. Neurosci. 9, 264. doi:10.3389/fnins.2015.00264

Strandberg, T.E., Pitkala, K.H., Linnavuori, K.H., Tilvis, R.S., 2003. Impact of viral and bacterial burden on cognitive impairment in elderly persons with cardiovascular diseases. Stroke 34, 2126–2131.

Strozyk, D., Dickson, D.W., Lipton, R.B., Katz, M., Derby, C.A., Lee, S., Wang, C., Verghese, J., 2017. Contribution of vascular pathology to the clinical expression of dementia. Neurobiol. Aging 31, 1710–1720. doi:10.1016/j.neurobiolaging.2008.09.011

Suh, H.-S., Zhao, M.-L., Derico, L., Choi, N., Lee, S.C., 2013. Insulin-like growth factor 1 and 2 (IGF1, IGF2) expression in human microglia: differential regulation by inflammatory mediators. J. Neuroinflammation 10, 37. doi:10.1186/1742-2094-10-37

Sun, A., Liu, M., Nguyen, X. V, Bing, G., 2003. P38 MAP kinase is activated at early stages in Alzheimer's disease brain. Exp. Neurol. 183, 394–405.

Swardfager, W., Yu, D., Ramirez, J., Cogo-Moreira, H., Szilagyi, G., Holmes, M.F., Scott, C.J.M., Scola, G., Chan, P.C.P., Chen, J., Chan, P.C.P., Sahlas, D.J., Herrmann, N., Lanctôt, K.L., Andreazza, A.C., Pettersen, J.A., Black, S.E., 2017. Peripheral inflammatory markers indicate microstructural damage within periventricular white matter hyperintensities in Alzheimer's disease: A preliminary report. Alzheimer's Dement. Diagnosis, Assess. Dis. Monit. 7, 56–60. doi:10.1016/j.dadm.2016.12.011

Sweeney, M.D., Zhao, Z., Montagne, A., Nelson, A.R., Zlokovic, B. V, 2018. Blood-Brain Barrier: From Physiology to Disease and Back. Physiol. Rev. 99, 21–78. doi:10.1152/physrev.00050.2017

Tai, L.M., Holloway, K.A., Male, D.K., Loughlin, A.J., Romero, I.A., 2010. Amyloid-β-induced occludin down-regulation and increased permeability in human brain endothelial cells is mediated by MAPK activation. J. Cell. Mol. Med. 14, 1101–1112. doi:10.1111/j.1582-4934.2009.00717.x

Takechi, R., Lam, V., Brook, E., Giles, C., Fimognari, N., Mooranian, A., Al-Salami, H., Coulson, S.H., Nesbit, M., Mamo, J.C.L., 2017. Blood-Brain Barrier Dysfunction Precedes Cognitive Decline and Neurodegeneration in Diabetic Insulin Resistant Mouse Model: An Implication for Causal Link . Front. Aging Neurosci. .

Tanaka, S., Kondo, H., Kanda, K., Ashino, T., Nakamachi, T., Sekikawa, K., Iwakura, Y., Shioda, S., Numazawa, S., Yoshida, T., 2011. Involvement of interleukin-1 in lipopolysaccaride-induced microglial activation and learning and memory deficits. J. Neurosci. Res. 89, 506–514. doi:10.1002/jnr.22582

Tang, Y., Le, W., 2016. Differential Roles of M1 and M2 Microglia in Neurodegenerative Diseases. Mol. Neurobiol. 53, 1181–1194. doi:10.1007/s12035-014-9070-5

Tate, J.A., Snitz, B.E., Alvarez, K.A., Nahin, R.L., Weissfeld, L.A., Lopez, O., Angus, D.C., Shah, F., Ives, D.G., Fitzpatrick, A.L., Williamson, J.D., Arnold, A.M., DeKosky, S.T., Yende, S., 2014. Infection hospitalization increases risk of dementia in the elderly. Crit. Care Med. 42, 1037–1046. doi:10.1097/CCM.0000000000000123

Taubert, M., Draganski, B., Anwander, A., Muller, K., Horstmann, A., Villringer, A., Ragert, P., 2010. Dynamic properties of human brain structure: learning-related changes in cortical areas and associated fiber connections. J. Neurosci. 30, 11670–11677. doi:10.1523/JNEUROSCI.2567-10.2010

Terrisse, A.D., PUECH, N., ALLART, S., GOURDY, P., XUEREB, J.M., PAYRASTRE, B., SIÉ, P., 2010. Internalization of microparticles by endothelial cells promotes platelet/endothelial cell interaction under flow. J. Thromb. Haemost. 8, 2810–2819. doi:10.1111/j.1538-7836.2010.04088.x

Thal, L.J., Ferris, S.H., Kirby, L., Block, G.A., Lines, C.R., Yuen, E., Assaid, C., Nessly, M.L., Norman, B.A., Baranak, C.C., Reines, S.A., 2005. A randomized, double-blind, study of rofecoxib in patients with mild cognitive impairment. Neuropsychopharmacology 30, 1204–1215. doi:10.1038/sj.npp.1300690

Thirumangalakudi, L., Samany, P.G., Owoso, A., Wiskar, B., Grammas, P., 2006. Angiogenic proteins are expressed by brain blood vessels in Alzheimer's disease. J. Alzheimers. Dis. 10, 111–118. doi:10.3233/jad-2006-10114

Thomas, H.B., Moots, R.J., Edwards, S.W., Wright, H.L., 2015. Whose Gene Is It Anyway? The Effect of Preparation Purity on Neutrophil Transcriptome Studies. PLoS One 10, e0138982.

Thomas, L.M., Salter, R.D., 2010. Activation of macrophages by P2X7-induced microvesicles from myeloid cells is mediated by phospholipids and is partially dependent on TLR4. J. Immunol. 185, 3740–3749. doi:10.4049/jimmunol.1001231

Tietz, S., Engelhardt, B., 2015. Brain barriers: Crosstalk between complex tight junctions and adherens junctions. J. Cell Biol. 209, 493–506. doi:10.1083/jcb.201412147

Timár, C.I., Lőrincz, Á.M., Csépányi-Kömi, R., Vályi-Nagy, A., Nagy, G., Buzás, E.I., Iványi, Z., Kittel, Á., Powell, D.W., McLeish, K.R., Ligeti, E., 2013. Antibacterial effect of microvesicles released from human neutrophilic granulocytes. Blood 121, 510 LP – 518.

Tomasini, R., Samir, A.A., Vaccaro, M.I., Pebusque, M.J., Dagorn, J.C., Iovanna, J.L., Dusetti, N.J., 2001. Molecular and functional characterization of the stress-induced protein (SIP) gene and its two transcripts generated by alternative splicing. SIP induced by stress and promotes cell death. J. Biol. Chem. 276, 44185–44192. doi:10.1074/jbc.M105647200

Tomimoto, H., 2015. White matter integrity and cognitive dysfunction: Radiological and neuropsychological correlations. Geriatr. Gerontol. Int. doi:10.1111/ggi.12661

Tominaga, N., Kosaka, N., Ono, M., Katsuda, T., Yoshioka, Y., Tamura, K., Lötvall, J., Nakagama, H., Ochiya, T., 2015. Brain metastatic cancer cells release microRNA-181c-containing extracellular vesicles capable of destructing blood–brain barrier. Nat. Commun. 6, 6716. doi:10.1038/ncomms7716

Topakian, R., Barrick, T.R., Howe, F.A., Markus, H.S., 2010. Blood-brain barrier permeability is increased in normal-appearing white matter in patients with lacunar stroke and leucoaraiosis. J. Neurol. Neurosurg. Psychiatry 81, 192–197. doi:10.1136/jnnp.2009.172072

Trickler, W.J., Lantz, S.M., Murdock, R.C., Schrand, A.M., Robinson, B.L., Newport, G.D., Schlager, J.J., Oldenburg, S.J., Paule, M.G., Slikker, W., 2010. Silver nanoparticle induced blood-brain barrier inflammation and increased permeability in primary rat brain microvessel endothelial cells. Toxicol. Sci. kfq244.

Tuma, P.L., Hubbard, A.L., 2003. Transcytosis: crossing cellular barriers. Physiol. Rev. 83, 871–932. doi:10.1152/physrev.00001.2003

Turturici, G., Tinnirello, R., Sconzo, G., Geraci, F., 2014. Extracellular membrane vesicles as a mechanism of cell-to-cell communication: advantages and disadvantages. Am. J. Physiol. Cell

Physiol. 306, C621-33. doi:10.1152/ajpcell.00228.2013

Uberti, D., Carsana, T., Bernardi, E., Rodella, L., Grigolato, P., Lanni, C., Racchi, M., Govoni, S., Memo, M., 2002. Selective impairment of p53-mediated cell death in fibroblasts from sporadic Alzheimer's disease patients. J. Cell Sci. 115, 3131–3138.

Ulloa, F., Cotrufo, T., Ricolo, D., Soriano, E., Araújo, S., 2018. SNARE complex in axonal guidance and neuroregeneration. Neural Regen. Res. 13, 386–392. doi:10.4103/1673-5374.228710

Valenti, R., Huber, V., Iero, M., Filipazzi, P., Parmiani, G., Rivoltini, L., 2007. Tumor-Released Microvesicles as Vehicles of Immunosuppression. Cancer Res. 67, 2912 LP – 2915. doi:10.1158/0008-5472.CAN-07-0520

van den Biggelaar, A.H.J., Gussekloo, J., de Craen, A.J.M., Frölich, M., Stek, M.L., van der Mast, R.C., Westendorp, R.G.J., 2007. Inflammation and interleukin-1 signaling network contribute to depressive symptoms but not cognitive decline in old age. Exp. Gerontol. 42, 693–701.

Van Herreweghe, F., Festjens, N., Declercq, W., Vandenabeele, P., 2010. Tumor necrosis factor-mediated cell death: to break or to burst, that's the question. Cell. Mol. Life Sci. 67, 1567–1579. doi:10.1007/s00018-010-0283-0

van Uden, I.W.M., van der Holst, H.M., Tuladhar, A.M., van Norden, A.G.W., de Laat, K.F., Rutten-Jacobs, L.C.A., Norris, D.G., Claassen, J.A.H.R., van Dijk, E.J., Kessels, R.P.C., de Leeuw, F.-E., 2016. White Matter and Hippocampal Volume Predict the Risk of Dementia in Patients with Cerebral Small Vessel Disease: The RUN DMC Study. J. Alzheimers. Dis. 49, 863–873. doi:10.3233/JAD-150573

Verderio, C., Muzio, L., Turola, E., Bergami, A., Novellino, L., Ruffini, F., Riganti, L., Corradini, I., Francolini, M., Garzetti, L., Maiorino, C., Servida, F., Vercelli, A., Rocca, M., Libera, D.D., Martinelli, V., Comi, G., Martino, G., Matteoli, M., Furlan, R., 2012. Myeloid microvesicles are a marker and therapeutic target for neuroinflammation. Ann. Neurol. 72, 610–624. doi:10.1002/ana.23627

Vernooij, M.W., de Groot, M., van der Lugt, A., Ikram, M.A., Krestin, G.P., Hofman, A., Niessen, W.J., Breteler, M.M.B., 2008. White matter atrophy and lesion formation explain the loss of structural integrity of white matter in aging. Neuroimage 43, 470–477. doi:10.1016/j.neuroimage.2008.07.052

Vilchez, D., Saez, I., Dillin, A., 2014. The role of protein clearance mechanisms in organismal ageing and age-related diseases. Nat. Commun. 5, 1–13.

Vinters, H. V, 1987. Cerebral amyloid angiopathy. A critical review. Stroke 18, 311–324.

Viswanathan, A., Greenberg, S.M., 2008. Intracerebral hemorrhage. Handb. Clin. Neurol. 93, 767–790.

Vorbrodt, A.W., Dobrogowska, D.H., 1994. Immunocytochemical evaluation of blood-brain barrier to endogenous albumin in adult, newborn and aged mice. Folia Histochem. Cytobiol. 32, 63–70.

Wadhwani, K.C., Koistinaho, J., Balbo, A., Rapoport, S.I., 1991. Blood-nerve and blood-brain barrier permeabilities and nerve vascular space in Fischer-344 rats of different ages. Mech. Ageing Dev. 58, 177–190.

Waller, R., Baxter, L., Fillingham, D.J., Coelho, S., Pozo, J.M., Mozumder, M., Frangi, A.F., Ince, P.G., Simpson, J.E., Highley, J.R., 2019. Iba-1-/CD68+ microglia are a prominent feature of age-associated deep subcortical white matter lesions. PLoS One 14, e0210888.

Waller, R., Woodroofe, M.N., Wharton, S.B., Ince, P.G., Francese, S., Heath, P.R., Cudzich-Madry, A., Thomas, R.H., Rounding, N., Sharrack, B., Simpson, J.E., 2016. Gene expression profiling

of the astrocyte transcriptome in multiple sclerosis normal appearing white matter reveals a neuroprotective role. J. Neuroimmunol. 299, 139–146. doi:10.1016/j.jneuroim.2016.09.010

Wang, W.-X., Huang, Q., Hu, Y., Stromberg, A.J., Nelson, P.T., 2011. Patterns of microRNA expression in normal and early Alzheimer's disease human temporal cortex: white matter versus gray matter. Acta Neuropathol. 121, 193–205. doi:10.1007/s00401-010-0756-0

Wardlaw, J.M., Allerhand, M., Doubal, F.N., Valdes Hernandez, M., Morris, Z., Gow, A.J., Bastin, M., Starr, J.M., Dennis, M.S., Deary, I.J., 2014. Vascular risk factors, large-artery atheroma, and brain white matter hyperintensities. Neurology 82, 1331 LP – 1338. doi:10.1212/WNL.0000000000000312

Wardlaw, J.M., Doubal, F., Armitage, P., Chappell, F., Carpenter, T., Muñoz Maniega, S., Farrall, A., Sudlow, C., Dennis, M., Dhillon, B., 2009. Lacunar stroke is associated with diffuse blood–brain barrier dysfunction. Ann. Neurol. Off. J. Am. Neurol. Assoc. Child Neurol. Soc. 65, 194–202.

Wardlaw, J.M., Makin, S.J., Valdés Hernández, M.C., Armitage, P.A., Heye, A.K., Chappell, F.M., Muñoz-Maniega, S., Sakka, E., Shuler, K., Dennis, M.S., Thrippleton, M.J., 2017. Blood-brain barrier failure as a core mechanism in cerebral small vessel disease and dementia: evidence from a cohort study. Alzheimer's Dement. 13, 634–643. doi:https://doi.org/10.1016/j.jalz.2016.09.006

Wardlaw, J.M., Smith, C., Dichgans, M., 2013a. Mechanisms of sporadic cerebral small vessel disease: insights from neuroimaging. Lancet. Neurol. 12, 483–497. doi:10.1016/S1474-4422(13)70060-7

Wardlaw, J.M., Smith, E.E., Biessels, G.J., Cordonnier, C., Fazekas, F., Frayne, R., Lindley, R.I., O'Brien, J.T., Barkhof, F., Benavente, O.R., Black, S.E., Brayne, C., Breteler, M., Chabriat, H., Decarli, C., de Leeuw, F.-E., Doubal, F., Duering, M., Fox, N.C., Greenberg, S., Hachinski, V., Kilimann, I., Mok, V., Oostenbrugge, R. van, Pantoni, L., Speck, O., Stephan, B.C.M., Teipel, S., Viswanathan, A., Werring, D., Chen, C., Smith, C., van Buchem, M., Norrving, B., Gorelick, P.B., Dichgans, M., 2013b. Neuroimaging standards for research into small vessel disease and its contribution to ageing and neurodegeneration. Lancet. Neurol. 12, 822–838. doi:10.1016/S1474-4422(13)70124-8

Wei, Q., Li, Y.-X., Liu, M., Li, X., Tang, H., 2012. MiR-17-5p targets TP53INP1 and regulates cell proliferation and apoptosis of cervical cancer cells. IUBMB Life 64, 697–704. doi:10.1002/iub.1051

Weksler, B., Romero, I.A., Couraud, P.-O., 2013. The hCMEC/D3 cell line as a model of the human blood brain barrier. Fluids Barriers CNS 10, 16. doi:10.1186/2045-8118-10-16

Wen, Q., Mustafi, S.M., Li, J., Risacher, S.L., Tallman, E., Brown, S.A., West, J.D., Harezlak, J., Farlow, M.R., Unverzagt, F.W., Gao, S., Apostolova, L.G., Saykin, A.J., Wu, Y.-C., 2019. White matter alterations in early-stage Alzheimer's disease: A tract-specific study. Alzheimer's Dement. (Amsterdam, Netherlands) 11, 576–587. doi:10.1016/j.dadm.2019.06.003

Wen, W., Sachdev, P.S., 2004. Extent and distribution of white matter hyperintensities in stroke patients: the Sydney Stroke Study. Stroke 35, 2813–2819. doi:10.1161/01.STR.0000147034.25760.3d

Wharton, S.B., Brayne, C., Savva, G.M., Matthews, F.E., Forster, G., Simpson, J., Lace, G., Ince, P.G., 2011. Epidemiological neuropathology: the MRC Cognitive Function and Aging Study experience. J. Alzheimers. Dis. 25, 359–372. doi:10.3233/JAD-2011-091402

Wheeler, A.P., Bernard, G.R., 1999. Treating patients with severe sepsis. N. Engl. J. Med. 340, 207–214. doi:10.1056/NEJM199901213400307

Whitney, L.W., Ludwin, S.K., McFarland, H.F., Biddison, W.E., 2001. Microarray analysis of gene expression in multiple sclerosis and EAE identifies 5-lipoxygenase as a component of

inflammatory lesions. J. Neuroimmunol. 121, 40–48. doi:10.1016/s0165-5728(01)00438-6

Witlox, J., Eurelings, L.S.M., de Jonghe, J.F.M., Kalisvaart, K.J., Eikelenboom, P., van Gool, W.A., 2010. Delirium in elderly patients and the risk of postdischarge mortality, institutionalization, and dementia: a meta-analysis. JAMA 304, 443–451. doi:10.1001/jama.2010.1013

Wolf, P., 1967. The Nature and Significance of Platelet Products in Human Plasma. Br. J. Haematol. 13, 269–288. doi:10.1111/j.1365-2141.1967.tb08741.x

Wozniak, J.R., Lim, K.O., 2006. Advances in white matter imaging: a review of in vivo magnetic resonance methodologies and their applicability to the study of development and aging. Neurosci. Biobehav. Rev. 30, 762–774. doi:10.1016/j.neubiorev.2006.06.003

Wu, F., Liu, L., Zhou, H., 2017. Endothelial cell activation in central nervous system inflammation. J. Leukoc. Biol. 101, 1119–1132. doi:10.1189/jlb.3RU0816-352RR

Xu, L., Nirwane, A., Yao, Y., 2018. Basement membrane and blood-brain barrier. Stroke Vasc. Neurol. 4, 78–82. doi:10.1136/svn-2018-000198

Xue, S., Cai, X., Li, W., Zhang, Z., Dong, W., Hui, G., 2012. Elevated plasma endothelial microparticles in Alzheimer's disease. Dement. Geriatr. Cogn. Disord. 34, 174–180. doi:10.1159/000343491

Yaffe, K., Lindquist, K., Penninx, B.W., Simonsick, E.M., Pahor, M., Kritchevsky, S., Launer, L., Kuller, L., Rubin, S., Harris, T., 2003. Inflammatory markers and cognition in well-functioning African-American and white elders. Neurology 61, 76–80.

Yang, T., Martin, P., Fogarty, B., Brown, A., Schurman, K., Phipps, R., Yin, V.P., Lockman, P., Bai, S., 2015. Exosome Delivered Anticancer Drugs Across the Blood-Brain Barrier for Brain Cancer Therapy in Danio Rerio. Pharm. Res. 32, 2003–2014. doi:10.1007/s11095-014-1593-y

Yang, Y., Li, C.-C.H., Weissman, A.M., 2004. Regulating the p53 system through ubiquitination. Oncogene 23, 2096–2106. doi:10.1038/sj.onc.1207411

Yao, H., Mizoguchi, Y., Monji, A., Yakushiji, Y., Takashima, Y., Uchino, A., Yuzuriha, T., Hashimoto, M., 2019. Low-Grade Inflammation Is Associated with Apathy Indirectly via Deep White Matter Lesions in Community-Dwelling Older Adults: The Sefuri Study. Int. J. Mol. Sci. 20, 1905. doi:10.3390/ijms20081905

Yeretssian, G., Correa, R.G., Doiron, K., Fitzgerald, P., Dillon, C.P., Green, D.R., Reed, J.C., Saleh, M., 2011. Non-apoptotic role of BID in inflammation and innate immunity. Nature 474, 96.

Ylikoski, A., Erkinjuntti, T., Raininko, R., Sarna, S., Sulkava, R., Tilvis, R., 1995. White matter hyperintensities on MRI in the neurologically nondiseased elderly. Analysis of cohorts of consecutive subjects aged 55 to 85 years living at home. Stroke 26, 1171–1177.

Young, V.G., Halliday, G.M., Kril, J.J., 2008. Neuropathologic correlates of white matter hyperintensities. Neurology 71, 804 LP – 811. doi:10.1212/01.wnl.0000319691.50117.54

Yuan, B., Shi, H., Zheng, K., Su, Z., Su, H., Zhong, M., He, X., Zhou, C., Chen, H., Xiong, Q., Zhang, Y., Yang, Z., 2017. MCP-1-mediated activation of microglia promotes white matter lesions and cognitive deficits by chronic cerebral hypoperfusion in mice. Mol. Cell. Neurosci. 78, 52–58. doi:https://doi.org/10.1016/j.mcn.2016.08.003

Yujiri, T., Sather, S., Fanger, G.R., Johnson, G.L., 1998. Role of MEKK1 in cell survival and activation of JNK and ERK pathways defined by targeted gene disruption. Science (80-.). 282, 1911–1914.

Zarbock, A., Ley, K., 2008. Mechanisms and Consequences of Neutrophil Interaction with the Endothelium. Am. J. Pathol. 172, 1–7. doi:10.2353/ajpath.2008.070502

Zenaro, E., Pietronigro, E., Della Bianca, V., Piacentino, G., Marongiu, L., Budui, S., Turano, E., Rossi, B., Angiari, S., Dusi, S., 2015. Neutrophils promote Alzheimer's disease-like pathology and cognitive decline via LFA-1 integrin. Nat. Med. 21, 880–886.

Zhang, C.E., Wong, S.M., van de Haar, H.J., Staals, J., Jansen, J.F.A., Jeukens, C.R., Hofman, P.A.M., van Oostenbrugge, R.J., Backes, W.H., 2017. Blood–brain barrier leakage is more widespread in patients with cerebral small vessel disease. Neurology 88, 426–432.

Zhang, G.-S., Tian, Y., Huang, J.-Y., Tao, R.-R., Liao, M.-H., Lu, Y.-M., Ye, W.-F., Wang, R., Fukunaga, K., Lou, Y.-J., Han, F., 2013. The γ-Secretase Blocker DAPT Reduces the Permeability of the Blood–Brain Barrier by Decreasing the Ubiquitination and Degradation of Occludin During Permanent Brain Ischemia. CNS Neurosci. Ther. 19, 53–60. doi:10.1111/cns.12032

Zhang, H., Goudeva, L., Immenschuh, S., Schambach, A., Skokowa, J., Eiz-Vesper, B., Blasczyk, R., Figueiredo, C., 2015. miR-155 is associated with the leukemogenic potential of the class IV granulocyte colony-stimulating factor receptor in $CD34^{+}$ progenitor cells. Mol. Med. 20, 736—746. doi:10.2119/molmed.2014.00146

Zhang, S.-C., Ge, B., Duncan, I.D., 1999. Adult brain retains the potential to generate oligodendroglial progenitors with extensive myelination capacity. Proc. Natl. Acad. Sci. 96, 4089 LP – 4094. doi:10.1073/pnas.96.7.4089

Zhou, X., Spittau, B., Krieglstein, K., 2012. TGFbeta signalling plays an important role in IL4-induced alternative activation of microglia. J. Neuroinflammation 9, 210. doi:10.1186/1742-2094-9-210

Zhu, X., Lee, H., Raina, A.K., Perry, G., Smith, M.A., 2002. The role of mitogen-activated protein kinase pathways in Alzheimer's disease. Neurosignals 11, 270–281.

Zlokovic, B. V., 2005. Neurovascular mechanisms of Alzheimer's neurodegeneration. Trends Neurosci. doi:10.1016/j.tins.2005.02.001

Zlokovic, B. V, 2011. Neurovascular pathways to neurodegeneration in Alzheimer's disease and other disorders. Nat. Rev. Neurosci. 12, 723–38. doi:10.1038/nrn3114

Appendix I

The University Of Sheffield.

The Medical School

Dr V Ridger
Department of Cardiovascular Science
Medical School

Faculty of Medicine Dentistry & Health
Professor AP Weetman
Pro-Vice-Chancellor

Mrs Pauline Barnard
Research Ethics Administrator
Room LU116, L Floor
The Medical School
Beech Hill Road
Sheffield S10 2RX

Telephone: +44 (0) 114 271 2027
Fax: +44 (0) 114 226 8898
Email: p.a.whitaker@sheffield.ac.uk

24 April 2014

Dear Dr Ridger

Reference No: SMBRER310
Project Title: Studies of the function of platelets and leukocytes in blood and plasma from healthy volunteers

I am pleased to inform you that on 1 May 2014 the School's Ethics Reviewers **approved** the above-named project on ethics grounds, on the basis that you will adhere to and use the following documents that you submitted for ethics review:

i) Amended Ethics Application Form (dated 24/4/14)
ii) Consent form (dated 26/2/14)
iii) Healthy volunteer information sheet (dated 24/4/14)

If, during the course of the project, you need to deviate from the above-approved documents please inform me. The written approval of the School's Ethics Review Panel will be required for significant deviations from or significant changes to the above-approved documents. If you decide to terminate the project prematurely please inform me.

Yours sincerely

[redacted]

Pauline Barnard
School Research Ethics Administrator

2011 THE AWARDS AWARD WINNER UNIVERSITY OF THE YEAR

Appendix II

FOR CFAS OFFICE USE
Tissue request no. 16/03

AUTHORISATION TO USE TISSUE FROM THE COGNITIVE FUNCTION AND AGEING STUDY (CFAS) BIOLOGICAL RESOURCE

FOLLOWING CONSIDERATION BY THE CFAS MANAGEMENT COMMITTEE (CMC) AND BIOLOGICAL RESOURCE ADVISORY COMMITTEE (BRAC):

Study Title: Neurtrophil-derived microvesicle-induced blood brain barrier dysfunction in the ageing brain.

Head of proposed study:
Dr Julie Simpson
Additional Investigator: Anjana Ajikumar
Organisation: Sheffield Institute for Translational Neuroscience,
385A Glossop Road, Sheffield, S10 2HQ

Telephone No: 0114 222 2235

Email: s.wharton@sheffield.ac.uk

CFAS TISSUE REQUEST NUMBER**: 16/03**

This project was reviewed by both CMC and BRAC committees and approval was given to release the requested tissue under the following REC approval:

Title of Ethical application: Cognitive Function and Ageing Studies: Diabetes, Defective Nutrient Signalling and Dementia: an Epidemiological Neuropathology approach.

REC No:15/SW/0246
IRAS No: 184134

[redacted]

Professor Carol Brayne
Chief Investigator CFAS

Date: 27/07/2017

Appendix III

The list of dysregulated gene list obtained from the microarray analysis of the endothelial cells obtained from DSCL, NAWM and control cases is attached as a file in the electronic version under the name ‘post-mortem microarray data’.

Appendix IV

Top 20 dysregulated gene list obtained from the microarray analysis of NMV treated hCMEC/D3 cells v control non-treated cells are attached as a folder in the electronic version under the name ‘top dysregulated genes’. Furthermore, top 20 dysregulated genes in DSCL v NAWM, NAWM v Control and control v DSCL is also listed in the folder.